Structure-Driven Chirality-Induced Spin Selectivity in Self-Sorted Azahelicenes via Facile Electrosynthesis

Zuowei Sun[1,†], Shaokun Tao[1,†], Haojie Zhang[2], Yun Yang[1], Minghui Wang[1], Li Chen[1], Yi Tan[1], Haiyan Fu[1], Ruixiang Li[1], Dan Li[2], Hua Chen[1], Dong Luo*[,2], Xueli Zheng*[,1] & Weichao Xue*[,1]

[1]*Key Laboratory of Green Chemistry & Technology, Ministry of Education, College of Chemistry, Sichuan University*

Chengdu 610064, Sichuan, P. R. China.

[2]*College of Chemistry and Materials Science, Guangdong Provincial Key Laboratory of Supramolecular Coordination Chemistry, Jinan University*

Guangzhou 510632, Guangdong, P. R. China

**Corresponding author.*

[†]*These authors contributed equally.*

Email: weichaoxue@scu.edu.cn; zhengxueli@scu.edu.cn; luodong@jnu.edu.cn

Supporting Information

Table of Contents

1 General Information

All reactions were performed in flame-dried glassware using conventional Schlenk techniques under a static pressure of nitrogen unless otherwise stated. Liquids and solutions were transferred with syringes. Unless otherwise specified, all reagents were purchased from commercial sources and used without further purification. All electrodes were commercially obtained and used as received: platinum plate (Shanghai Yueci Electronics, 99.99% purity), graphite felt (Tianjin Carbon Factory, 5 mm thickness), and graphite rod (Tianjin Carbon Factory, 5 mm diameter). Analytical thin layer chromatography (TLC) was performed on silica gel 60 F254/0.25 mm glass plates by *Merck*. Flash column chromatography was performed on silica gel 12–120 (40–63 μm, 60 Å, 12–120 g) by *SepaBean machine* using the indicated solvents. ^{1}H and ^{13}C NMR spectra were recorded on *Bruker* AVANCE IIIHD 400 NMR spectrometers in $CDCl_3$ or DMSO-d_6 solutions. Chemical shifts are reported in parts per million (ppm) and are referenced to the residual solvent resonance as the internal standard. Chemical shifts of the NMR spectra are reported relative to $CDCl_3$ (^{1}H NMR: δ = 7.26 ppm, ^{13}C NMR: δ = 77.0 ppm), DMSO-d_6 (^{1}H NMR: δ = 2.50 ppm, ^{13}C NMR: δ = 39.5 ppm). Data are reported as follows: chemical shift, multiplicity (s = singlet, d = doublet, t = triplet, q = quartet, m = multiplet, br = broad signal), coupling constants (Hz), and integration. Enantiomeric analyses were determined by analytical high performance liquid chromatography (HPLC) on an *Agilent Technologies* 1220 Infinity II instrument. Chiral HPLC separations were carried out using a Shimadzu LC-20AT instrument. High resolution electrospray ionisation mass spectra (HR-ESI-MS) were recorded on a *SCIEX* X500R QTOF instrument. Cyclic voltammetry was performed using a CHI760E analyzer with a scan rate of 100 mV/s at room temperature to investigate the oxidation potentials. Single crystals suitable for X-ray diffraction analyses were obtained from their solution on a *Bruker* APEX-II CCD diffractometer. UV-Vis spectra were recorded on a *Thermo Scientific* GENESYS 180 UV-Visible spectrophotometer, and the fluorescence spectra were recorded on a *Techcomp* FL970 spectrometer at room temperature. CD spectra were recorded on automatic mode using a Bio Logic MOS-500 multifunctional circular dichroism spectrometer, and the CPL spectra were measured with a JASCO CPL-300 spectrophotometer at room temperature. The transient photoluminescence decay characteristics and absolute PL

quantum yield were measured on a *Horiba JobinYvon* Fluorolog-3 spectrofluorometer. AFM Topography and magnetic conductive probe atomic force microscope (mc-AFM) measurements were performed using Oxford MFP-3D Origin at room temperature.

2 Optimization Study

2.1 Optimization Study of Redox Mediators

Table S1. Screening of the optimal quantity of redox mediators[a].

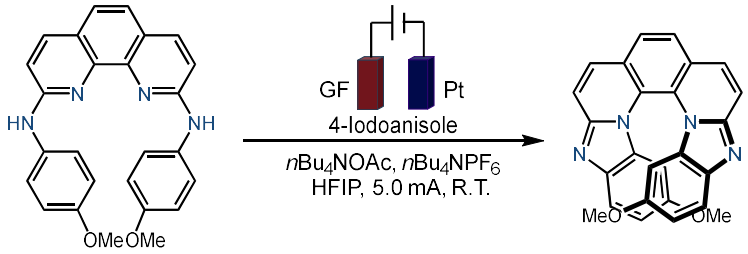

5a **5**

Entry	4-Iodoanisole [mol%]	Yield [%][b]
1	40	59
2	30	60
3	25	69
4	20	68
5	10	56
6	5	64
7	1	60
8	0	66

[a]Reaction conditions: undivided cell, GF as anode, Pt as cathode, **5a** (0.10 mmol), 4-iodoanisole, nBu$_4$NOAc (0.40 mmol), nBu$_4$NPF$_6$ (0.200 M), HFIP (2.50 mL), 5.0 mA, 2 h, R.T. [b]^{1}H NMR yield, using 1,3,5-trimethoxybenzene as internal standard.

2.2 Optimization Study of Electrode

Table S2. Screening of the electrode sheet[a].

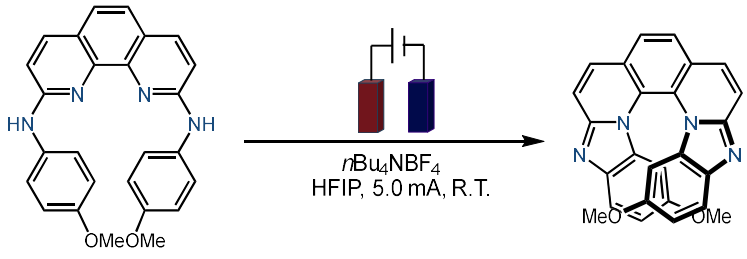

5a **5**

Entry	Electrode	Yield [%][b]
1	GF | GF	66
2	GF | Pt	69
3	Pt | Pt	46
4	Graphite | Pt	27
5	Graphite | Graphite	32
6	Pt | GF	22
7	Pt | Graphite	34

[a]Reaction conditions: undivided cell, **5a** (0.10 mmol), nBu$_4$NBF$_4$ (0.100 M), HFIP (2.50 mL), 5.0 mA, 2 h, R.T. [b]^{1}H NMR yield, using 1,3,5-trimethoxybenzene as internal standard.

2.3 Optimization Study of Current

Table S3. Screening of the reaction current[a].

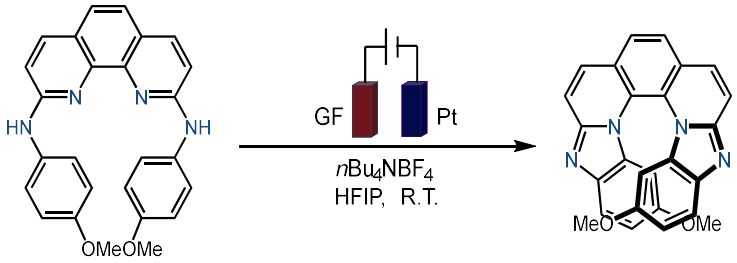

5a **5**

Entry	Current [mA]	Yield [%][b]
1	2.5 mA, 4.0 h	64
2	5.0 mA, 2.0 h	69
3	7.5 mA, 1.3 h	68
4	10.0 mA, 1.0 h	65
5	12.5 mA, 0.8 h	57

[a]Reaction conditions: undivided cell, GF as anode, Pt as cathode, **5a** (0.10 mmol), *n*Bu_4NBF_4 (0.100 M), HFIP (2.50 mL), R.T. [b]^{1}H NMR yield, using 1,3,5-trimethoxybenzene as internal standard.

2.4 Optimization Study of Electrolyte

Table S4. Screening of the type of electrolyte[a].

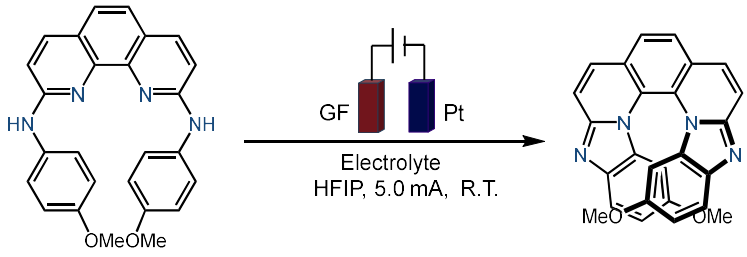

5a **5**

Entry	Electrolyte	Yield [%][b]
1	$LiClO_4$	49
2	$LiBF_4$	28
3	nBu$_4$NBF$_4$	69
4	nBu$_4$NPF$_6$	61
5	nBu$_4$NClO$_4$	54
6	nBu$_4$NI	40

[a]Reaction conditions: undivided cell, GF as anode, Pt as cathode, **5a** (0.10 mmol), electrolyte (0.100 M), HFIP (2.50 mL), 5.0 mA, 2 h, R.T. [b]^{1}H NMR yield, using 1,3,5-trimethoxybenzene as internal standard. Unless otherwise stated, nBu$_4$NBF$_4$ was used as the supporting electrolyte due to its superior electrochemical stability under the reaction conditions.

Table S5. Screening of the electrolyte concentration[a].

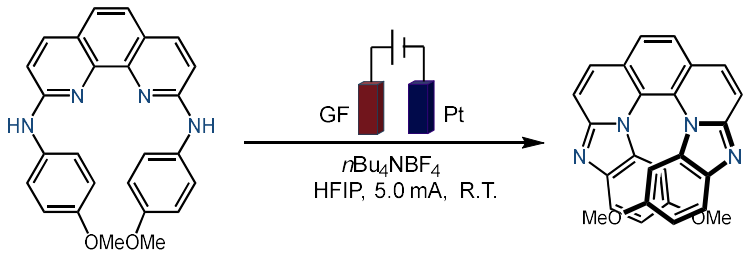

5a **5**

Entry	nBu$_4$NBF$_4$	Yield [%][b]
1	0.100 M	69
2	0.150 M	88
3	0.200 M	90
4	0.250 M	90

[a]Reaction conditions: undivided cell, GF as anode, Pt as cathode, **5a** (0.10 mmol), nBu$_4$NBF$_4$, HFIP (2.50 mL), 5.0 mA, 2 h, R.T. [b]^{1}H NMR yield, using 1,3,5-trimethoxybenzene as internal standard.

2.5 Optimization Study of Solvent

Table S6. Screening of the solvent[a].

Since the oxidation potential of substrates in electrochemical oxidation correlates with their electron density, condition optimization was first carried out using electron-rich substrates. A trifluoromethyl-substituted substrate was then selected as a representative electron-deficient system for condition screening. Only HFIP afforded the product in 23% yield (entry 5), while other alcohol solvents resulted in trace conversion. However, the HFIP/H_2O (5/1) mixed solvent supplies protons for cathodic hydrogen evolution, facilitating the anodic oxidation.

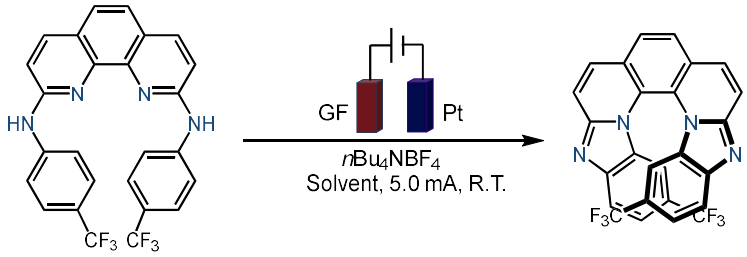

11a **11**

Entry	Solvent	Yield [%][c]
1	MeOH	Trace
2	EtOH	Trace
3	*i*-PrOH	Trace
4	*n*-BuOH	Trace
5	HFIP	23
6[b]	H_2O	N.R.
7[b]	*V*(HFIP)/*V*(H_2O) = 2.5/0.5	52
8[b]	*V*(HFIP)/*V*(H_2O) = 2.0/1.0	34
9[b]	*V*(HFIP)/*V*(H_2O) = 1.5/1.5	17
10[b]	*V*(HFIP)/*V*(H_2O) = 1.0/2.0	Trace
11[b]	*V*(HFIP)/*V*(H_2O) = 0.5/2.5	Trace

[a]Reaction conditions: undivided cell, GF as anode, Pt as cathode, **11a** (0.10 mmol), *n*Bu_4NBF_4 (0.100 M), solvent (2.50 mL), 5.0 mA, 2 h, R.T. [b]Solvent (3.00 mL), otherwise identical to a. [c]^{1}H NMR yield, using 1,3,5-trimethoxybenzene as internal standard.

Table S7. Screening of the electrolyte concentration[a].

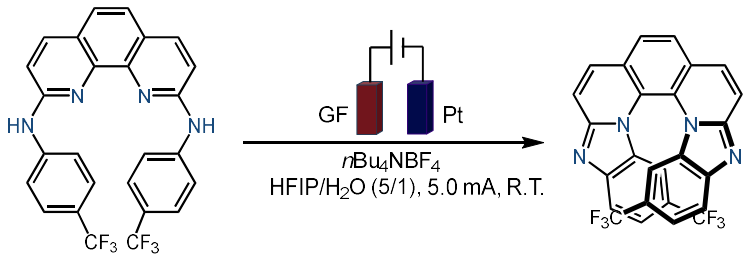

11a **11**

Entry	Electrolyte concentration	Yield [%][b]
1	0.100 M nBu$_4$NBF$_4$	52
2	0.150 M nBu$_4$NBF$_4$	66
3	0.200 M nBu$_4$NBF$_4$	70

[a]Reaction conditions: undivided cell, GF as anode, Pt as cathode, **11a** (0.10 mmol), nBu$_4$NBF$_4$, V(HFIP)/V(H$_2$O) = 5/1 (3.00 mL), 5.0 mA, 2 h, R.T. [b]^{1}H NMR yield, using 1,3,5-trimethoxybenzene as internal standard.

3 Experimental Details for the Substrate

3.1 General Procedure for Synthesis of Substrate Type 1 (GP1)

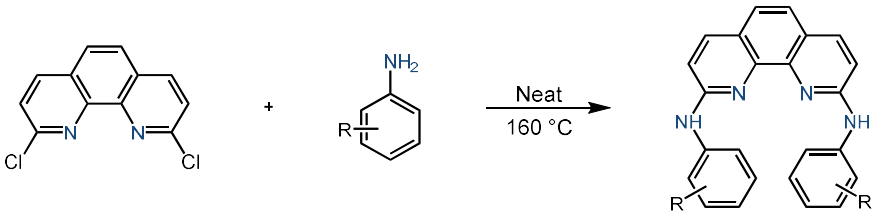

A dried two-neck round-bottom flask equipped with a magnetic stir bar was connected to a Schlenk line and purged with N_2. The flask was charged with 2,9-dichloro-1,10-phenanthroline (4.0 mmol, 1.00 equiv.) and an aromatic amine (20.0 mmol, 5.00 equiv.) and then heated at 160 °C for 4 h. If the solid did not melt, anhydrous dimethyl sulfoxide (20.0 mL) was added. After cooling to room temperature, saturated aqueous $NaHCO_3$ (50.0 mL) was added. The mixture was extracted with dichloromethane (50.0 mL × 3), and the combined organic layers were dried over anhydrous sodium sulfate. The solvent was removed under reduced pressure, and the crude residue was purified by column chromatography on silica gel to afford the desired product.[1]

3.2 General Procedure for Synthesis of Substrate Type 2 (GP2)

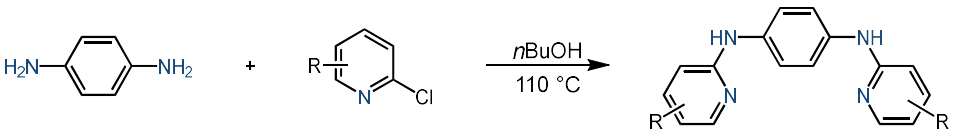

A dried two-neck round-bottom flask equipped with a magnetic stir bar was connected to a Schlenk line and purged with N_2. To the flask were added *p*-phenylenediamine (4.0 mmol, 1.00 equiv.) and an N-heteroaryl chloride (10.0 mmol, 2.50 equiv.), followed by *n*-butanol (20.0 mL). The reaction mixture was heated at 110 °C for 24 h. After cooling to room temperature, saturated aqueous $NaHCO_3$ (50.0 mL) was added. The mixture was extracted with dichloromethane (50.0 mL × 3), and the combined organic layers were dried over anhydrous sodium sulfate. The solvent was removed under reduced pressure, and the crude residue was purified by column chromatography on silica gel to afford the desired product.[2]

3.3 General Procedure for Synthesis of Substrate Type 3 (GP3)

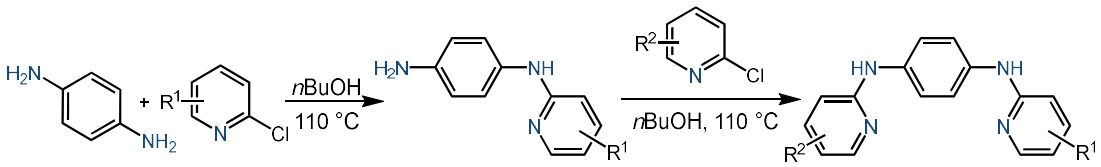

A dried two-neck round-bottom flask equipped with a magnetic stir bar was connected to a Schlenk line and purged with N_2. To the flask were added *p*-phenylenediamine (4.0 mmol, 1.00 equiv.) and an N-heteroaryl chloride (4.0 mmol, 1.00 equiv.), followed by *n*-butanol (20.0 mL). The reaction mixture was heated at 110 °C for 24 h. After cooling to room temperature, a second N-heteroaryl chloride (4.0 mmol, 1.00 equiv.) was added, and the mixture was heated at 110 °C for another 24 h. Upon cooling to room temperature, saturated aqueous $NaHCO_3$ (50.0 mL) was added. The mixture was extracted with dichloromethane (50.0 mL × 3), and the combined organic layers were dried over anhydrous sodium sulfate. The solvent was removed under reduced pressure, and the crude residue was purified by column chromatography on silica gel to afford the desired product.

3.4 Characterization Data of the Substrate

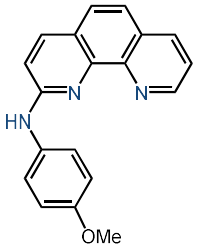

1a
$C_{19}H_{15}N_3O$
M = 301.35 g/mol

***N*-(4-methoxyphenyl)-1,10-phenanthrolin-2-amine** (**1a**): Prepared from 2,9-dichloro-1,10-phenanthroline (1.00 g, 4.0 mmol) and 4-methoxyaniline (1.23 g, 10.0 mmol) according to **GP1**. Purification by flash column chromatography on silica gel using petroleum ether and ethyl acetate to afford **1a** as a grey solid (0.720 g, 60% yield).

R_f = 0.20 (PE/EA = 4/1). **^{1}H NMR** (400 MHz, DMSO-d_6) δ 9.45 (s, 1H), 9.16–9.02 (m, 1H), 8.38 (d, J = 8.2 Hz, 1H), 8.20 (d, J = 8.8 Hz, 2H), 8.15 (d, J = 8.8 Hz, 1H), 7.79 (d, J = 8.8 Hz, 1H), 7.72–7.61 (m, 2H), 7.19 (d, J = 8.8 Hz, 1H), 6.96 (d, J = 8.8 Hz, 2H), 3.77 (s, 3H). **^{13}C NMR** (100 MHz, DMSO-d_6) δ 154.7, 153.8, 149.3, 144.9, 144.7, 137.0, 135.9, 135.0, 128.9, 126.4, 122.5, 122.5, 121.7, 119.7, 114.0, 113.6, 55.2. **HRMS** (ESI-TOF) for $C_{19}H_{16}N_3O^+$ $[M+H]^+$: calculated 302.1288, found 302.1288.

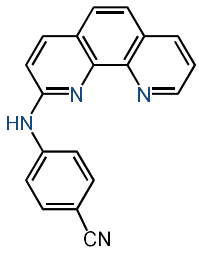

2a
$C_{19}H_{12}N_4$
M = 296.33 g/mol

4-((1,10-phenanthrolin-2-yl)amino)benzonitrile (**2a**): Prepared from 2,9-dichloro-1,10-phenanthroline (1.00 g, 4.0 mmol) and 4-aminobenzonitrile (1.18 g, 10.0 mmol) according to **GP1**. Purification by flash column chromatography on silica gel using petroleum ether and ethyl acetate to afford **2a** as a white solid (0.750 g, 63% yield).

$\mathbf{R}_f$ = 0.20 (PE/EA = 1/1). **^{1}H NMR** (400 MHz, DMSO-d_6) δ 10.16 (s, 1H), 9.12 (dd, J = 4.2, 1.8 Hz, 1H), 8.54 (d, J = 8.8 Hz, 2H), 8.43 (dd, J = 8.2, 1.8 Hz, 1H), 8.31 (d, J = 8.6 Hz, 1H), 7.87 (d, J = 8.6 Hz, 1H), 7.83–7.75 (m, 3H), 7.74–7.68 (m, 1H), 7.34 (d, J = 8.8 Hz, 1H). **^{13}C NMR** (100 MHz, DMSO-d_6) δ 153.7, 149.8, 145.8, 144.7, 144.4, 137.8, 136.0, 133.2, 128.9, 126.3, 123.4, 123.2, 122.9, 119.8, 118.0, 114.4, 101.7. **HRMS** (ESI-TOF) for $C_{19}H_{13}N_4^+$ $[M+H]^+$: calculated 297.1135, found 297.1136.

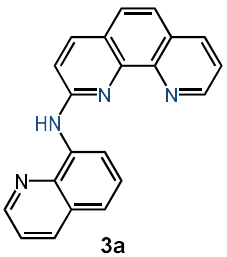

3a
$C_{21}H_{14}N_4$
M = 322.37 g/mol

***N*-(quinolin-8-yl)-1,10-phenanthrolin-2-amine** (**3a**): Prepared from 2,9-dichloro-1,10-phenanthroline (1.00 g, 4.0 mmol) and quinolin-8-amine (1.44 g, 10.0 mmol) according to **GP1**. Purification by flash column chromatography on silica gel using ethyl acetate to afford **3a** as a yellow solid (0.730 g, 57% yield).

R_f = 0.40 (EA). **^{1}H NMR** (400 MHz, $CDCl_3$) δ 9.74 (s, 1H), 9.58 (dd, *J* = 8.0, 1.2 Hz, 1H), 9.22 (dd, *J* = 4.2, 1.8 Hz, 1H), 8.83 (dd, *J* = 4.2, 1.8 Hz, 1H), 8.21 (dd, *J* = 8.2, 1.8 Hz, 1H), 8.17 (dd, *J* = 8.2, 1.8 Hz, 1H), 8.09 (d, *J* = 8.8 Hz, 1H), 7.76 (t, *J* = 8.0 Hz, 1H), 7.70 (d, *J* = 8.8 Hz, 1H), 7.62–7.56 (m, 2H), 7.47–7.42 (m, 2H), 7.40 (d, *J* = 8.8 Hz, 1H). **^{13}C NMR** (100 MHz, $CDCl_3$) δ 154.2, 149.9, 147.5, 145.6, 145.6, 138.8, 137.4, 137.0, 136.4, 135.9, 129.3, 128.3, 128.3, 126.3, 123.5, 122.8, 122.5, 121.4, 118.9, 114.3, 114.2. **HRMS** (ESI-TOF) for $C_{21}H_{15}N_4^+$ $[M+H]^+$: calculated 323.1291, found 323.1286.

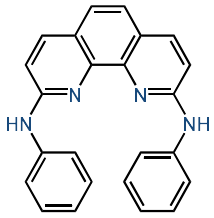

4a
$C_{24}H_{18}N_4$
M = 362.44 g/mol

***N*²,*N*⁹-diphenyl-1,10-phenanthroline-2,9-diamine** (**4a**): Prepared from 2,9-dichloro-1,10-phenanthroline (1.00 g, 4.0 mmol) and aniline (1.86 g, 20.0 mmol) according to **GP1**. Purification by flash column chromatography on silica gel using petroleum ether and ethyl acetate to afford **4a** as a white solid (1.07 g, 74% yield).

R*f* = 0.30 (PE/EA = 3/1). **¹H NMR** (400 MHz, $CDCl_3$) δ 7.97 (d, *J* = 8.8 Hz, 2H), 7.45 (s, 2H), 7.43–7.31 (m, 10H), 7.26 (d, *J* = 8.8 Hz, 2H), 7.14–7.07 (m, 2H). **¹³C NMR** (100 MHz, $CDCl_3$) δ 155.1, 144.6, 140.5, 138.3, 129.6, 124.4, 123.6, 122.6, 121.3, 110.9. **HRMS** (ESI-TOF) for $C_{24}H_{19}N_4^+$ $[M+H]^+$: calculated 363.1604, found 363.1603.

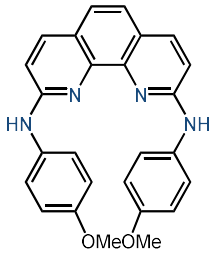

5a
$C_{26}H_{22}N_4O_2$
M = 422.49 g/mol

***N*²,*N*⁹-bis(4-methoxyphenyl)-1,10-phenanthroline-2,9-diamine** (**5a**): Prepared from 2,9-dichloro-1,10-phenanthroline (1.00 g, 4.0 mmol) and 4-methoxyaniline (2.46 g, 20.0 mmol) according to **GP1**. Purification by flash column chromatography on silica gel using petroleum ether and ethyl acetate to afford **5a** as a yellow solid (1.35 g, 80% yield).

$\mathbf{R}_f$ = 0.40 (PE/EA = 1/1). **^{1}H NMR** (400 MHz, $CDCl_3$) δ 7.91 (d, *J* = 8.8 Hz, 2H), 7.39 (s, 2H), 7.30–7.26 (m, 4H), 7.16 (s, 2H), 7.05 (d, *J* = 8.8 Hz, 2H), 6.93–6.88 (m, 4H), 3.81 (s, 6H). **^{13}C NMR** (100 MHz, $CDCl_3$) δ 156.9, 156.3, 144.6, 138.2, 133.3, 125.1, 124.1, 122.3, 114.9, 110.1, 55.7. **HRMS** (ESI-TOF) for $C_{26}H_{23}N_4O_2^+$ $[M+H]^+$: calculated 423.1816, found 423.1820.

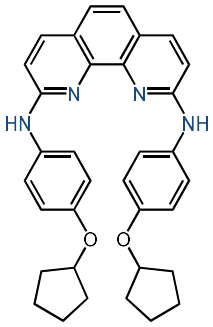

6a
$C_{34}H_{34}N_4O_2$
M = 530.67 g/mol

***N*²,*N*⁹-bis(4-(cyclopentyloxy)phenyl)-1,10-phenanthroline-2,9-diamine** (**6a**): Prepared from 2,9-dichloro-1,10-phenanthroline (1.00 g, 4.0 mmol) and 4-(cyclopentyloxy)aniline (3.55 g, 20.0 mmol) according to **GP1**. Purification by flash column chromatography on silica gel using petroleum ether and ethyl acetate to afford **6a** as a brown solid (1.59 g, 75% yield).

R_f = 0.30 (PE/EA = 1/1). **^{1}H NMR** (400 MHz, $CDCl_3$) δ 7.91 (d, *J* = 8.8 Hz, 2H), 7.39 (s, 2H), 7.26 (d, *J* = 8.8 Hz, 4H), 7.06 (d, *J* = 8.8 Hz, 2H), 6.89 (d, *J* = 8.8 Hz, 4H), 4.79–4.72 (m, 2H), 1.94–1.75 (m, 12H), 1.68–1.57 (m, 4H). **^{13}C NMR** (100 MHz, $CDCl_3$) δ 156.2, 155.4, 144.1, 138.1, 132.5, 125.0, 123.8, 122.0, 116.4, 109.9, 32.9, 24.1. **HRMS** (ESI-TOF) for $C_{34}H_{35}N_4O_2^+$ $[M+H]^+$: calculated 531.2755, found 531.2751.

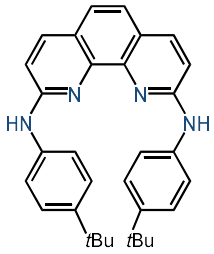

7a

$C_{32}H_{34}N_4$

M = 474.65 g/mol

***N*²,*N*⁹-bis(4-(tert-butyl)phenyl)-1,10-phenanthroline-2,9-diamine** (**7a**): Prepared from 2,9-dichloro-1,10-phenanthroline (1.00 g, 4.0 mmol) and 4-(*tert*-butyl)aniline (2.98 g, 20.0 mmol) according to **GP1**. Purification by flash column chromatography on silica gel using petroleum ether and ethyl acetate to afford **7a** as a yellow solid (1.42 g, 75% yield).

$\mathbf{R}_f$ = 0.30 (PE/EA = 7/3). **^{1}H NMR** (400 MHz, $CDCl_3$) δ 7.95 (d, J = 8.8 Hz, 2H), 7.42 (s, 2H), 7.40–7.36 (m, 4H), 7.32–7.24 (m, 8H), 1.34 (s, 18H). **^{13}C NMR** (100 MHz, $CDCl_3$) δ 155.6, 147.0, 144.6, 138.2, 137.7, 126.5, 124.2, 122.4, 121.9, 110.3, 34.6, 31.6. **HRMS** (ESI-TOF) for $C_{32}H_{35}N_4^+$ $[M+H]^+$: calculated 475.2856, found 475.2863.

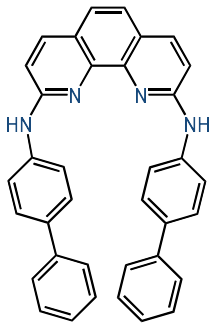

8a
$C_{36}H_{26}N_4$
M = 514.63 g/mol

***N*²,*N*⁹-di([1,1'-biphenyl]-4-yl)-1,10-phenanthroline-2,9-diamine** (**8a**): Prepared from 2,9-dichloro-1,10-phenanthroline (1.00 g, 4.0 mmol) and 4-(cyclopentyloxy)aniline (3.38 g, 20.0 mmol) according to **GP1**. Purification by flash column chromatography on silica gel using petroleum ether and ethyl acetate to afford **8a** as a yellow solid (1.65 g, 80% yield).

R*f* = 0.40 (PE/EA = 1/1). **^{1}H NMR** (800 MHz, $CDCl_3$) δ 8.03 (dd, *J* = 8.8, 3.8 Hz, 2H), 7.62–7.60 (m, 4H), 7.59–7.56 (m, 8H), 7.49 (d, *J* = 3.8 Hz, 2H), 7.42–7.39 (m, 4H), 7.33–7.30 (m, 4H), 7.25 (s, 2H). **^{13}C NMR** (200 MHz, $CDCl_3$) δ 154.6, 140.6, 139.5, 138.4, 136.4, 128.8, 128.1, 127.0, 126.8, 124.2, 122.6, 121.2, 111.3. **HRMS** (ESI-TOF) for $C_{36}H_{27}N_4^+$ $[M+H]^+$: calculated 515.2230, found 515.2237.

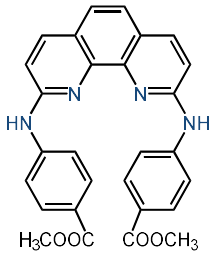

9a
$C_{28}H_{22}N_4O_4$
M = 478.51 g/mol

Dimethyl 4,4'-((1,10-phenanthroline-2,9-diyl)bis(azanediyl))dibenzoate (**9a**): Prepared from 2,9-dichloro-1,10-phenanthroline (1.00 g, 4.0 mmol) and methyl 4-aminobenzoate (3.02 g, 20.0 mmol) according to **GP1**. Purification by flash column chromatography on silica gel using petroleum ether and ethyl acetate to afford **9a** as a white solid (1.24 g, 65% yield).

$\mathbf{R}_f$ = 0.30 (PE/EA = 7/3). **^{1}H NMR** (400 MHz, DMSO-d_6) δ 9.99 (s, 2H), 8.41 (d, J = 8.8 Hz, 4H), 8.24 (d, J = 8.8 Hz, 2H), 7.76 (d, J = 8.8 Hz, 4H), 7.64 (s, 2H), 7.29 (d, J = 8.8 Hz, 2H), 3.75 (s, 6H). **^{13}C NMR** (100 MHz, DMSO-d_6) δ 165.9, 153.5, 146.1, 143.3, 137.7, 130.8, 124.1, 122.9, 120.8, 116.7, 114.6, 51.5. **HRMS** (ESI-TOF) for $C_{28}H_{23}N_4O_4^+$ $[M+H]^+$: calculated 479.1714, found 479.1719.

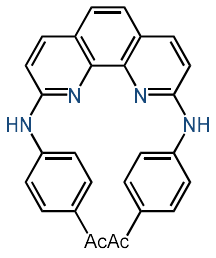

10a
$C_{28}H_{22}N_4O_2$
M = 446.51 g/mol

1,1'-(((1,10-phenanthroline-2,9-diyl)bis(azanediyl))bis(4,1-phenylene))bis(ethan-1-one) (**10a**): Prepared from 2,9-dichloro-1,10-phenanthroline (1.00 g, 4.0 mmol) and 1-(4-aminophenyl)ethan-1-one (2.70 g, 20.0 mmol) according to **GP1**. Purification by flash column chromatography on silica gel using petroleum ether and ethyl acetate to afford **10a** as a yellow solid (1.20 g, 67% yield).

$\mathbf{R_f}$ = 0.30 (PE/EA = 4/1). **^{1}H NMR** (400 MHz, DMSO-d_6) δ 10.04 (s, 2H), 8.47 (d, J = 8.6 Hz, 4H), 8.25 (d, J = 8.8 Hz, 2H), 7.80 (d, J = 8.6 Hz, 4H), 7.66 (s, 2H), 7.31 (d, J = 8.8 Hz, 2H), 2.40 (s, 6H). **^{13}C NMR** (100 MHz, DMSO-d_6) δ 196.2, 154.0, 146.7, 143.8, 138.1, 130.4, 129.4, 124.6, 123.5, 117.0, 115.2, 26.4. **HRMS** (ESI-TOF) for $C_{28}H_{23}N_4O_2^+$ $[M+H]^+$: calculated 447.1816, found 447.1840.

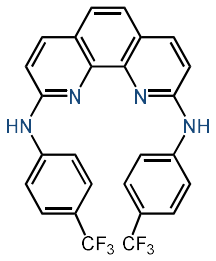

11a
$C_{26}H_{16}F_6N_4$
M = 498.43 g/mol

***N*²,*N*⁹-bis(4-(trifluoromethyl)phenyl)-1,10-phenanthroline-2,9-diamine** (**11a**): Prepared from 2,9-dichloro-1,10-phenanthroline (1.00 g, 4.0 mmol) and 4-(trifluoromethyl)aniline (3.22 g, 20.0 mmol) according to **GP1**. Purification by flash column chromatography on silica gel using petroleum ether and ethyl acetate to afford 10a as a white solid (1.53 g, 77% yield).

$\mathbf{R}_f$ = 0.30 (PE/EA = 7/3). **^{1}H NMR** (400 MHz, DMSO-d_6) δ 9.98 (s, 2H), 8.56 (d, J = 8.6 Hz, 4H), 8.20 (d, J = 8.8 Hz, 2H), 7.60 (s, 2H), 7.50 (d, J = 8.6 Hz, 4H), 7.29 (d, J = 8.8 Hz, 2H). **^{13}C NMR** (100 MHz, DMSO-d_6) δ 153.66, 145.29, 143.34, 137.63, 126.10, 126.05, 124.09, 123.40, 122.91, 120.47, 120.15, 117.06, 114.61. **HRMS** (ESI-TOF) for $C_{26}H_{17}F_6N_4^+$ $[M+H]^+$: calculated 499.1352, found 499.1373.

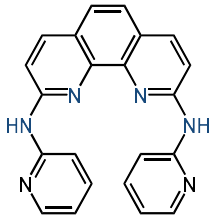

12a
$C_{22}H_{16}N_6$
M = 364.41 g/mol

***N*²,*N*⁹-di(pyridin-2-yl)-1,10-phenanthroline-2,9-diamine** (**12a**): Prepared from 2,9-dichloro-1,10-phenanthroline (1.00 g, 4.0 mmol) and pyridin-2-amine (1.88 g, 20.0 mmol) according to **GP1**. Purification by flash column chromatography on silica gel using dichloromethane and ethanol to afford **12a** as a yellow solid (0.46 g, 31% yield).

R*f* = 0.20 (DCM/EtOH = 40/1). **¹H NMR** (400 MHz, $CDCl_3$) δ 8.42–7.92 (m, 8H), 7.83 (d, *J* = 8.8 Hz, 2H), 7.64–7.50 (m, 4H), 6.91 (s, 2H). **HRMS** (ESI-TOF) for $C_{22}H_{17}N_6^+$ $[M+H]^+$: calculated 365.1509, found 365.1518.

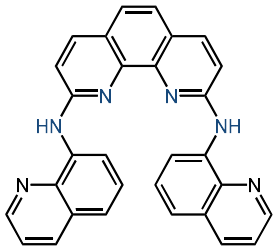

13a
$C_{30}H_{20}N_6$
M = 464.53 g/mol

***N*²,*N*⁹-di(quinolin-8-yl)-1,10-phenanthroline-2,9-diamine** (**13a**): Prepared from 2,9-dichloro-1,10-phenanthroline (1.00 g, 4.0 mmol) and quinolin-8-amine (2.88 g, 20.0 mmol) according to **GP1**. Purification by flash column chromatography on silica gel using petroleum ether and ethyl acetate to afford **13a** as a yellow solid (1.24 g, 67% yield).

R*f* = 0.30 (PE/EA = 3/7). **^{1}H NMR** (400 MHz, $CDCl_3$) δ 10.16 (dd, *J* = 7.8, 1.2 Hz, 2H), 9.72 (s, 2H), 8.88 (dd, *J* = 4.2, 1.8 Hz, 2H), 8.20 (dd, *J* = 8.2, 1.8 Hz, 2H), 8.09 (d, *J* = 8.6 Hz, 2H), 7.59 (t, *J* = 8.0 Hz, 2H), 7.55 (s, 2H), 7.48 (dd, *J* = 8.2, 4.2 Hz, 2H), 7.42 (dd, *J* = 8.2, 1.2 Hz, 2H), 7.31 (d, *J* = 8.6 Hz, 2H). **^{13}C NMR** (100 MHz, $CDCl_3$) δ 154.0, 147.6, 144.7, 138.8, 137.6, 137.4, 136.6, 129.2, 128.4, 124.6, 123.1, 121.6, 118.4, 115.1, 113.9. **HRMS** (ESI-TOF) for $C_{30}H_{21}N_6^+$ $[M+H]^+$: calculated 465.1822, found 465.1818.

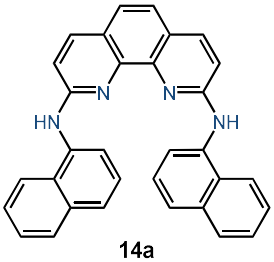

14a
$C_{32}H_{22}N_4$
M = 462.56 g/mol

***N*²,*N*⁹-di(naphthalen-1-yl)-1,10-phenanthroline-2,9-diamine** (**14a**): Prepared from 2,9-dichloro-1,10-phenanthroline (1.00 g, 4.0 mmol) and naphthalen-1-amine (2.86 g, 20.0 mmol) according to **GP1**. Purification by flash column chromatography on silica gel using petroleum ether and ethyl acetate to afford **14a** as a yellow solid (1.29 g, 70% yield).

R_f = 0.30 (PE/EA = 3/7). **^{1}H NMR** (400 MHz, $CDCl_3$) δ 8.18 (d, *J* = 8.2 Hz, 2H), 7.96–7.85 (m, 4H), 7.76 (d, *J* = 8.2 Hz, 2H), 7.57–7.45 (m, 8H), 7.42 (s, 2H), 6.94 (d, *J* = 8.8 Hz, 2H). **^{13}C NMR** (100 MHz, $CDCl_3$) δ 157.0, 144.5, 138.3, 136.3, 134.9, 130.0, 128.6, 126.6, 126.6, 126.1, 126.1, 124.3, 122.9, 122.6, 121.3, 110.9. **HRMS** (ESI-TOF) for $C_{32}H_{23}N_4^+$ $[M+H]^+$: calculated 463.1917, found 463.1920.

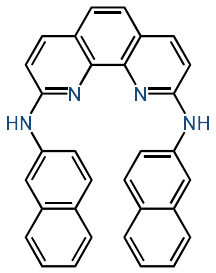

15a
$C_{32}H_{22}N_4$
M = 462.56 g/mol

***N*²,*N*⁹-di(naphthalen-2-yl)-1,10-phenanthroline-2,9-diamine** (**15a**): Prepared from 2,9-dichloro-1,10-phenanthroline (1.00 g, 4.0 mmol) and naphthalen-2-amine (2.86 g, 20.0 mmol) according to **GP1**. Purification by flash column chromatography on silica gel using petroleum ether and ethyl acetate to afford **15a** as a yellow solid (0.650 g, 35% yield).

R_f = 0.30 (PE/EA = 3/1). **^{1}H NMR** (400 MHz, DMSO-d_6) δ 9.70 (s, 2H), 8.81 (d, *J* = 2.2 Hz, 2H), 8.30 (dd, *J* = 8.8, 2.2 Hz, 2H), 8.19 (d, *J* = 8.8 Hz, 2H), 7.59 (s, 2H), 7.51 (t, *J* = 8.8 Hz, 4H), 7.30 (d, *J* = 8.8 Hz, 2H), 7.18 (d, *J* = 8.2 Hz, 2H), 7.07 (ddd, *J* = 8.2, 6.8, 1.2 Hz, 2H), 6.84 (ddd, *J* = 8.2, 6.8, 1.2 Hz, 2H). **^{13}C NMR** (100 MHz, DMSO-d_6) δ 154.09, 143.75, 139.38, 137.20, 134.00, 128.64, 128.34, 126.94, 126.86, 125.31, 123.71, 122.83, 122.39, 119.75, 114.40, 112.19. **HRMS** (ESI-TOF) for $C_{32}H_{23}N_4^+$ $[M+H]^+$: calculated 463.1917, found 463.1920.

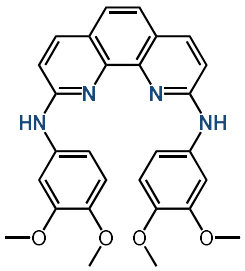

16a
$C_{28}H_{26}N_4O_4$
M = 482.54 g/mol

***N*²,*N*⁹-bis(3,4-dimethoxyphenyl)-1,10-phenanthroline-2,9-diamine** (**16a**): Prepared from 2,9-dichloro-1,10-phenanthroline (1.00 g, 4.0 mmol) and 3,4-dimethoxyaniline (3.06 g, 20.0 mmol) according to **GP1**. Purification by flash column chromatography on silica gel using petroleum ether and ethyl acetate to afford **16a** as a dark yellow solid (0.370 g, 19% yield). $\mathbf{R}_f$ = 0.20 (PE/EA = 1/1). **^{1}H NMR** (400 MHz, $CDCl_3$) δ 9.24 (s, 2H), 8.17 (dd, *J* = 8.8, 2.4 Hz, 2H), 8.06 (d, *J* = 8.8 Hz, 2H), 7.48 (s, 2H), 7.39 (d, *J* = 2.4 Hz, 2H), 7.10 (d, *J* = 8.8 Hz, 2H), 6.65 (d, *J* = 8.8 Hz, 2H), 3.66 (s, 6H), 3.64 (s, 6H). **^{13}C NMR** (100 MHz, $CDCl_3$) δ 156.1, 149.5, 146.2, 138.1, 133.5, 123.9, 122.1, 115.2, 111.8, 110.3, 107.7, 56.2, 55.9. **HRMS** (ESI-TOF) for $C_{28}H_{27}N_4O_4^+$ $[M+H]^+$: calculated 483.2027, found 483.2026.

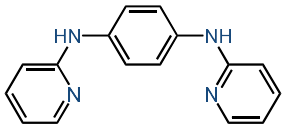

17a
$C_{16}H_{14}N_4$
M = 262.32 g/mol

***N*^{1},*N*^{4}-di(pyridin-2-yl)benzene-1,4-diamine** (**17a**): Prepared from *p*-phenylenediamine (0.430 g, 4.0 mmol) and 2-chloropyridine (1.14 g, 10.0 mmol) according to **GP2**. Purification by flash column chromatography on silica gel using petroleum ether and ethyl acetate to afford **17a** as a grey solid (0.760 g, 72% yield).

R$_f$ = 0.30 (EA). **^{1}H NMR** (400 MHz, DMSO-d_6) δ 11.12 (s, 2H), 8.05–7.96 (m, 4H), 7.53 (s, 4H), 7.32 (d, J = 8.8 Hz, 2H), 7.01 (t, J = 6.6 Hz, 2H). **^{13}C NMR** (100 MHz, DMSO-d_6) δ 152.2, 143.6, 138.0, 134.3, 125.3, 114.0, 113.3. **HRMS** (ESI-TOF) for $C_{16}H_{15}N_4^+$ $[M+H]^+$: calculated 263.1291, found 263.1292.

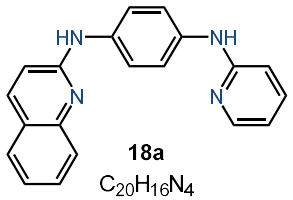

18a
$C_{20}H_{16}N_4$
M = 312.38 g/mol

***N*^{1}-(pyridin-2-yl)-*N*^{4}-(quinolin-2-yl)benzene-1,4-diamine** (**18a**): Prepared from *p*-phenylenediamine (0.430 g, 4.0 mmol), 2-chloropyridine (0.450 g, 4.0 mmol) and 2-chloroquinoline (0.650 g, 4.0 mmol) according to **GP3**. Purification by flash column chromatography on silica gel using petroleum ether and ethyl acetate to afford **18a** as a yellow solid (1.02 g, 82% yield).

R$_f$ = 0.30 (EA) **^{1}H NMR** (400 MHz, DMSO-d_6) δ 9.27 (s, 1H), 8.88 (s, 1H), 8.15–8.07 (m, 1H), 7.99 (d, J = 9.0 Hz, 1H), 7.87 (d, J = 9.0 Hz, 2H), 7.74–7.58 (m, 4H), 7.57–7.48 (m, 2H), 7.29–7.18 (m, 1H), 7.01 (d, J = 9.0 Hz, 1H), 6.82–6.74 (m, 1H), 6.71–6.62 (m, 1H). **^{13}C NMR** (100 MHz, DMSO-d_6) δ 156.2, 154.3, 147.3, 147.2, 137.0, 136.6, 135.6, 134.9, 129.3, 127.4, 126.1, 123.4, 122.2, 119.2, 118.9, 114.0, 113.6, 110.0. **HRMS** (ESI-TOF) for $C_{20}H_{17}N_4^+$ $[M+H]^+$: calculated 313.1448, found 313.1450.

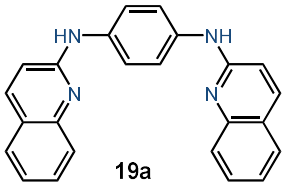

19a
$C_{24}H_{18}N_4$
M = 362.44 g/mol

***N*^{1},*N*^{4}-di(quinolin-2-yl)benzene-1,4-diamine** (**19a**): Prepared from *p*-phenylenediamine (0.430 g, 4.0 mmol) and 2-chloroquinoline (1.64 g, 10.0 mmol) according to **GP2**. Purification by flash column chromatography on silica gel using petroleum ether and ethyl acetate to afford **19a** as a yellow solid (1.19 g, 82% yield).

R$_f$ = 0.30 (EA). **^{1}H NMR** (400 MHz, Methanol-d_4) δ 8.06 (d, *J* = 9.2 Hz, 2H), 7.71–7.64 (m, 8H), 7.59–7.53 (m, 2H), 7.33–7.27 (m, 2H), 7.00 (d, *J* = 9.2 Hz, 2H). **^{13}C NMR** (100 MHz, Methanol-d_4) δ 160.4, 155.4, 141.4, 137.1, 132.3, 129.3, 125.5, 124.8, 124.0, 114.9. **HRMS** (ESI-TOF) for $C_{24}H_{19}N_4^+$ $[M+H]^+$: calculated 363.1603, found 363.1611.

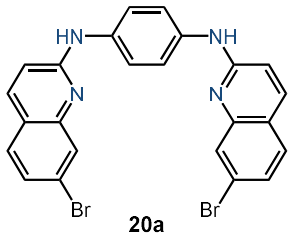

20a
$C_{24}H_{16}Br_2N_4$
M = 520.23 g/mol

***N*^{1},*N*^{4}-bis(7-bromoquinolin-2-yl)benzene-1,4-diamine** (**20a**): Prepared from *p*-phenylenediamine (0.430 g, 4.0 mmol) and 7-bromo-2-chloroquinoline (2.43 g, 10.0 mmol) according to **GP2**. Purification by flash column chromatography on silica gel using petroleum ether, dichloromethane and ethyl acetate to afford **20a** as a dark green solid (1.20 g, 58% yield). $\mathbf{R}_f$ = 0.60 (DCM/EA = 1/1). **^{1}H NMR** (400 MHz, DMSO-d_6) δ 9.51 (s, 2H), 8.03 (d, J = 9.0 Hz, 2H), 7.95 (s, 4H), 7.89 (d, J = 2.0 Hz, 2H), 7.67 (d, J = 8.6 Hz, 2H), 7.40 (dd, J = 8.6, 2.0 Hz, 2H), 7.07 (d, J = 9.0 Hz, 2H). **^{13}C NMR** (100 MHz, DMSO-d_6) δ 155.3, 148.7, 137.0, 135.7, 129.8, 128.5, 125.6, 123.0, 122.7, 119.7, 115.1. **HRMS** (ESI-TOF) for $C_{24}H_{17}N_4^+$ $[M+H]^+$: calculated 518.9814, found 518.9817.

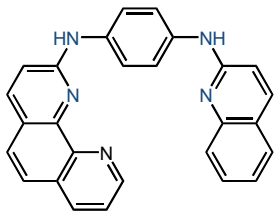

21a
$C_{27}H_{19}N_5$
M = 413.48 g/mol

***N*^{1}-(1,10-phenanthrolin-2-yl)-*N*^{4}-(quinolin-2-yl)benzene-1,4-diamine** (**21a**): repared from *p*-phenylenediamine (0.430 g, 4.0 mmol), 2-chloroquinoline (0.650 g, 4.0 mmol) and 2-chloro-1,10-phenanthroline (0.860 g, 4.0 mmol) according to **GP3**. Purification by flash column chromatography on silica gel using petroleum ether and ethyl acetate to afford **21a** as a yellow solid (1.16 g, 70% yield).

R$_f$ = 0.20 (EA). **^{1}H NMR** (400 MHz, $CDCl_3$) δ 9.13 (dd, *J* = 4.4, 1.8 Hz, 1H), 8.21 (dd, *J* = 8.2, 1.8 Hz, 1H), 8.02 (d, *J* = 8.8 Hz, 1H), 7.93 (d, *J* = 8.8 Hz, 1H), 7.79 (dd, *J* = 8.4, 1.1 Hz, 1H), 7.69–7.62 (m, 4H), 7.62–7.53 (m, 3H), 7.45–7.33 (m, 3H), 7.33–7.28 (m, 2H), 6.97 (d, *J* = 8.8 Hz, 1H), 6.94–6.83 (m, 1H). **^{13}C NMR** (100 MHz, $CDCl_3$) δ 156.2, 154.4, 149.6, 147.6, 145.1, 138.1, 137.8, 136.7, 136.0, 135.1, 129.9, 129.4, 127.5, 126.7, 126.5, 124.1, 123.6, 123.4, 123.2, 122.6, 122.1, 121.9, 111.8, 110.1. **HRMS** (ESI-TOF) for $C_{27}H_{20}N_5^+$ $[M+H]^+$: calculated 414.1713, found 414.1715.

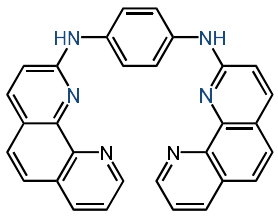

22a
$C_{30}H_{20}N_6$
M = 464.53 g/mol

***N*^{1},*N*^{4}-di(1,10-phenanthrolin-2-yl)benzene-1,4-diamine** (**22a**): Prepared from *p*-phenylenediamine (0.430 g, 4.0 mmol) and 2-chloro-1,10-phenanthroline (2.15 g, 10.0 mmol) according to **GP2**. Purification by flash column chromatography on silica gel using petroleum ether and ethyl acetate to afford **22a** as a grey solid (1.49 g, 80% yield).

R$_f$ = 0.20 (EA). **^{1}H NMR** (400 MHz, DMSO-d_6) δ 9.73–9.54 (m, 2H), 9.23–9.08 (m, 2H), 8.51–8.35 (m, 2H), 8.35–8.12 (m, 6H), 7.90–7.64 (m, 6H), 7.38–7.20 (m, 2H). **^{13}C NMR** (100 MHz, DMSO-d_6) δ 154.8, 149.4, 146.0, 145.3, 138.0, 136.0, 134.9, 129.0, 126.5, 122.6, 121.7, 119.1, 113.7. **HRMS** (ESI-TOF) for $C_{30}H_{21}N_6^+$ $[M+H]^+$: calculated 465.1822, found 465.1829.

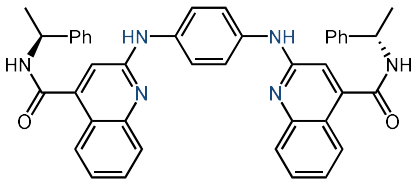

23a
$C_{42}H_{36}N_6O_2$
M = 656.29 g/mol

2,2'-(1,4-phenylenebis(azanediyl))bis(*N*-((*S*)-1-phenylethyl)quinoline-4-carboxamide) (**23a**): Prepared from *p*-phenylenediamine (0.430 g, 4.0 mmol) and (*S*)-2-chloro-*N*-(1-phenylethyl)quinoline-4-carboxamide (3.11 g, 10.0 mmol) according to **GP2**. Purification by flash column chromatography on silica gel using petroleum ether and ethyl acetate to afford **23a** as a yellow solid (1.84 g, 70% yield).

$\mathbf{R_f}$ = 0.50 (PE/EA = 4/1). **^{1}H NMR** (400 MHz, DMSO-d_6) δ 8.67 (s, 2H), 8.39 (d, J = 8.0 Hz, 2H), 7.12 (s, 4H), 6.94 (dd, J = 8.4, 1.4 Hz, 2H), 6.89 (dd, J = 8.4, 1.4 Hz, 2H), 6.75 (td, J = 8.0, 1.6 Hz, 2H), 6.66–6.59 (m, 4H), 6.55 (t, J = 7.6 Hz, 4H), 6.49–6.38 (m, 4H), 6.24 (s, 2H), 4.46–4.38 (m, 2H), 1.66 (m, 6H). **^{13}C NMR** (100 MHz, DMSO-d_6) δ 166.4, 154.0, 148.0, 145.0, 143.7, 135.8, 130.1, 128.9, 127.3, 127.1, 126.5, 125.4, 123.2, 120.5, 119.6, 112.5, 48.9, 22.9. **HRMS** (ESI-TOF) for $C_{42}H_{36}N_6O_2^+$ $[M+H]^+$: calculated 657.2973, found 657.2972.

4 Experimental Details for the Aza[5–9]helicenes

4.1 General Procedure for Synthesis of Helicenes Type 1 (GP4)

To a 15.0 mL Schlenk tube equipped with a magnetic stir bar were added the pre-prepared substrate (0.10 mmol, 1.00 equiv.), nBu$_4$NBF$_4$ (0.50 mmol, 5.00 equiv.), and HFIP (2.50 mL) in sequence. Platinum plate (10 × 15 × 1 mm^3) and graphite felt (10 × 15 × 3 mm^3) were used as the cathode and anode, respectively. Constant current electrolysis (5.0 mA) was carried out at room temperature for 2 h. After the reaction completed as monitored with TLC, the electrodes were washed with DCM (10.0 mL) and EtOH (10.0 mL), and the washings were combined with the reaction solution. The solvent was removed under reduced pressure, and the crude residue was purified by column chromatography on silica gel to afford the desired product.

4.2 General Procedure for Synthesis of Helicenes Type 2 (GP5)

For electron-deficient substrates, only HFIP afforded the product in 23% yield, while other alcohol solvents resulted in trace conversion. However, the HFIP/H$_2$O (5/1) mixed solvent supplies protons for cathodic hydrogen evolution, thereby facilitating the anodic oxidation.

To a 15.0 mL Schlenk tube equipped with a magnetic stir bar were added the pre-prepared substrate (0.10 mmol, 1.00 equiv.), nBu$_4$NBF$_4$ (0.60 mmol, 6.0 equiv.), and HFIP/H$_2$O (5/1, 3.00 mL) in sequence. Platinum plate (10 × 15 × 1 mm^3) and graphite felt (10 × 15 × 3 mm^3) were used as the cathode and anode, respectively. Constant current electrolysis (5.0 mA) was carried out at room temperature for 2 h. After the reaction completed as monitored with TLC, the electrodes were washed with DCM (10.0 mL) and EtOH (10.0 mL), and the washings were combined with the reaction solution. The solvent was removed under reduced pressure, and the crude residue was purified by column chromatography on silica gel to afford the desired product.

4.3 General Procedure for Synthesis of Helicenes Type 3 (GP6)

To a 15.0 mL Schlenk tube equipped with a magnetic stir bar were added the pre-prepared substrate (0.10 mmol, 1.00 equiv.), nBu$_4$NBF$_4$ (0.50 mmol, 5.00 equiv.), nBu$_4$NOAc (0.40 mmol, 10.0 equiv.), 1-iodo-4-methoxybenzene (0.050 mmol, 50 mol%), and HFIP (2.50 mL) in sequence. Platinum plate (10 × 15 × 1 mm^3) and graphite felt (10 × 15 × 3 mm^3) were used as the cathode and anode, respectively. Constant current electrolysis (10.0 mA) was carried out at room temperature for 2 h. After the reaction completed as monitored with TLC, the electrodes were washed with DCM (10.0 mL) and EtOH (10.0 mL), and the washings were combined with the reaction solution. The solvent was removed under reduced pressure, and the crude residue was purified by column chromatography on silica gel to afford the desired product.

4.4 Gram-Scale Experiment

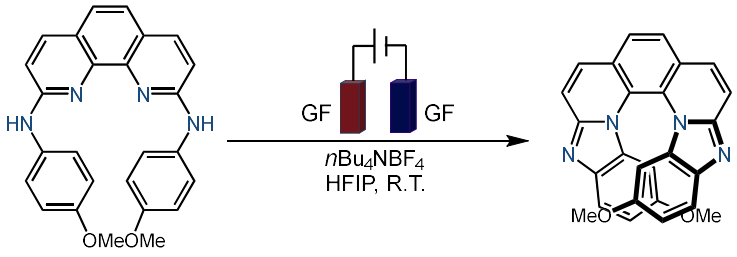

5a
2.4 mmol, 1.01 g

5
0.72 g, 73%

Given the broad substrate scope of the electrochemical oxidative C-N coupling strategy for the construction of azahelicenes, we further evaluated its practicality. Using **5a** as the model substrate, the reaction was successfully scaled up by 24-fold (2.40 mmol, 1.01 g). Notably, although a Pt plate had provided slightly higher yields during optimization, a graphite felt (GF) cathode was selected for scale-up, as both electrodes required proportional enlargement and GF allows for easier expansion to larger surface areas.

To a 100 mL Schlenk flask equipped with a magnetic stir bar were added the substrate **5a** (2.40 mmol, 1.01 g), nBu$_4$NBF$_4$ (12.0 mmol, 3.95 g), and HFIP (60.0 mL) in sequence. Graphite felts (40 × 75 × 3 mm^3) were used as the cathode and anode. Constant current electrolysis (80 mA) was carried out at room temperature for 5 h. After the reaction completed as monitored with TLC, the electrodes were washed with DCM (30.0 mL) and EtOH (30.0 mL), and the washings were combined with the reaction solution. The solvent was removed under reduced pressure.

Purification by flash column chromatography on silica gel using petroleum ether and ethyl acetate to afford **5** as a yellow solid (0.720 g, 73% yield).

4.5 Characterization Data of the Helicenes

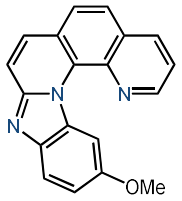

1
$C_{19}H_{13}N_3O$
M = 299.33 g/mol

12-methoxybenzo[4,5]imidazo[1,2-*a*][1,10]phenanthroline (**1**): Prepared from **1a** (30.1 mg, 0.10 mmol), nBu$_4$NBF$_4$ (165 mg, 0.50 mmol), and HFIP (2.50 mL) according to **GP4**. Purification by flash column chromatography on silica gel using petroleum ether and ethyl acetate to afford **1** as a yellow solid (23.8 mg, 80% yield).

R$_f$ = 0.30 (EA). **^{1}H NMR** (400 MHz, $CDCl_3$) δ 9.06 (dd, J = 4.2, 1.8 Hz, 1H), 8.44 (d, J = 2.6 Hz, 1H), 8.30 (dd, J = 8.2, 1.8 Hz, 1H), 7.89 (d, J = 9.0 Hz, 1H), 7.82–7.76 (m, 3H), 7.67–7.58 (m, 2H), 7.22 (dd, J = 9.0, 2.6 Hz, 1H), 3.93 (s, 3H). **^{13}C NMR** (100 MHz, $CDCl_3$) δ 153.9, 149.1, 147.0, 149.9, 139.2, 136.4, 133.8, 133.0, 128.8, 128.5, 127.2, 124.8, 124.5, 122.4, 120.0, 119.9, 115.3, 103.6, 55.9. **HRMS** (ESI-TOF) for $C_{19}H_{14}N_3O^+$ $[M+H]^+$: calculated 300.1131, found 300.1132.

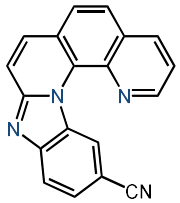

2
$C_{19}H_{10}N_4$
M = 294.32 g/mol

Benzo[4,5]imidazo[1,2-*a*][1,10]phenanthroline-12-carbonitrile (**2**): Prepared from **2a** (29.6 mg, 0.10 mmol), nBu$_4$NBF$_4$ (198 mg, 0.60 mmol), and HFIP/H_2O (5/1, 3.00 mL) according to **GP5**. Purification by flash column chromatography on silica gel using petroleum ether and ethyl acetate to afford **2** as a yellow solid (15.8 mg, 54% yield). $\mathbf{R}_f$ = 0.300 (PE/EA = 3/7). **^{1}H NMR** (400 MHz, $CDCl_3$) δ 9.61–9.53 (m, 1H), 9.18 (dd, J = 4.2, 1.8 Hz, 1H), 8.42 (dd, J = 8.4, 1.8 Hz, 1H), 8.04 (d, J = 8.4 Hz, 1H), 7.99–7.91 (m, 4H), 7.79–7.72 (m, 2H). **^{13}C NMR** (100 MHz, $CDCl_3$) δ 151.7, 148.0, 147.9, 138.9, 136.7, 133.3, 132.2, 129.9, 128.8, 127.6, 127.2, 125.9, 125.6, 124.9, 123.3, 120.7, 120.6, 119.6, 102.6. **HRMS** (ESI-TOF) for $C_{19}H_{11}N_4^+$ $[M+H]^+$: calculated 295.0978, found 295.0983.

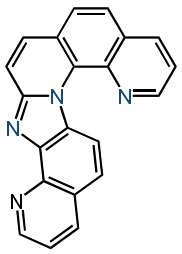

3
$C_{21}H_{12}N_4$
M = 320.36 g/mol

Quinolino[8',7':4,5]imidazo[1,2-*a*][1,10]phenanthroline (**3**): Prepared from **3a** (32.2 mg, 0.10 mmol), nBu$_4$NBF$_4$ (165 mg, 0.50 mmol), and HFIP (2.50 mL) according to **GP4**. Purification by flash column chromatography on silica gel using petroleum ether and ethyl acetate to afford **3** as a yellow solid (12.8 mg, 40% yield).

R$_f$ = 0.30 (EA). **^{1}H NMR** (400 MHz, $CDCl_3$) δ 9.16–9.08 (m, 2H), 9.03 (d, J = 9.4 Hz, 1H), 8.39 (dd, J = 8.2, 1.8 Hz, 1H), 8.35 (dd, J = 8.2, 1.8 Hz, 1H), 8.12 (d, J = 9.2 Hz, 1H), 7.98–7.91 (m, 2H), 7.84 (d, J = 9.2 Hz, 1H), 7.71–7.64 (m, 2H), 7.55 (dd, J = 8.2, 4.4 Hz, 1H). **^{13}C NMR** (100 MHz, $CDCl_3$) δ 149.6, 148.8, 147.6, 136.3, 135.7, 132.7, 132.6, 128.8, 128.3, 127.3, 126.1, 125.3, 125.0, 122.6, 121.1, 120.7, 120.4, 119.0. **HRMS** (ESI-TOF) for $C_{21}H_{13}N_4^+$ $[M+H]^+$: calculated 321.1135, found 321.1132.

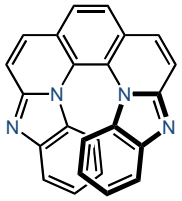

4
$C_{24}H_{14}N_4$
M = 358.40 g/mol

Benzo[4,5]imidazo[1,2-*a*]benzo[4,5]imidazo[2,1-*k*][1,10]phenanthroline (**4**): Prepared fr om **4a** (36.2 mg, 0.10 mmol), nBu$_4$NBF$_4$ (165 mg, 0.50 mmol), and HFIP (2.50 mL) according to **GP4**. Purification by flash column chromatography on silica gel using di chloromethane and methanol to afford **4** as a yellow solid (28.9 mg, 81% yield).

R$_f$ = 0.30 (DCM/MeOH = 50/1). **^{1}H NMR** (400 MHz, DMSO-d_6) δ 8.24–8.16 (m, 4H), 7.99 (d, J = 9.4 Hz, 2H), 7.72 (d, J = 8.4 Hz, 2H), 7.10 (ddd, J = 8.2, 7.2, 1.2 Hz, 2H), 6.50 (ddd, J = 8.2, 7.2, 1.2 Hz, 2H), 5.88 (d, J = 8.4 Hz, 2H). **^{13}C NMR** (100 MHz, DMSO-d_6) δ 147.6, 142.7, 132.3, 130.3, 125.5, 125.1, 124.1, 121.5, 120.8, 119.3, 118.8, 112.2. **HRMS** (ESI-TOF) for $C_{24}H_{15}N_4^+$ $[M+H]^+$: calculated 359.1291, found 359.1296.

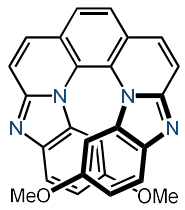

5
$C_{26}H_{18}N_4O_2$
M = 418.46 g/mol

10,15-dimethoxybenzo[4,5]imidazo[1,2-*a*]benzo[4,5]imidazo[2,1-*k*][1,10]phenanthroline (**5**): Prepared from **5a** (42.2 mg, 0.10 mmol), nBu$_4$NBF$_4$ (165 mg, 0.50 mmol), and HFIP (2.50 mL) according to **GP4**. Purification by flash column chromatography on silica gel using dichloromethane and methanol to afford **5** as a yellow solid (35.4 mg, 85% yield).

R$_f$ = 0.30 (DCM/MeOH = 40/1). **^{1}H NMR** (400 MHz, $CDCl_3$) δ 7.93 (s, 2H), 7.87 (d, J = 9.4 Hz, 2H), 7.81 (d, J = 9.4 Hz, 2H), 7.69 (d, J = 9.0 Hz, 2H), 6.82 (dd, J = 9.0, 2.4 Hz, 2H), 5.35 (d, J = 2.4 Hz, 2H), 3.16 (s, 6H). **^{13}C NMR** (100 MHz, DMSO-d_6) δ 153.9, 147.2, 137.0, 133.0, 129.1, 125.5, 125.0, 121.4, 119.7, 118.7, 115.0, 94.7, 54.4. **HRMS** (ESI-TOF) for $C_{26}H_{19}N_4O_2^+$ $[M+H]^+$: calculated 419.1503, found 419.1538.

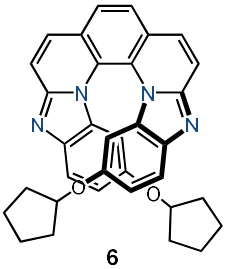

6
$C_{34}H_{30}N_4O_2$
M = 526.64 g/mol

10,15-bis(cyclopentyloxy)benzo[4,5]imidazo[1,2-a]benzo[4,5]imidazo[2,1-k][1,10]phenanthroline (**6**): Prepared from **6a** (53.1 mg, 0.10 mmol), *n*Bu_4NBF_4 (165 mg, 0.50 mmol), and HFIP (2.50 mL) according to **GP4**. Purification by flash column chromatography on silica gel using petroleum ether and ethyl acetate to afford **6** as a yellow solid (42.1 mg, 80% yield).

$\mathbf{R_f}$ = 0.30 (PE/EA = 1/1). **^{1}H NMR** (400 MHz, $CDCl_3$) δ 7.89 (s, 2H), 7.85 (d, *J* = 9.4 Hz, 2H), 7.78 (d, *J* = 9.4 Hz, 2H), 7.68 (d, *J* = 9.0 Hz, 2H), 6.81 (dd, *J* = 9.0, 2.4 Hz, 2H), 5.54 (d, *J* = 2.4 Hz, 2H), 3.90 (m, 2H), 1.71–1.45 (m, 16H). **^{13}C NMR** (100 MHz, $CDCl_3$) δ 153.8, 147.5, 137.6, 133.5, 128.6, 125.8, 124.5, 122.2, 120.3, 119.0, 117.0, 98.2, 80.6, 32.9, 32.5, 24.0, 23.9. **HRMS** (ESI-TOF) for $C_{34}H_{31}N_4O_2^+$ $[M+H]^+$: calculated 527.2442, found 527.2440.

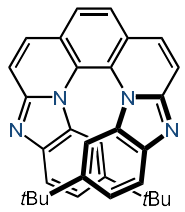

7
$C_{32}H_{30}N_4$
M = 470.62 g/mol

10,15-di-*tert*-butylbenzo[4,5]imidazo[1,2-*a*]benzo[4,5]imidazo[2,1-*k*][1,10]phenanthroline (**7**): Prepared from **7a** (47.5 mg, 0.10 mmol), nBu$_4$NBF$_4$ (165 mg, 0.50 mmol), and HFIP (2.50 mL) according to **GP4**. Purification by flash column chromatography on silica gel using petroleum ether and ethyl acetate to afford **7** as a yellow solid (30.0 mg, 64% yield).

R$_f$ = 0.30 (EA). **^{1}H NMR** (400 MHz, $CDCl_3$) δ 7.96–7.88 (m, 4H), 7.85 (d, J = 9.4 Hz, 2H), 7.73 (d, J = 8.8 Hz, 2H), 7.23 (dd, J = 8.8, 1.8 Hz, 2H), 5.95 (d, J = 1.8 Hz, 2H), 0.84 (s, 18H). **^{13}C NMR** (100 MHz, $CDCl_3$) δ 148.1, 145.2, 141.1, 132.9, 129.4, 126.0, 124.8, 123.4, 122.7, 119.5, 119.3, 108.9, 34.8, 31.1. **HRMS** (ESI-TOF) for $C_{32}H_{31}N_4^+$ $[M+H]^+$: calculated 471.2543, found 471.2567.

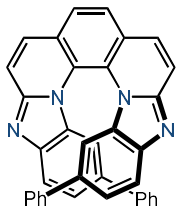

8
$C_{36}H_{22}N_4$
M = 510.60 g/mol

10,15-diphenylbenzo[4,5]imidazo[1,2-a]benzo[4,5]imidazo[2,1-k][1,10]phenanthroline (**8**): Prepared from **8a** (51.5 mg, 0.10 mmol), *n*Bu_4NBF_4 (165 mg, 0.50 mmol), and H FIP (2.50 mL) according to **GP4**. Purification by flash column chromatography on sili ca gel using petroleum ether and ethyl acetate to afford **8** as a yellow solid (31.1 mg, 60% yield).

$\mathbf{R_f}$ = 0.50 (EA). **^{1}H NMR** (800 MHz, $CDCl_3$) δ 7.99 (d, *J* = 9.2 Hz, 2H), 7.97 (s, 2H), 7.92 (d, *J* = 9.2 Hz, 4H), 7.39 (d, *J* = 8.0 Hz, 2H), 7.36 (t, *J* = 7.2 Hz, 4H), 7.24 (d, *J* = 7.2 Hz, 2H), 6.92 (d, *J* = 8.0 Hz, 4H), 6.19 (s, 2H). **^{13}C NMR** (200 MHz, $CDCl_3$) δ 148.5, 142.7, 141.0, 135.2, 133.2, 129.8, 128.6, 127.5, 126.9, 126.0, 125.0, 124.9, 122.4, 120.1, 119.4, 111.1. **HRMS** (ESI-TOF) for $C_{36}H_{23}N_4^+$ $[M+H]^+$: calculated 511.1917, found 511.1919.

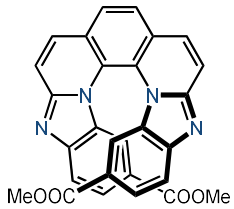

9
$C_{28}H_{18}N_4O_4$
M = 474.48 g/mol

Dimethyl benzo[4,5]imidazo[1,2-*a*]benzo[4,5]imidazo[2,1-*k*][1,10]phenanthroline-10,15-dicarboxylate (**9**): Prepared from **9a** (47.9 mg, 0.10 mmol), nBu$_4$NBF$_4$ (198 mg, 0.60 mmol), and HFIP/H_2O (5/1, 3.00 mL) according to **GP5**. Purification by flash column chromatography on silica gel using petroleum ether and ethyl acetate to afford **9** as a yellow solid (29.3 mg, 62% yield).

R$_f$ = 0.30 (EA). **^{1}H NMR** (400 MHz, $CDCl_3$) δ 8.07–8.01 (m, 6H), 7.84–7.79 (m, 4H), 6.64–6.59 (m, 2H), 3.73 (s, 6H). **^{13}C NMR** (100 MHz, $CDCl_3$) δ 166.3, 146.7, 145.9, 131.3, 126.4, 126.0, 122.8, 122.6, 119.7, 119.6, 115.3, 52.2. **HRMS** (ESI-TOF) for $C_{28}H_{19}N_4O_4^+$ $[M+H]^+$: calculated 475.1401, found 475.1400.

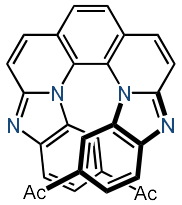

10
$C_{28}H_{18}N_4O_2$
M =442.48 g/mol

1,1'-(benzo[4,5]imidazo[1,2-a]benzo[4,5]imidazo[2,1-k][1,10]phenanthroline-10,15-diyl)bis(ethan-1-one) (**10**): Prepared from **10a** (44.7 mg, 0.10 mmol), *n*Bu_4NBF_4 (198 mg, 0.60 mmol), and HFIP/H_2O (5/1, 3.00 mL) according to **GP5**. Purification by flash co lumn chromatography on silica gel using ethyl acetate and methanol to afford **10** as a yellow solid 15.6 mg, 35% yield).

$\mathbf{R_f}$ = 0.15 (EA). **^{1}H NMR** (400 MHz, $CDCl_3$) δ 8.11–8.03 (m, 6H), 7.89–7.80 (m, 4H), 6.55 (s, 2H), 2.11 (s, 6H). **^{13}C NMR** (100 MHz, $CDCl_3$) δ 196.2, 150.1, 146.5, 132.1, 131.4, 130.3, 126.3, 125.7, 124.8, 122.3, 119.8, 119.5, 114.2, 26.0. **HRMS** (ESI-TOF) for $C_{28}H_{19}N_4O_2^+$ $[M+H]^+$: calculated 443.1503, found 443.1499.

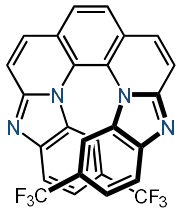

11
$C_{26}H_{12}F_6N_4$
M = 494.40 g/mol

10,15-bis(trifluoromethyl)benzo[4,5]imidazo[1,2-*a*]benzo[4,5]imidazo[2,1-*k*][1,10]phenanthroline (**11**): Prepared from **11a** (49.8 mg, 0.10 mmol), nBu$_4$NBF$_4$ (198 mg, 0.60 mmol), and HFIP/H_2O (5/1, 3.00 mL) according to **GP5**. Purification by flash column chromatography on silica gel using petroleum ether and ethyl acetate to afford **11** as a yellow solid 34.4 mg, 70% yield).

R$_f$ = 0.30 (EA). **^{1}H NMR** (400 MHz, DMSO-d_6) δ 8.37 (d, J = 9.4 Hz, 2H), 8.35 (s, 2H), 8.11 (d, J = 9.4 Hz, 2H), 7.89 (d, J = 8.6 Hz, 2H), 7.39 (d, J = 8.6 Hz, 2H), 6.10 (s, 2H). **^{13}C NMR** (100 MHz, $CDCl_3$) δ 149.55, 145.22, 131.62, 131.15, 126.16, 125.71, 125.64, 125.27, 125.05, 124.80, 123.37, 123.05, 122.23, 122.11, 121.39, 121.36, 120.68, 119.43, 110.13, 110.09. **HRMS** (ESI-TOF) for $C_{26}H_{13}F_6N_4^+$ $[M+H]^+$: calculated 495.1039, found 495.1062.

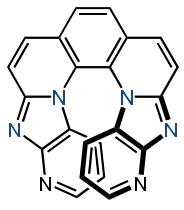

12

$C_{22}H_{12}N_6$

M =360.38 g/mol

Pyrido[2',3':4,5]imidazo[1,2-a]pyrido[2',3':4,5]imidazo[2,1-k][1,10]phenanthroline (**12**): Prepared from **12a** (36.4 mg, 0.10 mmol), *n*Bu$_4$NBF$_4$ (165 mg, 0.50 mmol), *n*Bu$_4$NOAc (0.40 mmol, 10.0 equiv.), 1-iodo-4-methoxybenzene (0.050 mmol, 50 mol%), and HFIP (2.50 mL) according to **GP6**. Purification by flash column chromatography on silica gel using ethyl acetate and methanol to afford **12** as a yellow solid (20.1 mg, 56% yield).

R$_f$ = 0.20 (EA). **^{1}H NMR** (400 MHz, DMSO-d_6) δ 8.44–8.33 (m, 6H), 8.15 (d, J = 9.4 Hz, 2H), 6.55 (dd, J = 8.4, 4.6 Hz, 2H), 6.30 (dd, J = 8.4, 1.6 Hz, 2H). HRMS (ESI-TOF) for C22H13N6+ [M+H]+: calculated 361.1196, found 361.1197.

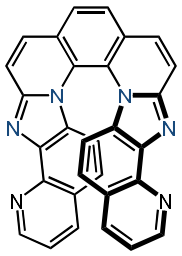

13
$C_{30}H_{16}N_6$
M = 460.50 g/mol

Quinolino[8',7':4,5]imidazo[1,2-*a*]quinolino[8',7':4,5]imidazo[2,1-*k*][1,10]phenanthroline (**13**): Prepared from **13a** (46.5 mg, 0.10 mmol), *n*Bu_4NBF_4 (165 mg, 0.50 mmol), and HFIP (2.50 mL) according to **GP4**. Purification by flash column chromatography on silica gel using ethyl acetate and methanol to afford **13** as a yellow solid (27.4 mg, 60% yield).

$\mathbf{R_f}$ = 0.20 (EA). **^{1}H NMR** (400 MHz, $CDCl_3$) δ 9.04 (dd, *J* = 4.4, 1.8 Hz, 2H), 8.20 (d, *J* = 9.4 Hz, 2H), 8.08 (s, 2H), 8.00 (d, *J* = 9.4 Hz, 2H), 7.89 (dd, *J* = 8.2, 1.8 Hz, 2H), 7.37 (dd, *J* = 8.2, 4.4 Hz, 2H), 6.79 (d, *J* = 9.0 Hz, 2H), 6.16 (d, *J* = 9.0 Hz, 2H). **^{13}C NMR** (100 MHz, $CDCl_3$) δ 150.1, 147.4, 141.6, 140.1, 136.0, 132.2, 128.6, 126.1, 125.5, 125.4, 122.1, 121.5, 121.1, 119.7, 112.9. **HRMS** (ESI-TOF) for $C_{30}H_{17}N_6^+$ $[M+H]^+$: calculated 461.1509, found 461.1506.

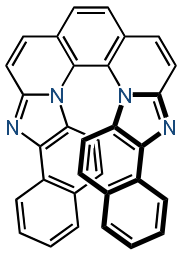

14
$C_{32}H_{18}N_4$
M = 458.52 g/mol

Naphtho[1',2':4,5]imidazo[1,2-*a*]naphtho[1',2':4,5]imidazo[2,1-*k*][1,10]phenanthroline (**14**): Prepared from **14a** (46.3 mg, 0.10 mmol), nBu$_4$NBF$_4$ (165 mg, 0.50 mmol), and HFIP (2.50 mL) according to **GP4**. Purification by flash column chromatography on si lica gel using ethyl acetate and methanol to afford **14** as a yellow solid (15.9 mg, 3 5% yield).

R$_f$ = 0.30 (EA). **^{1}H NMR** (400 MHz, DMSO-d_6) δ 8.68 (d, J = 8.2 Hz, 2H), 8.30 (s, 2H), 8.27–8.17 (m, 4H), 7.68–7.58 (m, 4H), 7.45–7.38 (m, 2H), 6.88 (d, J = 9.2 Hz, 2H), 6.04 (d, J = 9.2 Hz, 2H). **^{13}C NMR** (100 MHz, DMSO-d_6) δ 146.7, 139.4, 130.1, 129.2, 128.7, 128.0, 126.3, 125.7, 125.7, 125.6, 125.5, 122.3, 121.4, 121.2, 118.8, 112.2. **HRMS** (ESI-TOF) for $C_{32}H_{19}N_4^+$ $[M+H]^+$: calculated 459.1604, found 459.1616.

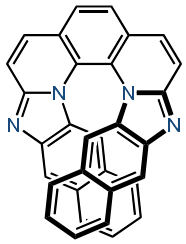

15
$C_{32}H_{18}N_4$
M = 458.52 g/mol

Naphtho[2',3':4,5]imidazo[1,2-*a*]naphtho[2',3':4,5]imidazo[2,1-*k*][1,10]phenanthroline (**15**): Prepared from **15a** (46.3 mg, 0.10 mmol), nBu$_4$NBF$_4$ (165 mg, 0.50 mmol), and HFIP (2.50 mL) according to **GP4**. Purification by flash column chromatography on si lica gel using petroleum ether and ethyl acetate to afford **15** as a yellow solid (16.9 mg, 37% yield).

R$_f$ = 0.20 (PE/EA = 30/70). **^{1}H NMR** (400 MHz, $CDCl_3$) δ 8.21 (s, 2H), 8.12 (d, J = 9.2 Hz, 2H), 8.02 (d, J = 9.2 Hz, 2H), 7.53 (d, J = 8.2 Hz, 2H), 7.29 (s, 4H), 7.20 (ddd, J = 8.2, 7.0, 1.2 Hz, 2H), 6.76 (ddd, J = 8.2, 7.0, 1.2 Hz, 2H), 5.92 (d, J = 8.2 Hz, 2H). **^{13}C NMR** (100 MHz, $CDCl_3$) δ 147.6, 141.3, 128.4, 128.0, 128.0, 127.4, 126.4, 126.1, 125.4, 125.0, 124.9, 123.8, 122.7, 117.7, 117.4, 116.9. **HRMS** (ESI-TOF) for $C_{32}H_{19}N_4^+$ $[M+H]^+$: calculated 459.1604, found 459.1618.

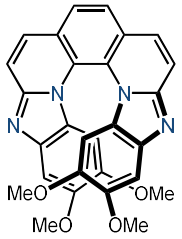

16

$C_{28}H_{22}N_4O_4$

M =478.51 g/mol

9,10,15,16-tetramethoxybenzo[4,5]imidazo[1,2-a]benzo[4,5]imidazo[2,1-k][1,10]phenanthroline (**16**): Prepared from **16a** (48.3 mg, 0.10 mmol), *n*Bu_4NBF_4 (165 mg, 0.50 mmol), and HFIP (2.50 mL) according to **GP4**. Purification by flash column chromatography on silica gel using petroleum ether and ethyl acetate to afford **16** as a green solid (20.1 mg, 42% yield).

$\mathbf{R_f}$ = 0.30 (EA). **^{1}H NMR** (400 MHz, DMSO-d_6) δ 8.19 (s, 2H), 8.09 (d, J = 9.4 Hz, 2H), 7.97 (d, J = 9.4 Hz, 2H), 7.27 (s, 2H), 5.39 (s, 2H), 3.74 (s, 6H), 3.06 (s, 6H). **^{13}C NMR** (100 MHz, $CDCl_3$) δ 148.5, 147.1, 145.7, 137.4, 127.5, 127.1, 125.6, 124.5, 121.8, 118.5, 100.2, 95.0, 55.9, 55.6. **HRMS** (ESI-TOF) for $C_{28}H_{23}N_4O_4^+$ $[M+H]^+$: calculated 479.1714, found 479.1710.

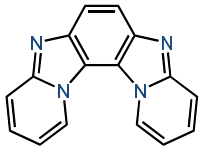

17
$C_{16}H_{10}N_4$
M = 258.28 g/mol

Pyrido[2''',1''':2'',3'']imidazo[4'',5'':3',4']benzo[1',2':4,5]imidazo[1,2-*a*]pyridine (**17**): Prepared from **17a** (26.2 mg, 0.10 mmol), nBu$_4$NBF$_4$ (165 mg, 0.50 mmol), and HFIP (2.50 mL) according to **GP4**. Purification by flash column chromatography on silica gel using petroleum ether and ethyl acetate to afford **17** as a green solid (19.0 mg, 74% yield).

R$_f$ = 0.40 (EA). **^{1}H NMR** (400 MHz, $CDCl_3$) δ 9.02 (d, J = 7.0 Hz, 2H), 8.11–8.05 (m, 2H), 7.84 (d, J = 9.2 Hz, 2H), 7.49–7.39 (m, 2H), 7.09–6.97 (m, 2H). **^{13}C NMR** (100 MHz, $CDCl_3$) δ 147.0, 141.6, 127.3, 126.8, 119.2, 119.1, 111.5. **HRMS** (ESI-TOF) for $C_{16}H_{11}N_4^+$ $[M+H]^+$: calculated 259.0978, found 259.0978.

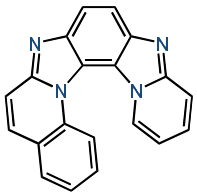

18
$C_{20}H_{12}N_4$
M = 308.34 g/mol

Pyrido[2''',1''':2'',3'']imidazo[4'',5'':3',4']benzo[1',2':4,5]imidazo[1,2-*a*]quinoline (**18**): Prepared from **18a** (26.2 mg, 0.10 mmol), nBu$_4$NBF$_4$ (165 mg, 0.50 mmol), and HFIP (2.50 mL) according to **GP4**. Purification by flash column chromatography on silica gel using petroleum ether and ethyl acetate to afford **18** as a brown solid (21.2 mg, 69% yield).

R$_f$ = 0.30 (EA). **^{1}H NMR** (400 MHz, $CDCl_3$) δ 8.31 (d, J = 7.2 Hz, 1H), 8.13–8.06 (m, 2H), 7.88–7.75 (m, 3H), 7.68–7.59 (m, 2H), 7.58–7.52 (m, 1H), 7.52–7.46 (m, 1H), 7.43–7.37 (m, 1H), 6.77–6.72 (m, 1H). **^{13}C NMR** (100 MHz, $CDCl_3$) δ 147.5, 147.1, 143.0, 141.4, 135.1, 131.7, 129.6, 128.7, 127.7, 127.2, 124.9, 124.6, 119.5, 119.1, 118.3, 118.2, 118.0, 116.4, 116.1, 109.5. **HRMS** (ESI-TOF) for $C_{20}H_{13}N_4^+$ $[M+H]^+$: calculated 309.1135, found 309.1131.

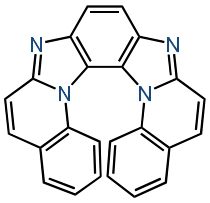

19
$C_{24}H_{14}N_4$
M = 358.40 g/mol

Quinolino[2''',1''':2'',3'']imidazo[4'',5'':3',4']benzo[1',2':4,5]imidazo[1,2-*a*]quinoline (**19**): Prepared from **19a** (36.2 mg, 0.10 mmol), *n*Bu_4NBF_4 (165 mg, 0.50 mmol), and HFIP (2.50 mL) according to **GP4**. Purification by flash column chromatography on silica gel using petroleum ether and ethyl acetate to afford **19** as a brown solid (25.1 mg, 71% yield).

$\mathbf{R_f}$ = 0.20 (EA). **^{1}H NMR** (400 MHz, $CDCl_3$) δ 8.15 (s, 2H), 7.74–7.66 (m, 6H), 7.37 (d, *J* = 8.4 Hz, 2H), 7.19–7.12 (m, 2H), 6.72–6.64 (m, 2H). **^{13}C NMR** (100 MHz, $CDCl_3$) δ 147.6, 143.0, 136.3, 130.4, 128.1, 126.8, 124.6, 123.4, 119.3, 118.5, 117.8, 117.5. **HRMS** (ESI-TOF) for $C_{24}H_{15}N_4^+$ $[M+H]^+$: calculated 359.1291, found 359.1292.

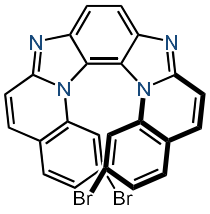

20

$C_{24}H_{12}Br_2N_4$

M = 516.20 g/mol

2,15-Dibromoquinolino[2’’’,1’’’:2’’,3’’]imidazo[4’’,5’’:3’,4’]benzo[1’,2’:4,5]imidazo[1,2-a]quinoline (**20**): Prepared from **20a** (52.0 mg, 0.10 mmol), *n*Bu_4NBF_4 (165 mg, 0.50 mmol), and HFIP (2.50 mL) according to **GP4**. Purification by flash column chromato graphy on silica gel using ethyl acetate and methanol to afford **20** as a green solid (2 6.5 mg, 55% yield).

$\mathbf{R_f}$ = 0.20 (EA). **^{1}H NMR** (400 MHz, DMSO-d_6) δ 8.13 (s, 2H), 8.06 (d, J = 9.4 Hz, 2H), 7.97 (d, J = 8.4 Hz, 2H), 7.86 (d, J = 9.4 Hz, 2H), 7.55 (d, J = 8.4 Hz, 2H), 7.48 (s, 2H). **^{13}C NMR** (100 MHz, $CDCl_3$). δ 147.1, 143.0, 136.1, 129.6, 129.4, 127.8, 122.5, 122.3, 121.1, 118.8, 118.0, 116.8. **HRMS** (ESI-TOF) for $C_{24}H_{13}Br_2N_4^+$ $[M+H]^+$: calculated 514.9501, found 514.9500.

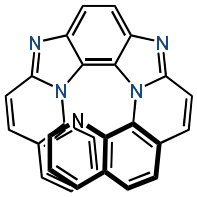

21
$C_{27}H_{15}N_5$
M = 409.45 g/mol

Quinolino[2''',1''':2'',3'']imidazo[4'',5'':3',4']benzo[1',2':4,5]imidazo[1,2-a][1,10]phenanthroline (**21**): Prepared from **21a** (36.2 mg, 0.10 mmol), *n*Bu_4NBF_4 (165 mg, 0.50 mmol), and HFIP (2.50 mL) according to **GP4**. Purification by flash column chromatography on silica gel using ethyl acetate and methanol to afford **21** as a brown solid (26.5 mg, 65% yield).

$\mathbf{R_f}$ = 0.20 (EA). **^{1}H NMR** (400 MHz, $CDCl_3$) δ 8.36–8.24 (m, 2H), 8.09 (d, *J* = 9.2 Hz, 1H), 7.96 (dd, *J* = 8.4, 2.8 Hz, 2H), 7.82–7.64 (m, 4H), 7.51 (d, *J* = 9.2 Hz, 1H), 7.39 (dd, *J* = 7.6, 1.4 Hz, 1H), 6.95–6.80 (m, 3H), 6.33 (m, 1H). **^{13}C NMR** (100 MHz, $CDCl_3$) δ 146.9, 141.5, 134.4, 134.3, 129.0, 128.5, 127.1, 126.5, 125.7, 125.2, 124.3, 123.5, 123.3, 122.8, 121.6, 120.4, 119.1, 118.9, 118.0, 117.7, 117.6. **HRMS** (ESI-TOF) for $C_{27}H_{16}N_5^+$ $[M+H]^+$: calculated 410.1400, found 410.1397.

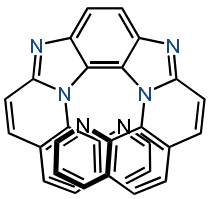

22
$C_{30}H_{16}N_6$
M = 460.50 g/mol

Phenanthoro[2''',1''':2'',3'']imidazo[4'',5'':3',4']benzo[1',2':4,5]imidazo[1,2-*a*]phenanthoroline (**22**): Prepared from **22a** (36.2 mg, 0.10 mmol), nBu$_4$NBF$_4$ (165 mg, 0.50 mmol), and HFIP (2.50 mL) according to **GP4**. Purification by flash column chromatography on silica gel using ethyl acetate and methanol to afford **22** as a brown solid (31.1 mg, 68% yield).

R$_f$ = 0.20 (EA). **^{1}H NMR** (400 MHz, $CDCl_3$) δ 8.38 (s, 2H), 7.97 (d, J = 9.2 Hz, 2H), 7.62 (dd, J = 8.2, 1.8 Hz, 2H), 7.58 (d, J = 9.2 Hz, 2H), 7.45 (dd, J = 4.2, 1.8 Hz, 2H), 7.40 (d, J = 8.4 Hz, 2H), 7.26 (d, J = 8.4 Hz, 2H), 6.77 (dd, J = 8.2, 4.2 Hz, 2H). **^{13}C NMR** (100 MHz, $CDCl_3$) δ 146.2, 142.1, 140.2, 134.2, 133.1, 127.7, 125.7, 125.4, 123.3, 123.1, 121.8, 119.2, 118.2. **HRMS** (ESI-TOF) for $C_{30}H_{17}N_6^+$ $[M+H]^+$: calculated 461.1509, found 461.1539.

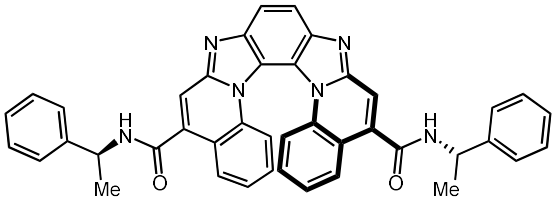

23

$C_{42}H_{32}N_6O_2$

M =652.76 g/mol

5,12-Di(N-((S)-1-phenylethyl)quinolino[2’’’,1’’’:2’’,3’’]imidazo[4’’,5’’:3’,4’]benzo[1’,2’:4,5]imidazo[1,2-a]quinoline (**23**): Prepared from **23a** (65.6 mg, 0.10 mmol), *n*Bu_4NBF_4 (165 mg, 0.50 mmol), and HFIP (2.50 mL) according to **GP4**. Purification by flash column chromatography on silica gel using petroleum ether and ethyl acetate to afford **23** as a brown solid (50.6 mg, 78% yield, dr = 1:1).

$\mathbf{R_f}$ = 0.40 (EA). **^{1}H NMR** (400 MHz, $CDCl_3$) δ 7.94 (d, *J* = 8.2 Hz, 2H), 7.83 (d, *J* = 8.2 Hz, 2H), 7.77–7.64 (m, 8H), 7.60–7.50 (m, 12H), 7.44–7.31 (m, 12H), 6.94 (t, *J* = 7.6 Hz, 2H), 6.88 (t, *J* = 7.6 Hz, 2H), 6.74 (d, *J* = 8.2 Hz, 2H), 6.69 (d, *J* = 8.2 Hz, 2H), 6.23 (t, *J* = 7.6 Hz, 2H), 6.16 (t, *J* = 7.6 Hz, 2H), 5.54–5.44 (m, 4H), 1.82–1.74 (m, 12H). **^{13}C NMR** (100 MHz, $CDCl_3$) δ 166.15, 166.09, 145.35, 142.87, 142.85, 142.82, 136.68, 136.66, 135.13, 135.04, 128.95, 128.91, 127.75, 126.84, 126.69, 126.43, 126.34, 126.31, 126.21, 124.98, 124.91, 120.01, 119.97, 118.74, 118.67, 118.33, 118.30, 116.75, 115.72, 115.65, 49.74, 49.67, 22.03, 21.95. **HRMS** (ESI-TOF) for $C_{42}H_{33}N_6O_2^+$ $[M+H]^+$: calculated 653.2660, found 653.2658.

5 Mechanistic Studies

5.1 Cyclic Voltammetry (CV) Experiments

Cyclic voltammograms were measured using a CHI 760E bipotentiostat equipped with electrochemical analysis software. A reaction was set up using general procedure with three electrodes: a steady-state glassy carbon electrode as working electrode, an Ag/AgCl (3.0 M KCl aq.) as reference electrode, and a platinum wire counter as electrode. The electrodes were polished with 0.05 μm aluminum oxide, ultrasonically rinsed with ethanol and ultrapure water before measurements. The solvent was deoxygenated by nitrogen bubbling for 0.5 h. The CV plotting convention was IUPAC. The starting point was 0.0 V.

5.2 Cyclic voltammetry (CV) experiments of substrate 5a

Cyclic voltammetry (CV) of the electron-rich substituted helicene **5a** and blank were performed in acetonitrile containing nBu$_4$NPF$_6$ (0.100 M, 10.0 mL) as the supporting electrolyte. A glassy carbon working electrode, a Pt wire counter electrode, and an Ag/AgCl (3.0 M KCl aq.) reference electrode were employed. The potential was scanned from 0.0 to 3.0 V at a sweep rate of 50 mV s^{-1}.

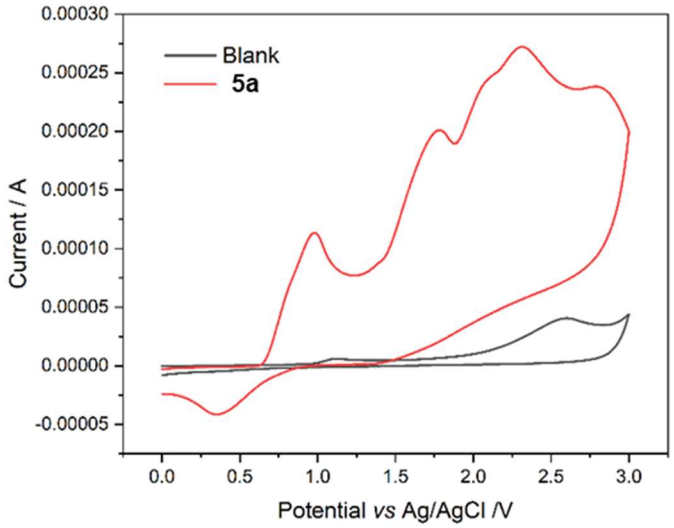

Figure S1. CV curves of blank and **5a**

5.3 Cyclic Voltammetry (CV) Experiments of Substrate 11a

Cyclic voltammetry (CV) of the electron-deficient substituted helicene **11a** and blank were performed in acetonitrile containing nBu$_4$NPF$_6$ (0.100 M, 100 mL) as the supporting electrolyte. A glassy carbon working electrode, a Pt wire counter electrode, and an Ag/AgCl (3.0 M KCl aq.) reference electrode were employed. The potential was scanned from 0.0 to 3.0 V at a sweep rate of 50 mV s^{-1}.

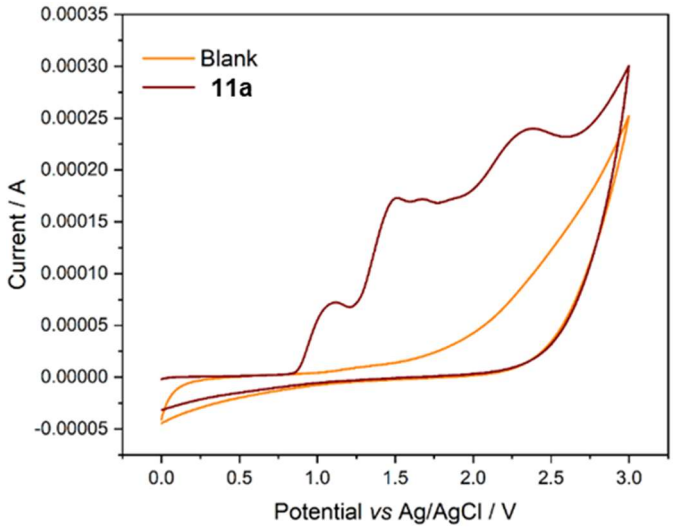

Figure S2. CV curves of blank and **11a**

The oxidation potential of **5a** (electron-rich) is lower than that of **11a** (electron-deficient), consistent with the substituent electronic effects. Multiple oxidation peaks were observed for **5a**, indicating a multistep electron-transfer process during oxidation.

5.4 Radical Probe Experiments.

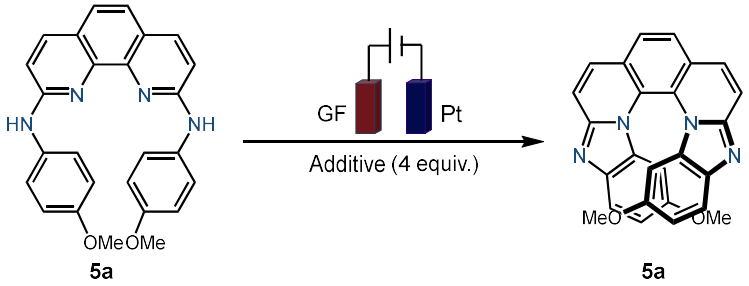

Additive	5
BHT	33%
TEMPO	35%

Figure S3. Radical probe experiments

A platinum plate (10 × 15 × 1 mm^3) and graphite felt (10 × 15 × 3 mm^3) were used as cathode and anode, respectively. To a 15.0 mL Schlenk tube equipped with a magnetic stir bar were added substrate **5a** (0.10 mmol, 1.00 equiv.), $n$$Bu_4NPF_6$ (0.50 mmol, 5.00 equiv.) and the radical inhibition reagent (0.40 mmol, 4.00 equiv.) in HFIP (2.50 mL).

The mixture was stirred and electrolyzed with a constant current of 5.0 mA at room temperature. After the reaction was completed as monitored with TLC, the electrodes were washed with DCM (10.0 mL) and EtOH (10.0 mL), and the washings were combined with the reaction solution. 1,3,5-trimethoxybenzene (0.20 mmol, 2.00 equiv.) was then added as an internal standard for yield determination by ^{1}H NMR. The solvent was removed under reduced pressure, and the residue was dissolved in DMSO-d_6 (0.50 mL) for ^{1}H NMR analysis.

Radical inhibition experiments were conducted by adding 4.00 equiv of BHT or TEMPO under the standard conditions. The yields decreased to 33% and 35%, respectively (vs. control), indicating the involvement of a radical pathway.

5.5 Proposed Mechanism

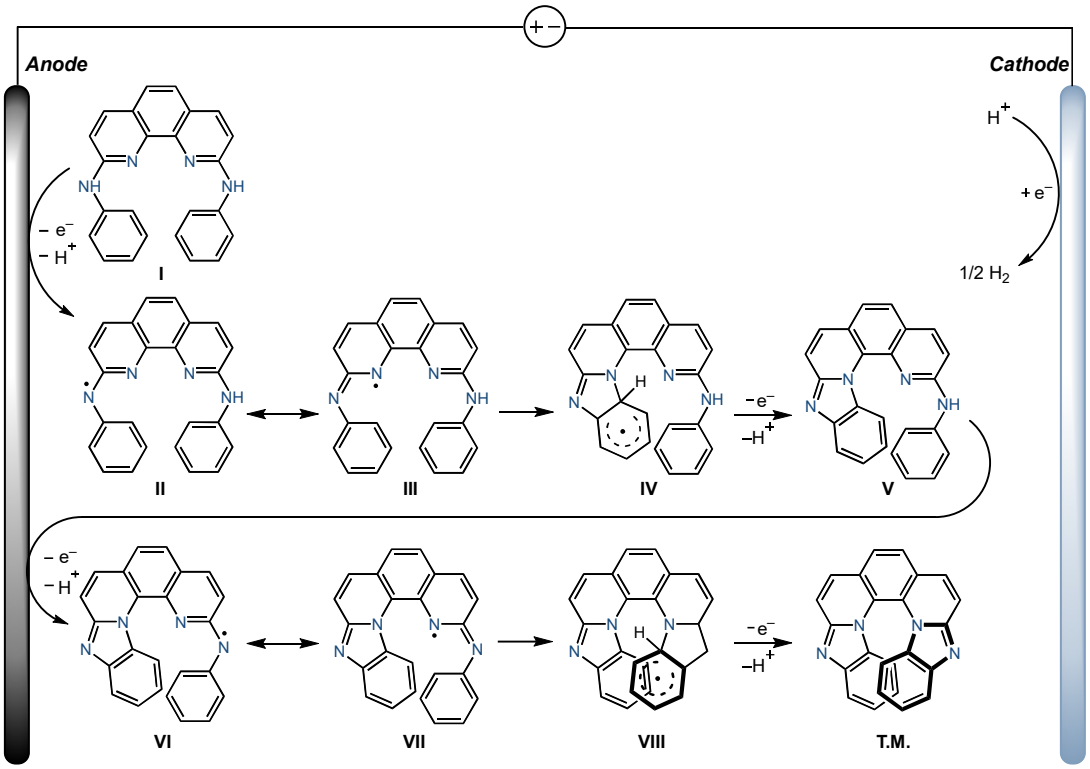

Figure S4. Proposed mechanism

As shown in Figure S4, substrate **I** undergoes anodic single-electron oxidation and deprotonation to afford radical intermediate **II**, which resonates to **III** and adds to the aromatic ring to give **IV**. A second anodic oxidation and deprotonation furnish the mono-C-N coupled product **V**. Further anodic oxidation of **V** generates radical intermediates **VI/VII**, which undergo radical addition to form **VIII**. Subsequent oxidation/deprotonation affords the bis-C-N coupled product **T.M.**. In parallel, proton reduction at the cathode releases H_2. The proposed mechanism is consistent with the multistep oxidation observed in the CV experiments.

6 Single Crystal Structures of Helicenes 11 and 20

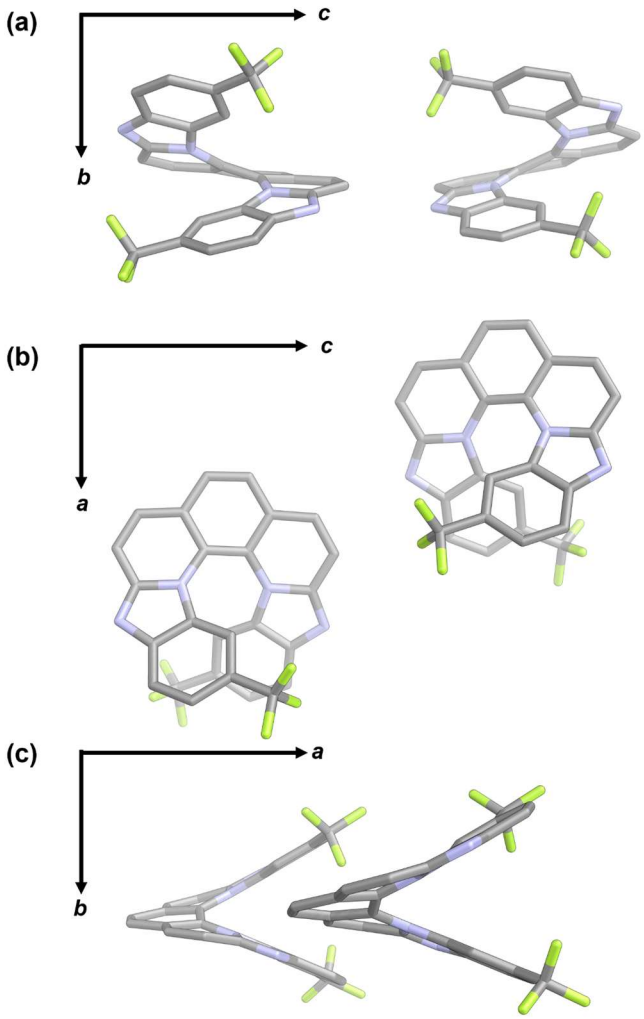

Figure S5. Single crystal structures of racemic helicene *rac*-**11**. Single crystals of *rac*-**11** suitable for X-ray diffraction were obtained by slow volatilization of a DMSO solution at room temperature over one week. (a–c) Helicene **11** in crystal view along (a) *a*-axis, (b) *b*-axis, and (c) *c*-axis.

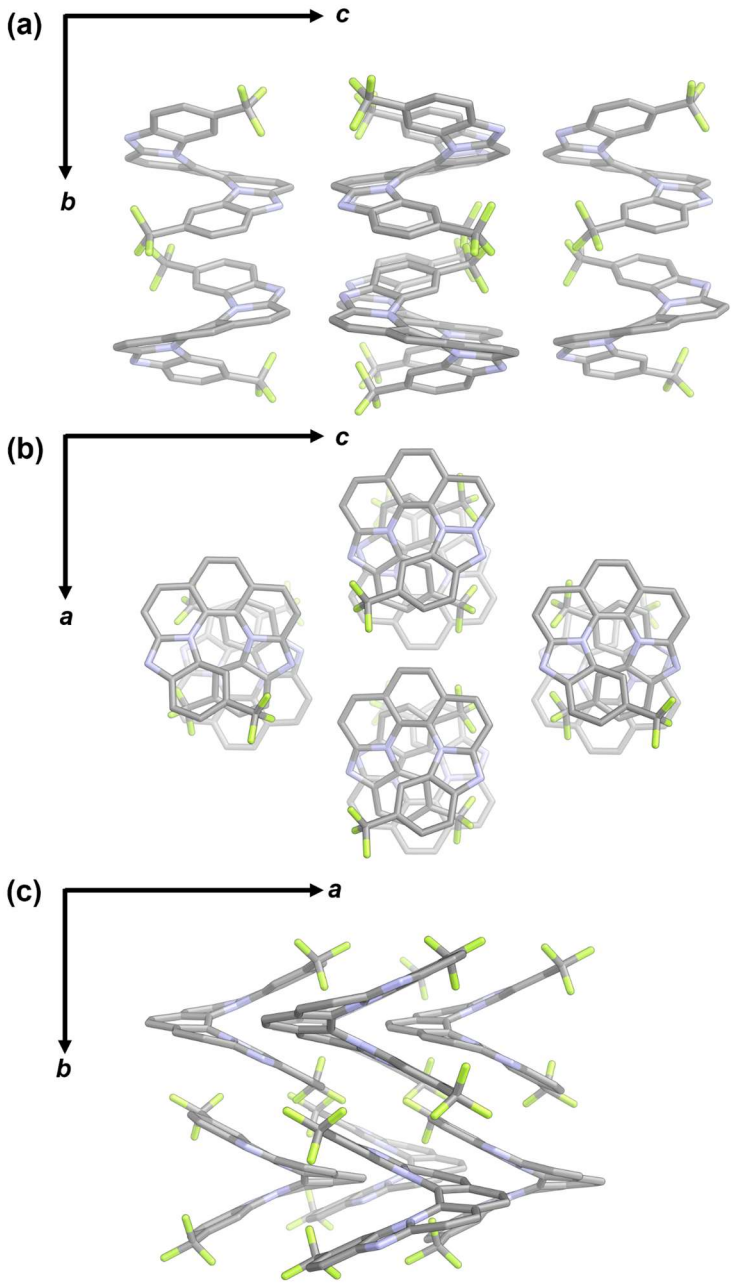

Figure S6. Packing diagram of crystal racemic helicene *rac*-**11**. (a–c) *rac*-**11** in crystal view along (a) *a*-axis, (b) *b*-axis, and (c) *c*-axis.

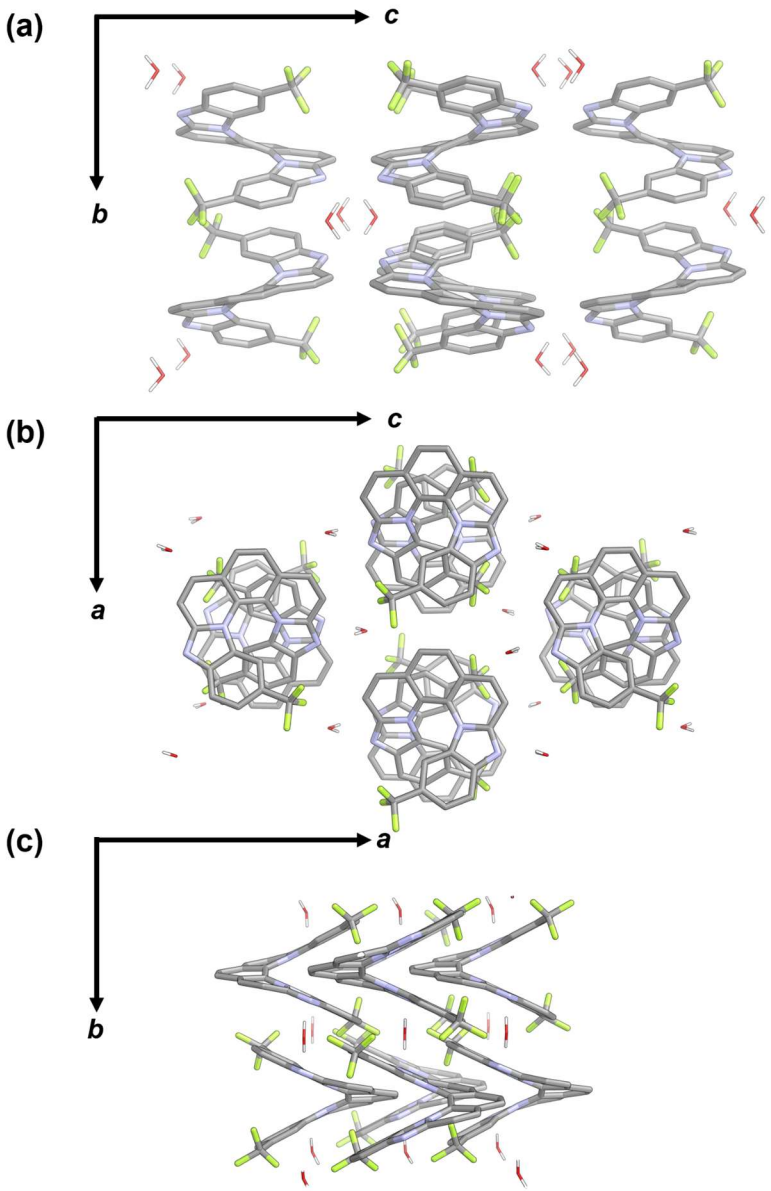

Figure S7. Packing diagram of crystal racemic helicene *rac*-**11**·H_2O. (a–c) *rac*-**11**·H_2O in crystal view along (a) *a*-axis, (b) *b*-axis, and (c) *c*-axis.

Table S8. Crystal data and structure refinement for *rac*-11·H_2O

Identification code	*rac*-**11**·H_2O
Empirical formula	$C_{26}H_{14}F_6N_4O$
Formula weight	512.41
Temperature/K	330
Crystal system	orthorhombic
Space group	Pnna
a/Å	9.9295(15)
b/Å	12.7666(17)
c/Å	17.765(3)
α/°	90
β/°	90
γ/°	90
Volume/Å^3	2252.0(6)
Z	4
ρ_{calc}g/cm^3	1.511
μ/mm^{-1}	0.129
F(000)	1040
Crystal size/mm^3	0.34 × 0.21 × 0.156
Radiation	MoKα (λ = 0.71073)
2θ range for data collection/°	3.928 to 49.992
Index ranges	-11 ≤ h ≤ 11, -15 ≤ k ≤ 13, -21 ≤ l ≤ 21
Reflections collected	29702
Independent reflections	1978 [R_{int} = 0.0634, R_{sigma} = 0.0238]
Data/restraints/parameters	1978/0/202
Goodness-of-fit on F^2	1.054
Final R indexes [I>=2σ (I)]	R_1 = 0.0488, wR_2 = 0.1218
Final R indexes [all data]	R_1 = 0.0694, wR_2 = 0.1420
Largest diff. peak/hole / e Å^{-3}	0.16/-0.21
CCDC number	2522083

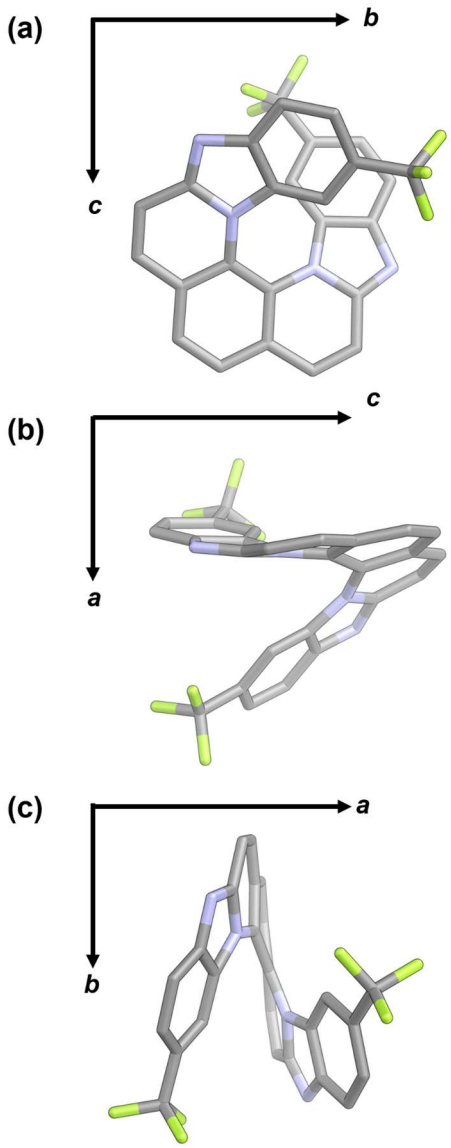

Figure S8. Single crystal structures of helicene *M*-**11**. Single crystals of *M*-**11** suitable for X-ray diffraction were obtained by slow vapor diffusion of diisopropyl ether into 1,2-dichloroethane solutions over 1 week at room temperature. (a–c) Helicene *M*-**11** in crystal view along (a) *a*-axis, (b) *b*-axis, and (c) *c*-axis.

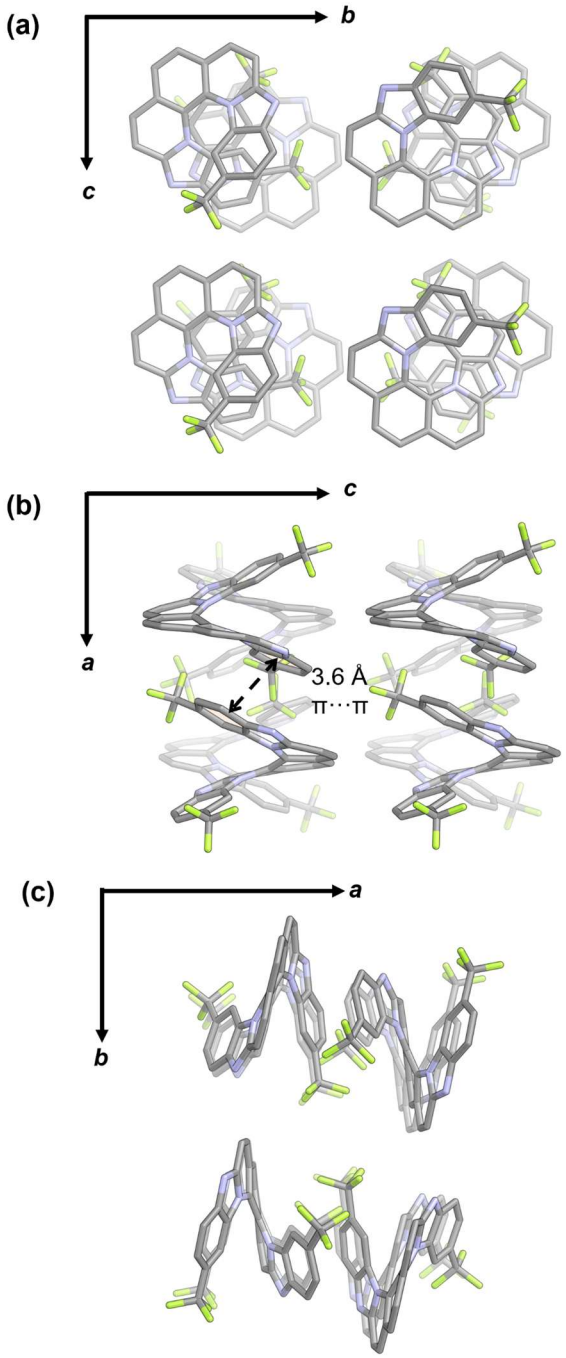

Figure S9. Packing diagram of crystal helicene *M*-**11**. (a–c) *M*-**11** in crystal view along (a) *a*-axis, (b) *b*-axis, and (c) *c*-axis.

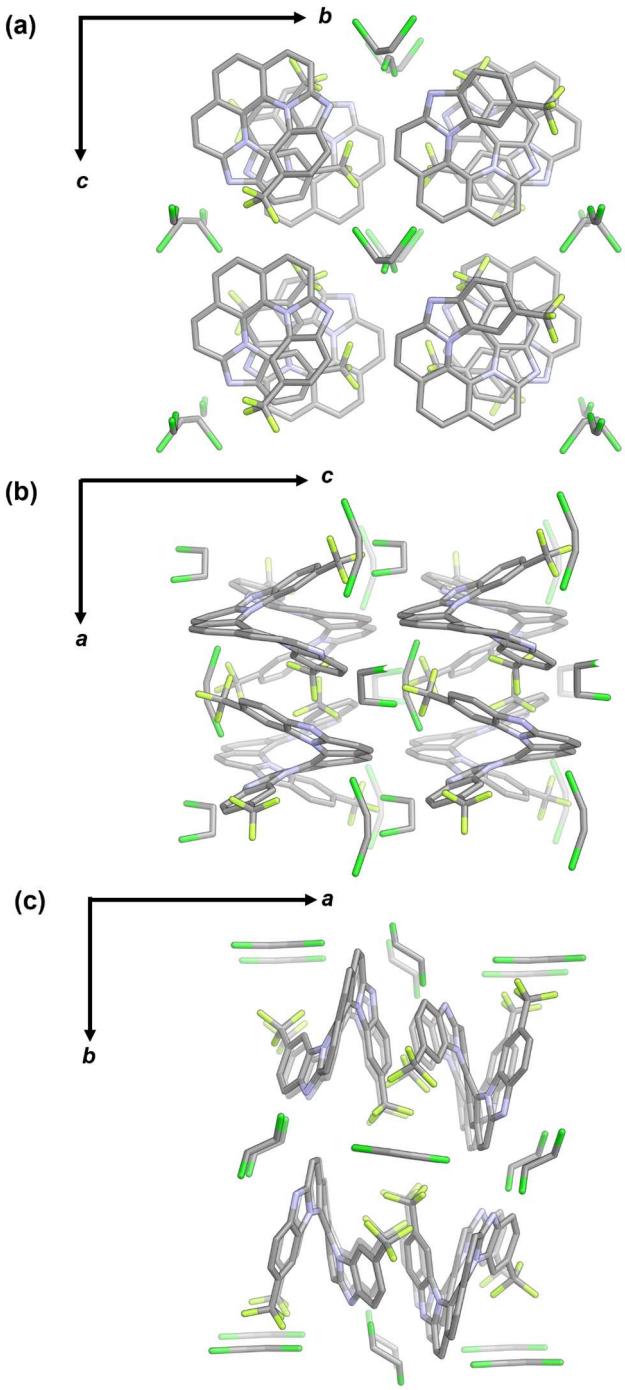

Figure S10. Packing diagram of crystal helicene *M*-**11** with 1,2-dichloroethane. (a–c) *M*-**11** with 1,2-dichloroethane in crystal view along (a) *a*-axis, (b) *b*-axis, and (c) *c*-axis.

Table S9. Crystal data and structure refinement for *M*-11 with 1,2-dichloroethane

Identification code	*M*-**11** with 1,2-dichloroethane
Empirical formula	$C_{28}H_{16}Cl_2F_6N_4$
Formula weight	593.35
Temperature/K	200
Crystal system	orthorhombic
Space group	$P2_12_12$
a/Å	12.9156(9)
b/Å	20.0304(13)
c/Å	9.9686(6)
α/°	90
β/°	90
γ/°	90
Volume/Å^3	2578.9(3)
Z	4
ρ_{calc}g/cm^3	1.528
μ/mm^{-1}	2.899
F(000)	1200
Crystal size/mm^3	0.39 × 0.34 × 0.28
Radiation	CuKα (λ = 1.54178)
2θ range for data collection/°	8.146 to 140.394
Index ranges	$-15 \leq h \leq 15$, $-20 \leq k \leq 24$, $-12 \leq l \leq 8$
Reflections collected	13766
Independent reflections	4666 [R_{int} = 0.0549, R_{sigma} = 0.0491]
Data/restraints/parameters	4666/18/381
Goodness-of-fit on F^2	1.061
Final R indexes [I>=2σ (I)]	R_1 = 0.0476, wR_2 = 0.1188
Final R indexes [all data]	R_1 = 0.0494, wR_2 = 0.1195
Largest diff. peak/hole / e Å^{-3}	0.39/-0.52
Flack parameter	0.132(7)
CCDC number	2522084

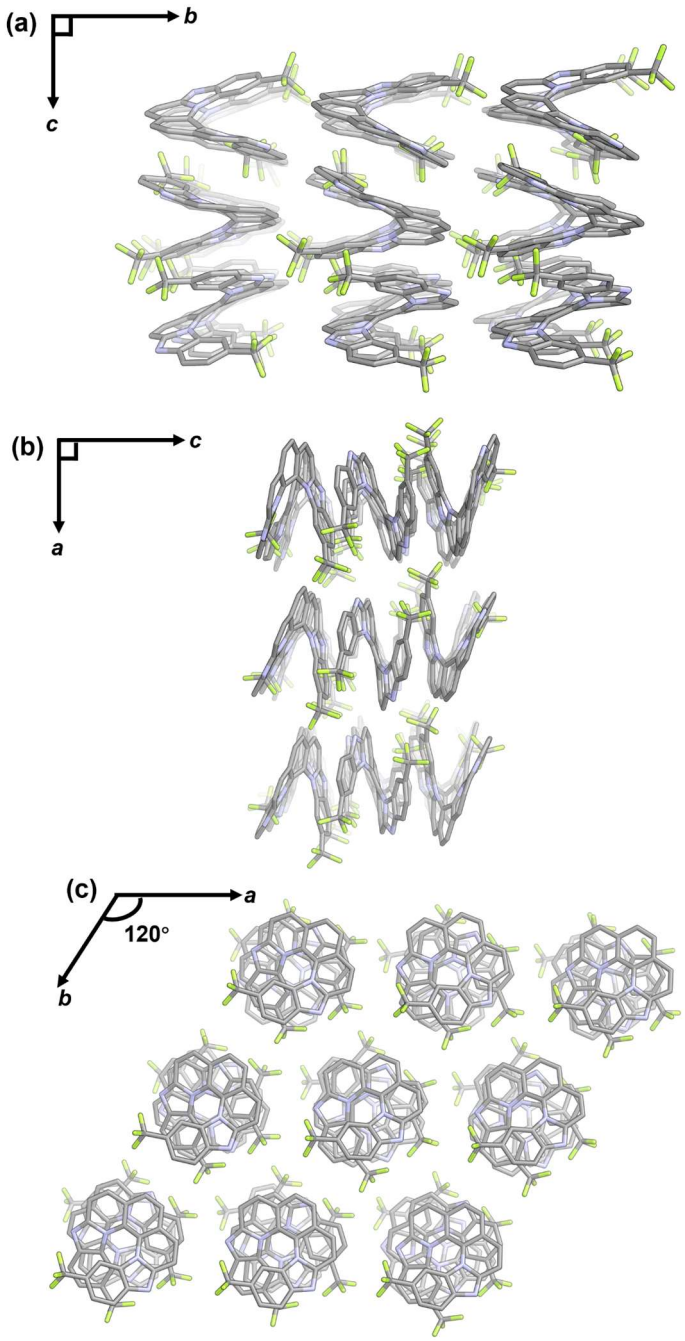

Figure S11. Single crystal structures of helicene *M*-**11**. Single crystals of *M*-**11** suitable for X-ray diffraction were obtained by slow vapor diffusion of diisopropyl ether into acetone solutions over 1 week at room temperature. (a–c) Helicene *M*-**11** in crystal view along (a) *a*-axis, (b) *b*-axis, and (c) *c*-axis.

Table S10. Crystal data and structure refinement for *M*-11 with acetone

Identification code	*M*-**11** with acetone
Empirical formula	$C_{26}H_{12}F_6N_4$
Formula weight	494.40
Temperature/K	193.00
Crystal system	trigonal
Space group	$P3_2$
a/Å	32.2229(6)
b/Å	32.2229(6)
c/Å	15.7246(4)
α/°	90
β/°	90
γ/°	120
Volume/Å^3	14139.7(6)
Z	27
ρ_{calc}g/cm^3	1.568
μ/mm^{-1}	1.151
F(000)	6750.0
Crystal size/mm^3	0.13 × 0.11 × 0.09
Radiation	CuKα (λ = 1.54178)
2θrange for data collection/°	5.484 to 149.826
Index ranges	$-40 \leq h \leq 40$, $-40 \leq k \leq 40$, $-15 \leq l \leq 19$
Reflections collected	334729
Independent reflections	36004 [R_{int} = 0.1674, R_{sigma} = 0.0695]
Data/restraints/parameters	36004/6229/2918
Goodness-of-fit on F^2	1.080
Final R indexes [I>=2σ (I)]	R_1 = 0.1394, wR_2 = 0.3314
Final R indexes [all data]	R_1 = 0.1692, wR_2 = 0.3522
Largest diff. peak/hole / e Å^{-3}	0.94/-0.73
Flack parameter	0.09(6)
CCDC number	2522089

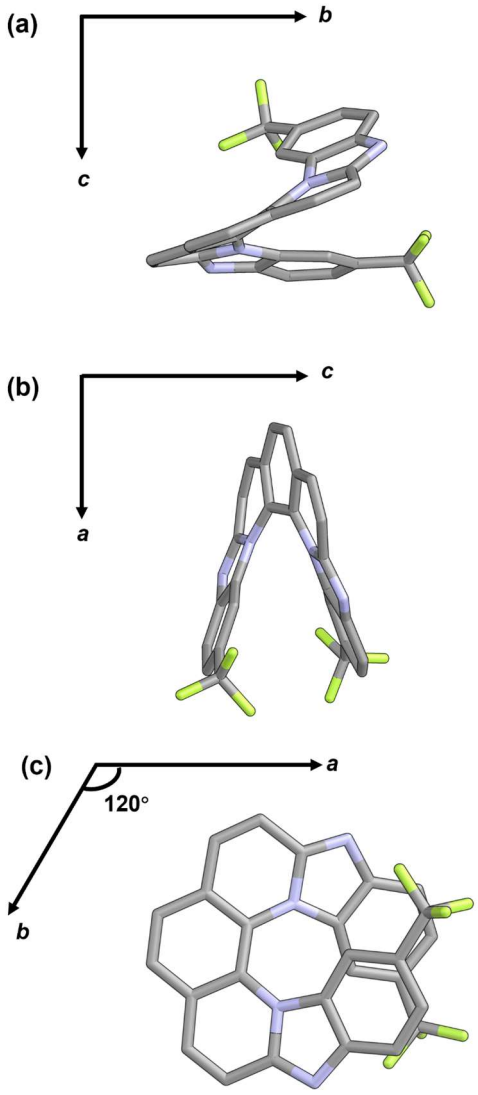

Figure S12. Single crystal structures of helicene *P*-**11**. Single crystals of *P*-**11** suitable for X-ray diffraction were obtained by slow vapor diffusion of diisopropyl ether into acetone solutions over 1 week at room temperature. (a–c) Helicene *P*-**11** in crystal view along (a) *a*-axis, (b) *b*-axis, and (c) *c*-axis.

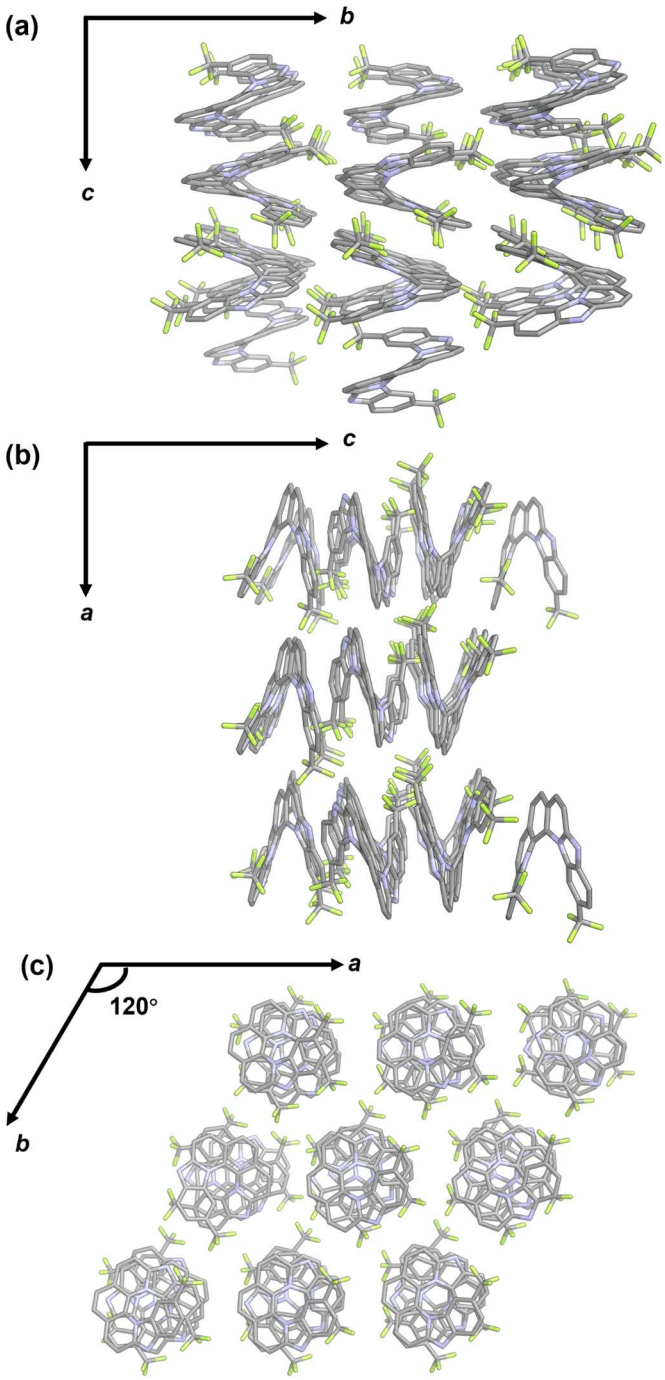

Figure S13. Packing diagram of crystal helicene *P*-**11**. (a–c) *P*-**11** in crystal view along (a) *a*-axis, (b) *b*-axis, and (c) *c*-axis.

Table S11. Crystal data and structure refinement for *P*-11

Identification code	*P*-**11**
Empirical formula	C26H12F6N4
Formula weight	494.40
Temperature/K	200.00
Crystal system	trigonal
Space group	P31
a/Å	32.2457(9)
b/Å	32.2457(9)
c/Å	15.7465(7)
α/°	90
β/°	90
γ/°	120
Volume/Å3	14179.4(10)
Z	27
ρcalcg/cm3	1.563
μ/mm-1	1.147
F(000)	6750.0
Crystal size/mm3	0.13 × 0.11 × 0.08
Radiation	CuKα (λ = 1.54178)
2θ range for data collection/°	5.482 to 140.738
Index ranges	-39 ≤ h ≤ 39, -39 ≤ k ≤ 39, -19 ≤ l ≤ 14
Reflections collected	127801
Independent reflections	33091 [Rint = 0.1146, Rsigma = 0.1071]
Data/restraints/parameters	33091/6859/2917
Goodness-of-fit on F2	1.127
Final R indexes [I>=2σ (I)]	R1 = 0.1101, wR2 = 0.2877
Final R indexes [all data]	R1 = 0.1519, wR2 = 0.3213
Largest diff. peak/hole / e Å-3	0.45/-0.35
Flack parameter	0.11(7)
CCDC number	2522088

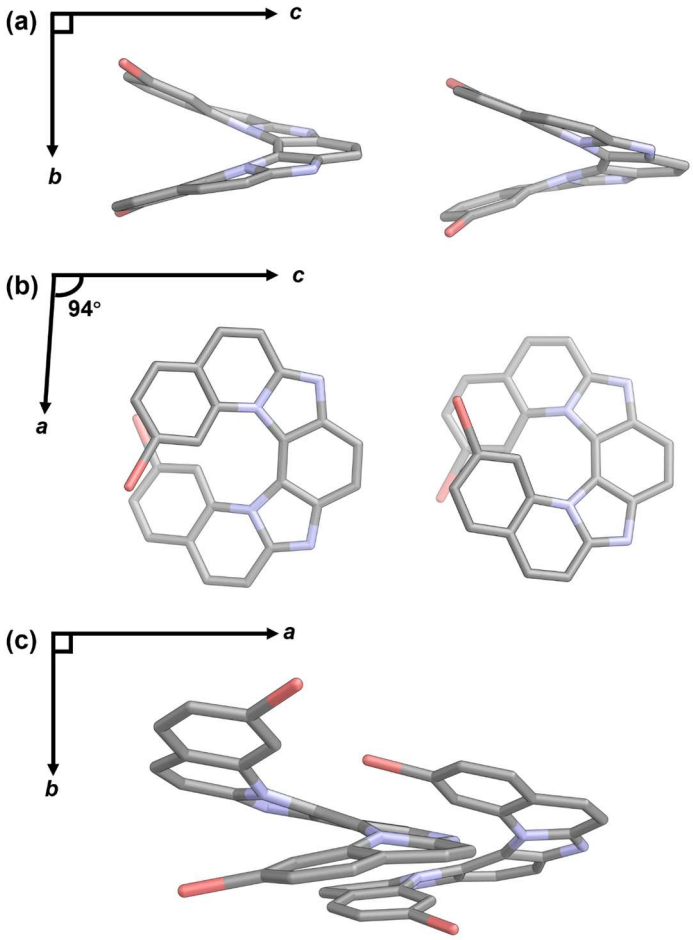

Figure S14. Single crystal structures of racemic helicene *rac*-**20**. Single crystals of *rac*-**20** suitable for X-ray diffraction were obtained by slow vapor diffusion of methanol into dichloromethane solutions over 1 week at room temperature. (a–c) Helicene *rac*-**20** in crystal view along (a) *a*-axis, (b) *b*-axis, and (c) *c*-axis.

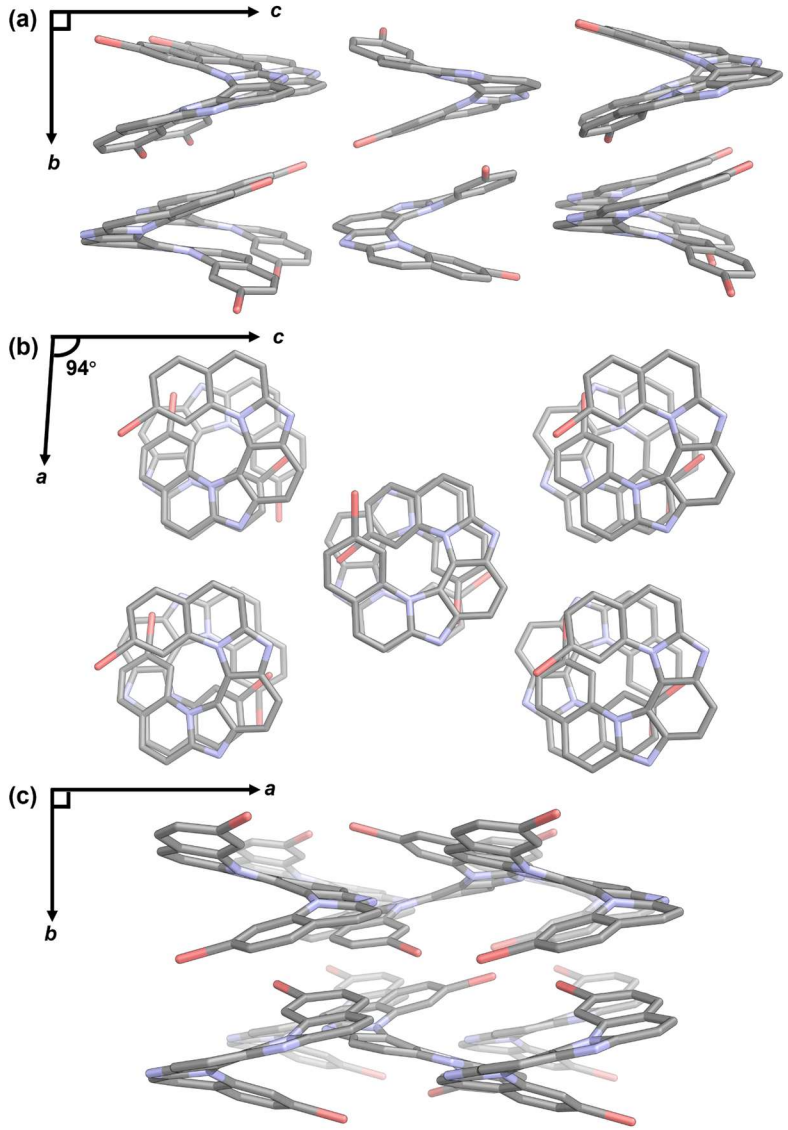

Figure S15. Packing diagram of crystal racemic helicene *rac*-**20**. (a–c) *rac*-**20** in crystal view along (a) *a*-axis, (b) *b*-axis, and (c) *c*-axis.

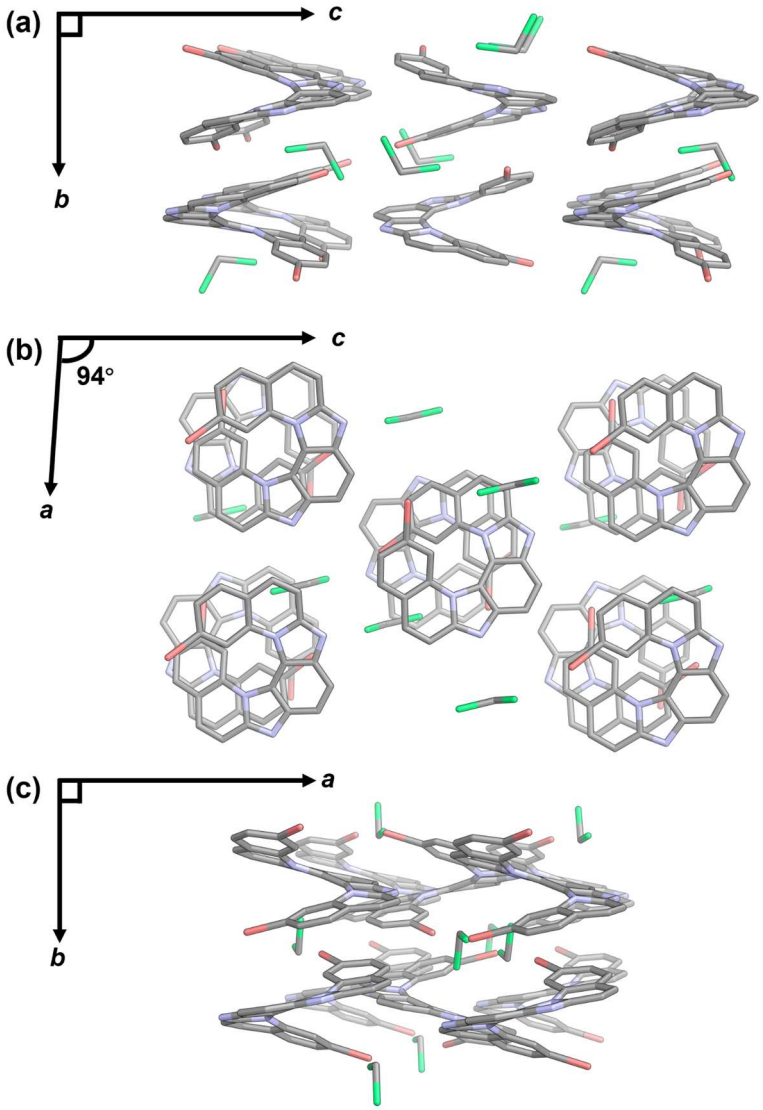

Figure S16. Packing diagram of crystal racemic helicene *rac*-**20**·CH_2Cl_2. (a–c) *rac*-**20**·CH_2Cl_2 in crystal view along (a) *a*-axis, (b) *b*-axis, and (c) *c*-axis.

Table S12. Crystal data and structure refinement for *rac*-20·CH_2Cl_2

Identification code	*rac*-**20**·CH_2Cl_2
Empirical formula	$C_{25}H_{14}Br_2Cl_2N_4$
Formula weight	601.12
Temperature/K	251
Crystal system	monoclinic
Space group	$P2_1/n$
a/Å	10.1623(10)
b/Å	11.5407(9)
c/Å	18.8777(18)
α/°	90
β/°	94.138(4)
γ/°	90
Volume/Å^3	2208.2(3)
Z	4
ρ_{calc}g/cm^3	1.808
μ/mm^{-1}	3.936
F(000)	1184
Crystal size/mm^3	0.37 × 0.18 × 0.13
Radiation	MoKα (λ = 0.71073)
2θ range for data collection/°	4.14 to 54.976
Index ranges	$-13 \leq h \leq 13$, $-14 \leq k \leq 14$, $-24 \leq l \leq 24$
Reflections collected	50346
Independent reflections	4977 [R_{int} = 0.0983, R_{sigma} = 0.0532]
Data/restraints/parameters	4977/0/298
Goodness-of-fit on F^2	1.013
Final R indexes [I>=2σ (I)]	R_1 = 0.0315, wR_2 = 0.0673
Final R indexes [all data]	R_1 = 0.0501, wR_2 = 0.0757
Largest diff. peak/hole / e Å^{-3}	0.46/-0.52
CCDC number	2522086

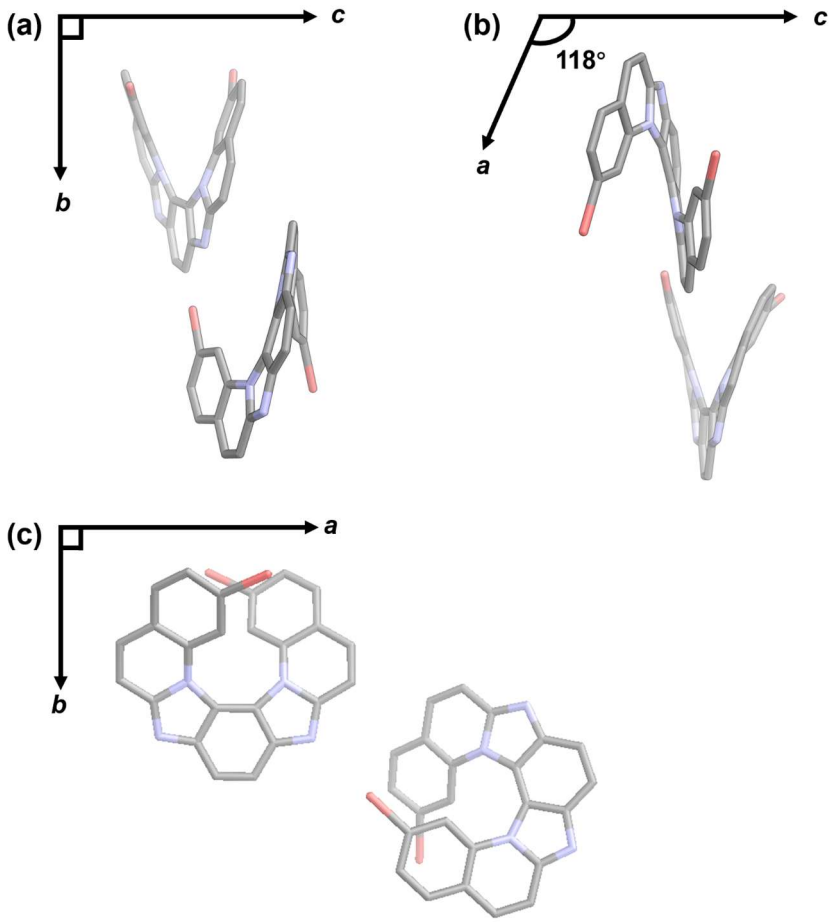

Figure S17. Single crystal structures of helicene *M*-**20**. Single crystals of *M*-**20** suitable for X-ray diffraction were obtained by slow vapor diffusion of methanol into dichloromethane solutions over 1 week at room temperature. (a–c) Helicene *M*-**20** in crystal view along (a) *a*-axis, (b) *b*-axis, and (c) *c*-axis.

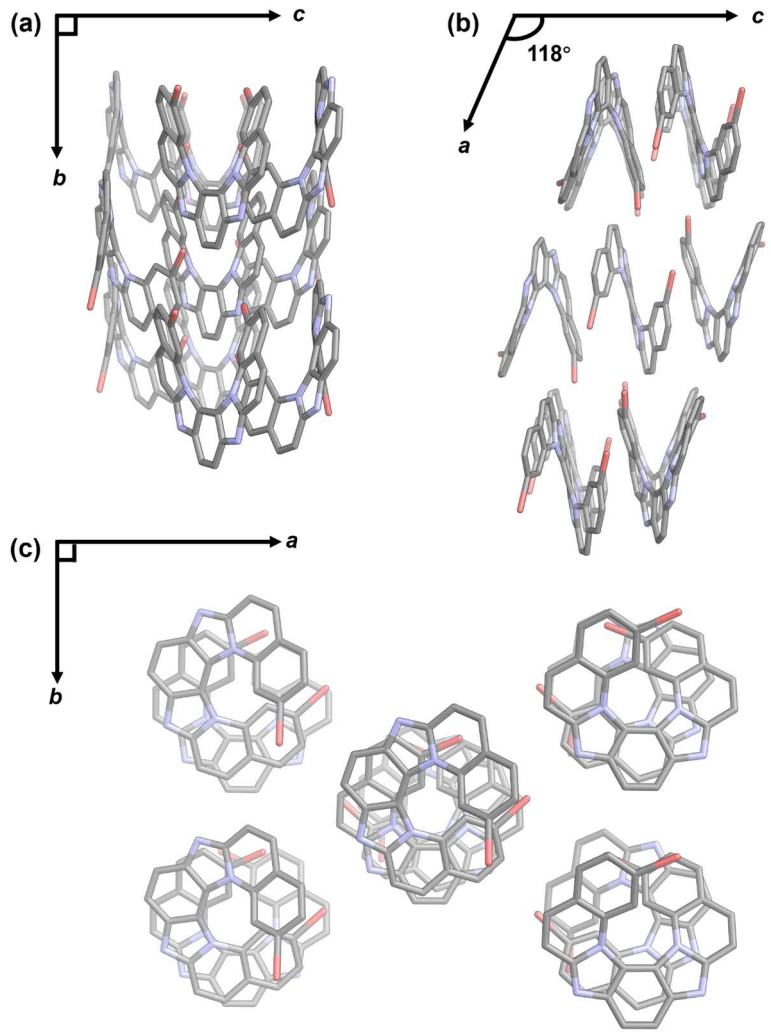

Figure S18. Packing diagram of crystal *M*-**20**. (a–c) *M*-**20** in crystal view along (a) *a*-axis, (b) *b*-axis, and (c) *c*-axis.

Table S13. Crystal data and structure refinement for *M*-20

Identification code	***M*-20**
Empirical formula	$C_{24}H_{12}Br_2N_4$
Formula weight	516.2
Temperature/K	256
Crystal system	monoclinic
Space group	C2
a/Å	20.1346(14)
b/Å	10.2688(7)
c/Å	15.6799(9)
α/°	90
β/°	117.915(2)
γ/°	90
Volume/Å^3	2864.7(3)
Z	6
ρ_{calc}g/cm^3	1.795
μ/mm^{-1}	4.265
F(000)	1524
Crystal size/mm^3	0.38 × 0.08 × 0.07
Radiation	MoKα (λ = 0.71073)
2θ range for data collection/°	4.124 to 54.99
Index ranges	$-26 \leq h \leq 26$, $-13 \leq k \leq 13$, $-19 \leq l \leq 20$
Reflections collected	41535
Independent reflections	6555 [R_{int} = 0.0933, R_{sigma} = 0.0643]
Data/restraints/parameters	6555/1/406
Goodness-of-fit on F^2	1.03
Final R indexes [I>=2σ (I)]	R_1 = 0.0325, wR_2 = 0.0631
Final R indexes [all data]	R_1 = 0.0485, wR_2 = 0.0692
Largest diff. peak/hole / e Å^{-3}	0.54/-0.41
Flack parameter	0.020(6)
CCDC number	2522087

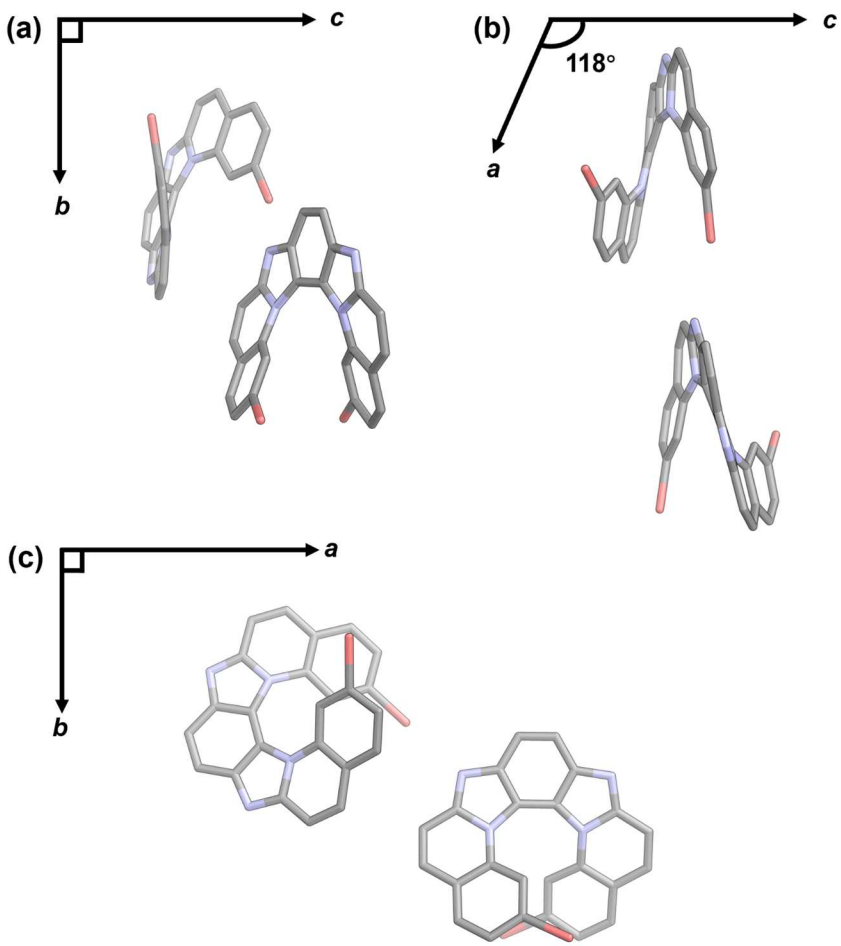

Figure S19. Single crystal structures of helicene *P*-**20**. Single crystals of *P*-**20** suitable for X-ray diffraction were obtained by slow vapor diffusion of methanol into dichloromethane solutions over 1 week at room temperature. (a–c) Helicene *P*-**20** in crystal view along (a) *a*-axis, (b) *b*-axis, and (c) *c*-axis.

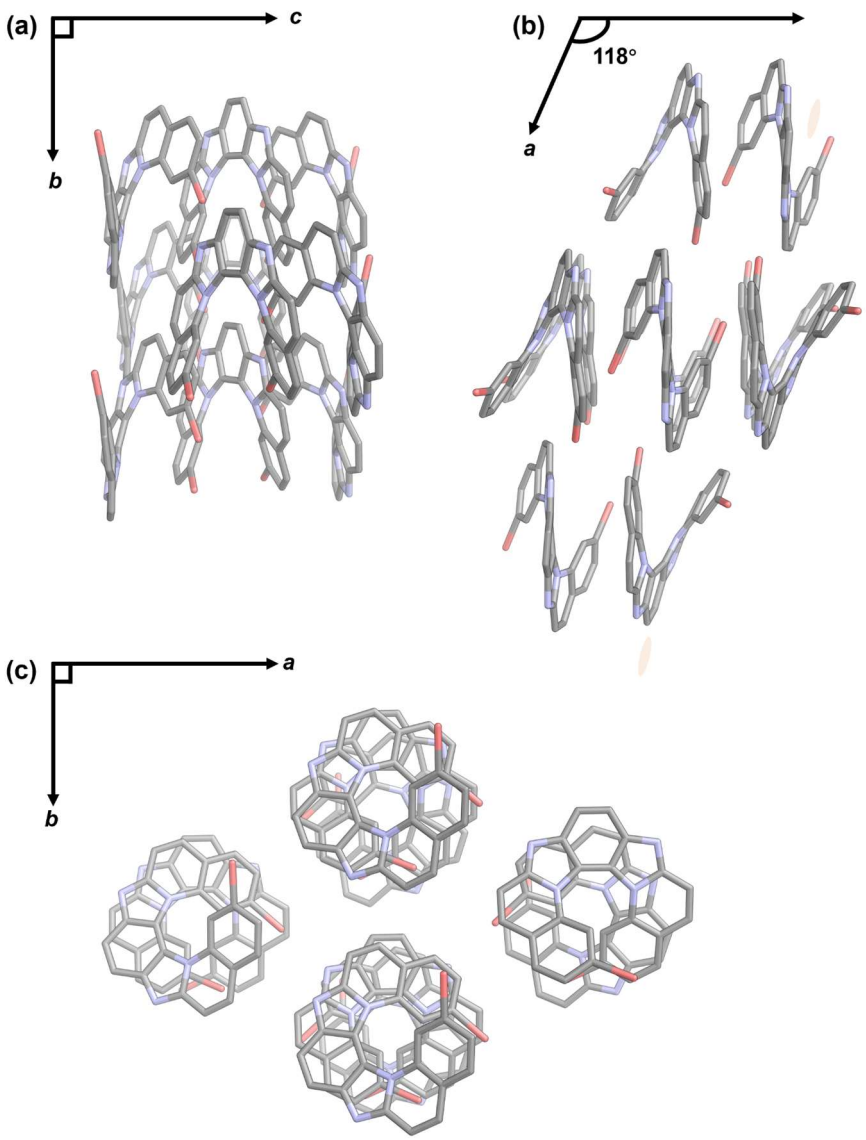

Figure S20. Packing diagram of crystal *P*-**20**. (a–c) *P*-**20** in crystal view along (a) *a*-axis, (b) *b*-axis, and (c) *c*-axis.

Table S14. Crystal data and structure refinement for *P*-20

Identification code	***P*-20**
Empirical formula	$C_{24}H_{12}Br_2N_4$
Formula weight	516.2
Temperature/K	209
Crystal system	monoclinic
Space group	C2
a/Å	20.0877(7)
b/Å	10.2487(3)
c/Å	15.6249(4)
α/°	90
β/°	117.8390(10)
γ/°	90
Volume/Å^3	2844.45(15)
Z	6
ρ_{calc}g/cm^3	1.808
μ/mm^{-1}	4.295
F(000)	1524
Crystal size/mm^3	0.42 × 0.12 × 0.08
Radiation	MoKα (λ = 0.71073)
2θ range for data collection/°	4.134 to 55.01
Index ranges	$-26 \leq h \leq 26$, $-13 \leq k \leq 13$, $-20 \leq l \leq 19$
Reflections collected	40311
Independent reflections	6511 [R_{int} = 0.0737, R_{sigma} = 0.0538]
Data/restraints/parameters	6511/1/406
Goodness-of-fit on F^2	1.032
Final R indexes [I>=2σ (I)]	R_1 = 0.0271, wR_2 = 0.0542
Final R indexes [all data]	R_1 = 0.0354, wR_2 = 0.0565
Largest diff. peak/hole / e Å^{-3}	0.24/-0.47
Flack parameter	0.012(5)
CCDC number	2522085

6.1 Chiral HPLC separations

Analytical chiral HPLC separation for compound **6**

Analytical chiral HPLC: Chiralpak IE-3 (0.46 cm I.D. × 25 cm L), DCM/EtOAc/DEA = 80/20/0.1(V/V/V), 1.0 mL/min, UV detection at 254 nm.

Racemic mixture:

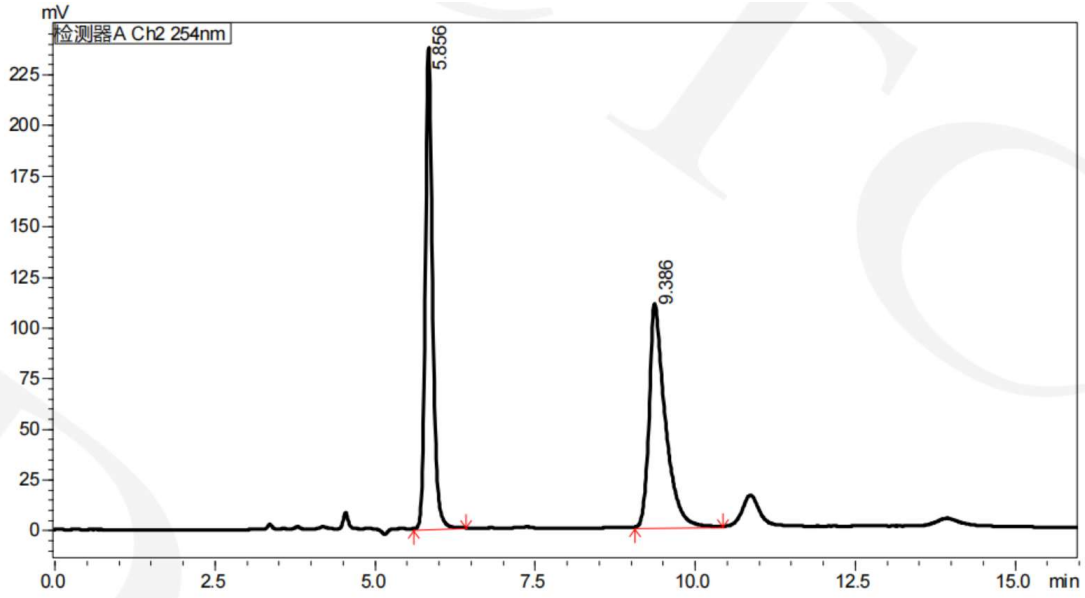

Peak	Ret. Time	Area	Area%	T.Plate	Tailing	Resolution
1	5.856	1882777	49.710	12153	1.214	--
2	9.386	1904743	50.290	7296	1.641	10.829

(+)-6: *ee* > 98%

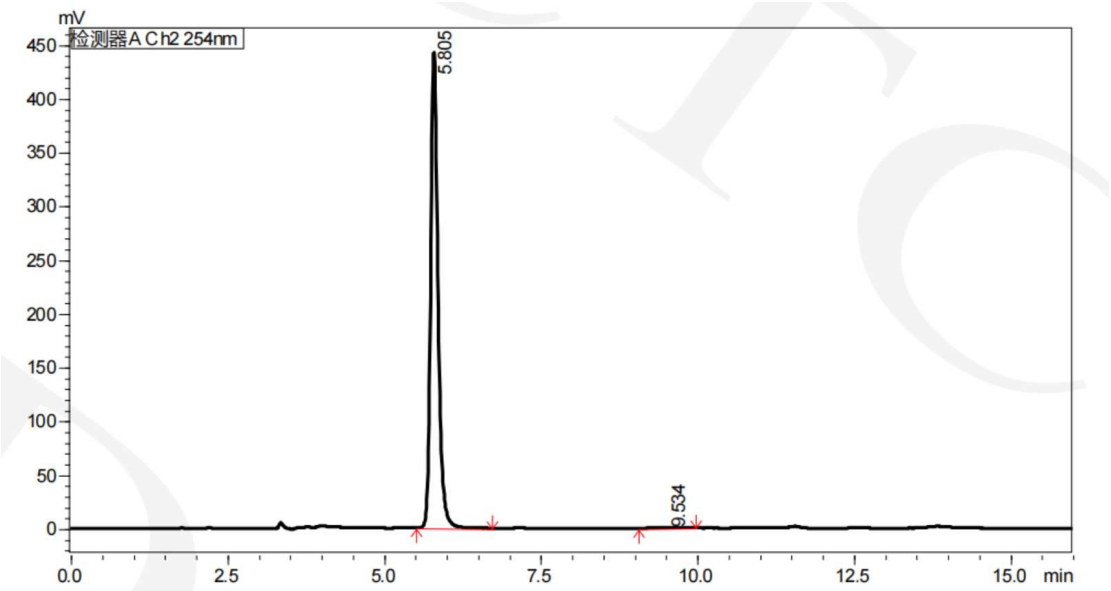

Peak	Ret. Time	Area	Area%	T.Plate	Tailing	Resolution
1	5.805	3624115	99.615	11341	1.264	--
2	9.534	13994	0.385	6832	1.012	10.977

(-)-6: *ee* > 98%

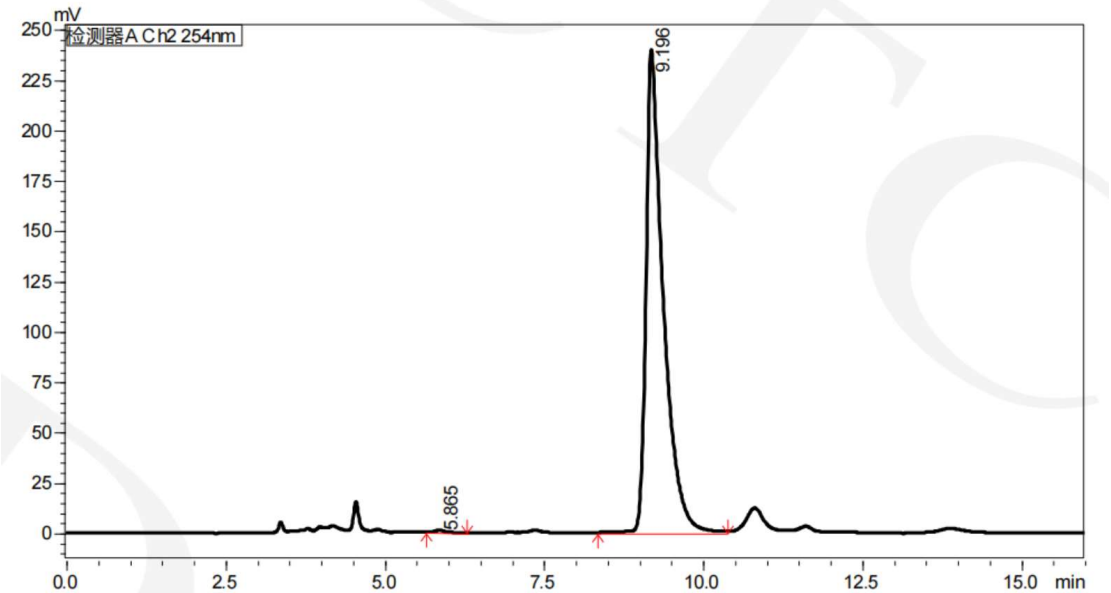

Peak	Ret. Time	Area	Area%	T.Plate	Tailing	Resolution
1	5.865	10468	0.232	10068	1.177	--
2	9.196	4494092	99.768	6061	1.893	9.431

Analytical chiral HPLC separation for compound **8**

Analytical chiral HPLC: Chiralpak IE (0.46 cm I.D. × 25 cm L), MeOH/DCM/DEA = 70/30/0.1 (V/V/V), 1.0 mL/min, UV detection at 254 nm.

Racemic mixture:

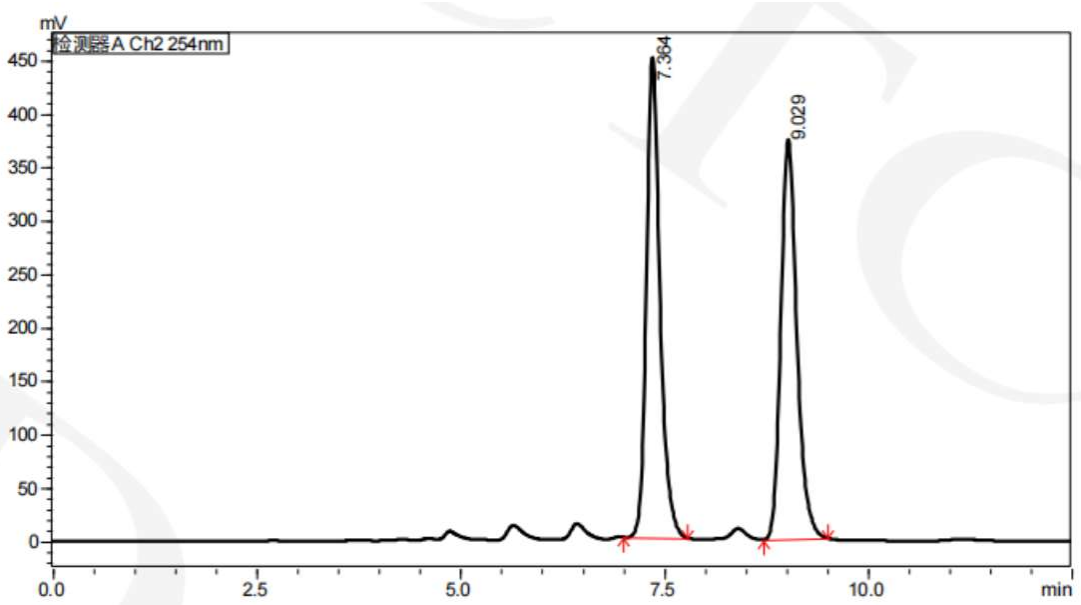

Peak	Ret. Time	Area	Area%	T.Plate	Tailing	Resolution
1	7.364	5206797	50.446	9554	1.251	--
2	9.029	5114673	49.554	10090	1.226	5.039

(+)-8: *ee* > 98%

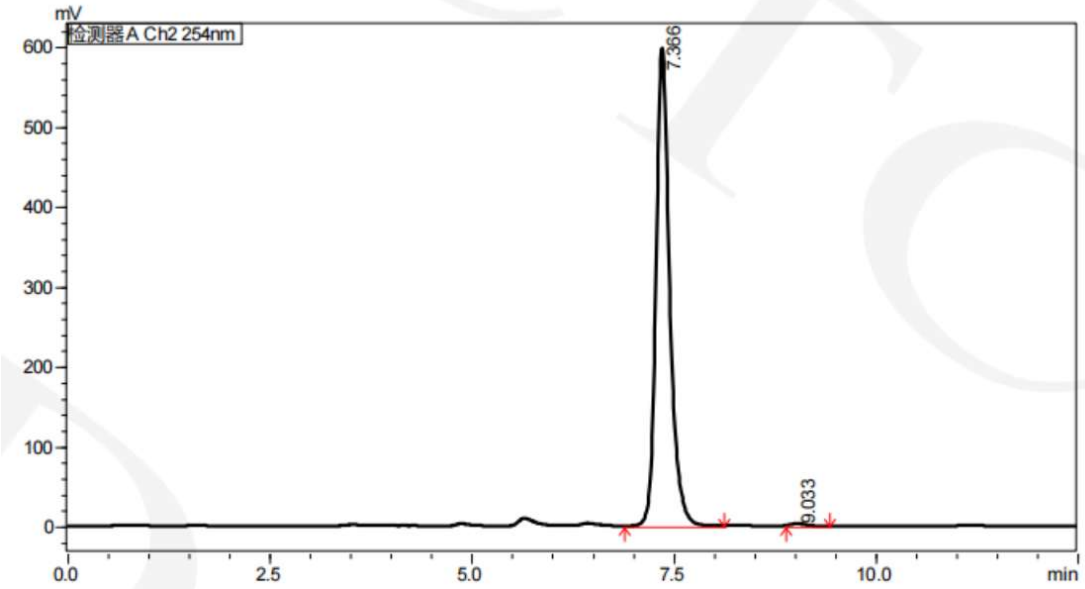

Peak	Ret. Time	Area	Area%	T.Plate	Tailing	Resolution
1	7.366	7056994	99.423	9440	1.255	--
2	9.033	5114673	0.577	10066	--	5.027

(-)-8: *ee* > 98%

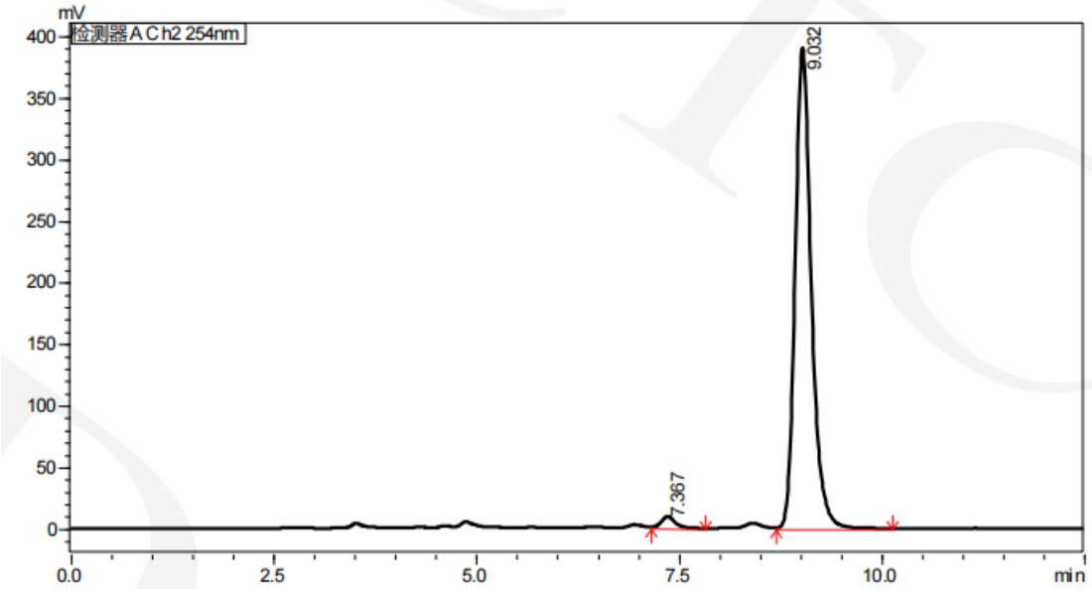

Peak	Ret. Time	Area	Area%	T.Plate	Tailing	Resolution
1	7.367	112492	2.035	8735	--	--
2	9.032	5416077	97.965	10031	1.243	4.927

Analytical chiral HPLC separation for compound **11**

Analytical chiral HPLC: Chiralpak IH (0.46 cm I.D. × 15 cm L), MeOH = 100%, 1.0 mL/min, UV detection at 254 nm.

Racemic mixture:

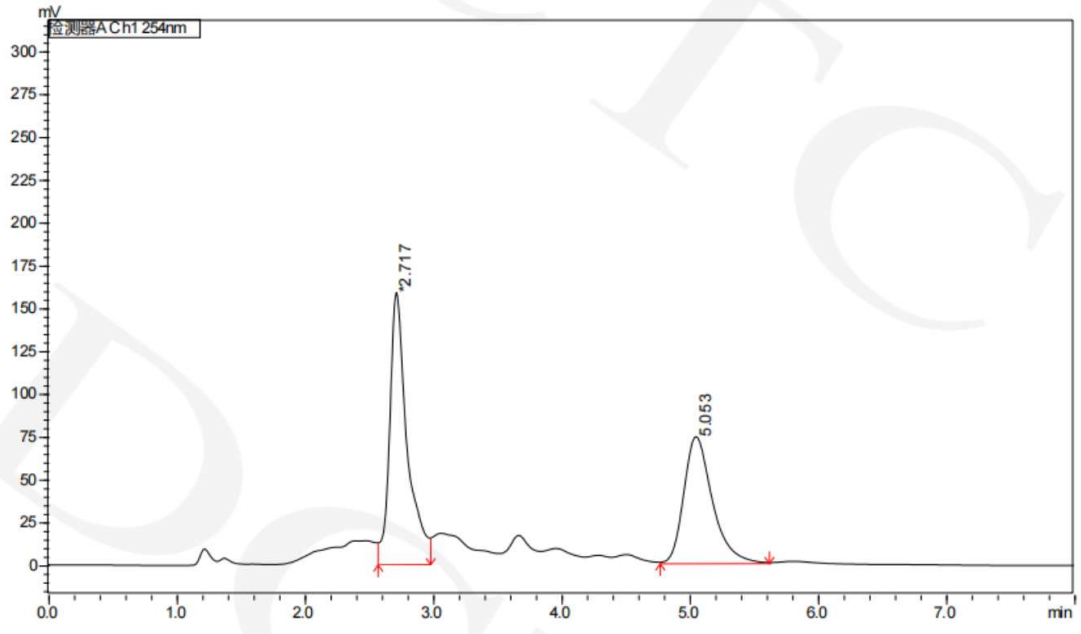

Peak	Ret. Time	Area	Area%	T.Plate	Tailing	Resolution
1	2.717	1494521	56.962	2261	--	--
2	5.053	1129210	43.038	2573	1.355	7.452

***P*-11**: *ee* > 98%

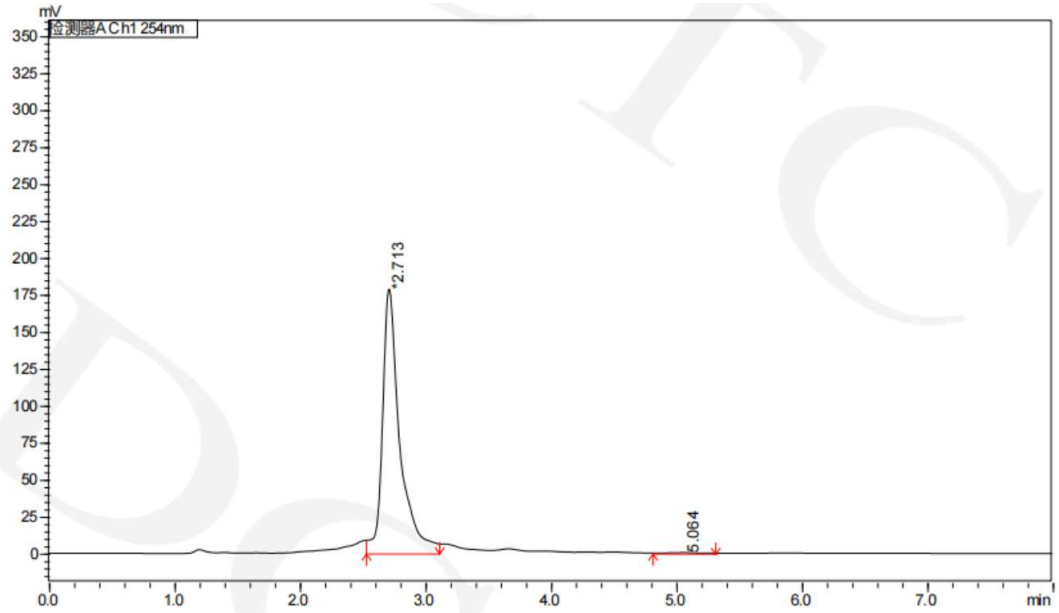

Peak	Ret. Time	Area	Area%	T.Plate	Tailing	Resolution
1	2.713	1709137	99.736	2318	1.505	--
2	5.064	4521	0.264	3046	--	7.938

***M*-11**: *ee* > 98%

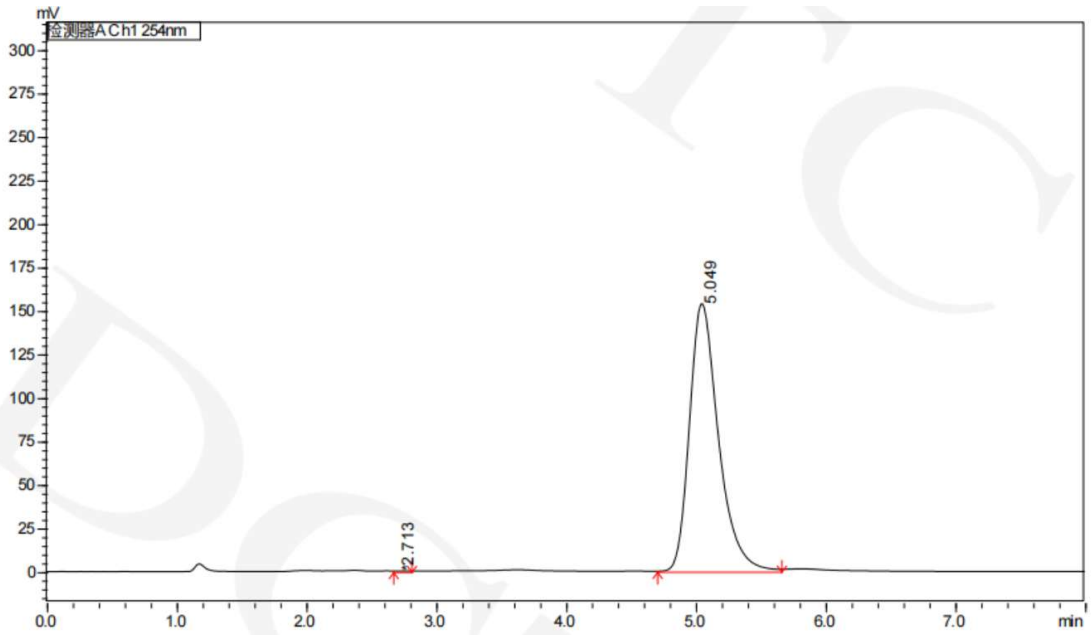

Peak	Ret. Time	Area	Area%	T.Plate	Tailing	Resolution
1	2.713	2317	0.097	193	--	--
2	5.049	2385950	99.903	2537	1.353	3.953

Analytical chiral HPLC separation for compound **13**

Analytical chiral HPLC: Chiralpak IB N-5 (0.46 cm I.D. × 25 cm L), MeOH/ACN/NH_3 in MeOH = 50/50/0.1 (V/V/V), 1.0 mL/min, UV detection at 254 nm.

Racemic mixture:

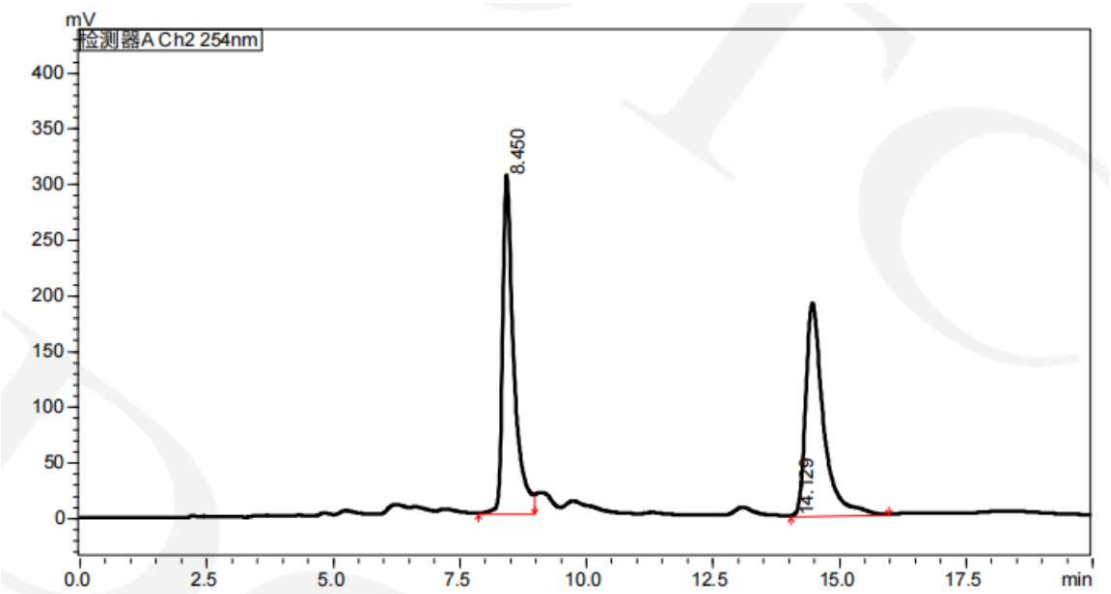

Peak	Ret. Time	Area	Area%	T.Plate	Tailing	Resolution
1	8.450	4628606	50.261	8531	--	--
2	14.129	4580448	49.739	1160	15.010	5.608

(+)-13: *ee* > 98%

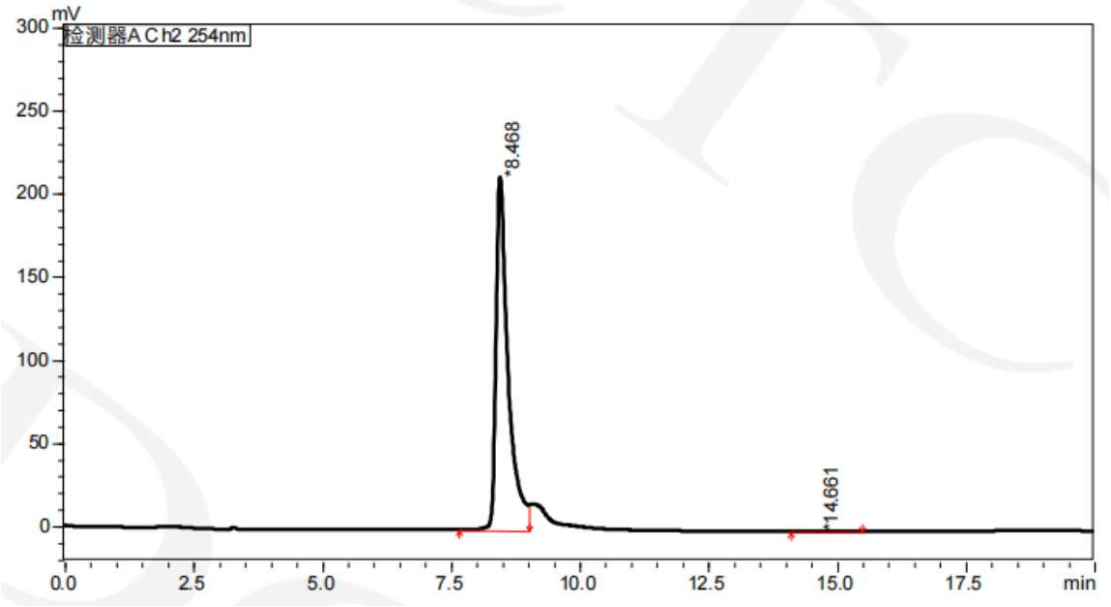

Peak	Ret. Time	Area	Area%	T.Plate	Tailing	Resolution
1	8.468	3477301	99.707	7681	--	--
2	14.661	10204	0.293	5813	1.651	10.718

(-)-13: *ee* > 98%

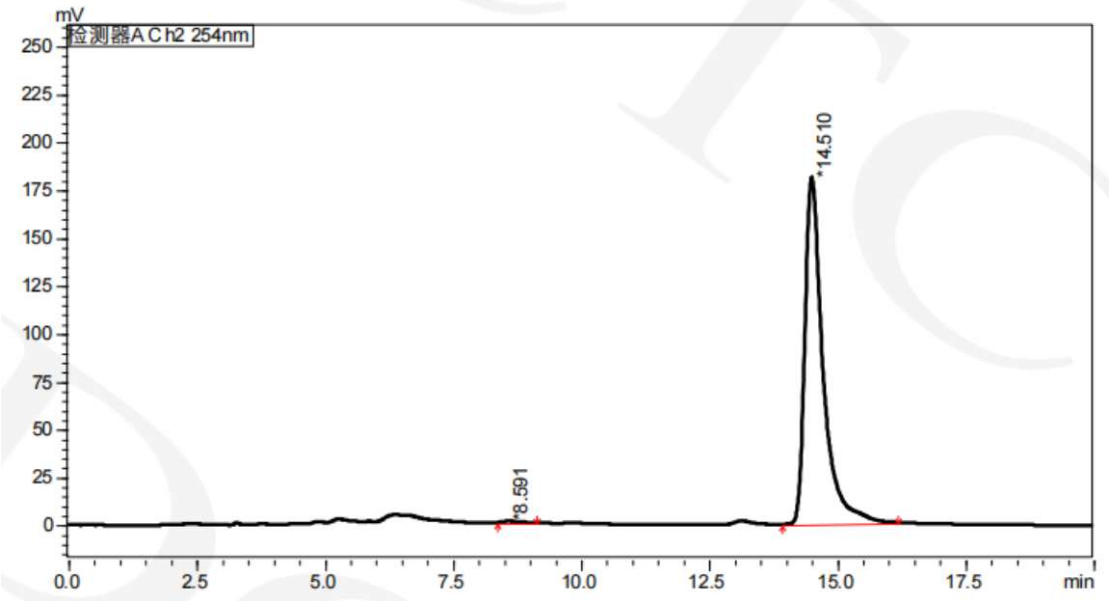

Peak	Ret. Time	Area	Area%	T.Plate	Tailing	Resolution
1	8.591	15970	0.358	2528	1.626	--
2	14.510	4448692	99.642	9750	1.731	9.314

Analytical chiral HPLC separation for compound **14**

Analytical chiral HPLC: Chiralpak IE-3 (0.46 cm I.D. × 25 cm L), DCM/EtOAc/DEA = 80/20/0.1 (V/V/V), 1.0 mL/min, UV detection at 254 nm.

Racemic mixture:

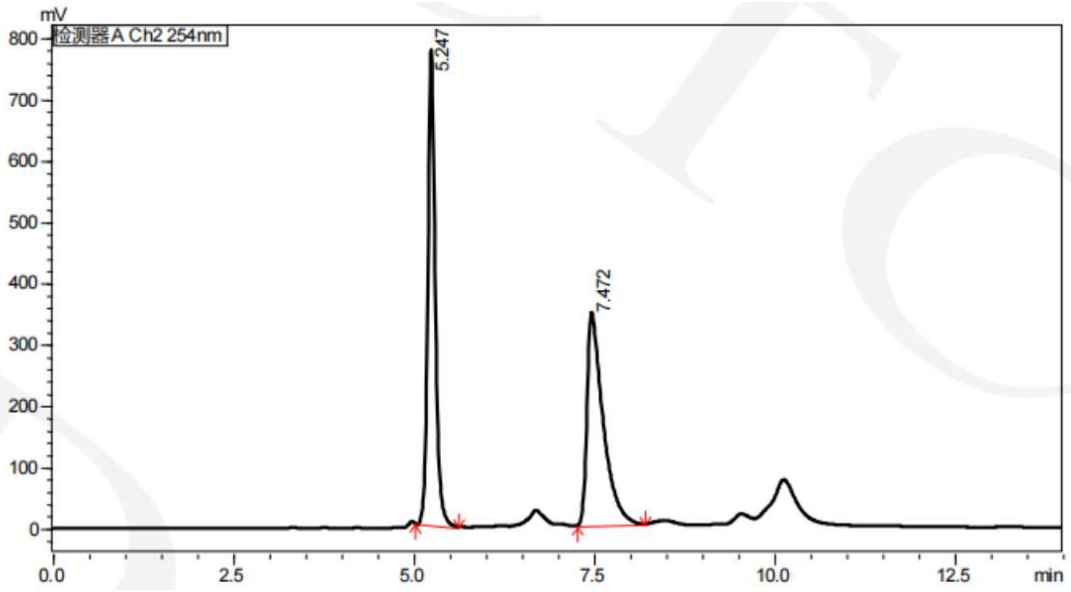

Peak	Ret. Time	Area	Area%	T.Plate	Tailing	Resolution
1	5.247	5470273	50.506	12042	1.173	--
2	7.472	5360647	49.494	5536	2.130	7.504

(+)-14: *ee* > 98%

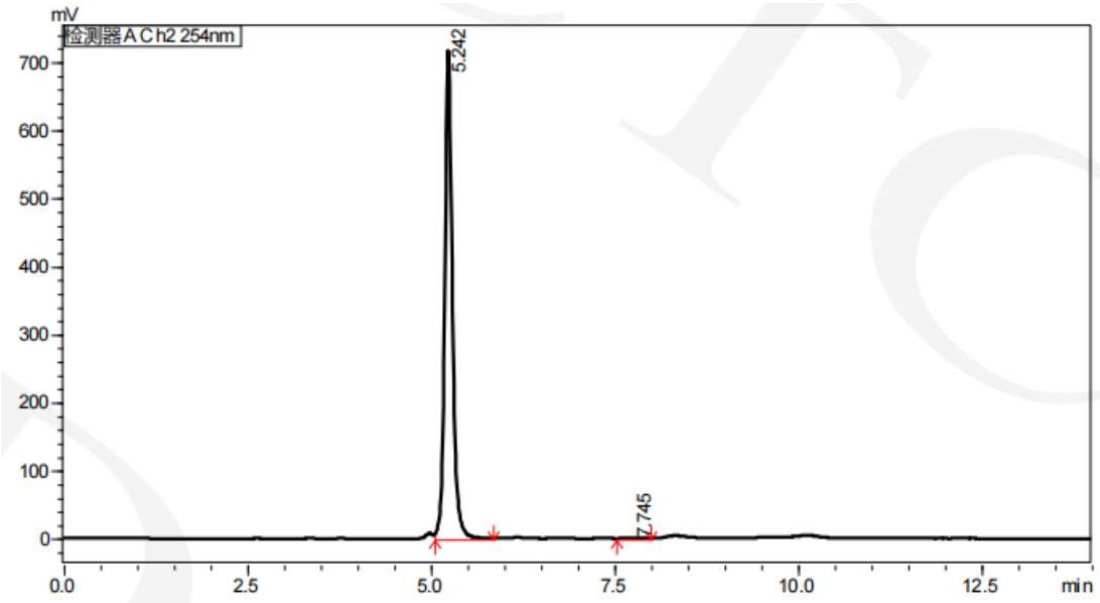

Peak	Ret. Time	Area	Area%	T.Plate	Tailing	Resolution
1	5.242	5188607	99.705	11828	1.158	--
2	7.745	15346	0.295	2168	--	5.833

(-)-14: *ee* > 98%

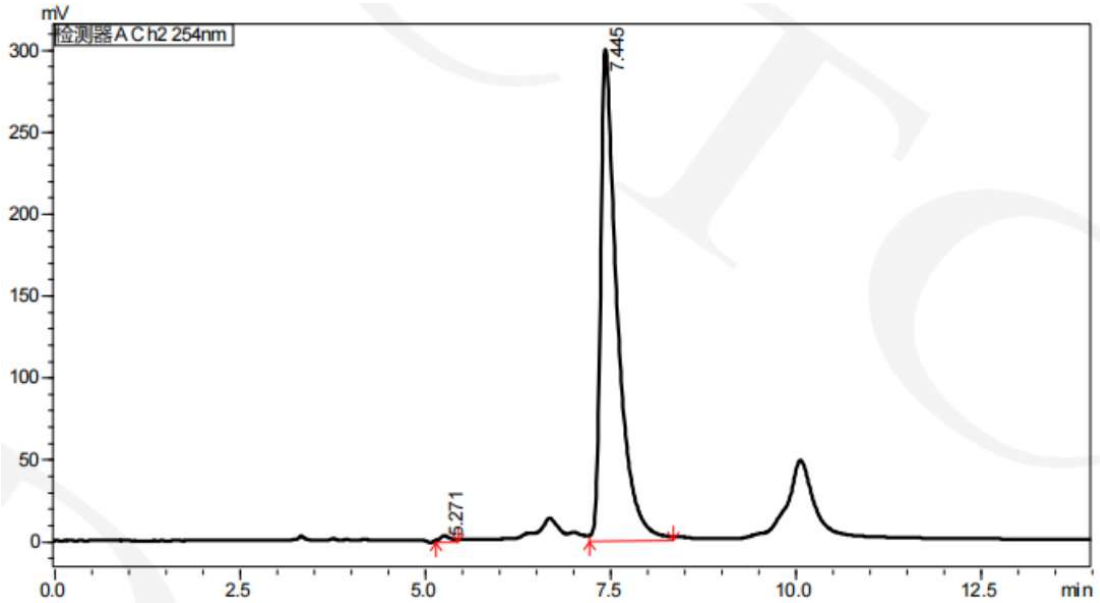

Peak	Ret. Time	Area	Area%	T.Plate	Tailing	Resolution
1	5.271	29205	0.618	6948	--	--
2	7.445	4699209	99.382	5801	2.144	6.753

Analytical chiral HPLC separation for compound **20**

Analytical chiral HPLC: Chiralpak IM (0.46 cm I.D. × 15 cm L), DCM/MeOH = 80/20 (V/V), 1.0 mL/min, UV detection at 254 nm.

Racemic mixture:

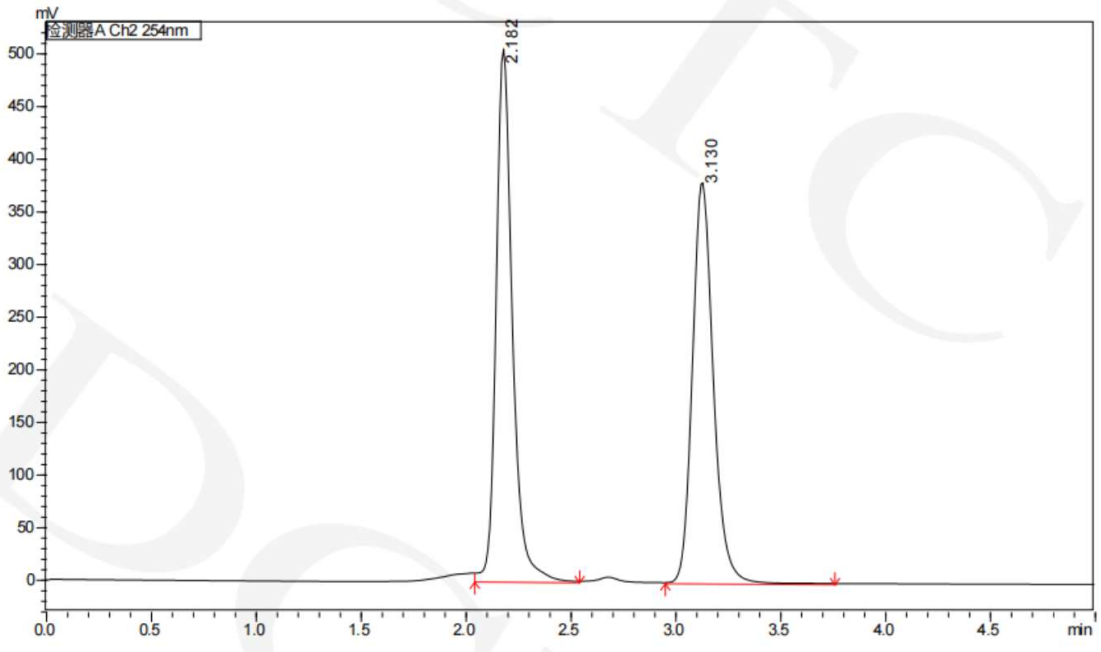

Peak	Ret. Time	Area	Area%	T.Plate	Tailing	Resolution
1	2.182	2732628	51.046	3380	1.261	--
2	3.130	2620688	48.954	4366	1.187	5.580

***M*-20**: *ee* > 98%

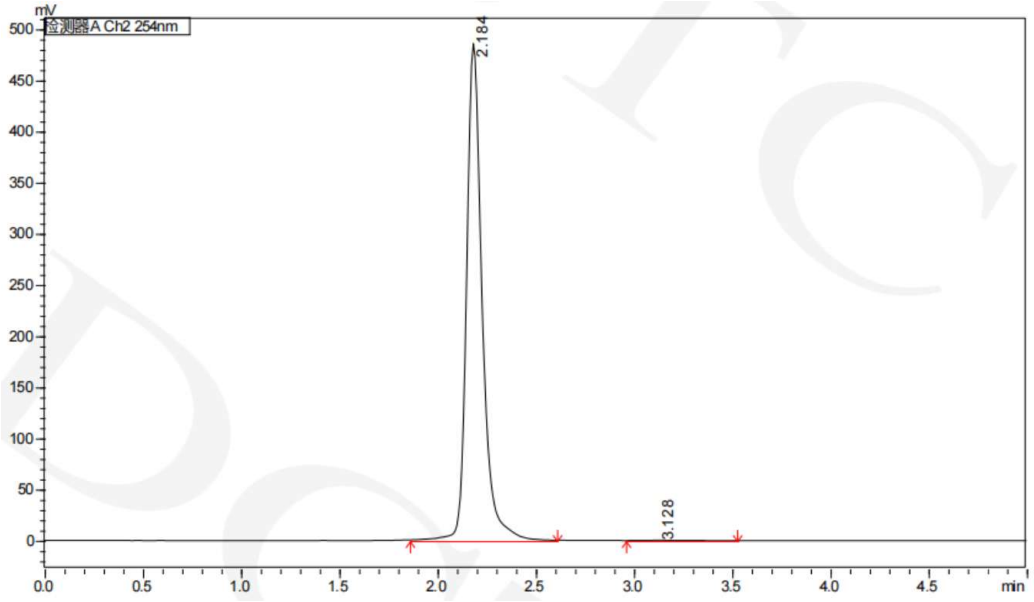

Peak	Ret. Time	Area	Area%	T.Plate	Tailing	Resolution
1	2.184	2688809	99.869	3271	1.304	--
2	3.128	3520	0.131	2626	1.588	4.754

***P*-20**: *ee* > 98%

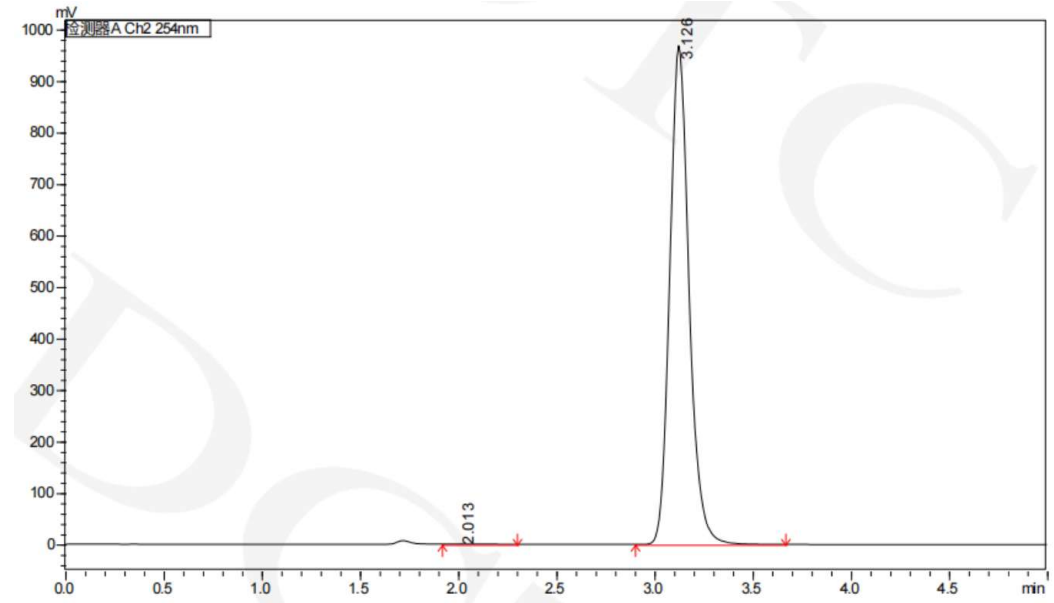

Peak	Ret. Time	Area	Area%	T.Plate	Tailing	Resolution
1	2.013	9451	0.143	337	--	--
2	3.126	6608466	99.857	4405	1.178	3.552

7 Photophysical Properties

7.1 UV-Vis Absorption and Fluorescence

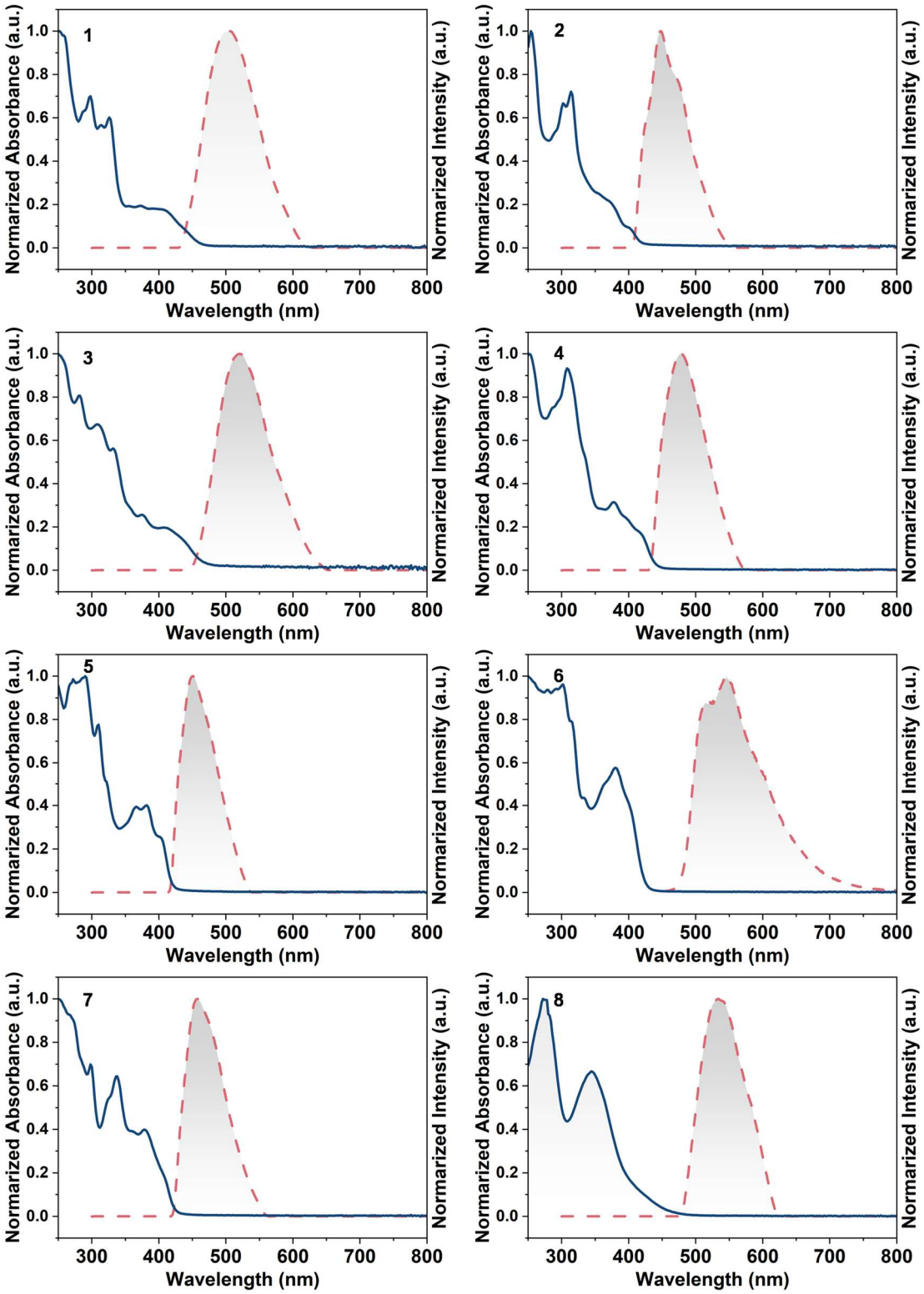

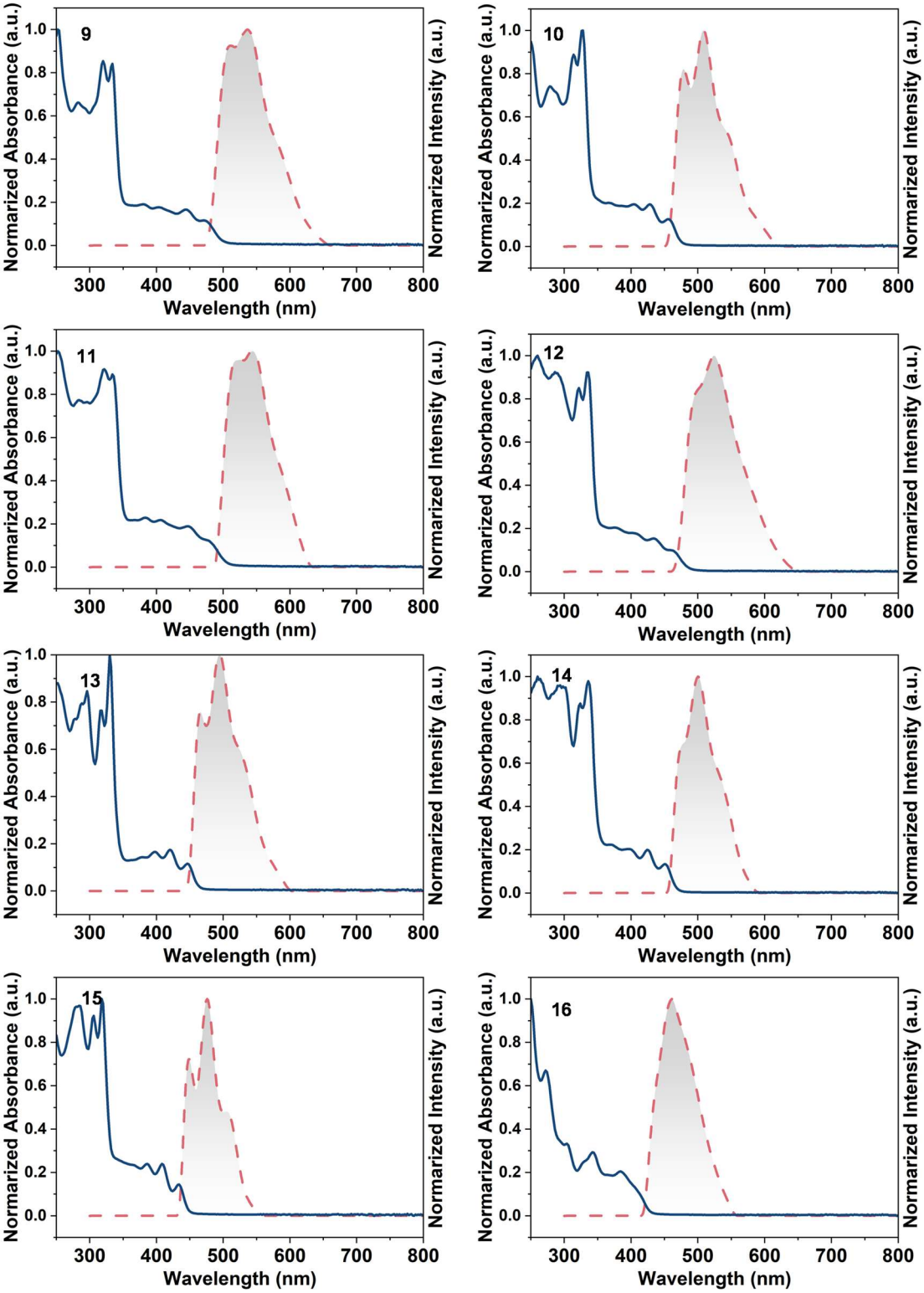
9
10
11
12
13
14
15
16
Normarized Absorbance (a.u.)
Normarized Intensity (a.u.)
Wavelength (nm)
0.0
0.2
0.4
0.6
0.8
1.0
300
400
500
600
700
800

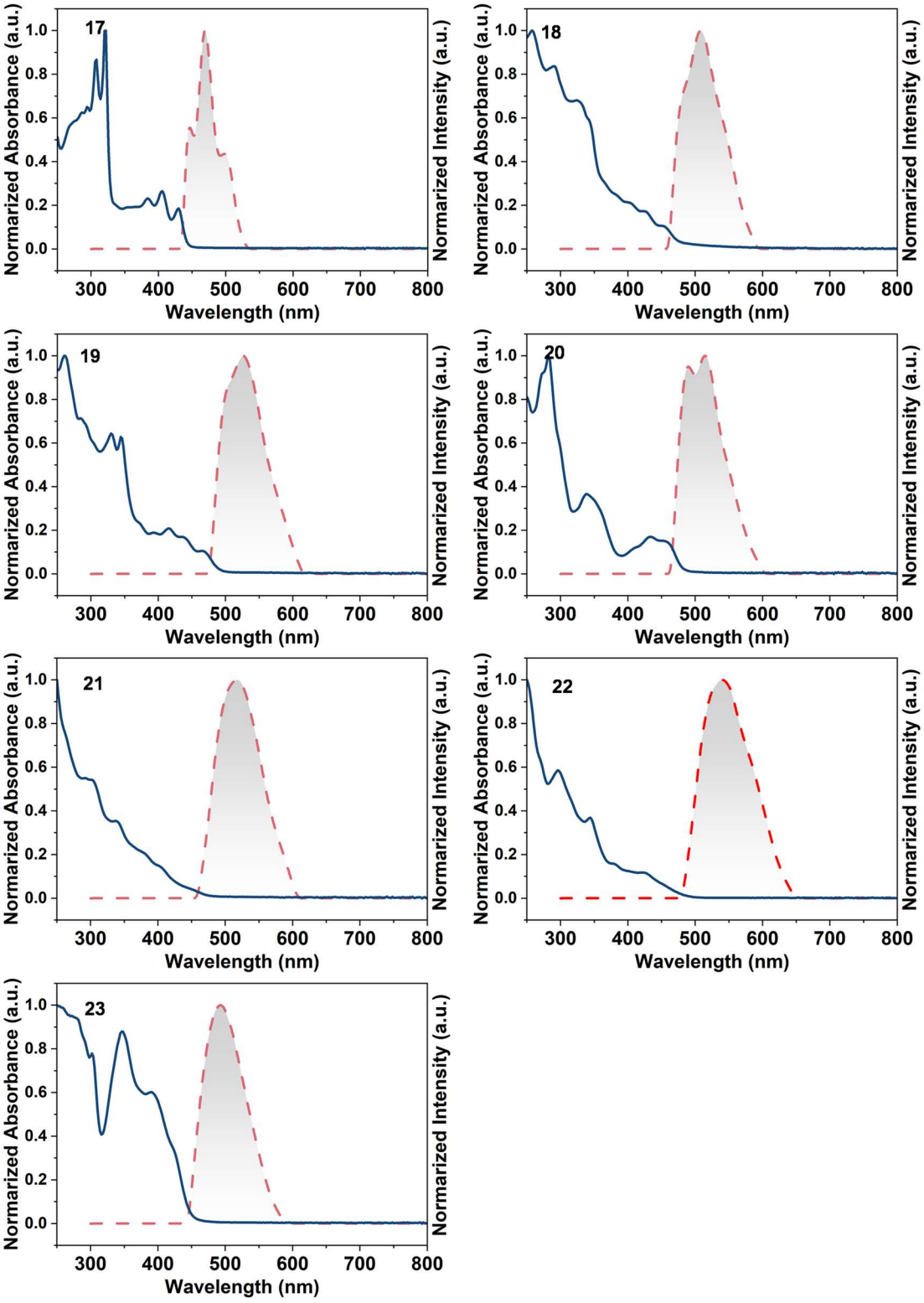

Figure S21. Absorption and fluorescence spectra of aza[5–9]helicenes **1–23**

7.2 Circular Dichroism (CD)

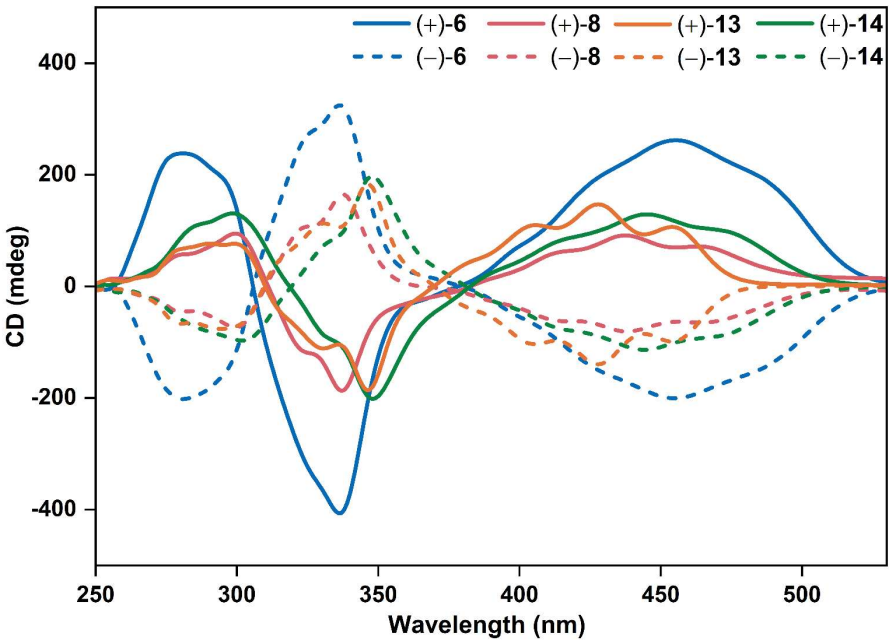

Figure S22. CD spectra of **6**, **8**, **13** and **14** in DCM (7.00×10^{-5} M, 298 K)

7.3 Circularly polarized luminescence (CPL)

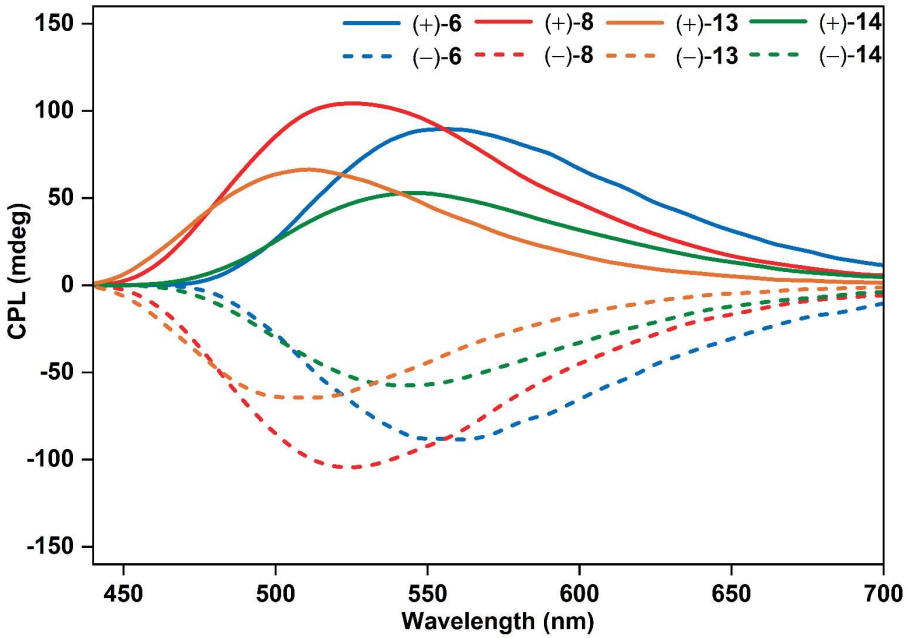

Figure S23. CPL (Ex at 340 nm) spectra of **6**, **8**, **13** and **14** in DCM (7.00×10^{-5} M, 298 K)

Table 15. Photophysical properties of aza[5–9]helicenes.

Helicene[a]	$\lambda_{max(abs)}$ (nm)[b]	$\lambda_{max(em)}$ (nm)[b,c]	Φ[c,d]	g_{lum}[e,f]
1 [5]H.	410	505	0.46	-
18 [6]H.	455	508	0.45	-
6 [7]H.	404	550	0.37	0.012
8 [7]H.	423	535	0.34	0.014
11 [7]H.	480	544	0.29	0.0083
13 [7]H.	448	495	0.35	0.0088
14 [7]H.	452	500	0.47	0.0065
20 [7]H.	459	516	0.03	0.0080
21 [8]H.	446	518	0.11	0.008[g]
22 [9]H.	427	541	0.04	0.027[g]

[a][n]H short for [n]helicene. [b]Concentration: 7.00×10^{-5} M in CH_2Cl_2. [c]Excitation wavelength: **1**: 410 nm, **18**: 450 nm, **6**: 400nm, **8**: 420, **11**: 470 nm, **13**: 460 nm, **14**: 450 nm, **20**: 470 nm, **21**: 400 nm, **22**: 425 nm. [d]Concentration: 7.00×10^{-6} M in CH_2Cl_2. [e] CPL excitation wavelength: **6**: 340 nm, **8**: 340 nm, **11**: 320 nm, **13**: 335 nm, **14**: 340 nm, **20**: 337 nm. [f]CPL emission wavelength: **6**: 550 nm, **8**: 530 nm, **11**: 480 nm, **13**: 504 nm, **14**: 523 nm, **20**: 470 nm. [g]g_{lum} values taken from reference 2.[2]

8 DFT Calculations

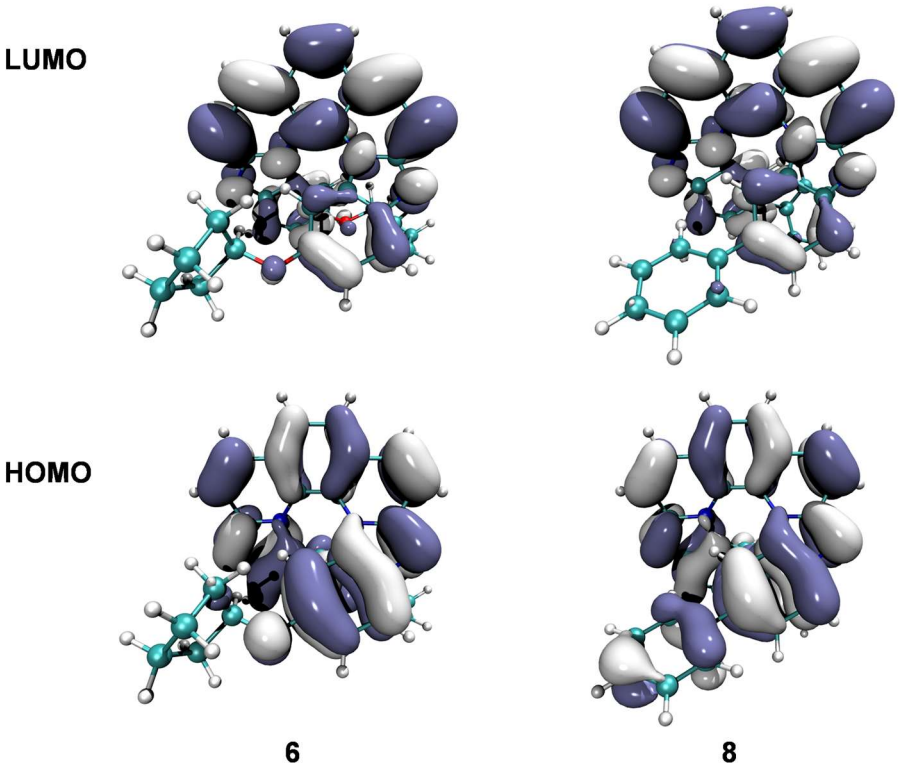

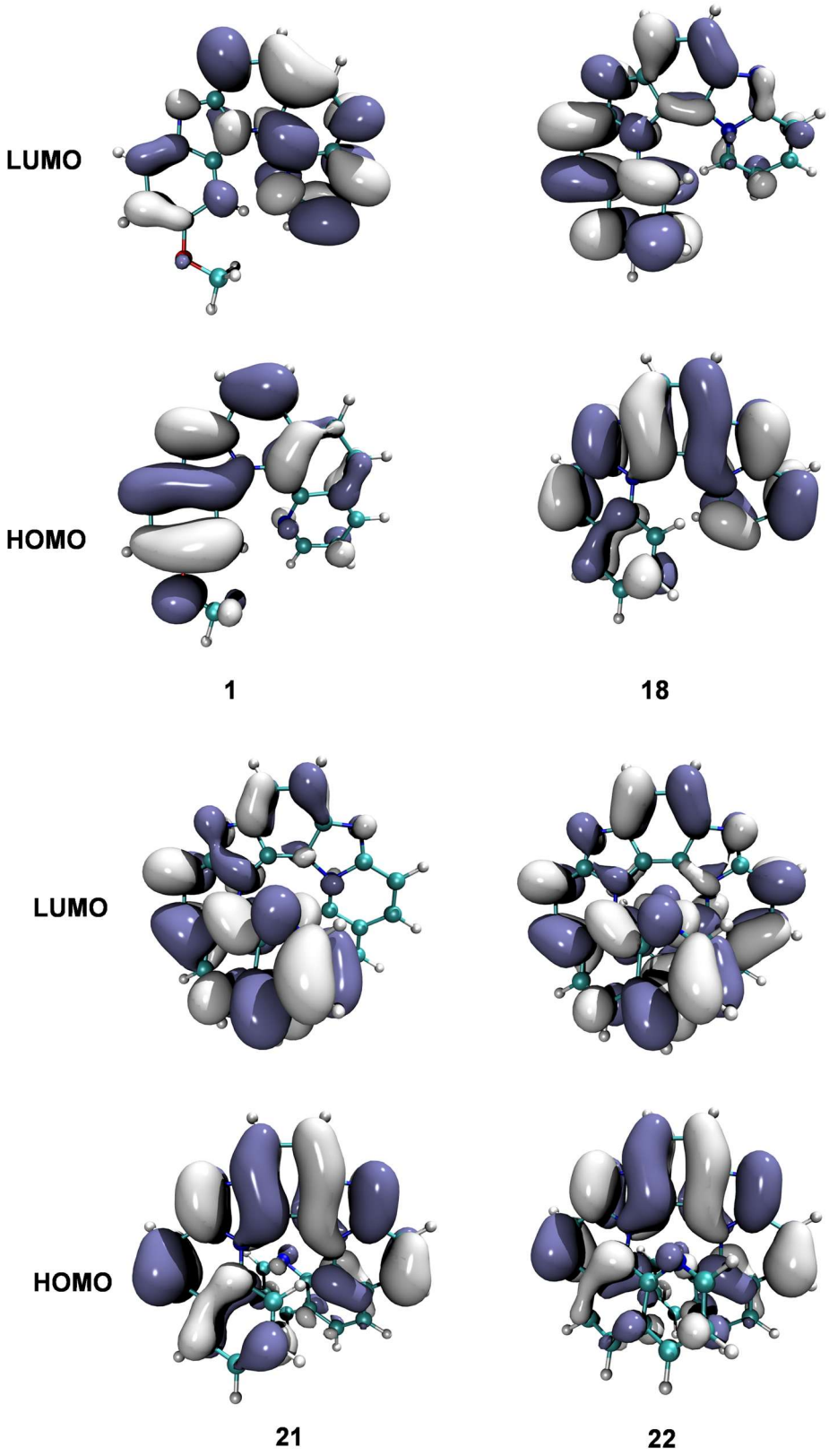

Figure S24. LUMOs and HOMOs of [5–9]helicenes **1**, **6**, **8**, **13**, **14**, **18**, **21** and **22** calculated at B3LYP/6-31G(d) level.

9 AFM Topography of the Thin Films of Helicene Enantiomers

AFM experiments were carried out to visualize the morphology of the helicene enantiomers of **11** and **20**. Samples were prepared by spin-coating a 10 µM DCM solution of the corresponding assembly onto freshly cleavaged HPOG. The results are summarized below.

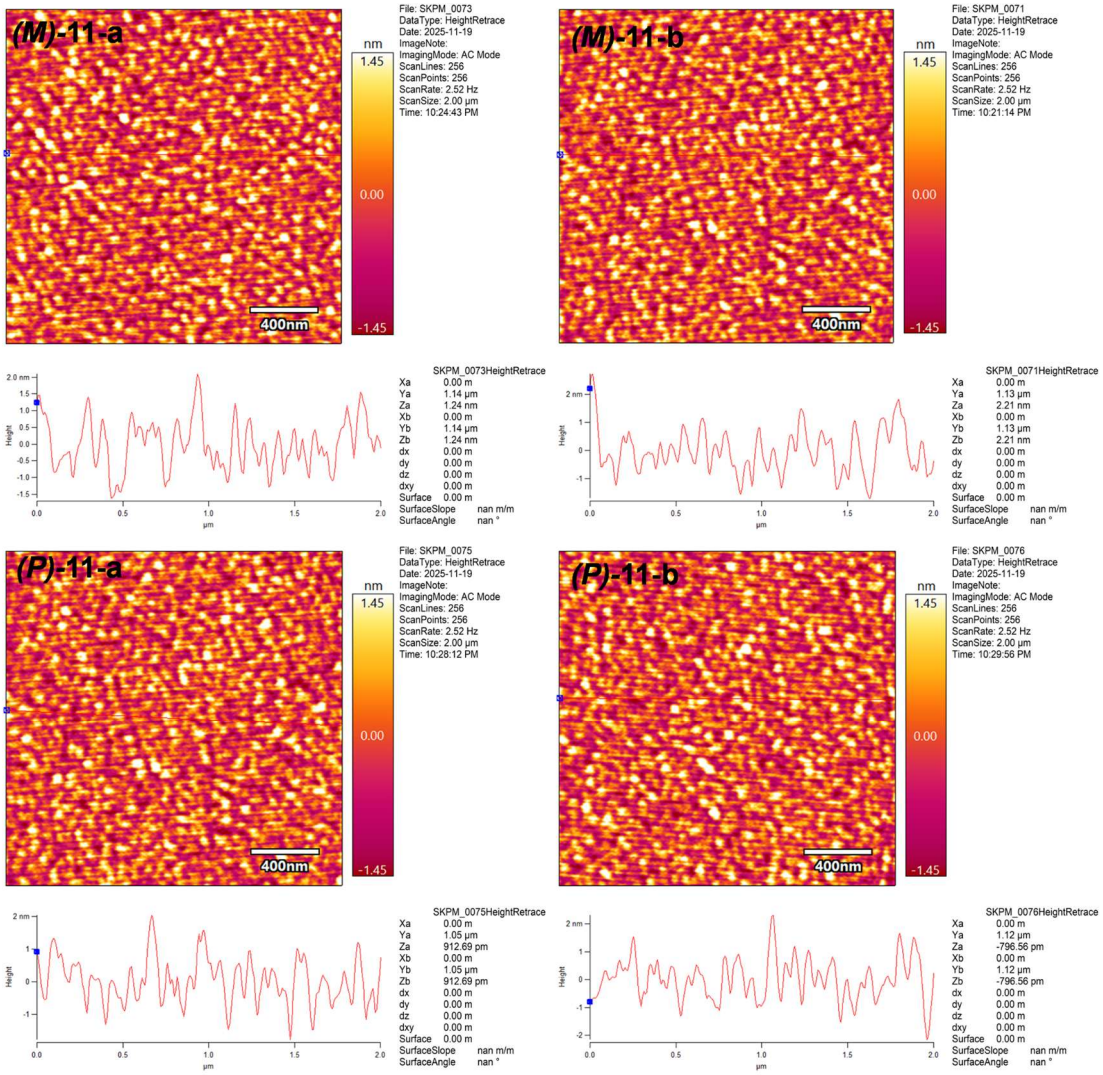

Figure S25. AFM studies for **(*M*)-11** and **(*P*)-11**. Insets: AFM height profile of the red line drawn in the AFM image. Note that the scanning area is different for (a) and (b).

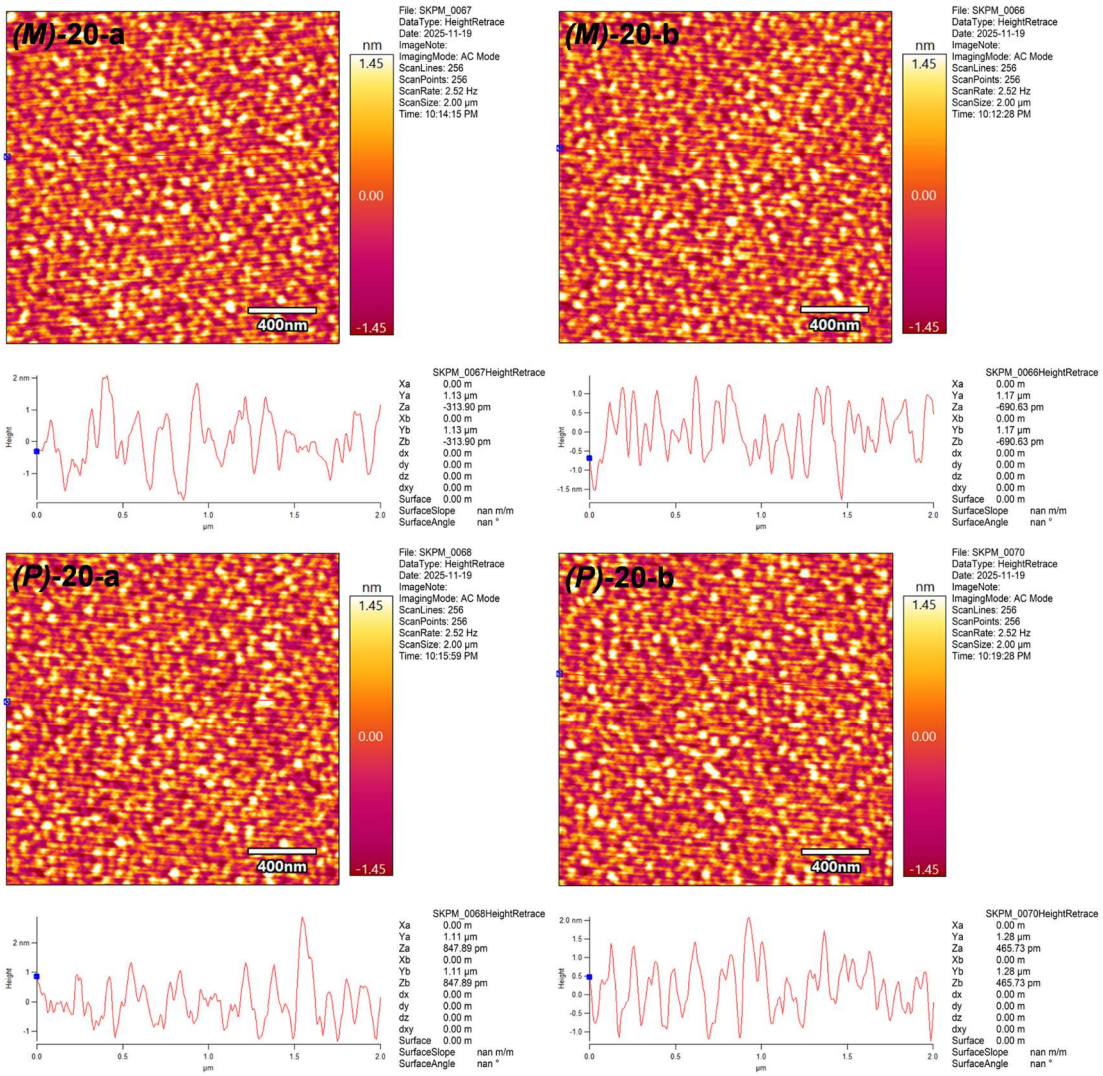

Figure S26. AFM studies for **(*M*)-20** and **(*P*)-20**. Insets: AFM height profile of the red line drawn in the AFM image. Note that the scanning area is different for (a) and (b).

AFM analysis indicates that the chiral *M*-helicenes or *P*-helicenes spin-coated onto the highly oriented pyrolytic graphite (HOPG) substrates exhibited the mean thickness of ±1 nm to ±1.5 nm, suggesting a uniform, flat morphology.

10 Spin Polarization of Thin Films of Helicene Enantiomers

Magnetic conductive probe atomic force microscope (mc-AFM) measurements were performed using Oxford MFP-3D Origin. The thin films of chiral helicenes were prepared on freshly cleaved HOPG substrates by spin-coating the helicene solution (10 μM). Current-voltage measurements (*I-V*) were recorded by performing voltage bias with the tip in contact with the surface of the film. The tests were carried out by a Co-Cr-coated AFM tips (MEPS-V2, Bruker, nominal tip radius of 12 nm with spring constant of ~3 N/m). Spin selective tests were performed by pre-magnetizing the AFM tips using a magnet (0.5 T) on up and down magnetization directions, in which tip+ means the field-up with respect to the substrate, while tip- means the field-down with respect to the substrate. When the testing time was over 1 h, the tip was re-magnetized. The *I-V* curves were measured across the bias from -2.0 V to +2.0 V, with a frequency of 0.5 Hz. In a similar way, the *I-V* curves of other helicenes were also recorded. For these helicenes, the *I-V* spectra refer to the measurements of longitudinal CISS effect, where spin selectivity occurs for electrons injected parallel to the helix axis.[3–5]

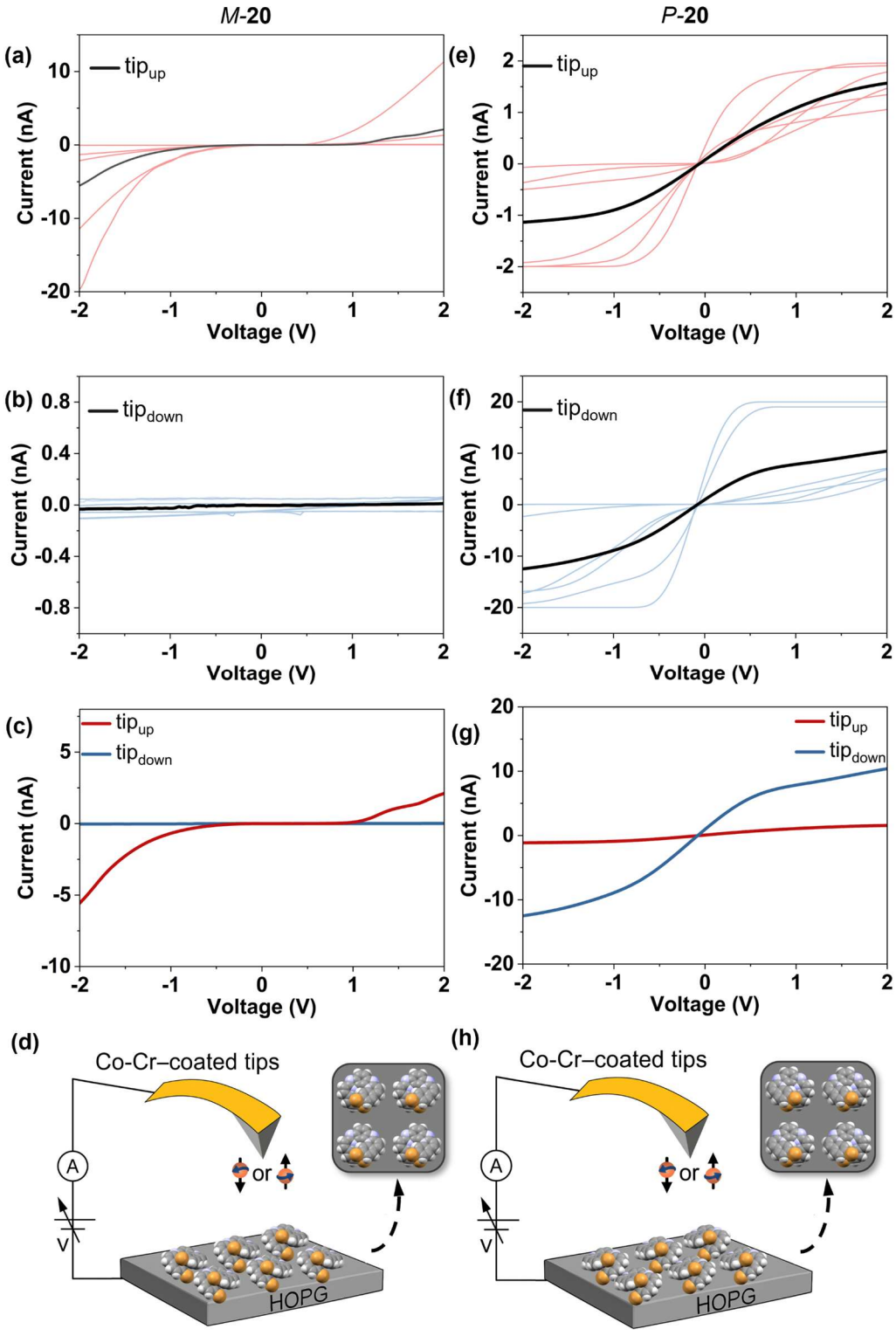

Figure S27. Spin-dependent conduction through the helicene *M*-**20** (**a**–**d**) and *P*-**20** (**e**–**h**) thin films. Each line (red and blue) represents one measurement, and the solid black lines represent the average of *I*-*V* curves. Note the ordinate scales are different in the individual figures to suit each *I*-*V* curves.

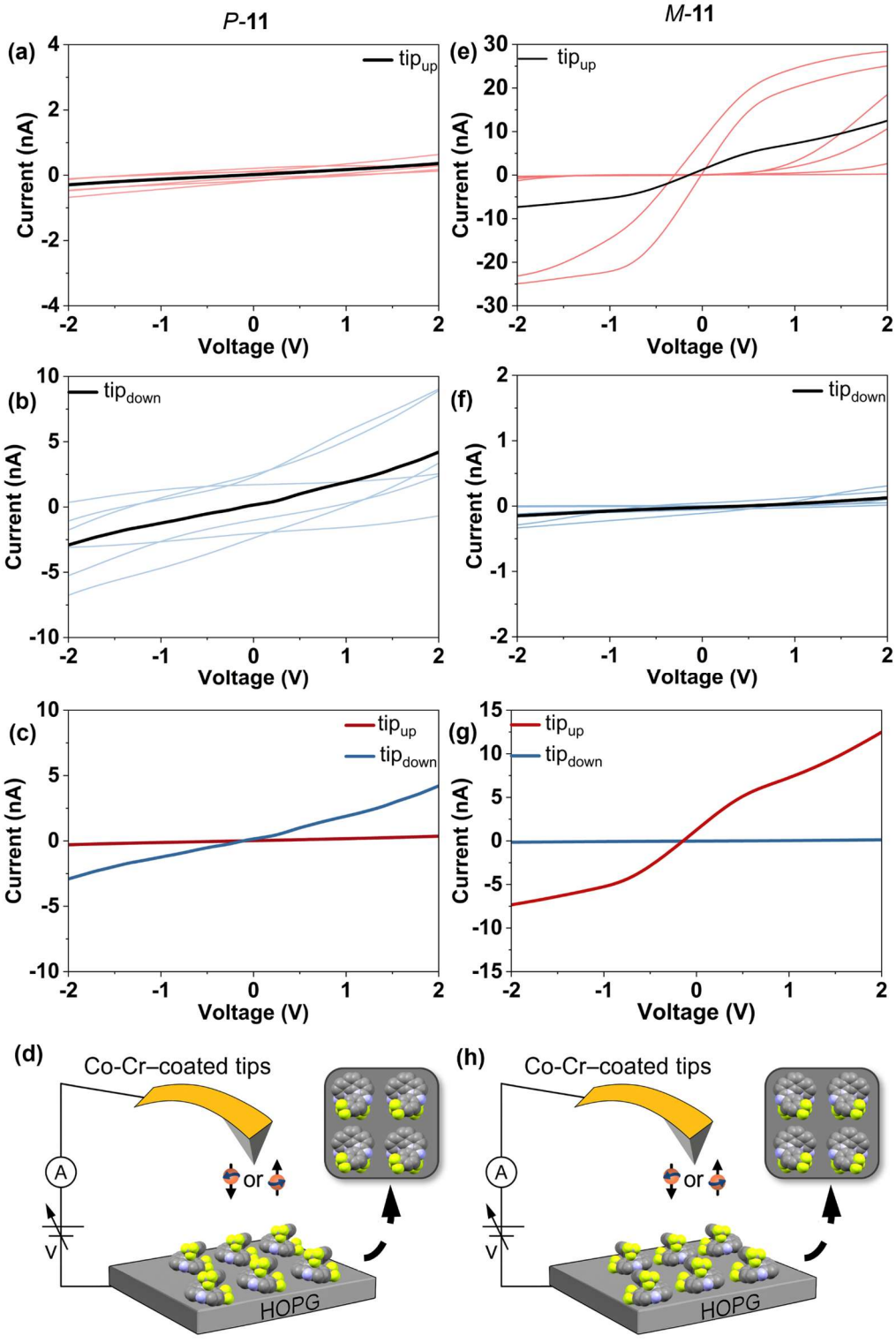

Figure S28. Spin-dependent conduction through the helicene *P*-**11** (**a**–**d**) and *M*-**11** (**e**–**h**) thin films. Each line (red and blue) represents one measurement, and the solid black lines represent the average of *I*-*V* curves. Note the ordinate scales are different in the individual figures to suit each *I*-*V* curves.

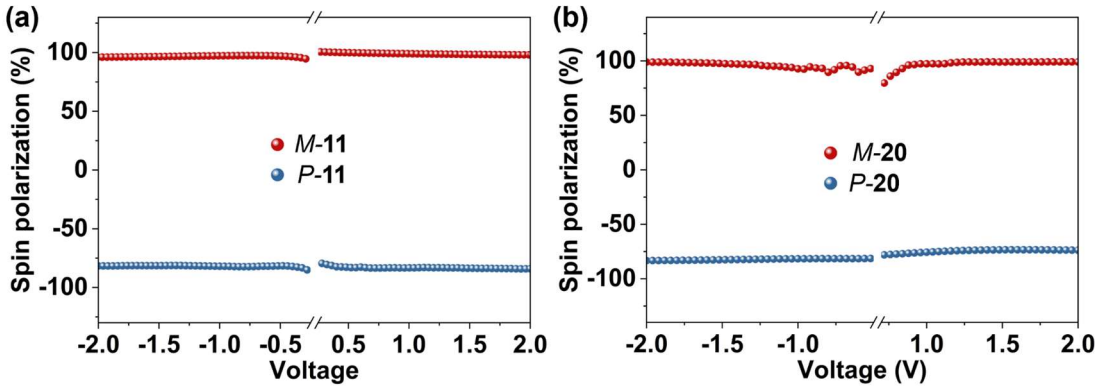

Figure S29. Spin polarization as a function of applied bias for *P*-**11** (blue) and *M*-**11** (red) samples (**a**) and for *P*-**20** (blue) and *M*-**20** (red) samples (**b**).

Table S16. Comparision of the comprehensive spin-selective properties of various categories of chiral systems.

No.	Categories	SP (%)	Spin current (nA)
1[6]	Molecular motors-1	25–60	150
2[7]	Molecular motors-2	44	< 0.15
3[8]	Molecular motors-3	14–96	3
4[9]	Molecular wires-1	32	< 1.0
5[10]	Molecular wires-2	50	2.4
6[11]	Helicenes-1	26	2
7[12]	Helicenes-2	60	2
8[13]	Helicenes-3	80	20
9[3]	Helicenes-4	80	1.2
10[14]	Helicenes-5	60	2
11[15]	Helicenes-6	50	0.6
12[16]	Helicenes-7	49	1
13[17]	Helicenes-8	40	4
14[18]	Chiral polymers-1	56	2.2
15[19]	Chiral polymers-2	52	< 0.1
16[20]	Chiral polymers-3	70	45
17[21]	Supramolecular polymers-1	65	1.5
18[22]	Supramolecular polymers-2	50	< 4.0
19[23]	Supramolecular polymers-3	90	0.5
20[24]	Hybrid perovskites-1	94	7
21[25]	Hybrid perovskites-2	80	10
22[26]	Hybrid perovskites-3	78	60
23[27]	Chiral MOF-1	96.9	3000
24[28]	Chiral MOF-2	94	2

Table S16 (continue). Comparision of the comprehensive spin-selective properties of various categories of chiral systems.

No.	Categories	SP (%)	Spin current (nA)
25[29]	Chiral MOF-3	42	0.6
26[30]	Chiral COF-1	83	2
27[31]	Chiral COF-2	90	< 20
28[32]	Chiral COF-3	72	15
29[4]	Molecular knots-1	88	400
30[33]	Molecular knots-2	> 60	-
31[34]	Quantum dots	30	1
32[35]	Oligopeptide/DNA	60	3
33[36]	Subphthalocyanines	50	2
34[37]	MoS2	75	0.6
35[5]	Chiral organic cages	90	150
36[5]	Cage-based helical supramolecular nanofibrils	82	330
37	Helicene **11** (This work)	**94**	**20**
38	Helicene **20** (This work)	**87**	**20**

11 NMR Spectra

***N*-(4-methoxyphenyl)-1,10-phenanthrolin-2-amine (1a)**: ^{1}H NMR (400 MHz, DMSO-d_6)

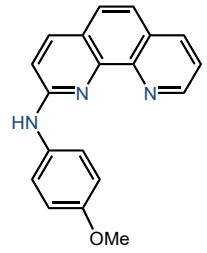

1a

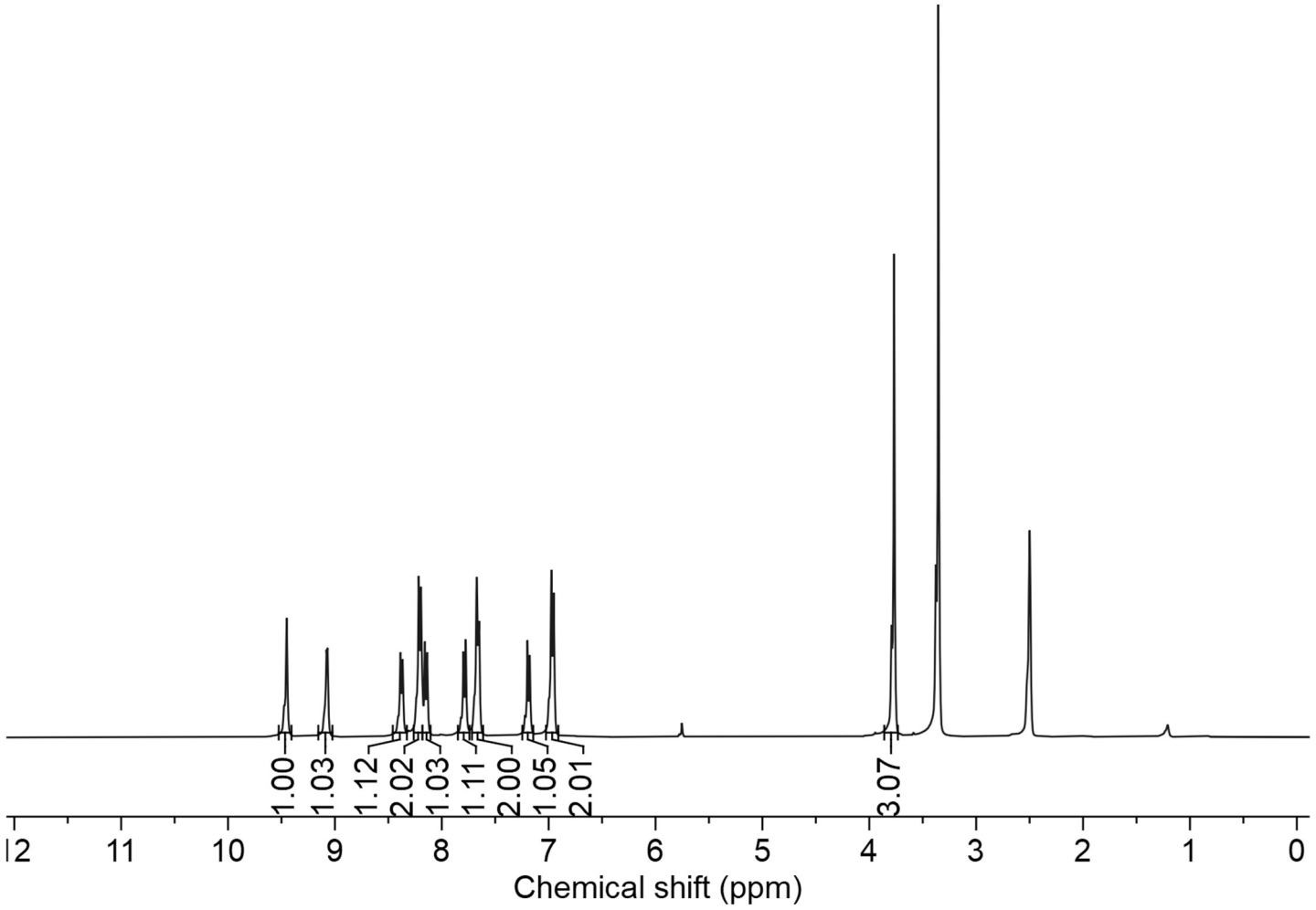

^{13}C NMR (100 MHz, DMSO-d_6)

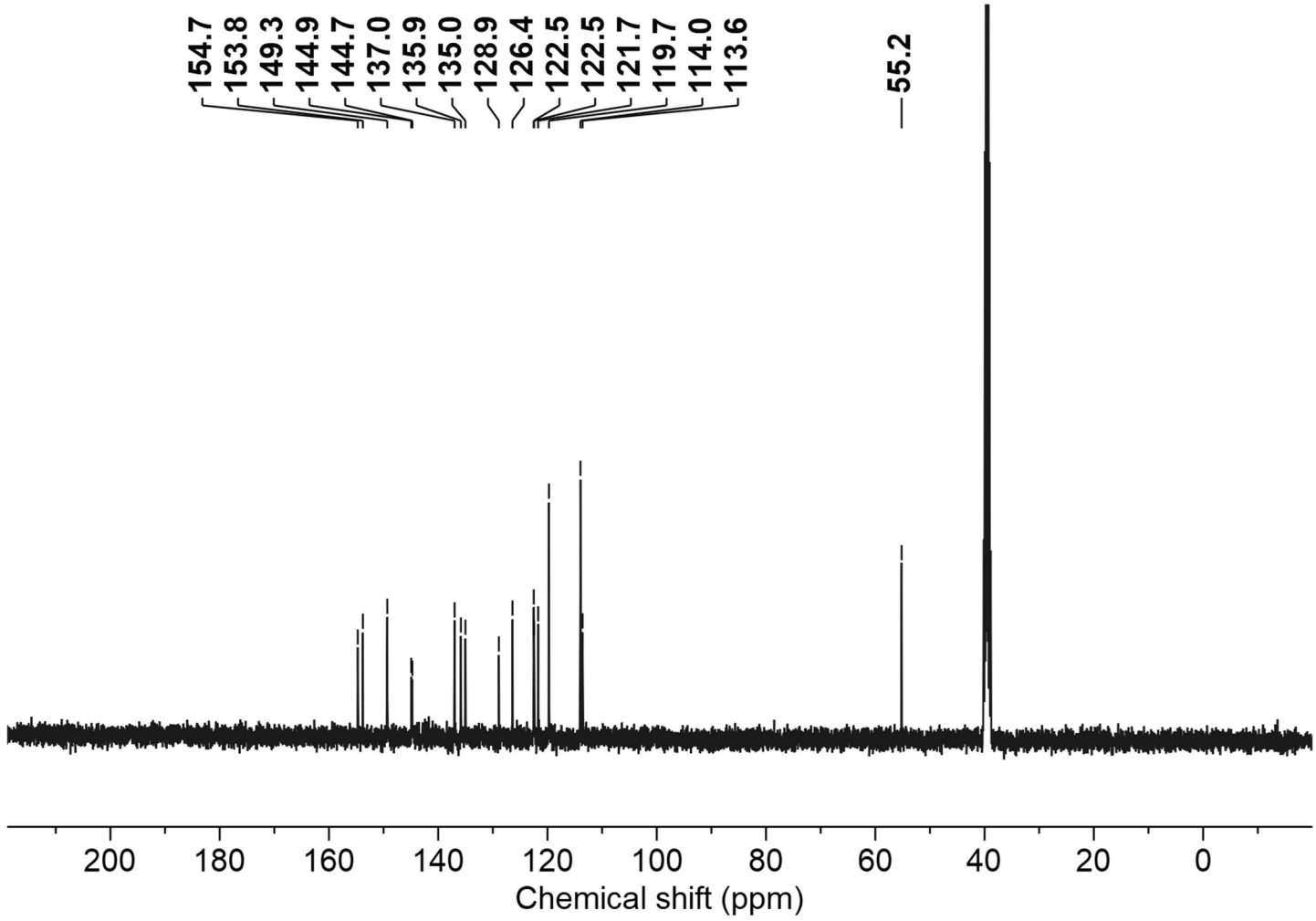

4-((1,10-phenanthrolin-2-yl)amino)benzonitrile (2a): ^{1}H NMR (400 MHz, DMSO-d_6)

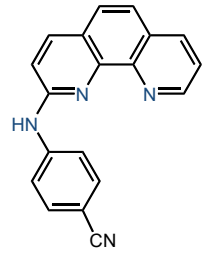

2a

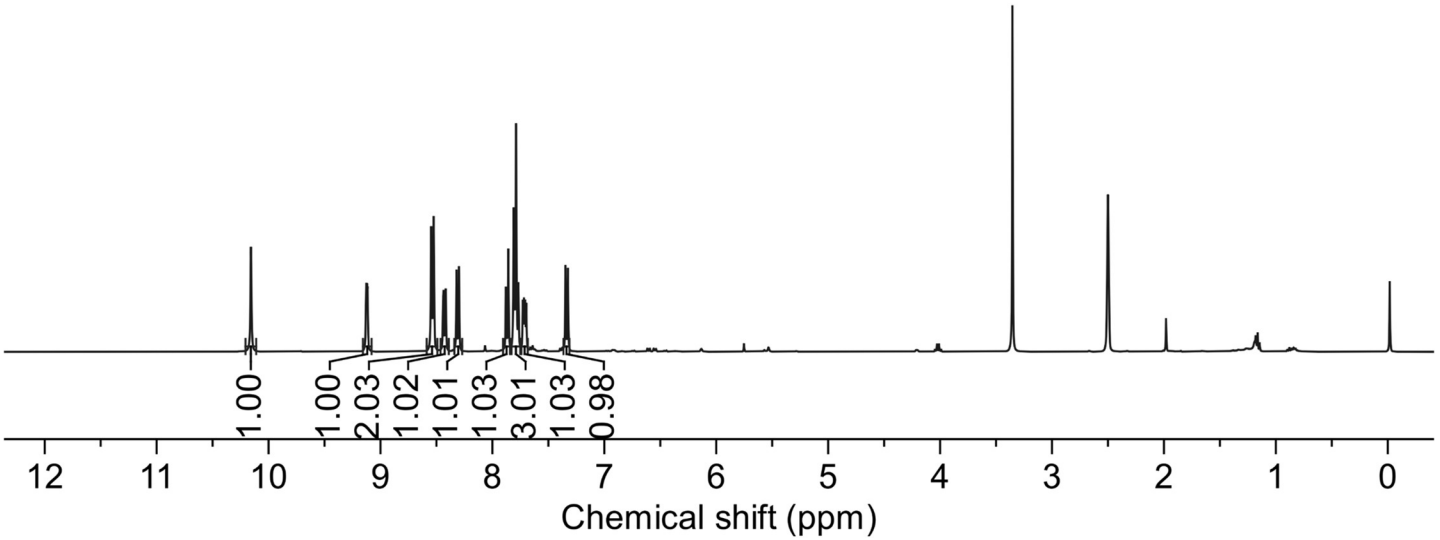

^{13}C NMR (100 MHz, DMSO-d_6)

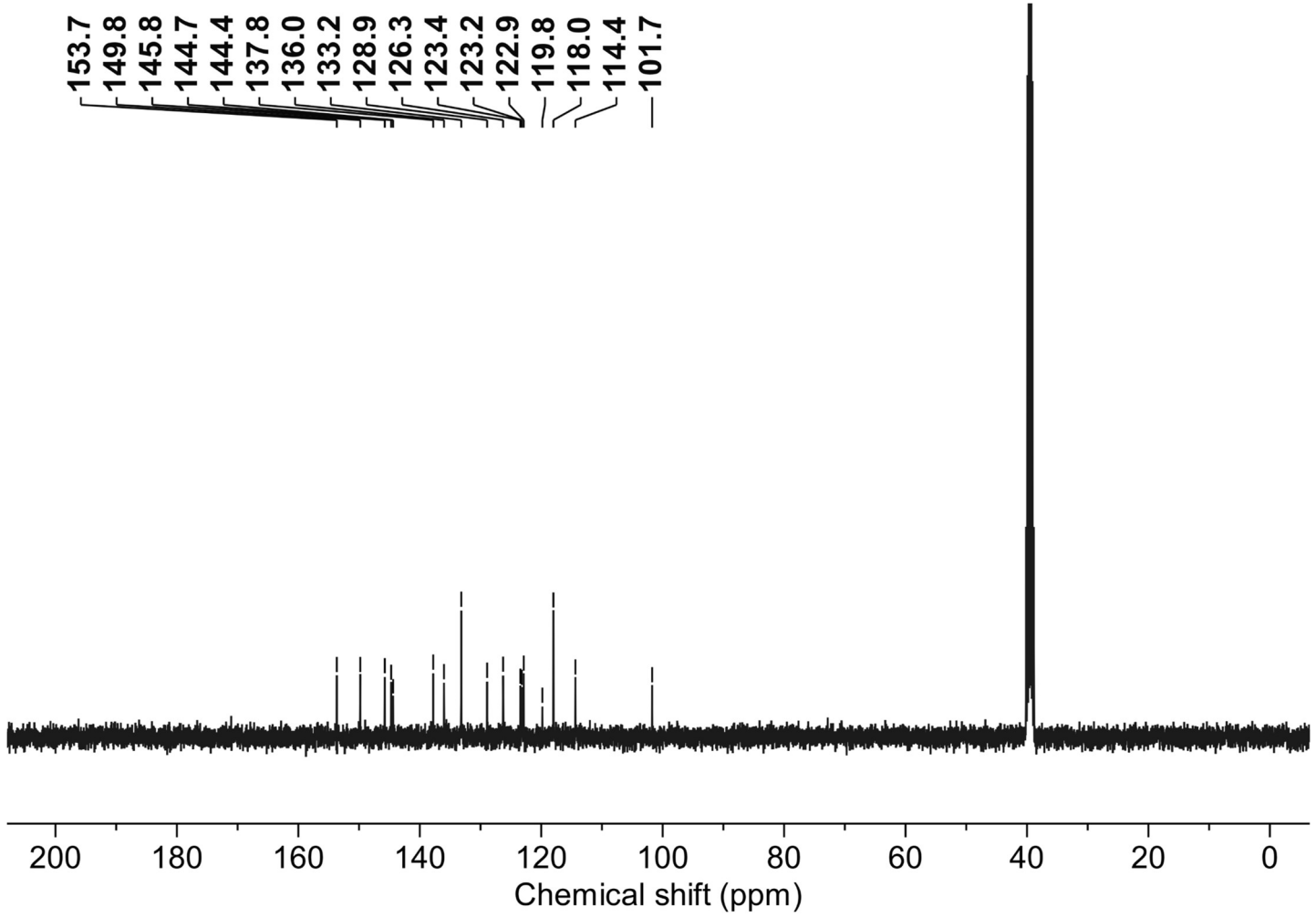

***N*-(quinolin-8-yl)-1,10-phenanthrolin-2-amine (3a)**: ^{1}H NMR (400 MHz, $CDCl_3$)

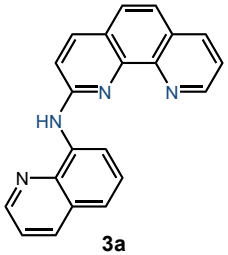

3a

..

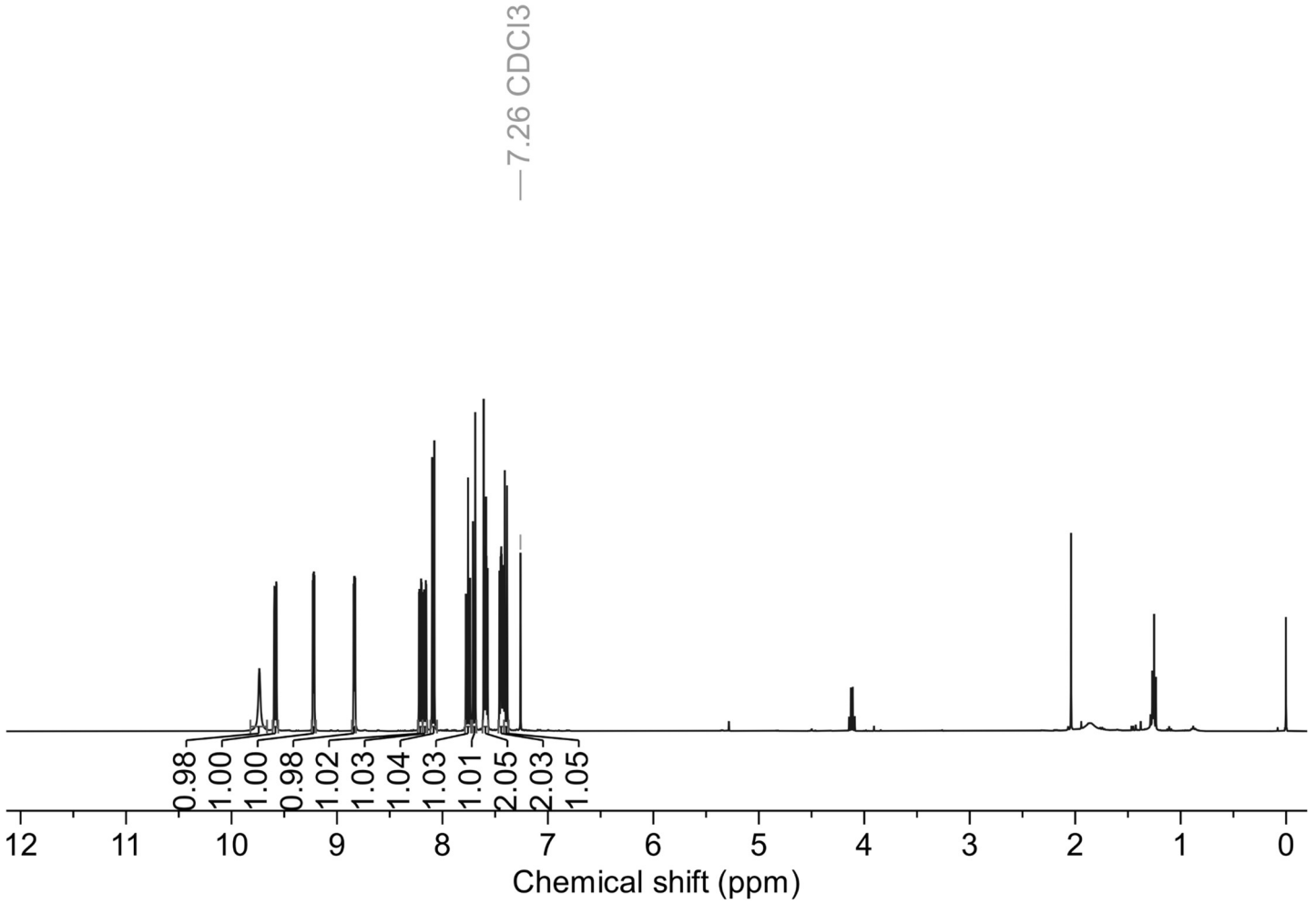

^{13}C NMR (100 MHz, $CDCl_3$)

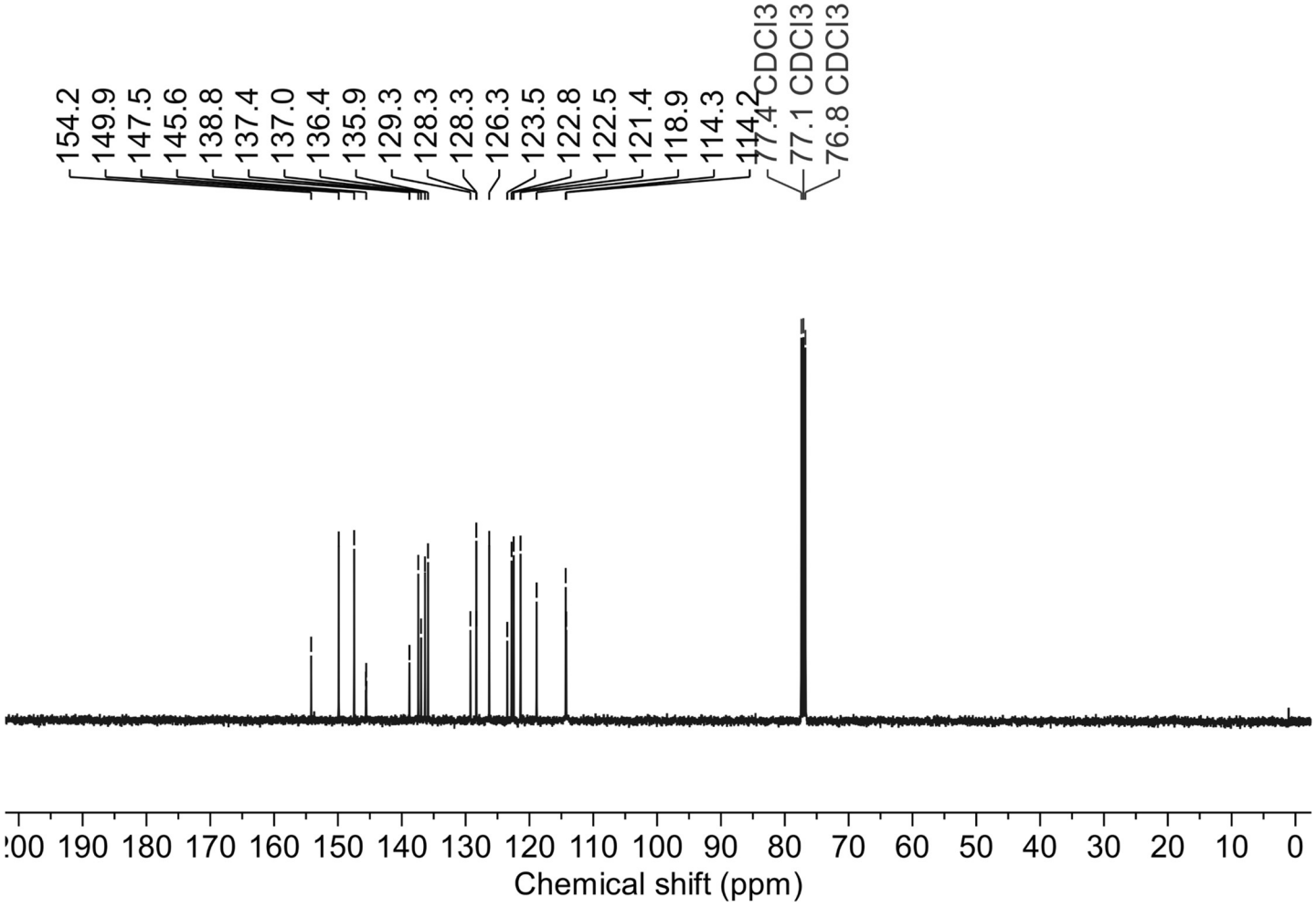

***N*^{2},*N*^{9}-diphenyl-1,10-phenanthroline-2,9-diamine** (**4a**):^{1}H NMR (400 MHz, $CDCl_3$)

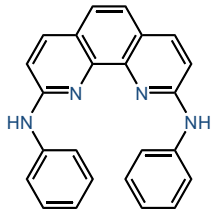

4a

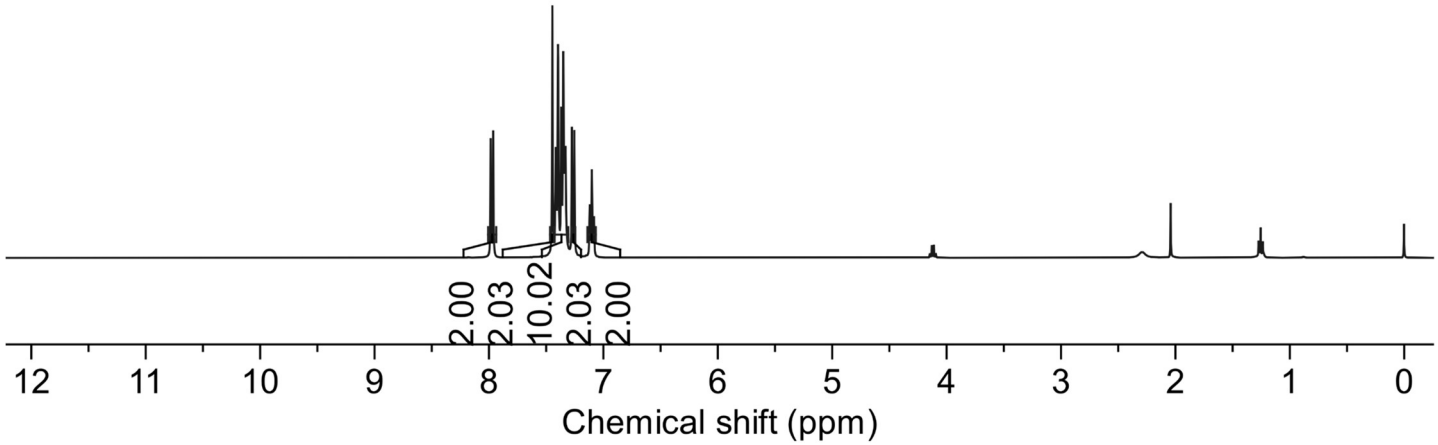

^{13}C NMR (100 MHz, $CDCl_3$)

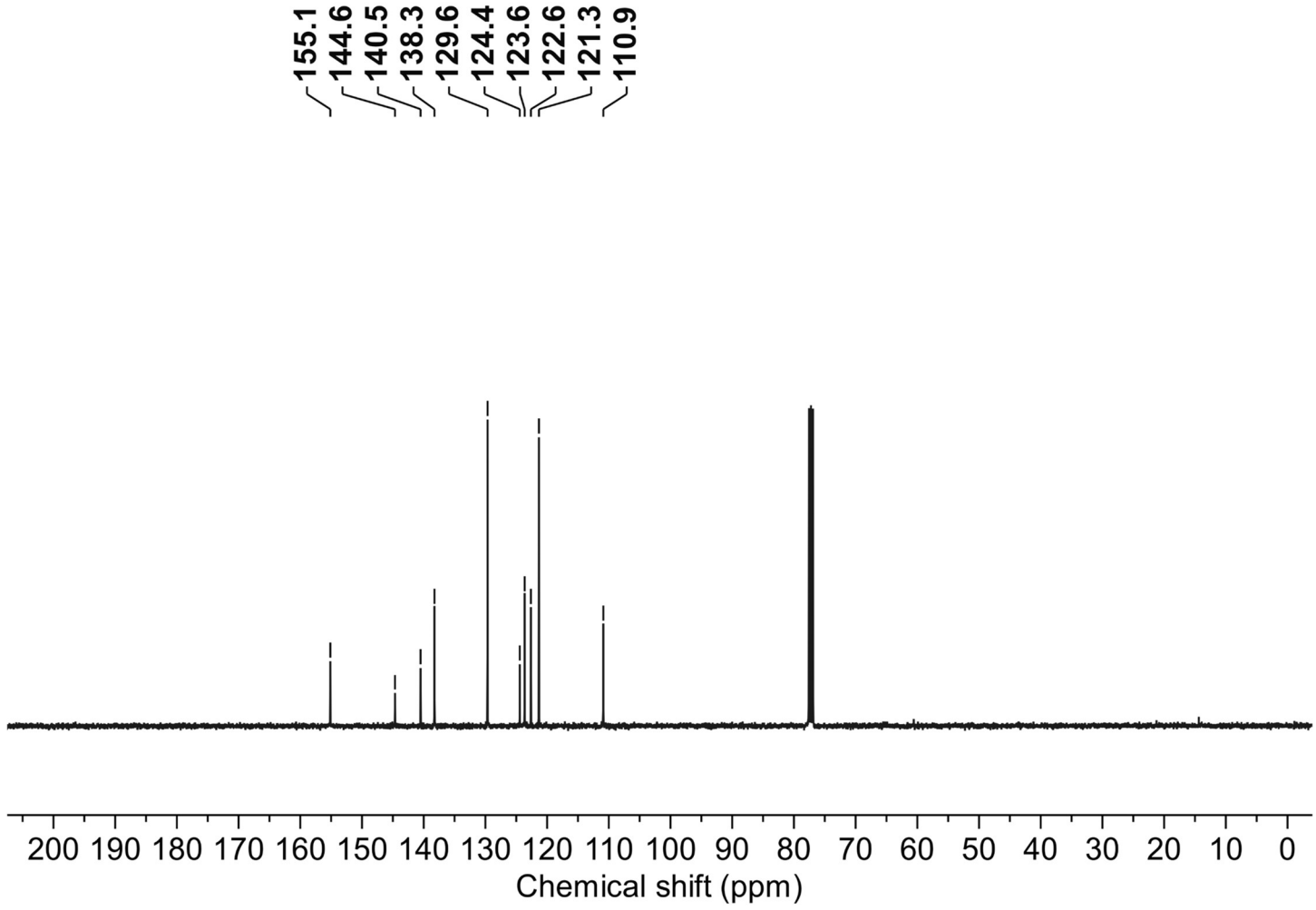

***N*²,*N*⁹-bis(4-methoxyphenyl)-1,10-phenanthroline-2,9-diamine** (**5a**): ^{1}H NMR (400 MHz, $CDCl_3$)

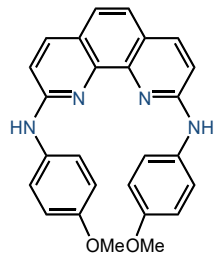

5a

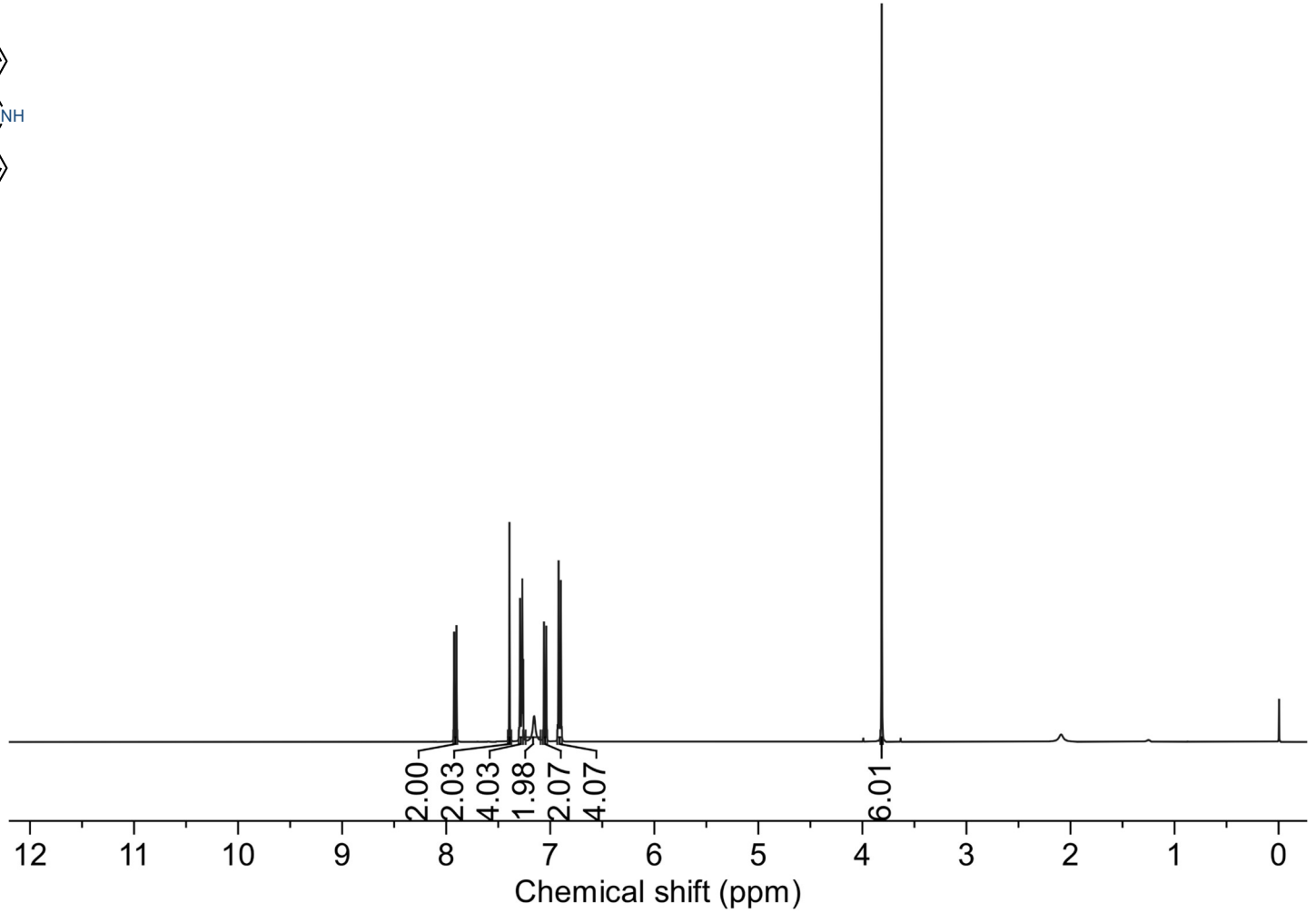

^{13}C NMR (100 MHz, $CDCl_3$)

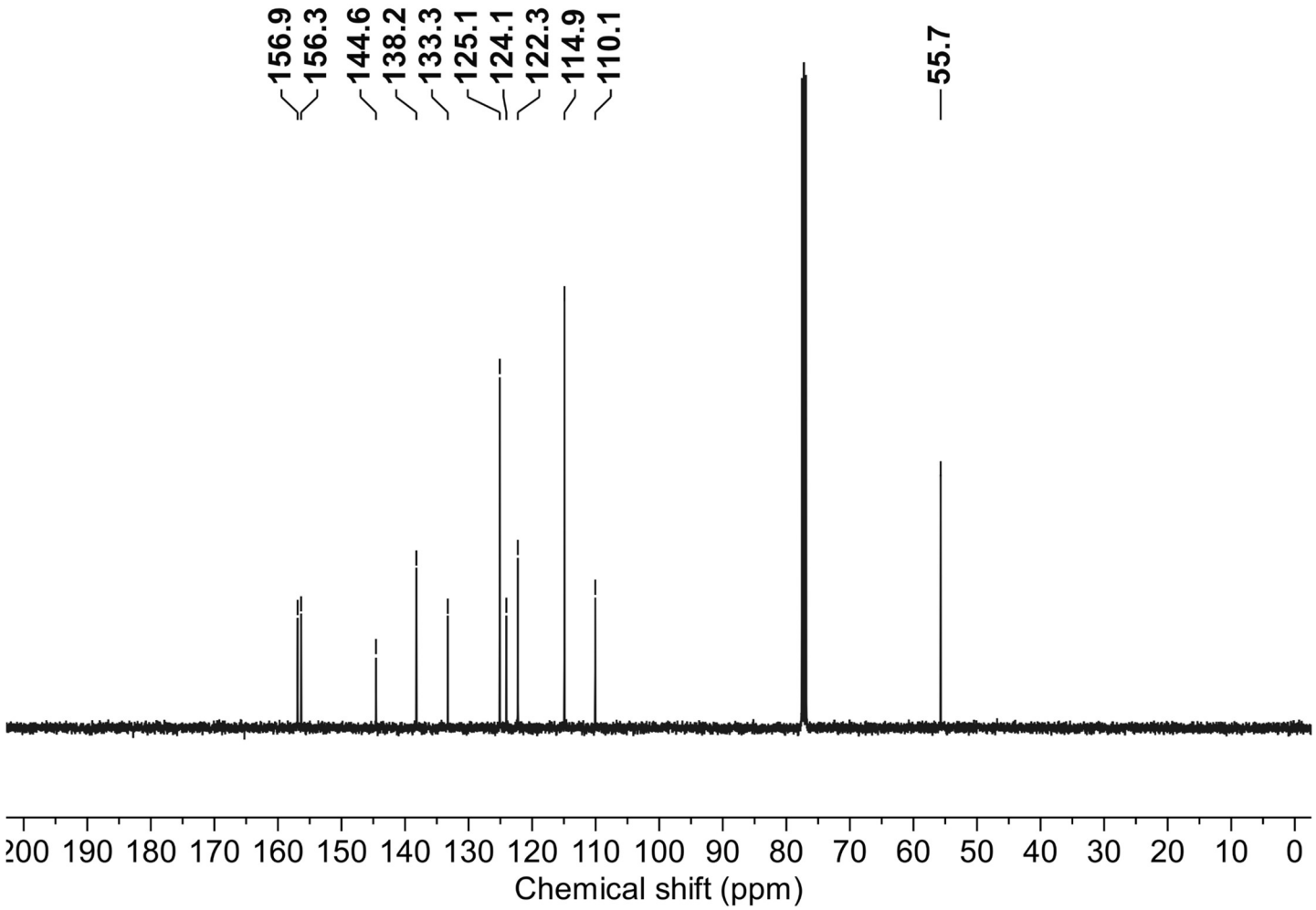

***N*²,*N*⁹-bis(4-(cyclopentyloxy)phenyl)-1,10-phenanthroline-2,9-diamine (6a)**: ^{1}H NMR (400 MHz, $CDCl_3$)

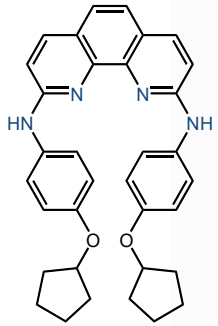

6a

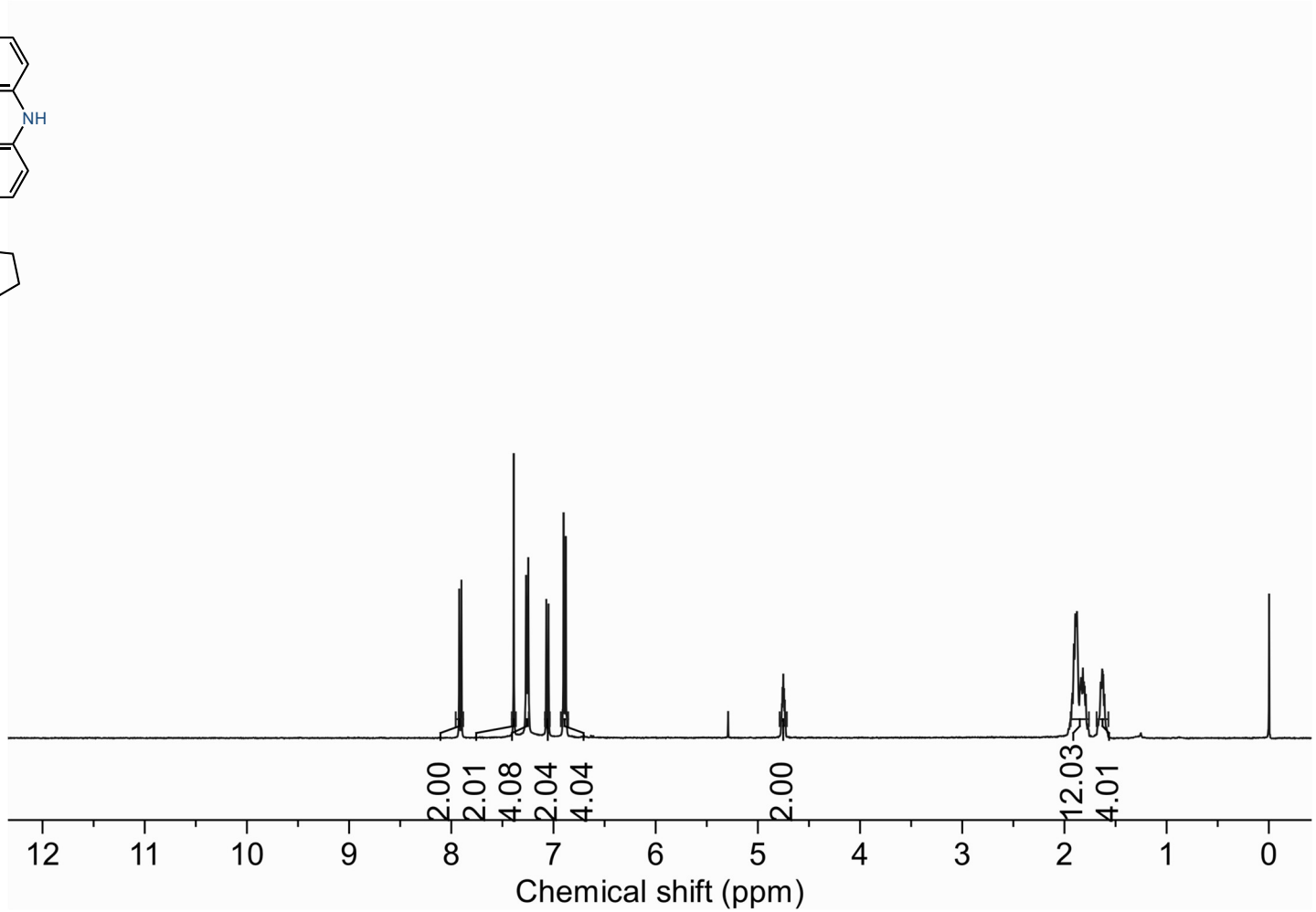

^{13}C NMR (100 MHz, $CDCl_3$)

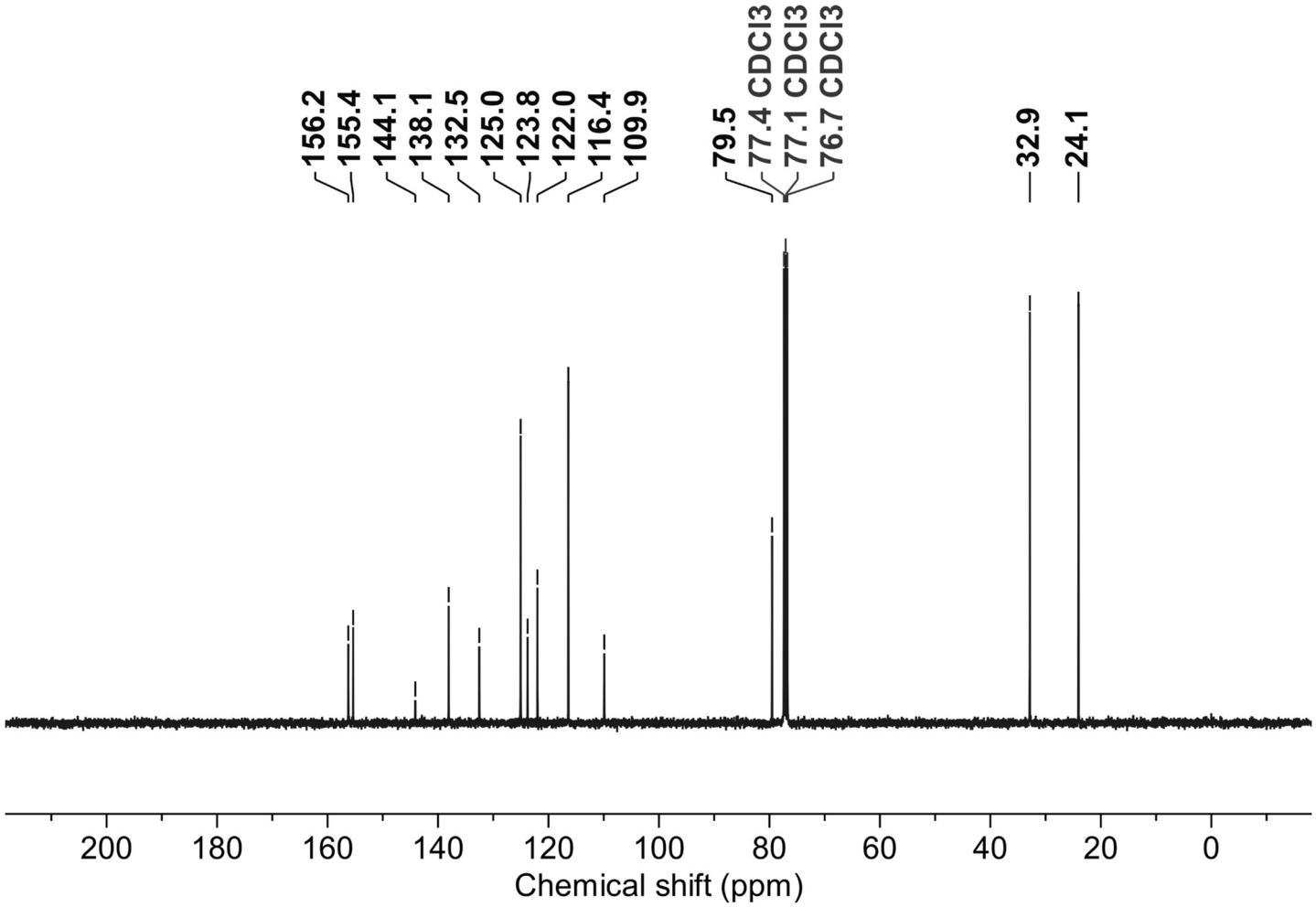

***N*²,*N*⁹-bis(4-(tert-butyl)phenyl)-1,10-phenanthroline-2,9-diamine (7a)**: ^{1}H NMR (400 MHz, $CDCl_3$)

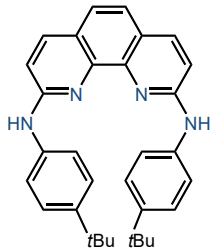

7a

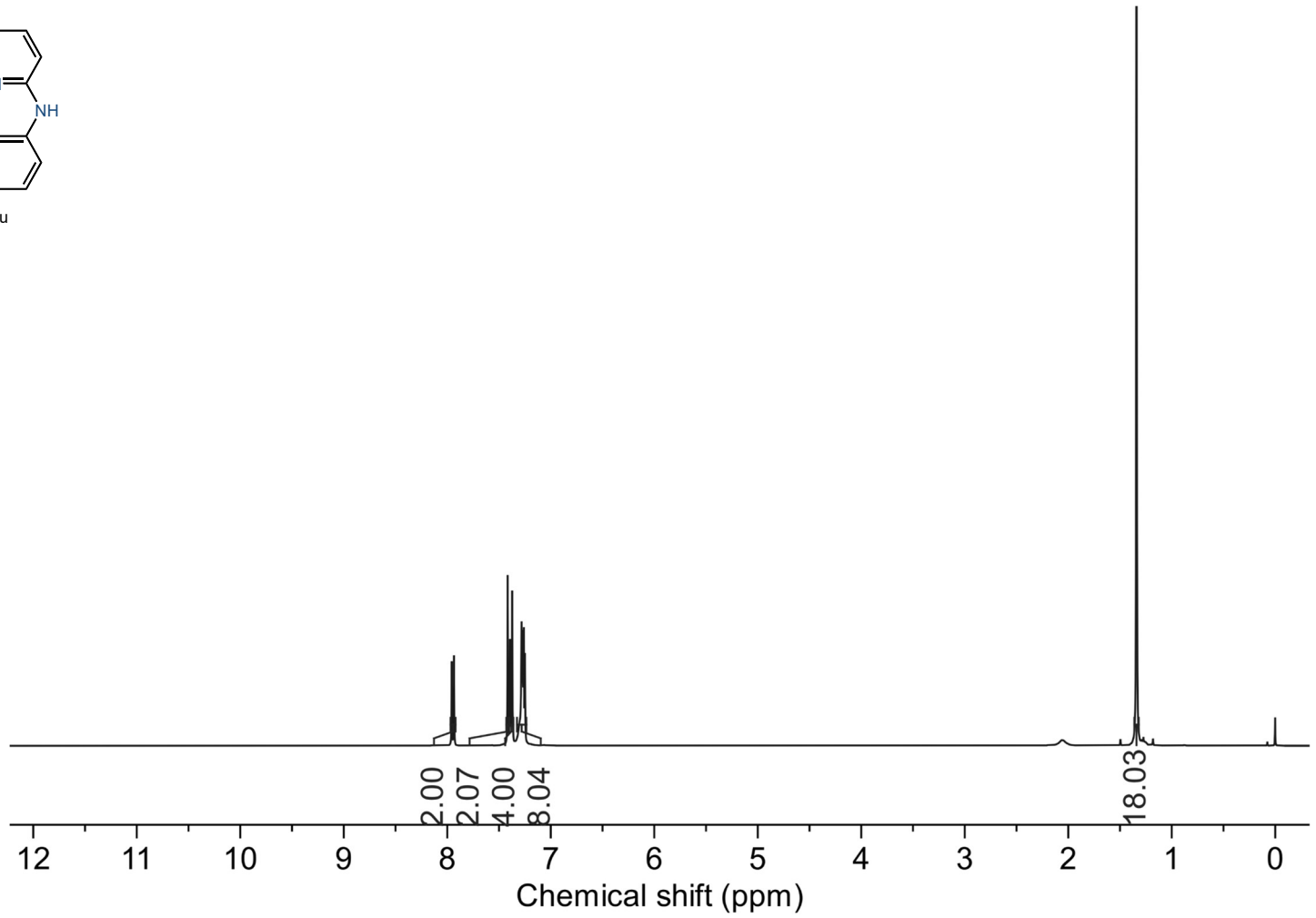

^{13}C NMR (100 MHz, $CDCl_3$)

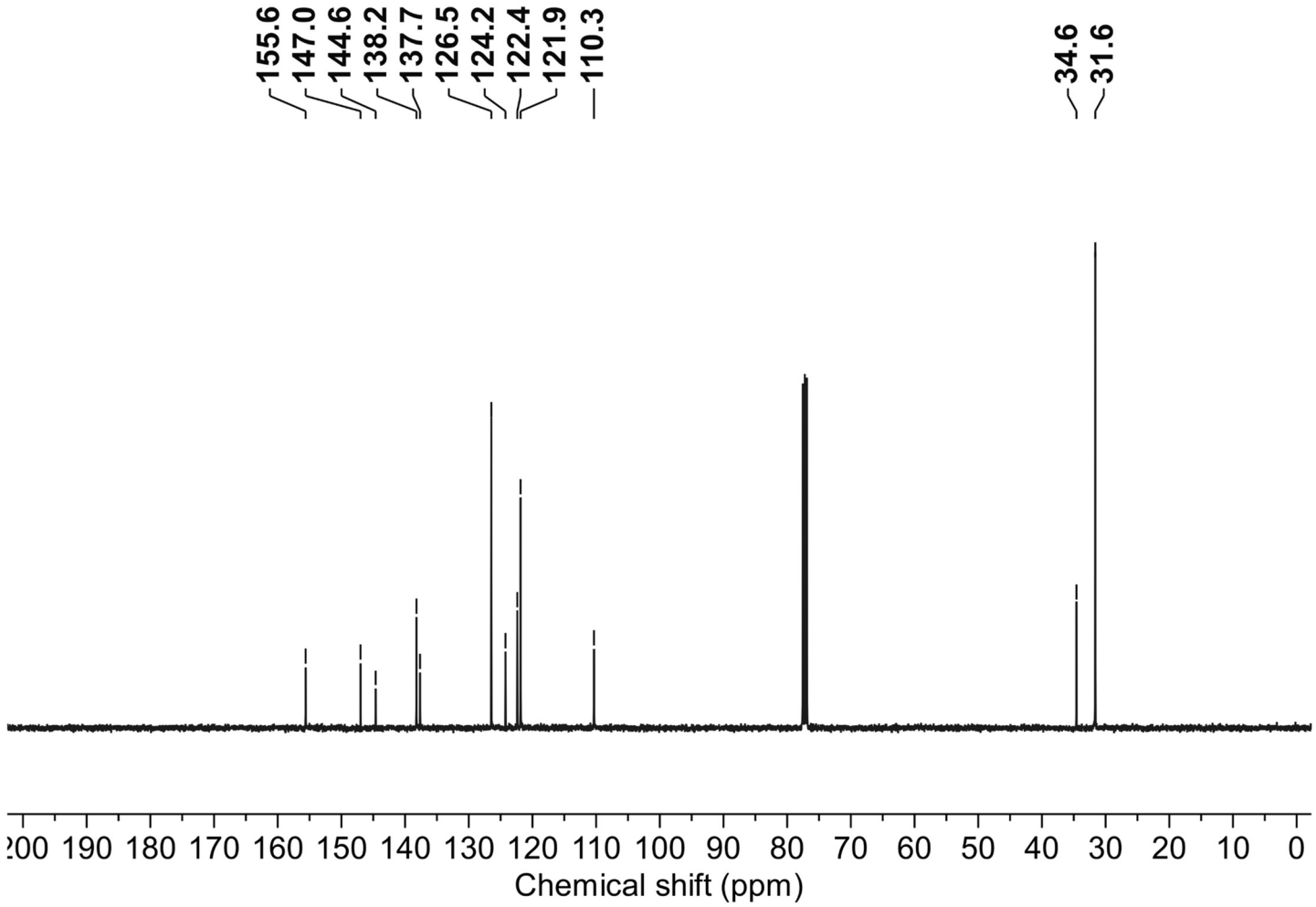

***N*²,*N*⁹-di([1,1'-biphenyl]-4-yl)-1,10-phenanthroline-2,9-diamine (8a)**: ^{1}H NMR (800 MHz, $CDCl_3$)

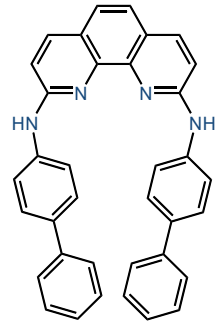

8a

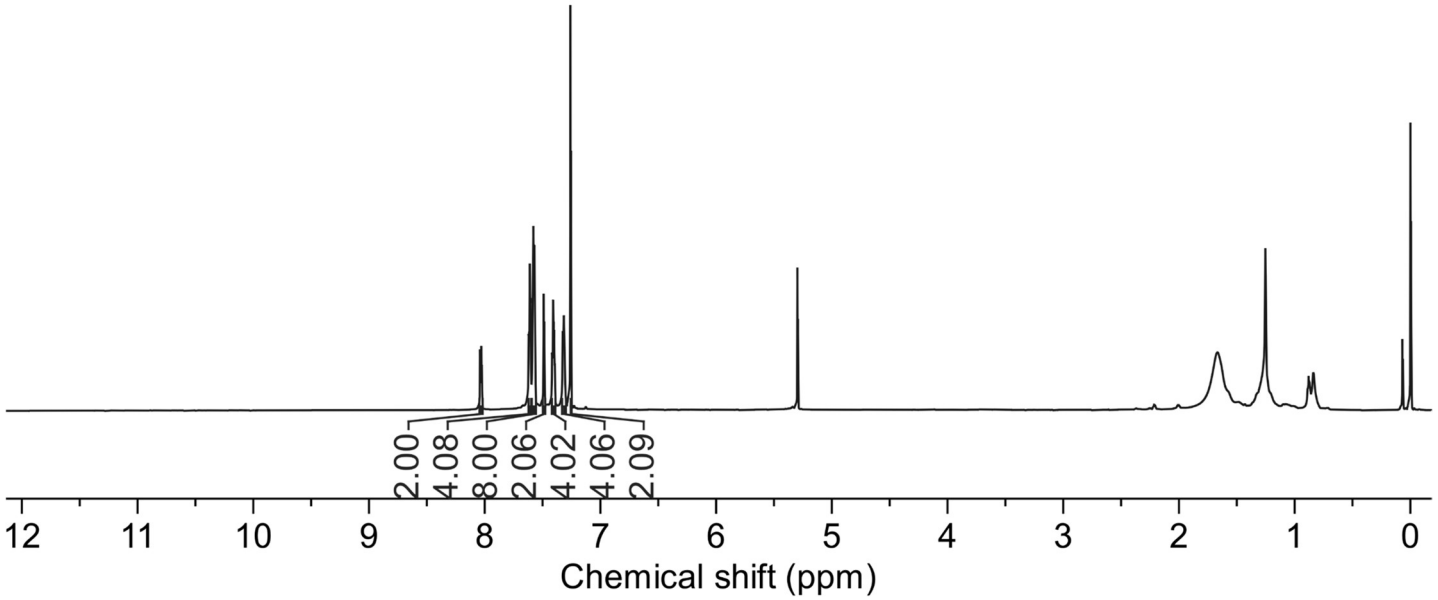

^{13}C NMR (200 MHz, $CDCl_3$)

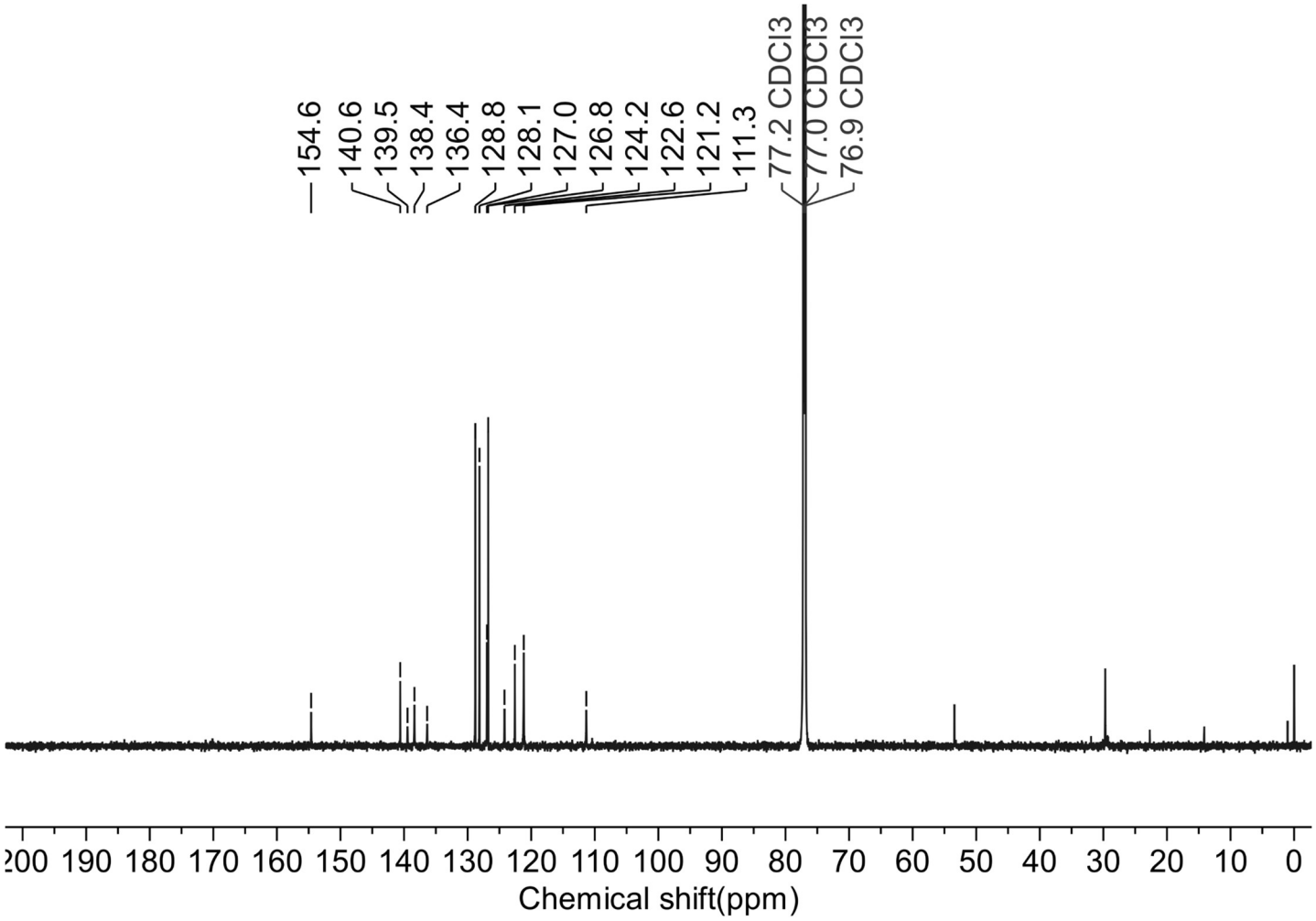

Dimethyl 4,4'-((1,10-phenanthroline-2,9-diyl)bis(azanediyl))dibenzoate (**9a**): ^{1}H NMR (400 MHz, DMSO-d_6)

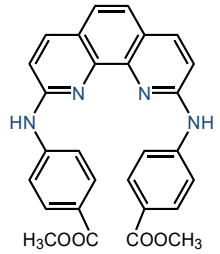

9a

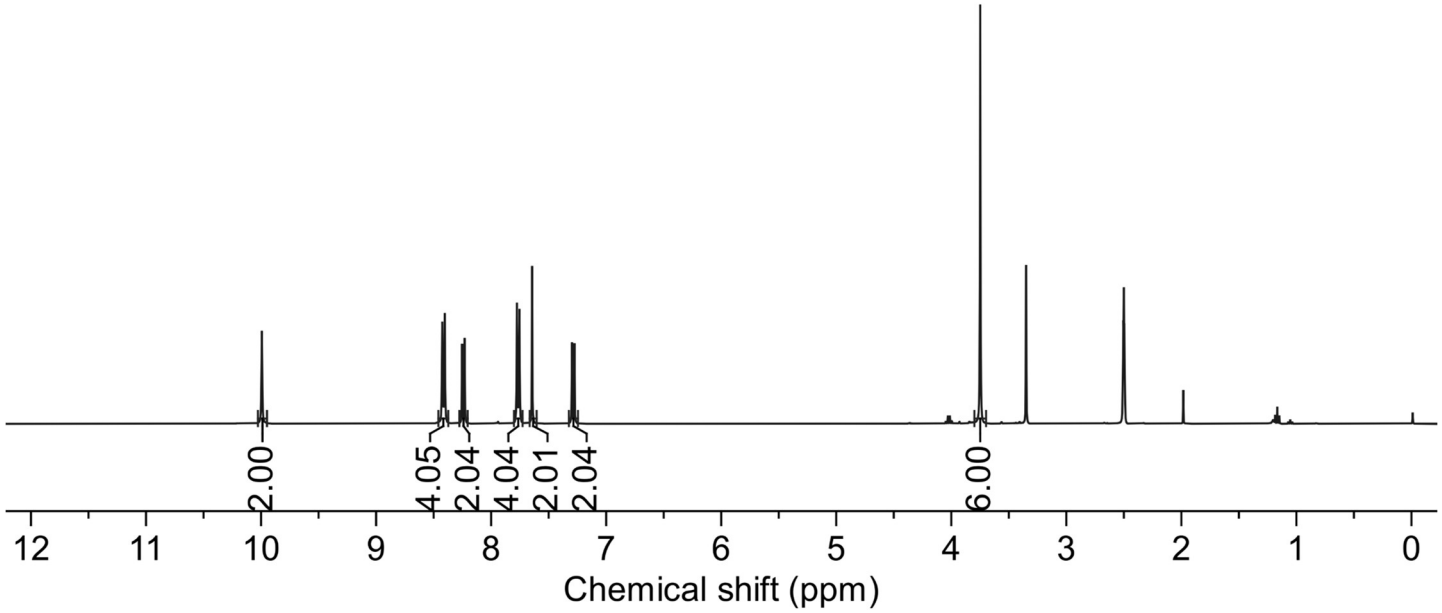

^{13}C NMR (100 MHz, DMSO-d_6)

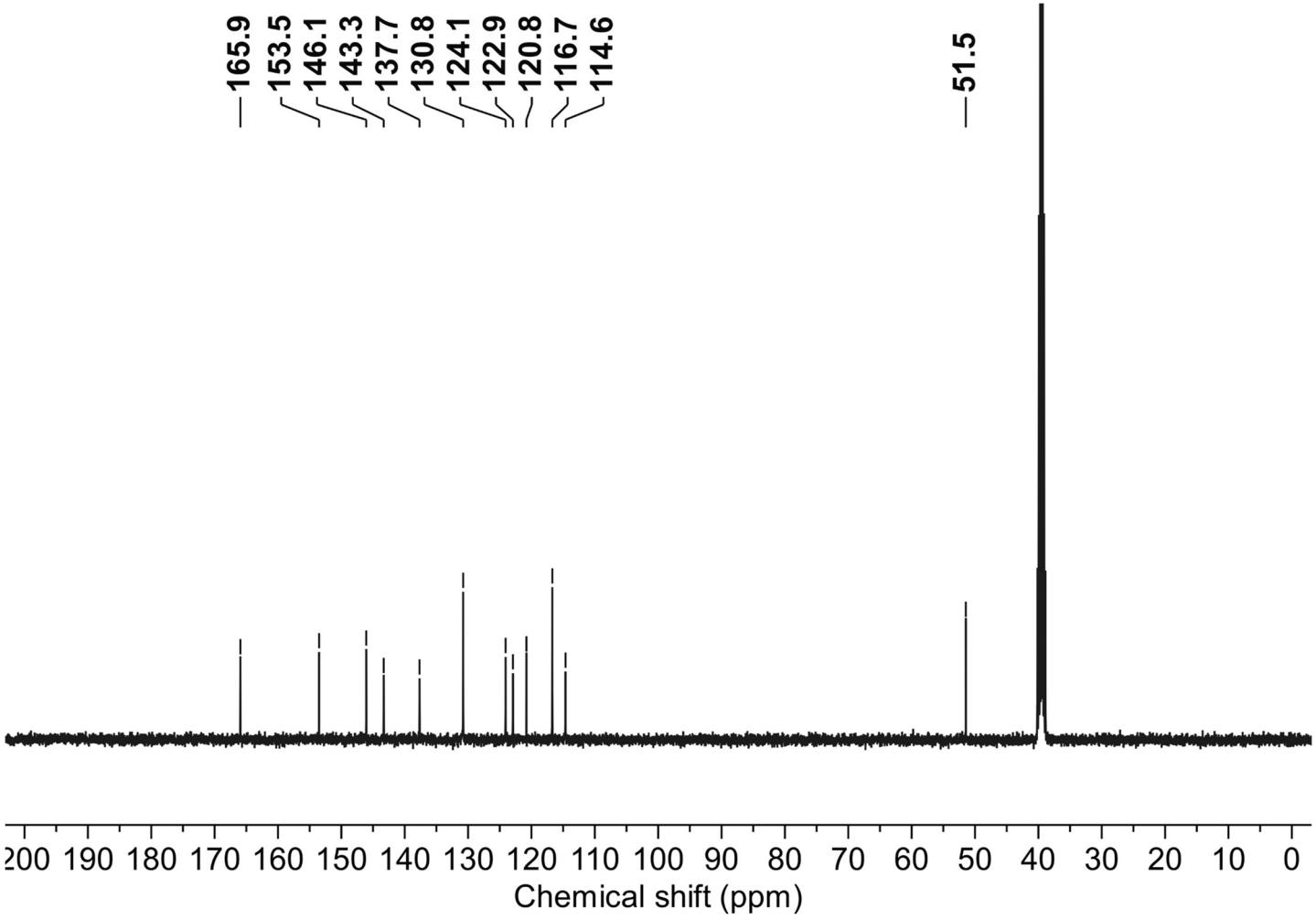

1,1'-(((1,10-phenanthroline-2,9-diyl)bis(azanediyl))bis(4,1-phenylene))bis(ethan-1-one) (**10a**): ^{1}H NMR (400 MHz, DMSO-d_6)

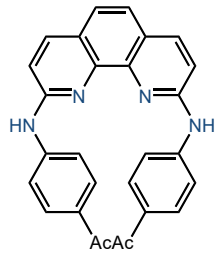

10a

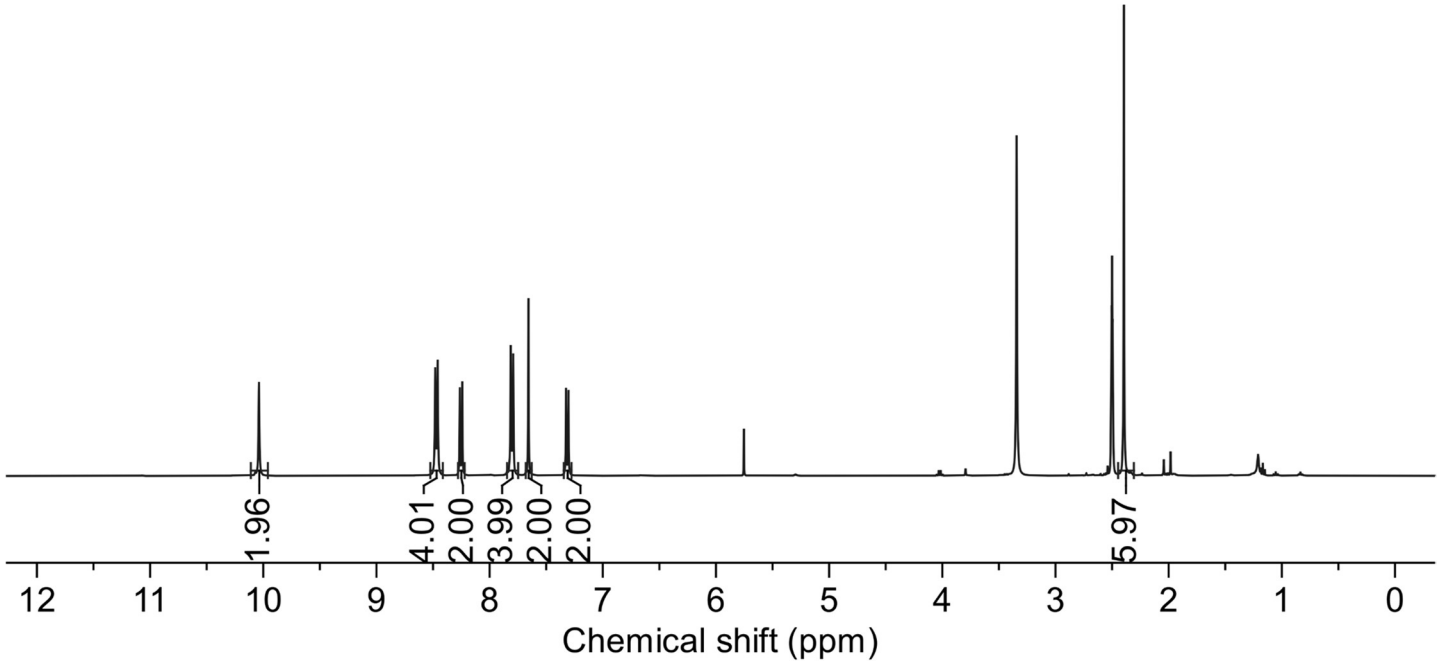

^{13}C NMR (100 MHz, DMSO-d_6)

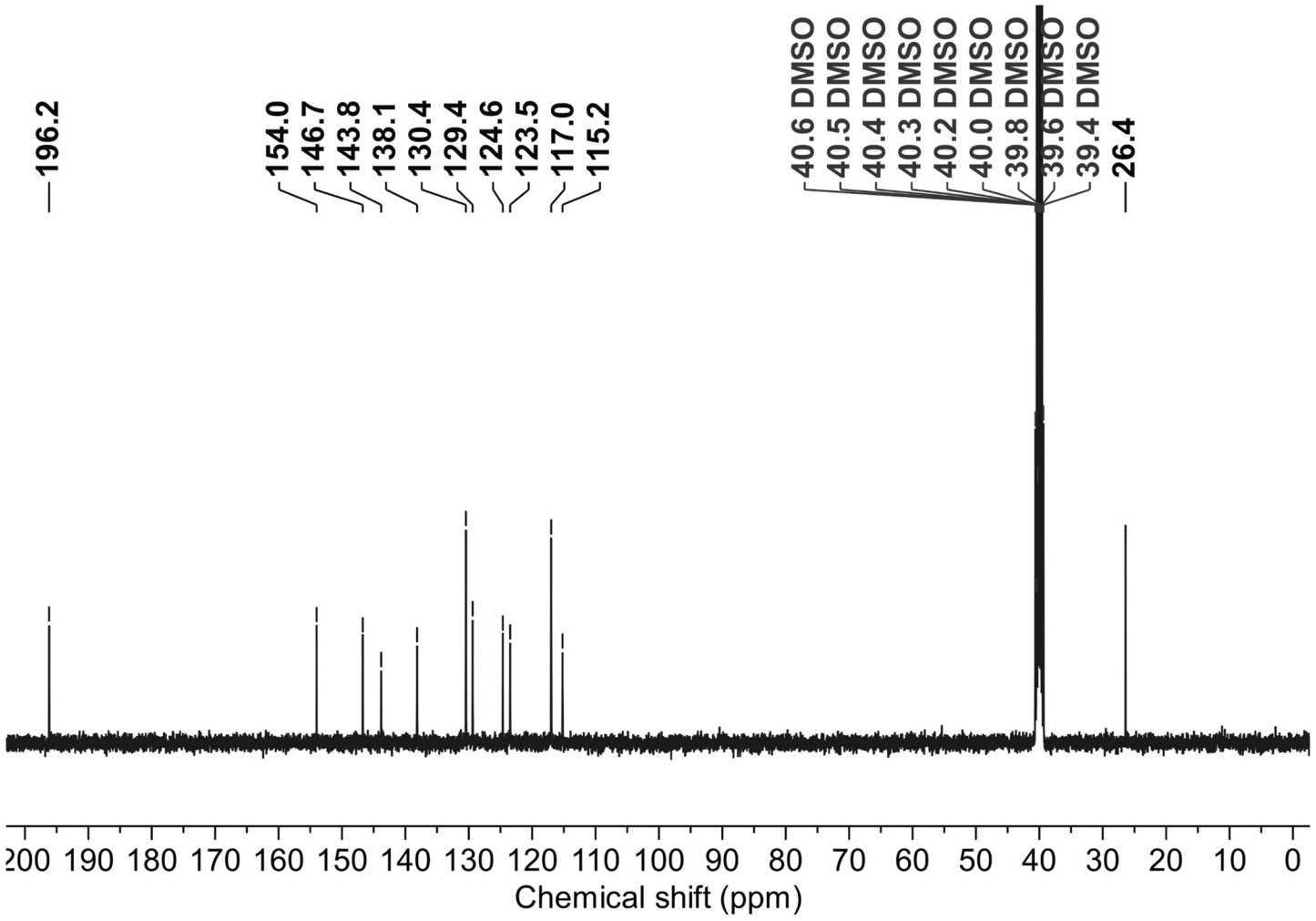

***N*²,*N*⁹-bis(4-(trifluoromethyl)phenyl)-1,10-phenanthroline-2,9-diamine (11a)**: ^{1}H NMR (400 MHz, DMSO-d_6)

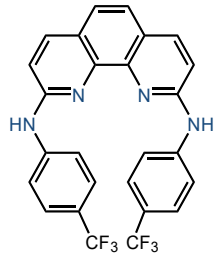

11a

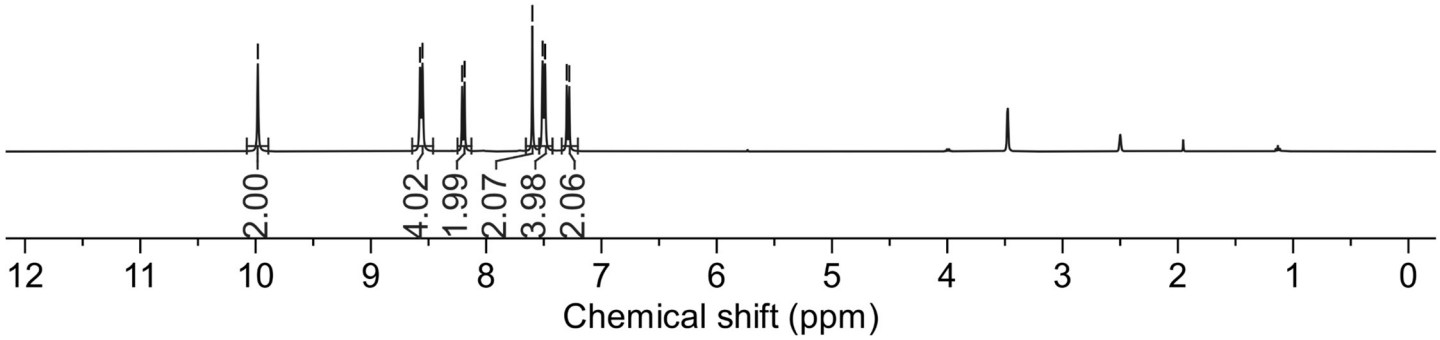

^{13}C NMR (100 MHz, DMSO-d_6)

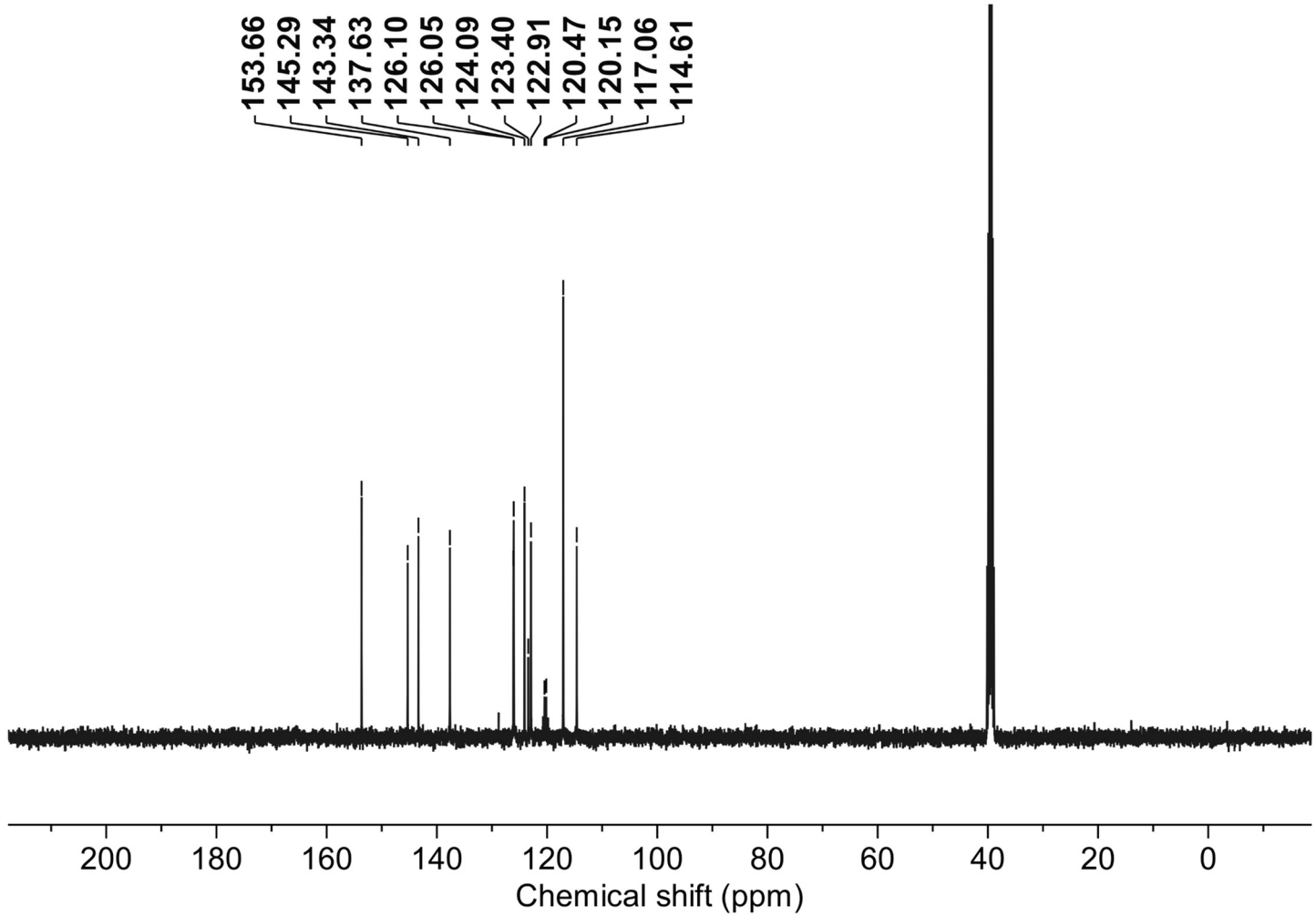

***N*²,*N*⁹-di(pyridin-2-yl)-1,10-phenanthroline-2,9-diamine (12a)**: ^{1}H NMR (400 MHz, $CDCl_3$)

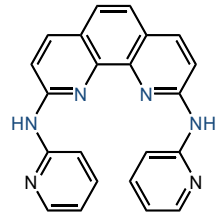

12a

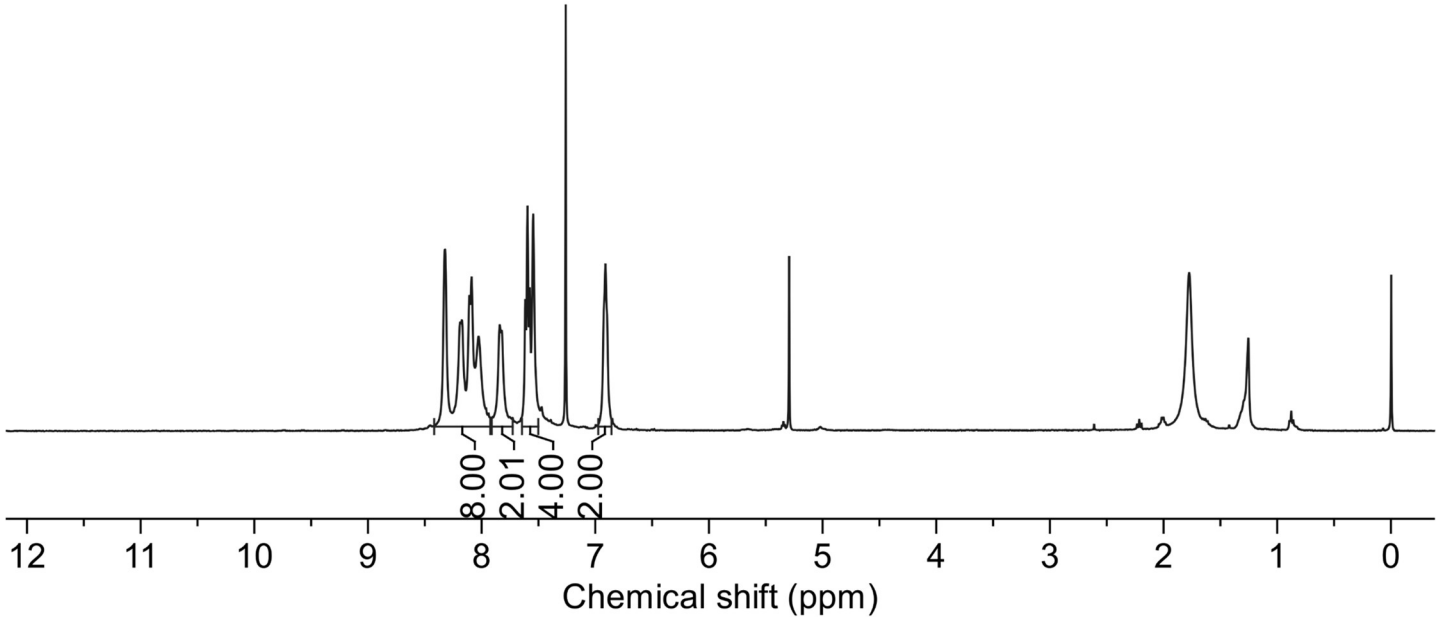

***N*²,*N*⁹-di(quinolin-8-yl)-1,10-phenanthroline-2,9-diamine (13a)**: ^{1}H NMR (400 MHz, $CDCl_3$)

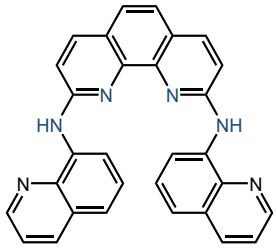

13a

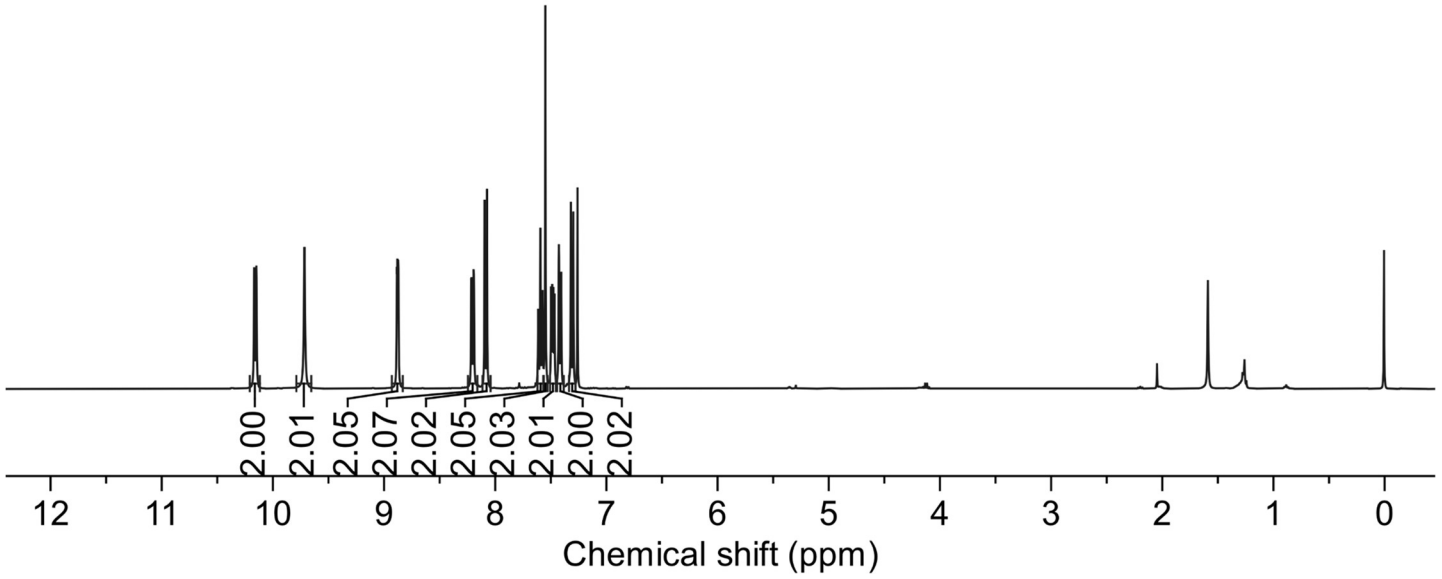

^{13}C NMR (100 MHz, $CDCl_3$)

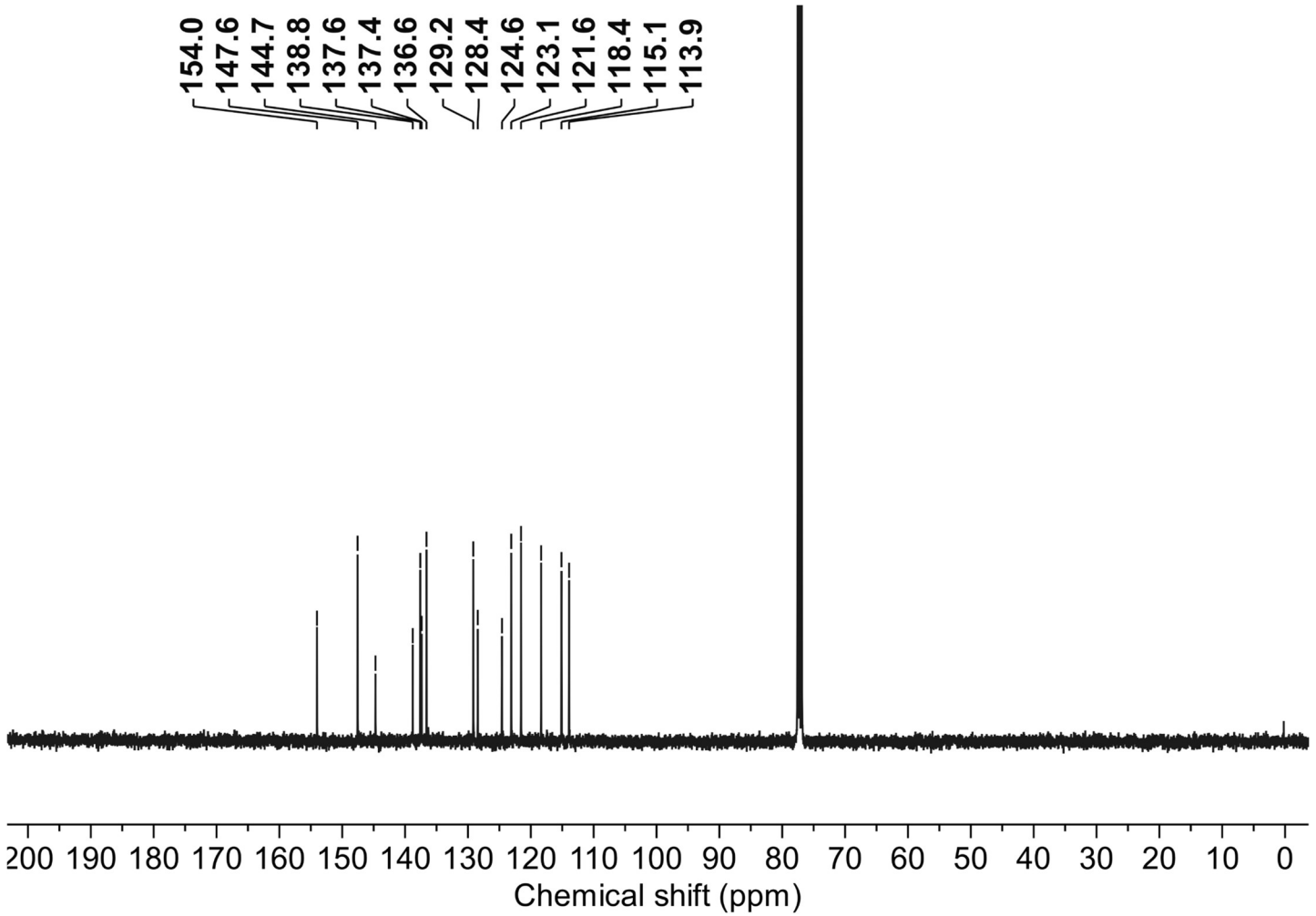

***N*²,*N*⁹-di(naphthalen-1-yl)-1,10-phenanthroline-2,9-diamine (14a)**: ^{1}H NMR (400 MHz, $CDCl_3$)

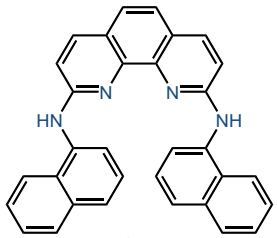

14a

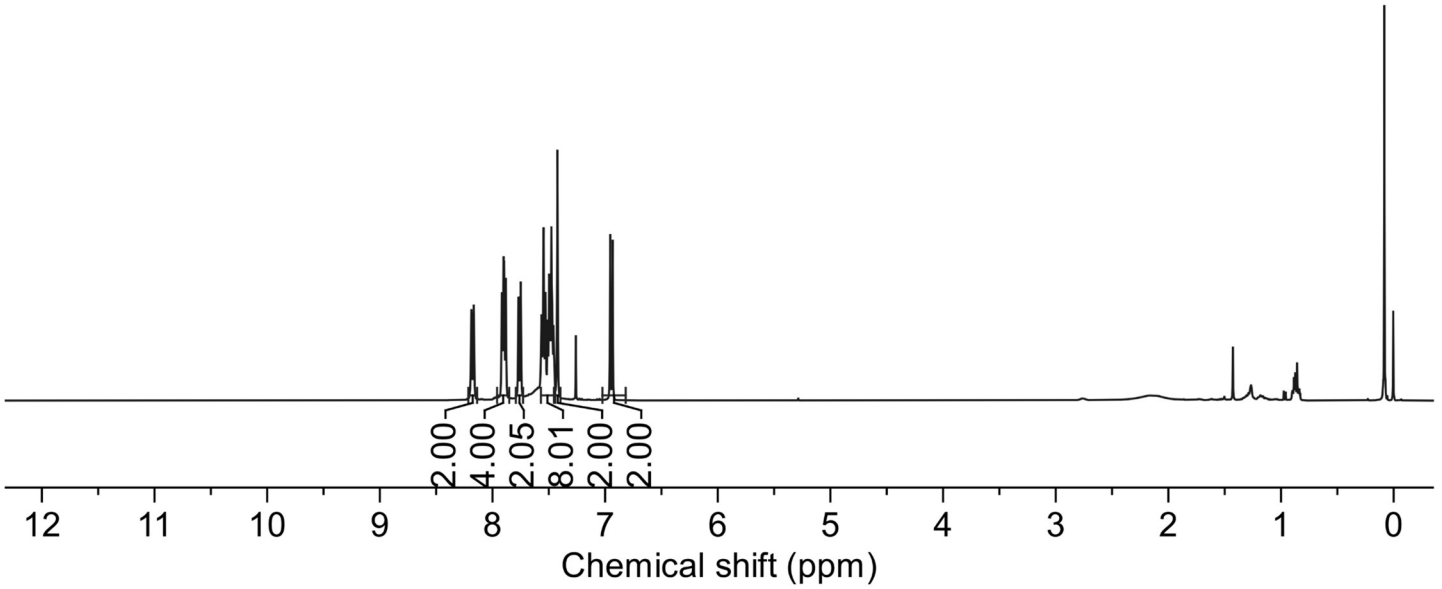

^{13}C NMR (100 MHz, $CDCl_3$)

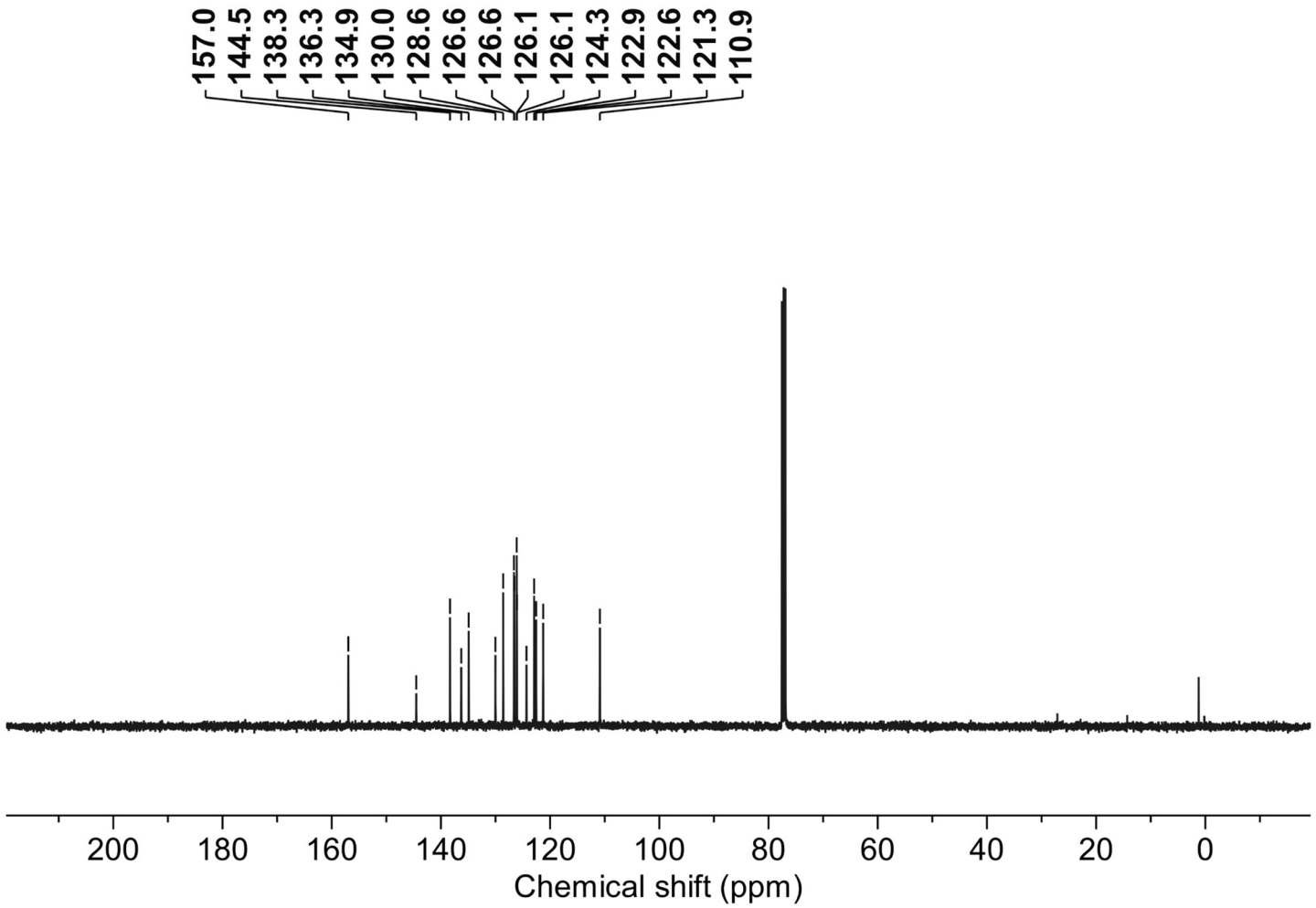

***N*²,*N*⁹-di(naphthalen-2-yl)-1,10-phenanthroline-2,9-diamine (15a)**: ^{1}H NMR (400 MHz, DMSO-d_6)

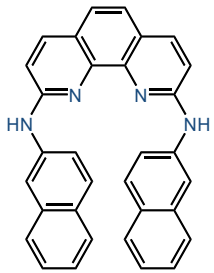

15a

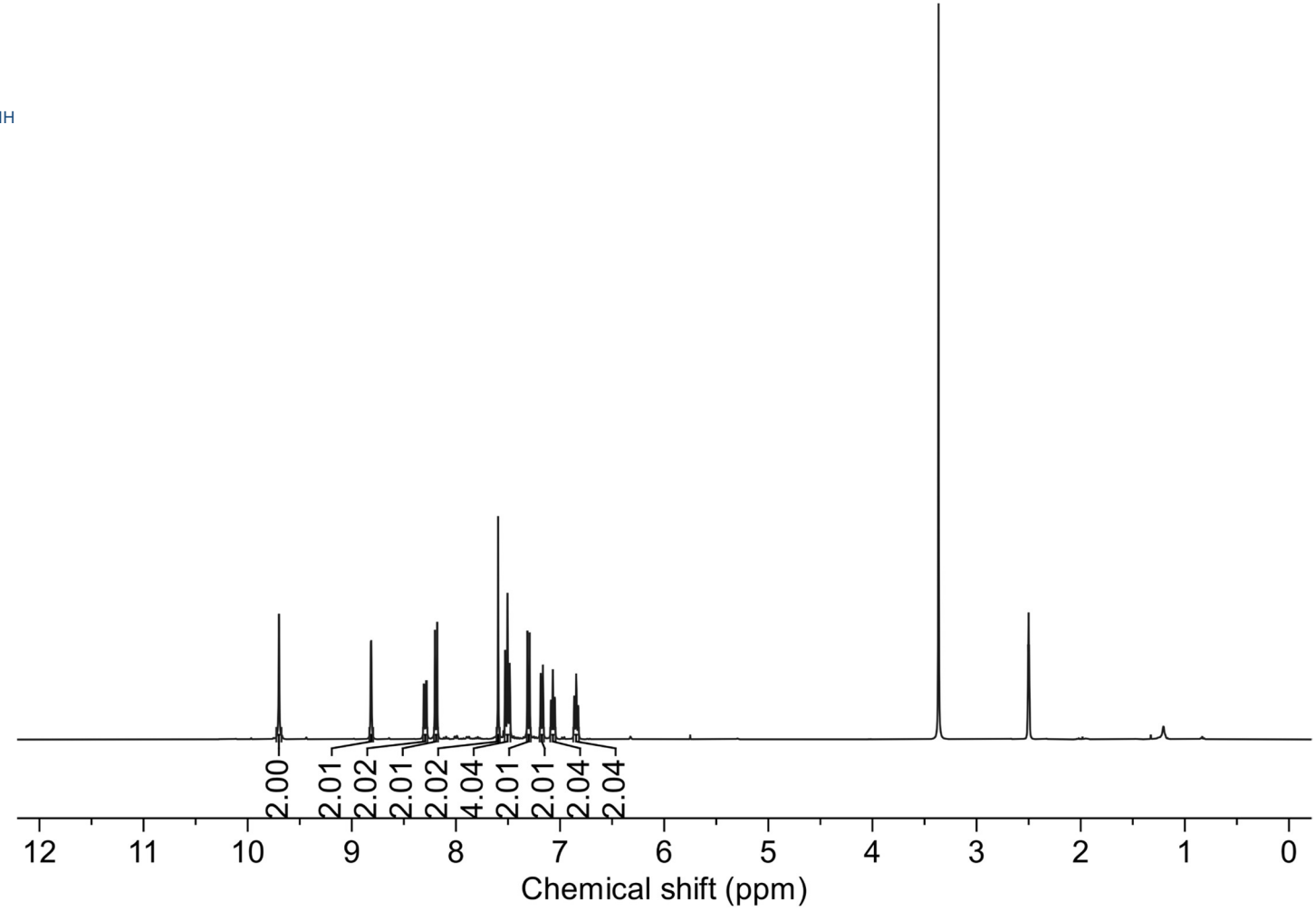

^{13}C NMR (100 MHz, DMSO-d_6)

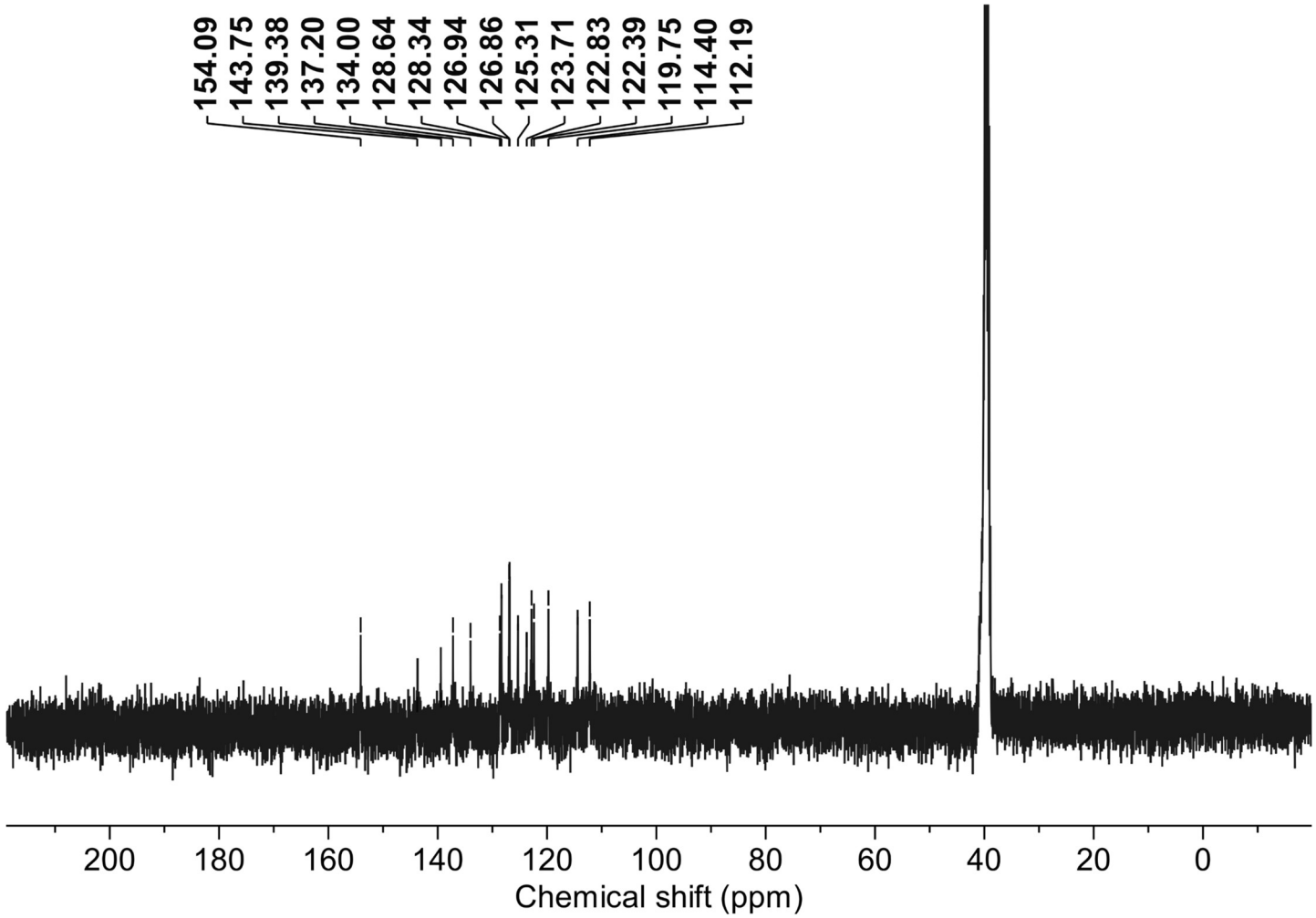

N^2,N^9-bis(3,4-dimethoxyphenyl)-1,10-phenanthroline-2,9-diamine (16a):: ^{1}H NMR (400 MHz, $CDCl_3$)

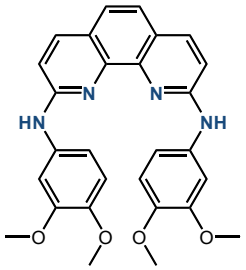

16a

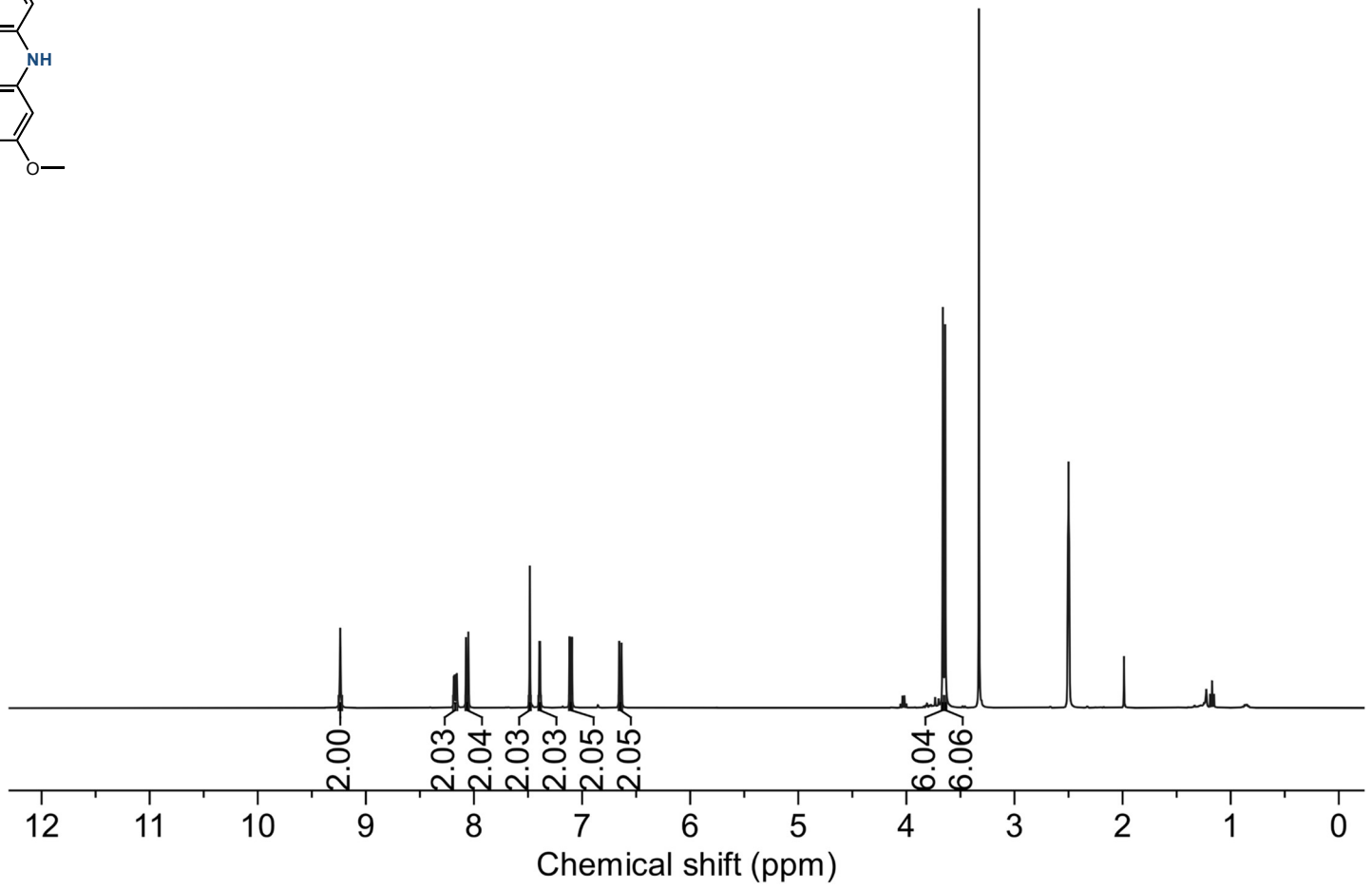

^{13}C NMR (100 MHz, $CDCl_3$)

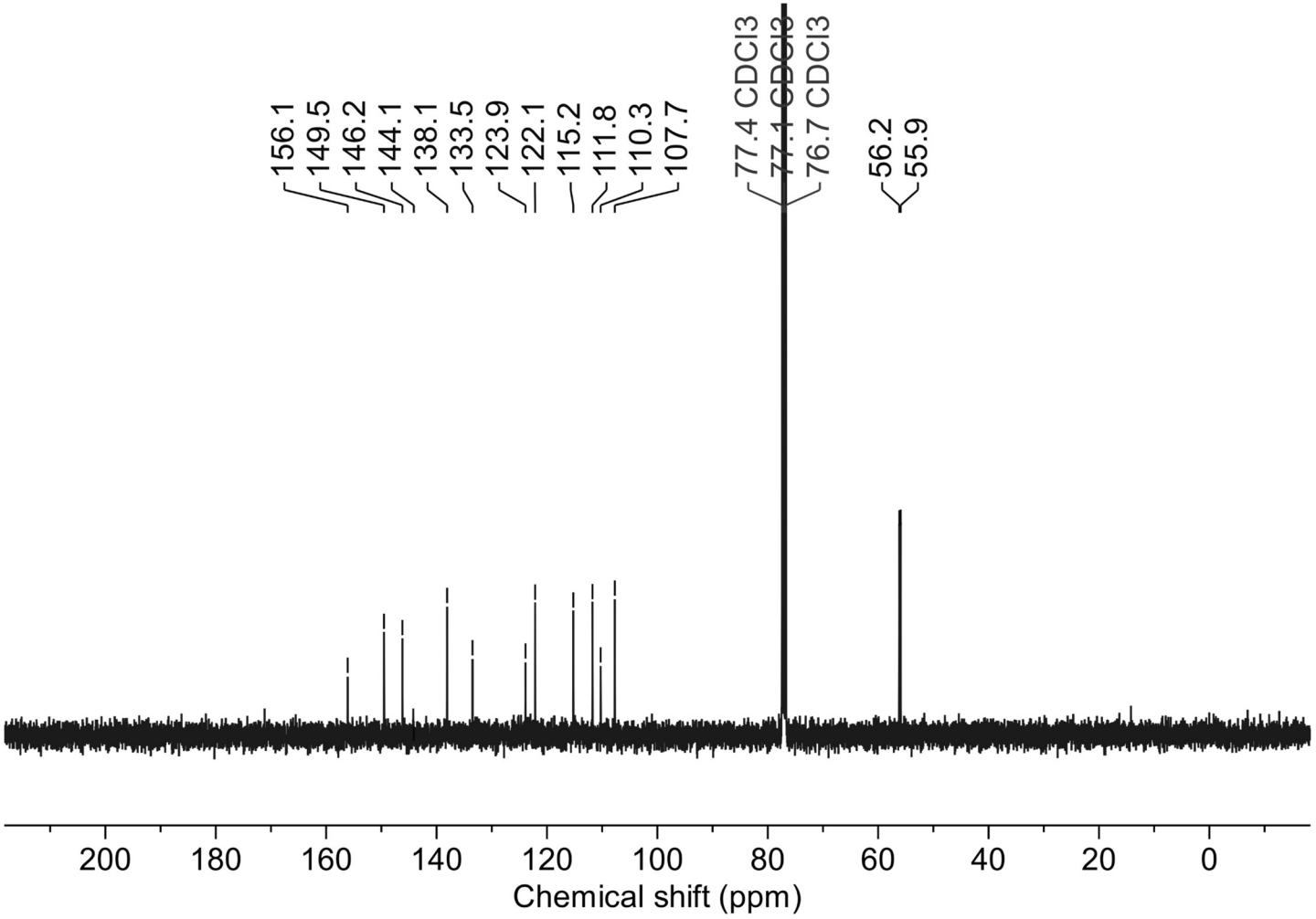

***N*^{1},*N*^{4}-di(pyridin-2-yl)benzene-1,4-diamine (17a)**: ^{1}H NMR (400 MHz, DMSO-d_6)

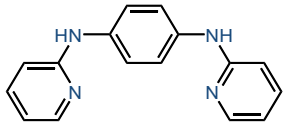

17a

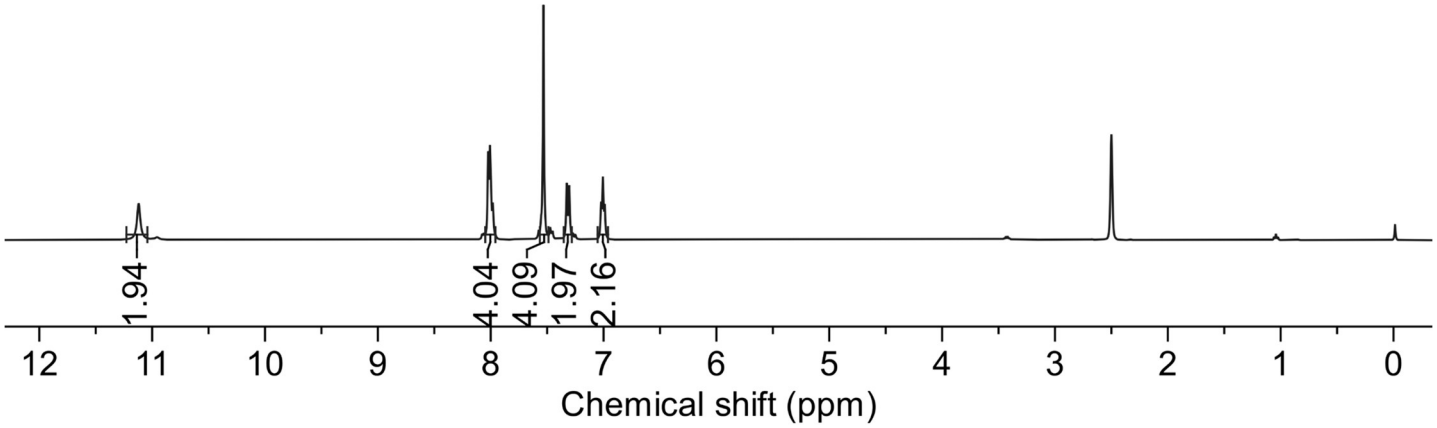

^{13}C NMR (100 MHz, DMSO-d_6)

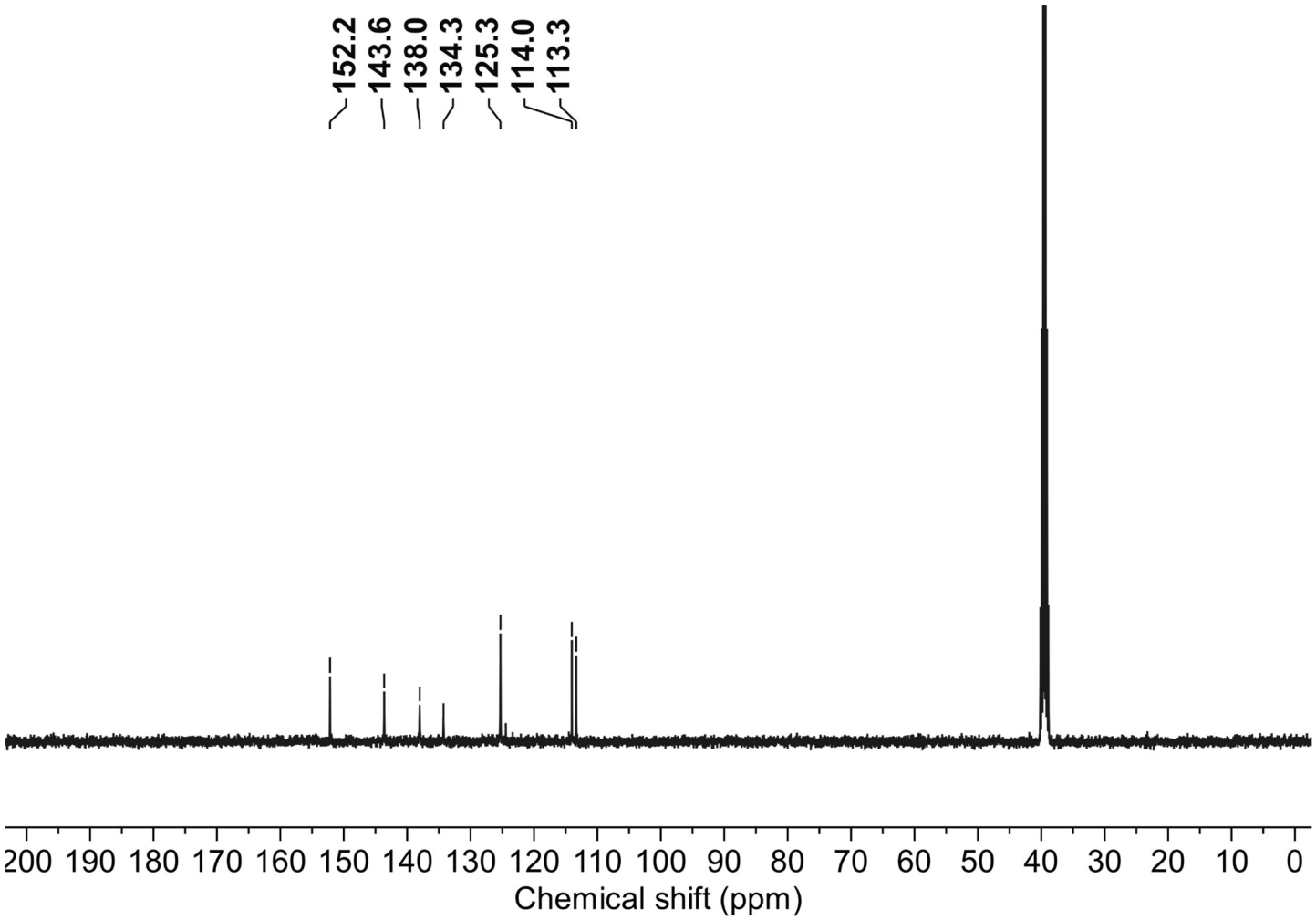

N^1-(pyridin-2-yl)-N^4-(quinolin-2-yl)benzene-1,4-diamine (**18a**): ^{1}H NMR (400 MHz, DMSO-d_6)

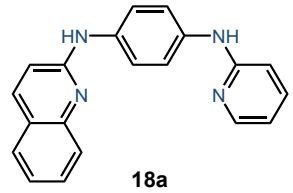

18a

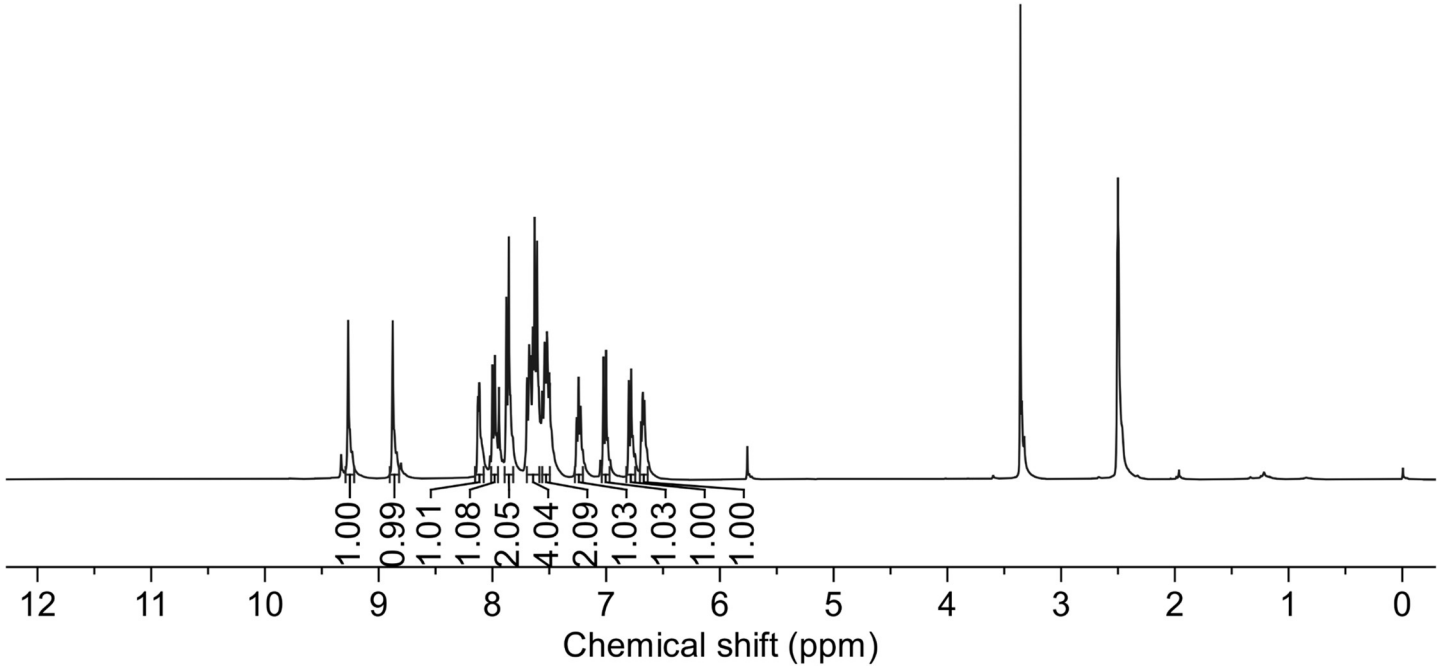

^{13}C NMR (100 MHz, DMSO-d_6)

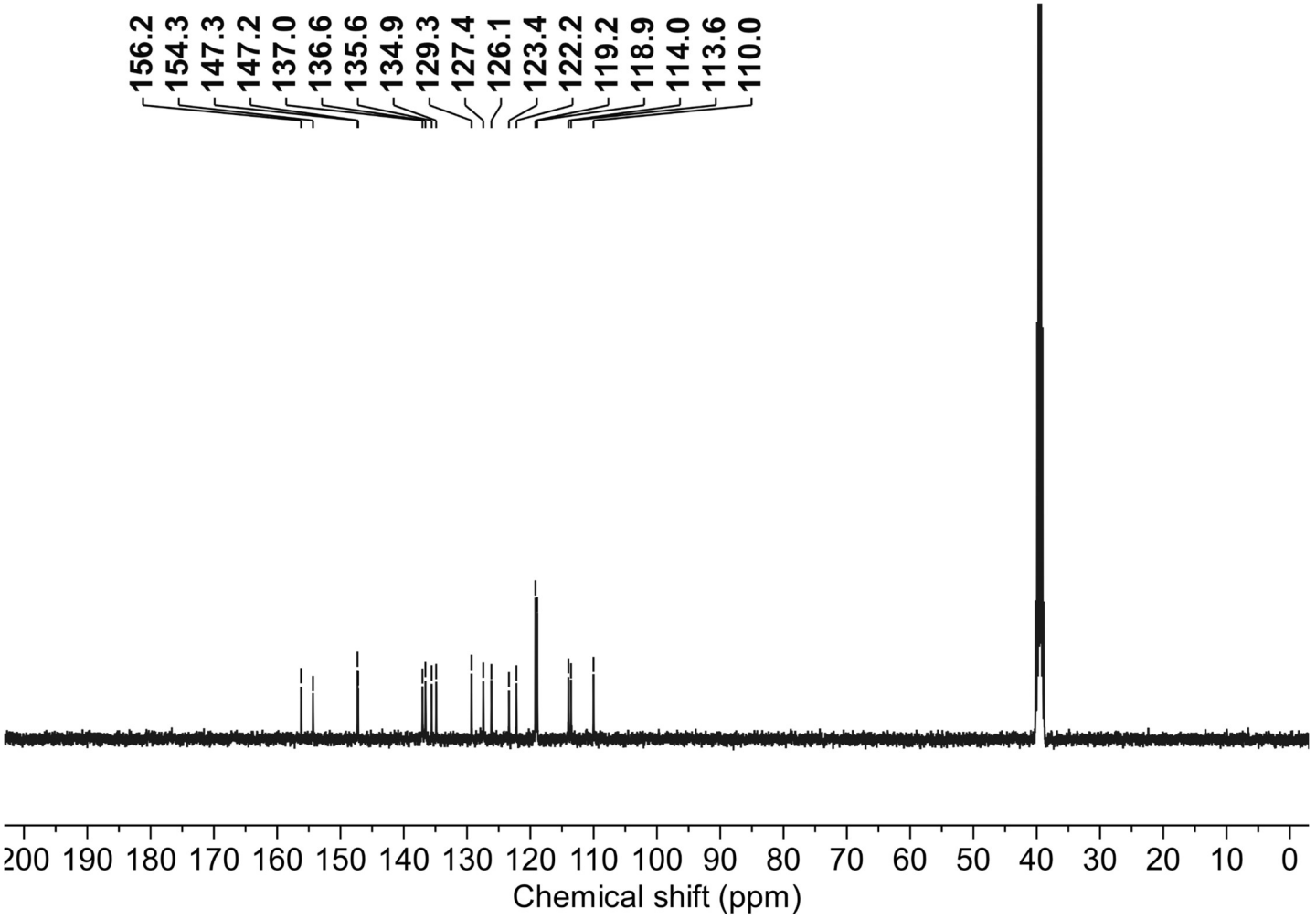

***N*^{1},*N*^{4}-di(quinolin-2-yl)benzene-1,4-diamine (19a)**: ^{1}H NMR (400 MHz, Methanol-d_4)

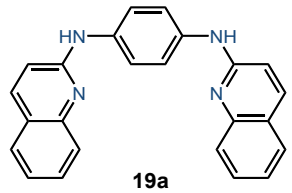

19a

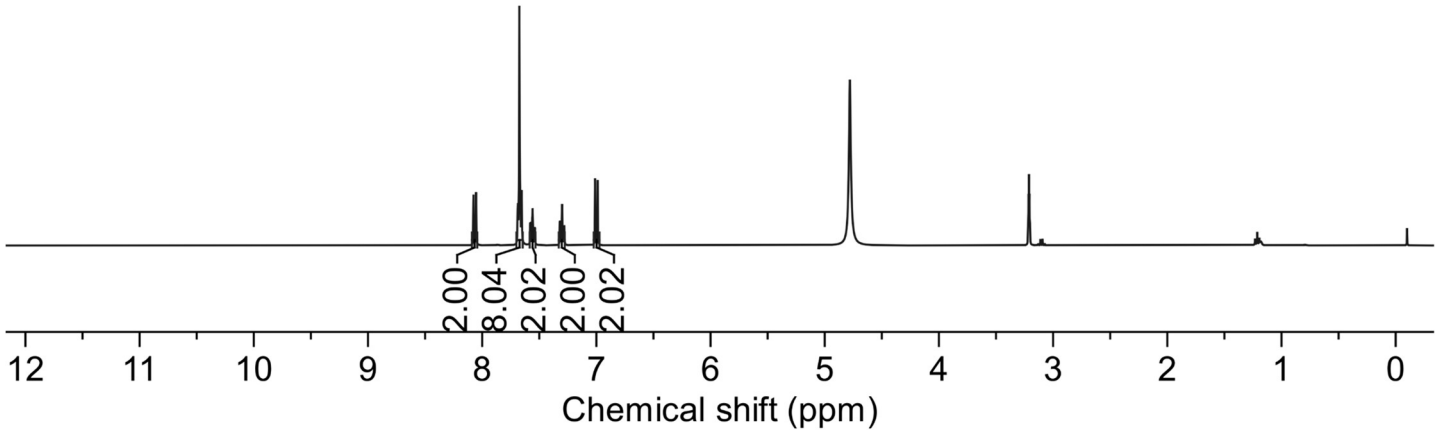

^{13}C NMR (100 MHz, Methanol-d_4)

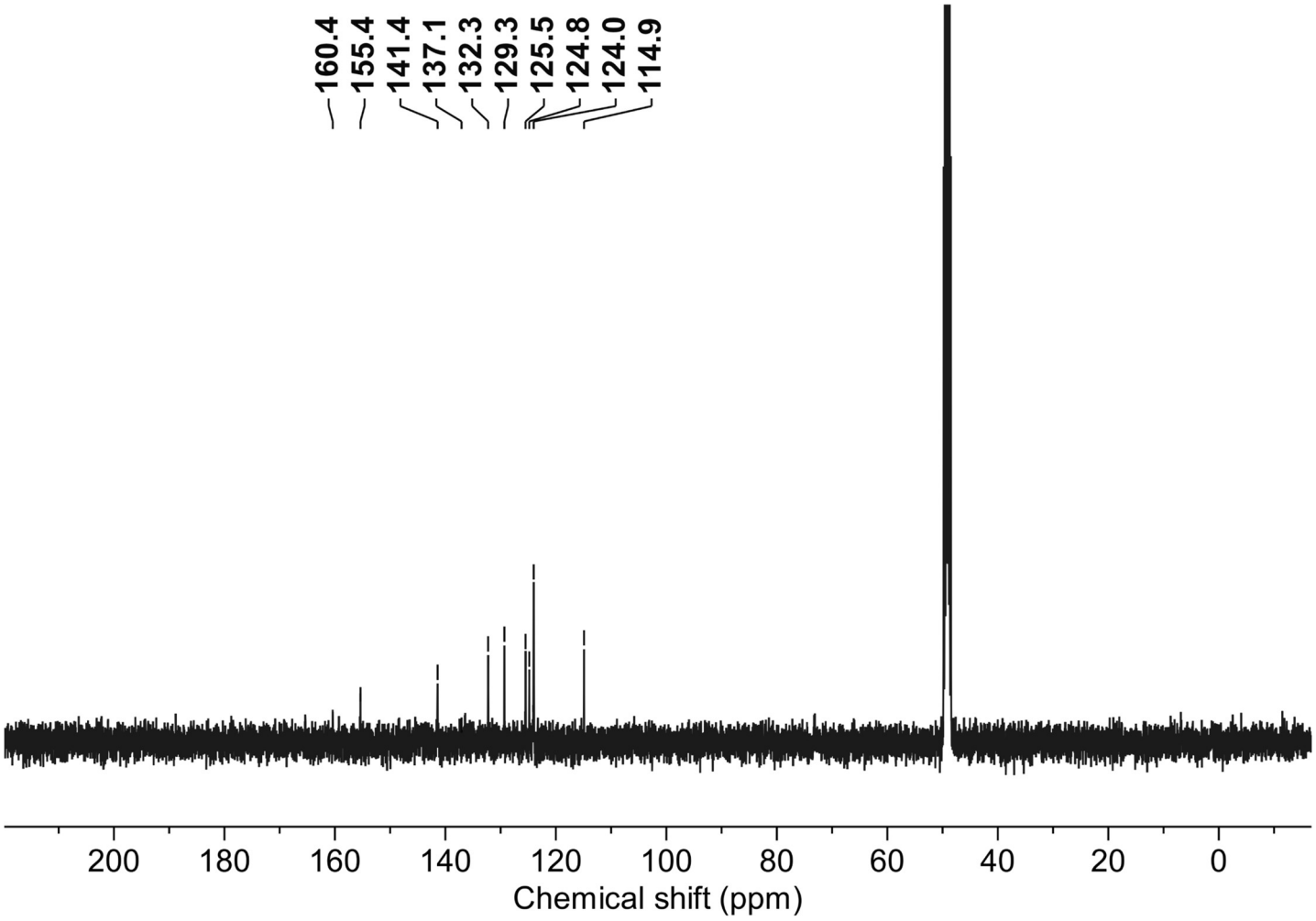

***N*^{1},*N*^{4}-bis(7-bromoquinolin-2-yl)benzene-1,4-diamine** (**20a**): ^{1}H NMR (400 MHz, DMSO-d_6)

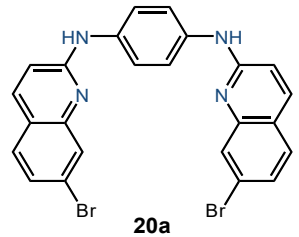

20a

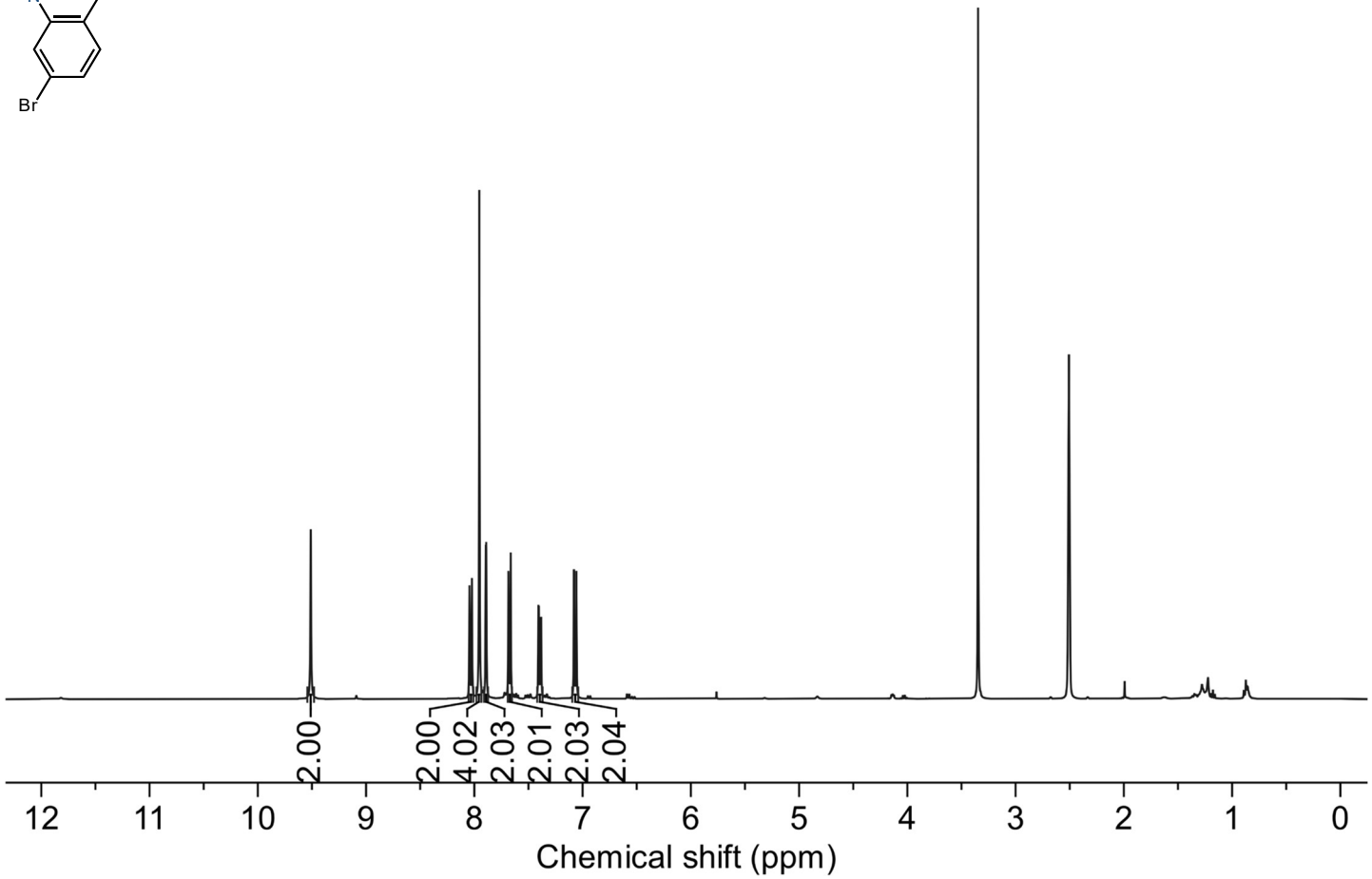

^{13}C NMR (100 MHz, DMSO-d_6)

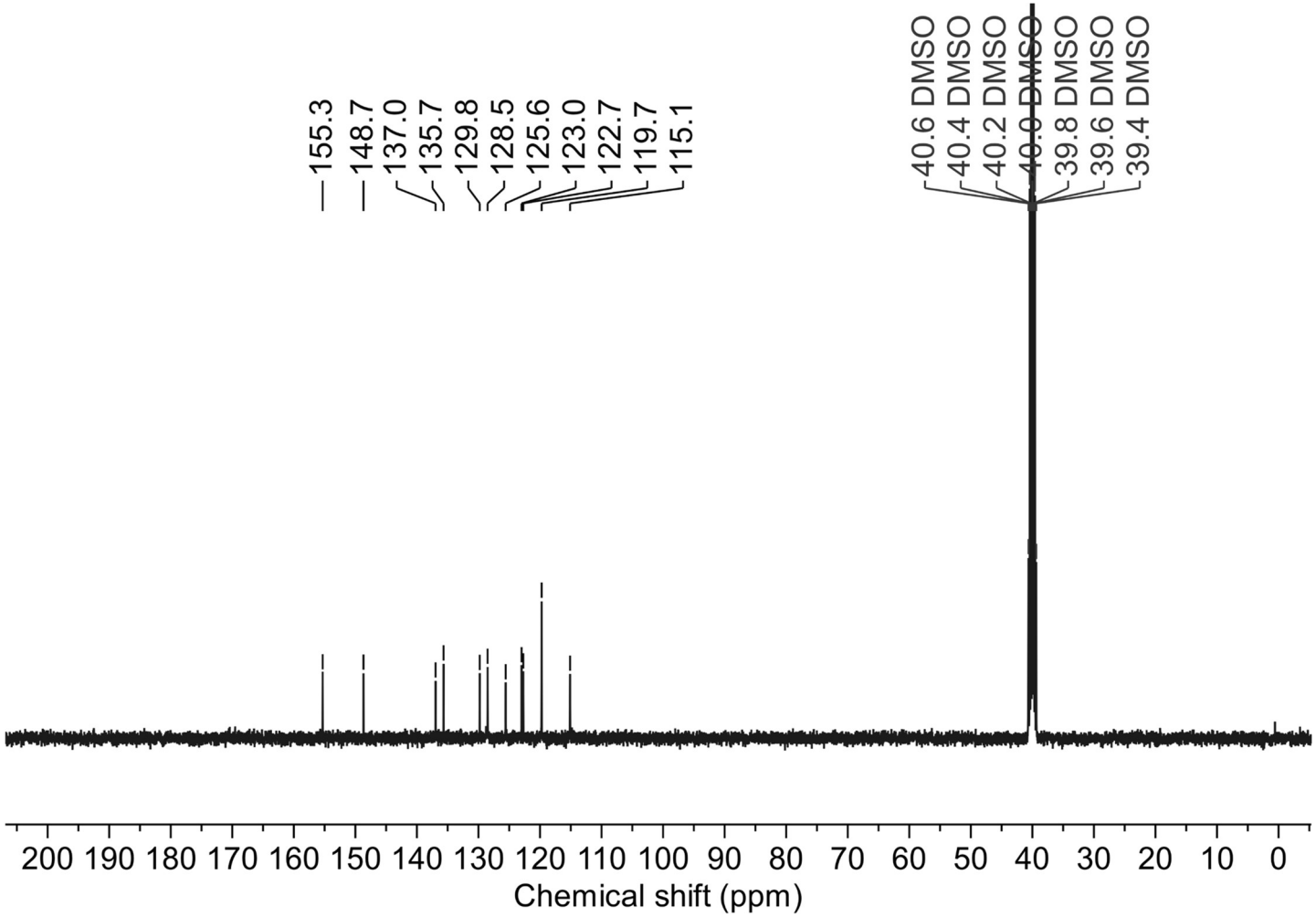

***N*^{1}-(1,10-phenanthrolin-2-yl)-*N*^{4}-(quinolin-2-yl)benzene-1,4-diamine** (**21a**): ^{1}H NMR (400 MHz, $CDCl_3$)

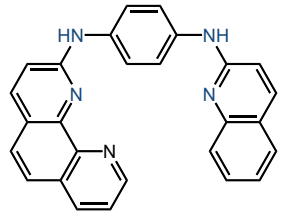

21a

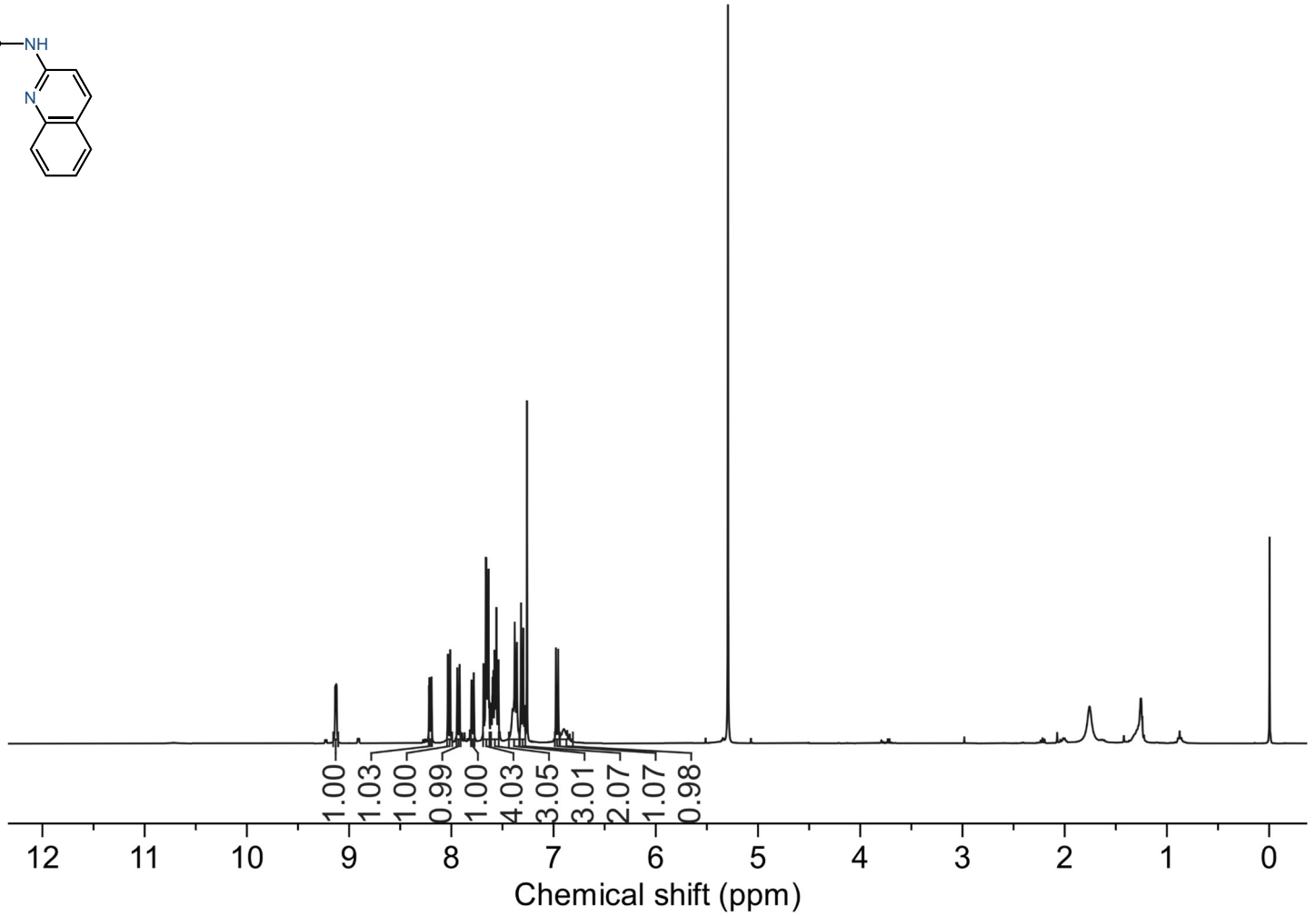

^{13}C NMR (100 MHz, $CDCl_3$)

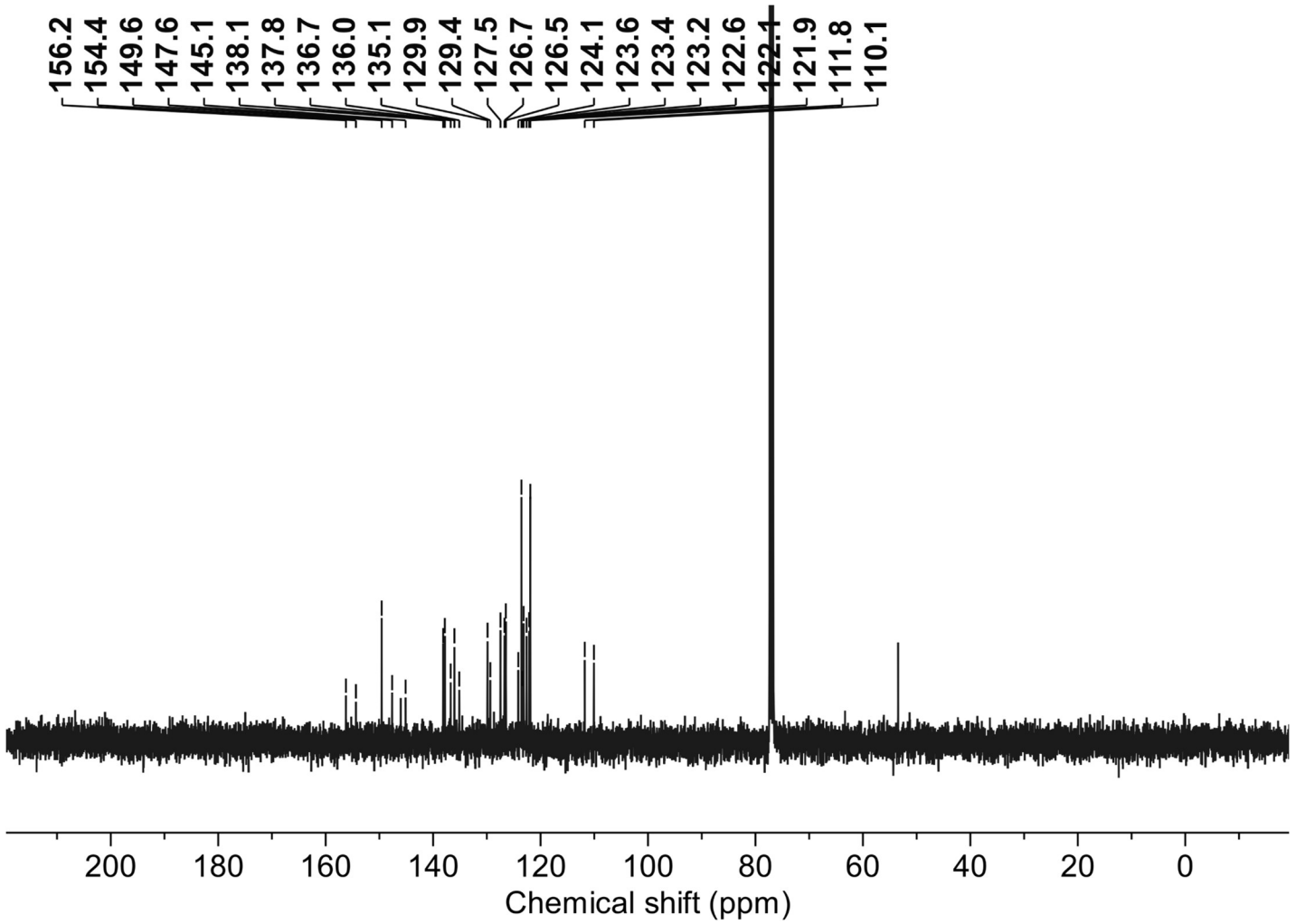

***N*^{1},*N*^{4}-di(1,10-phenanthrolin-2-yl)benzene-1,4-diamine (22a)**: ^{1}H NMR (400 MHz, DMSO-d_6)

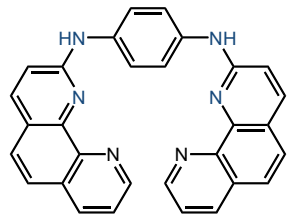

22a

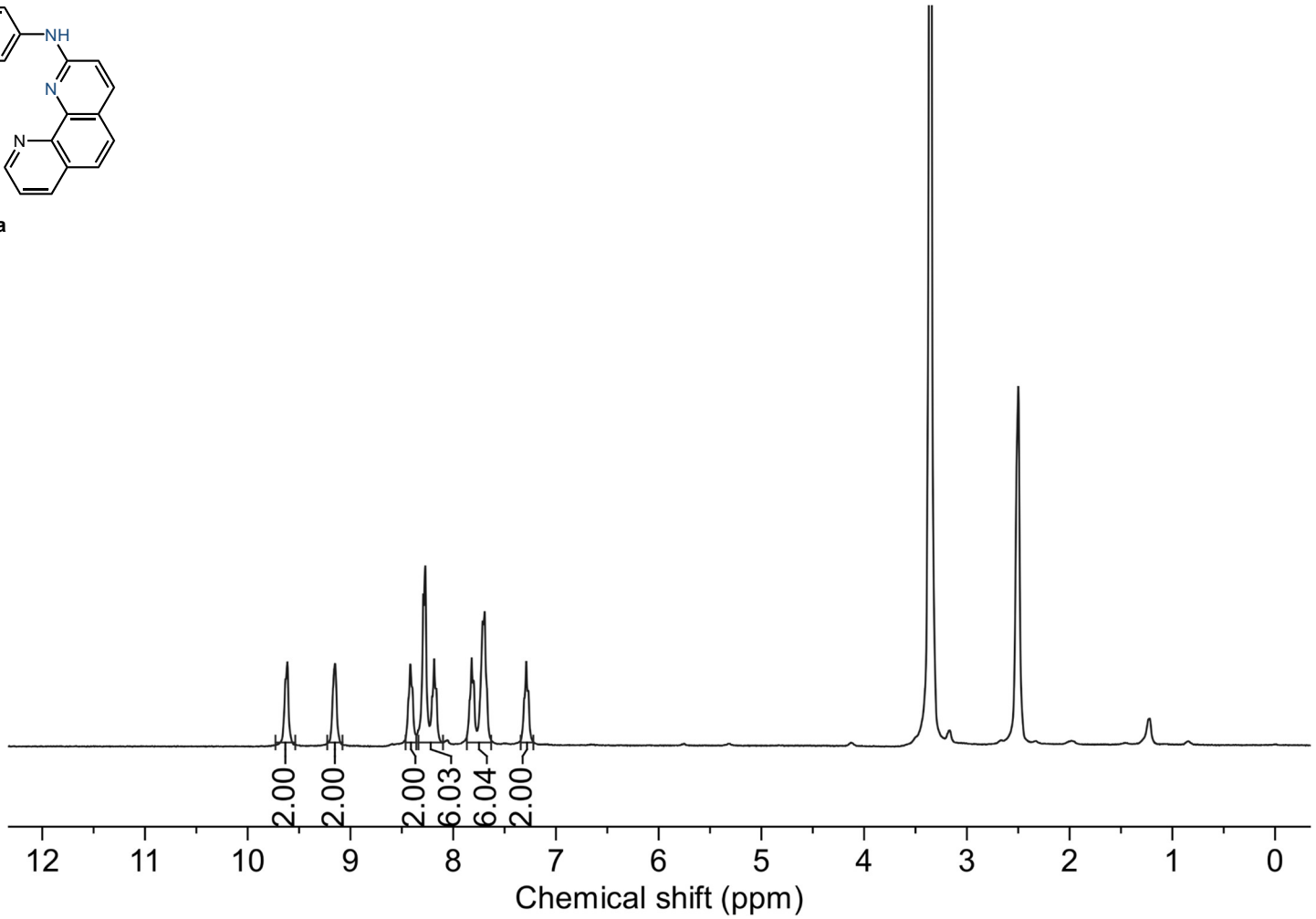

^{13}C NMR (100 MHz, DMSO-d_6)

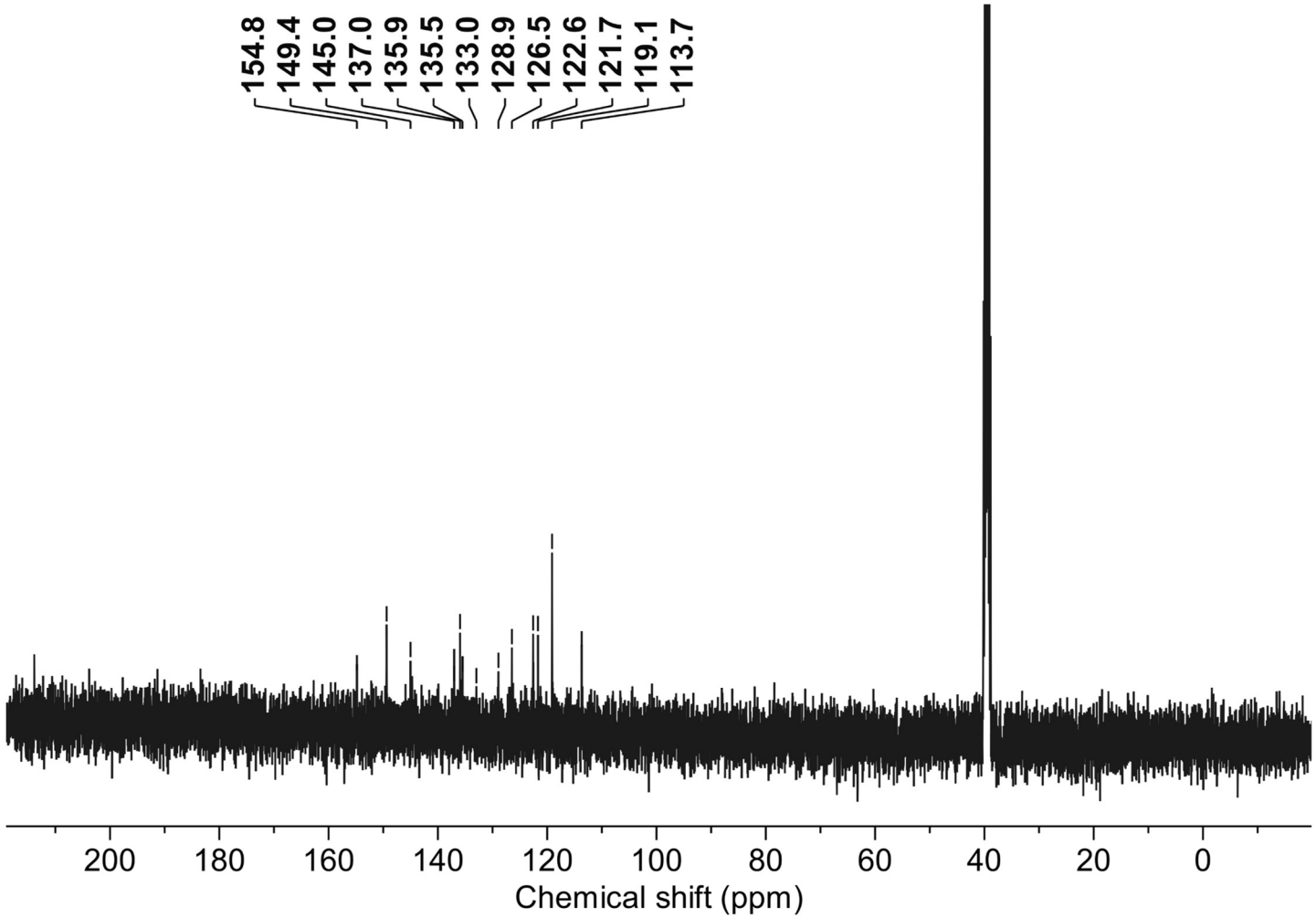

2,2'-(1,4-phenylenebis(azanediyl))bis(*N*-((*S*)-1-phenylethyl)quinoline-4-carboxamide) (23a): ^{1}H NMR (400 MHz, DMSO-d_6)

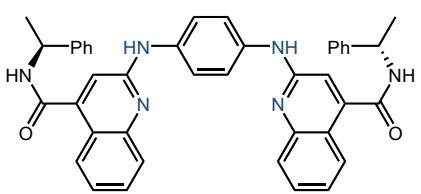

23a

^{13}C NMR (100 MHz, DMSO-d_6)

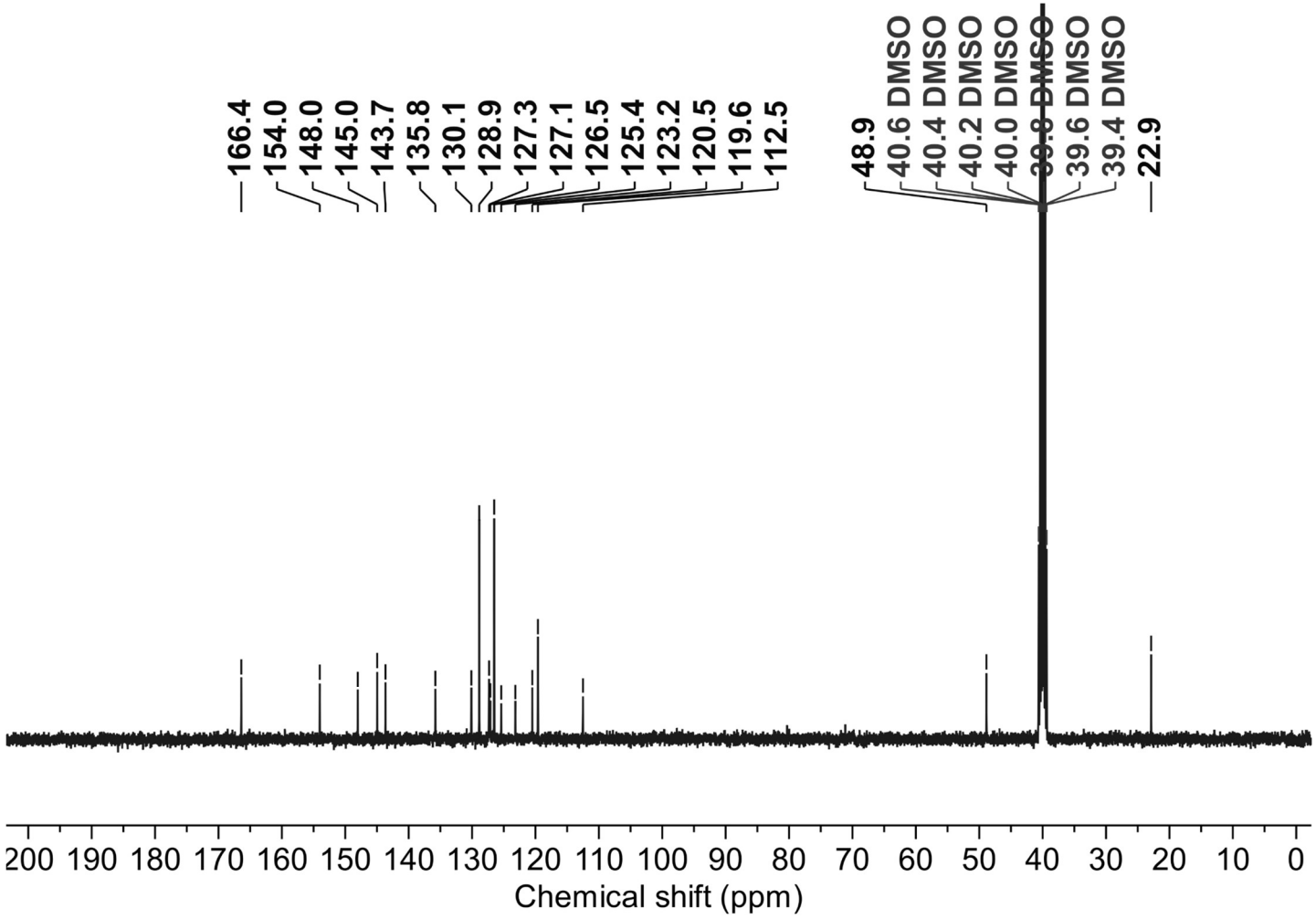

12-methoxybenzo[4,5]imidazo[1,2-*a*][1,10]phenanthroline (**1**): ^{1}H NMR (400 MHz, $CDCl_3$)

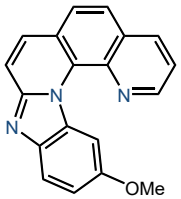

1

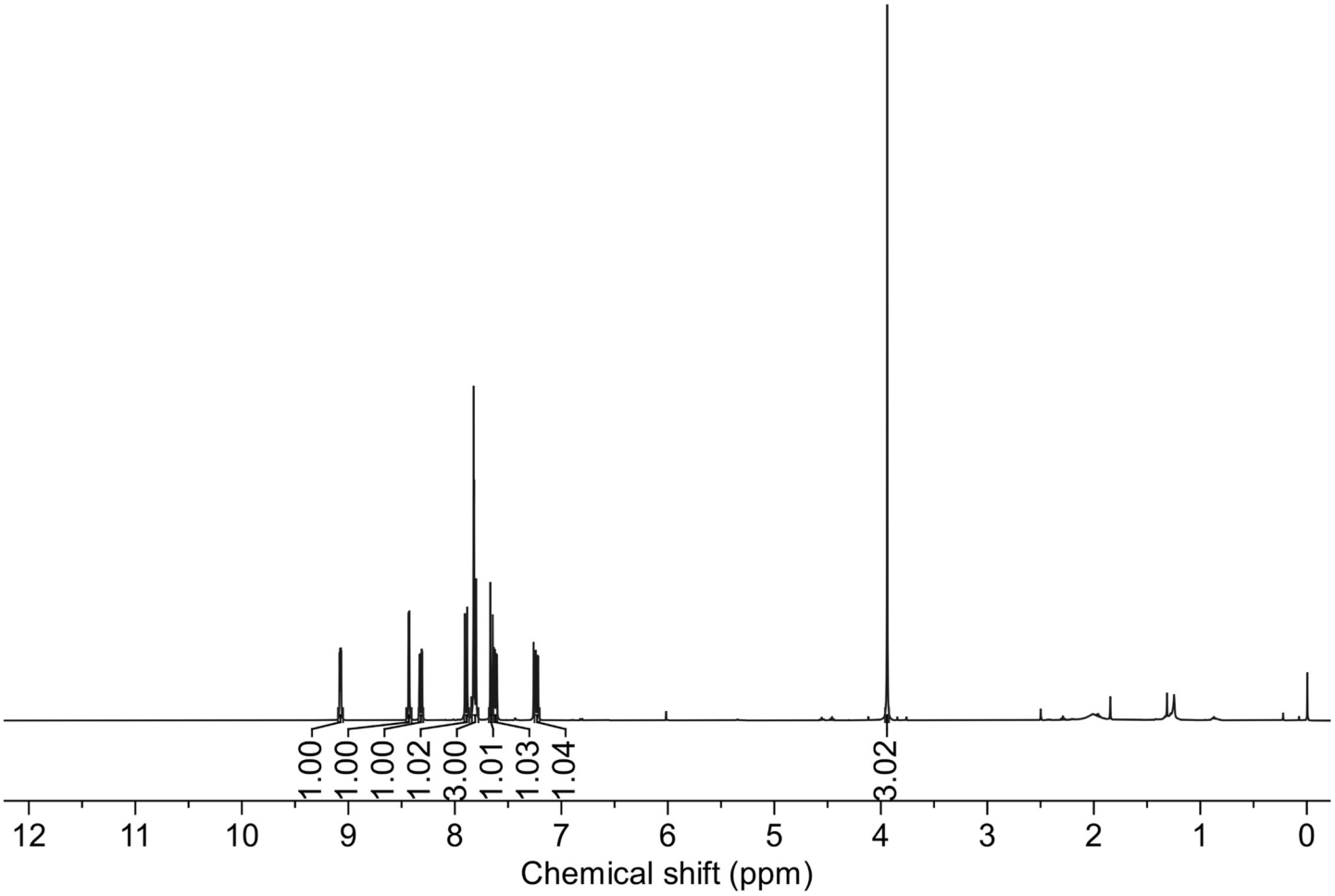

^{13}C NMR (100 MHz, $CDCl_3$)

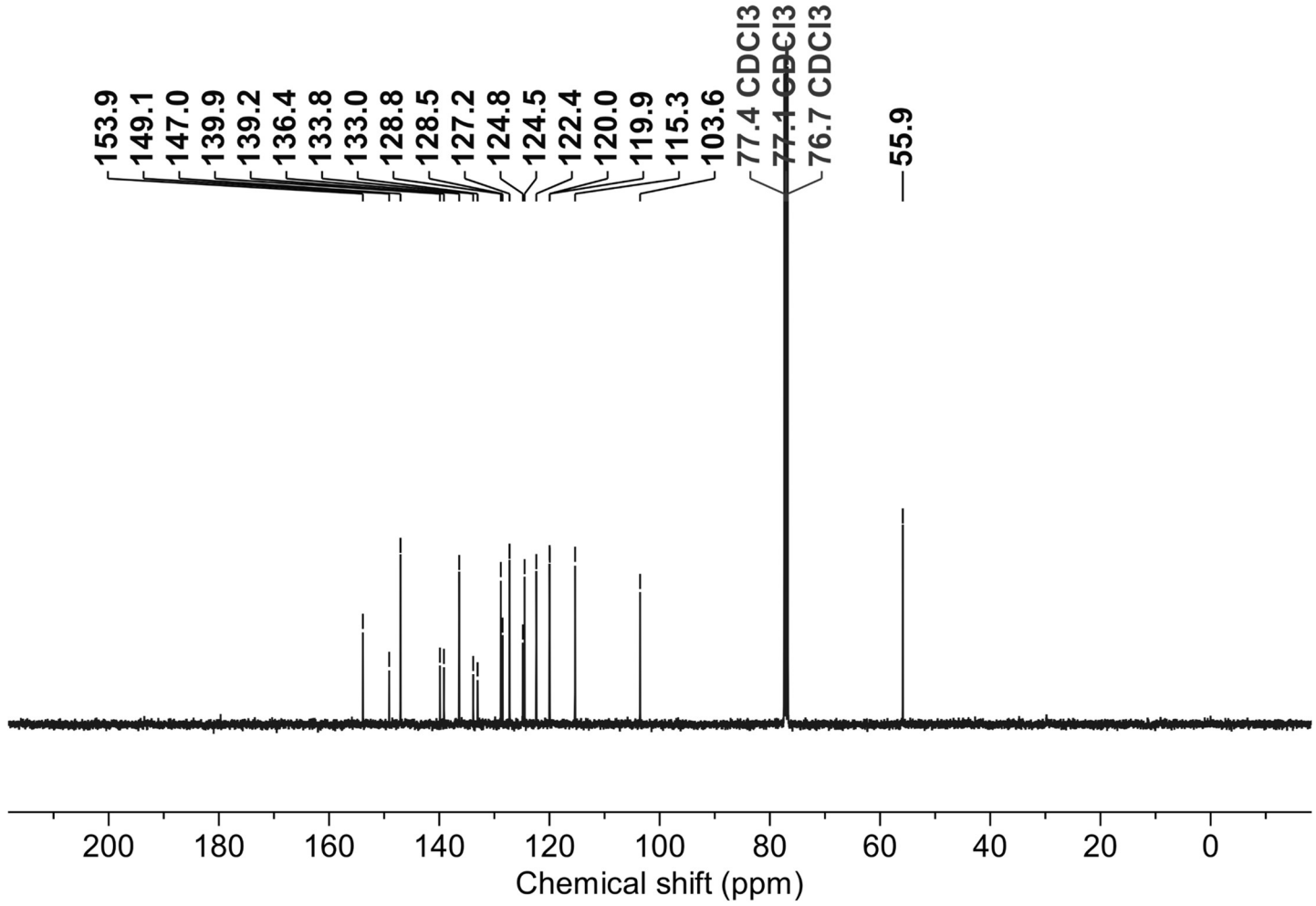

Benzo[4,5]imidazo[1,2-a][1,10]phenanthroline-12-carbonitrile (**2**): ^{1}H NMR (400 MHz, $CDCl_3$)

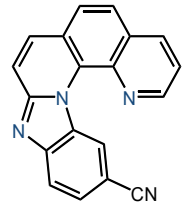

2

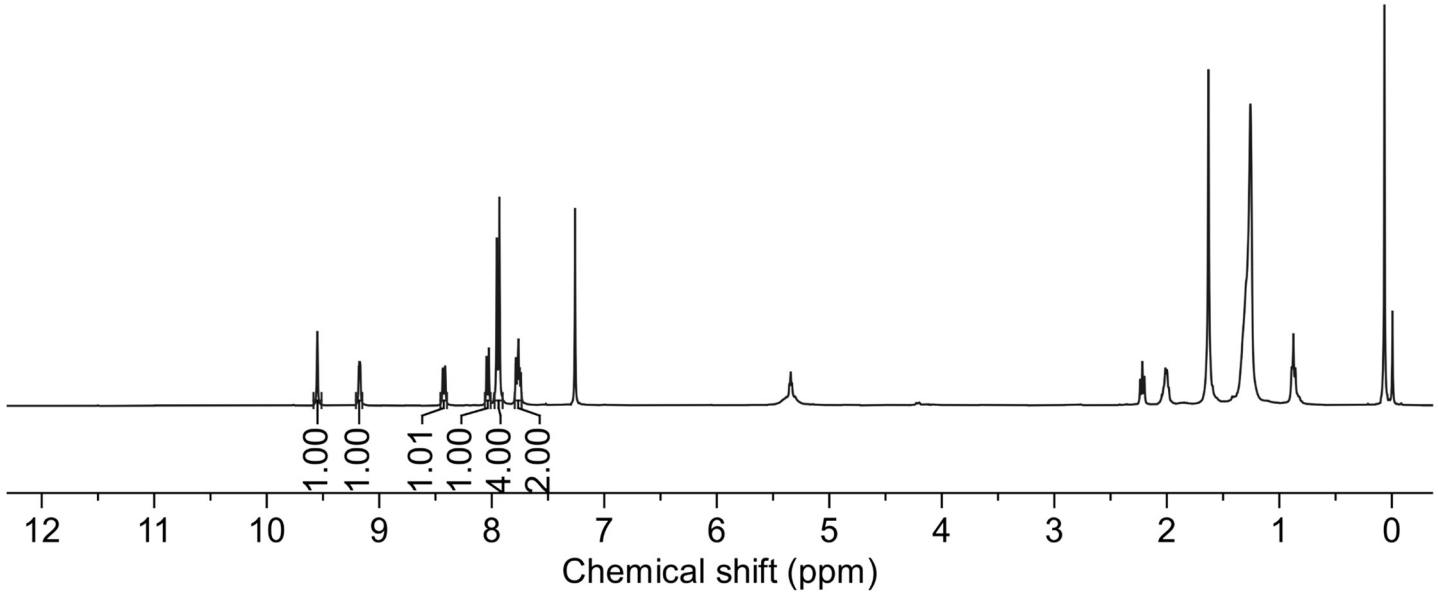

^{13}C NMR (100 MHz, $CDCl_3$)

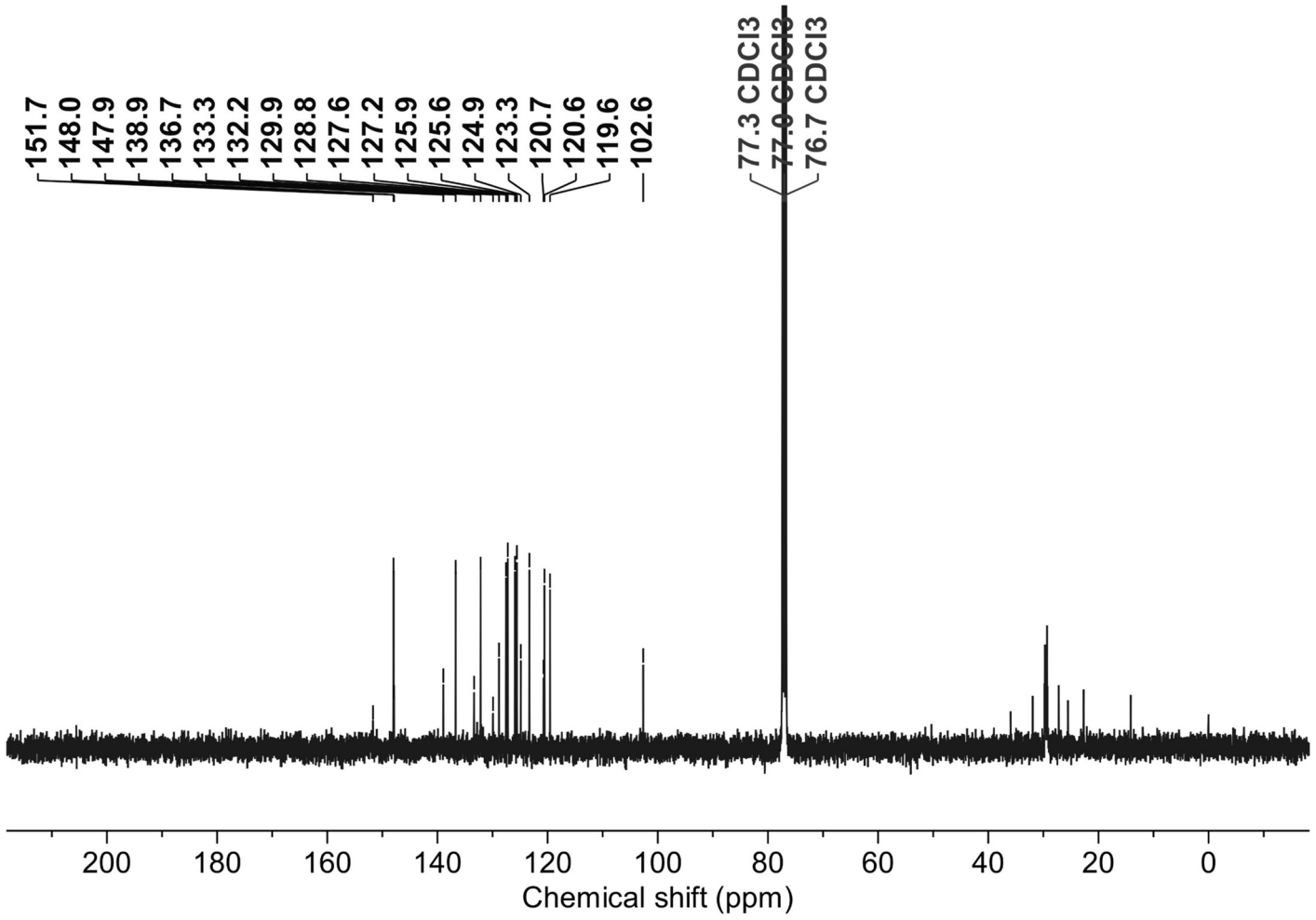

Quinolino[8',7':4,5]imidazo[1,2-a][1,10]phenanthroline (**3**): ^{1}H NMR (400 MHz, $CDCl_3$)

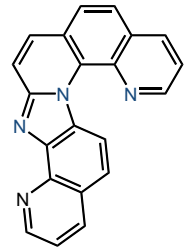

3

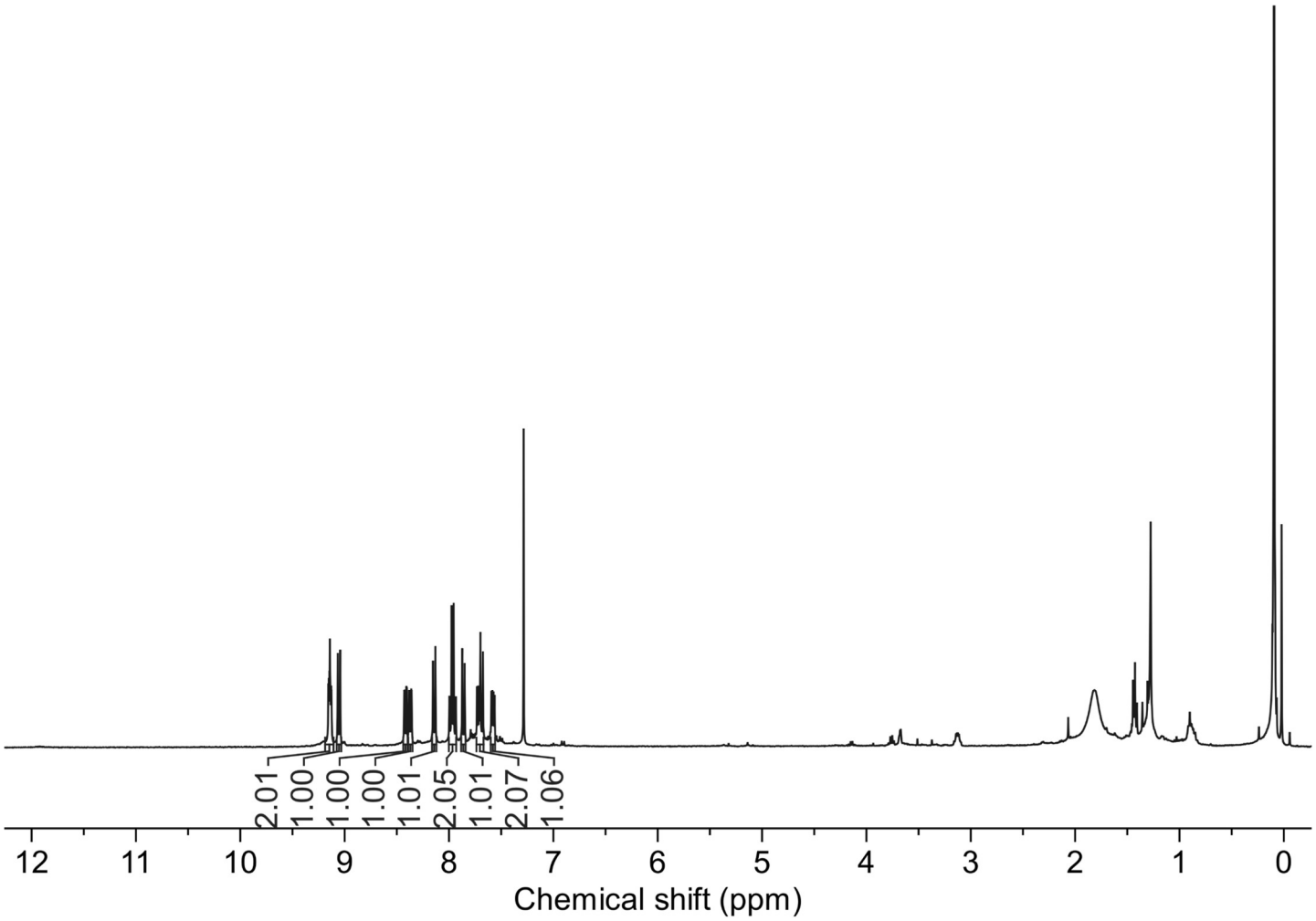

^{13}C NMR (100 MHz, $CDCl_3$)

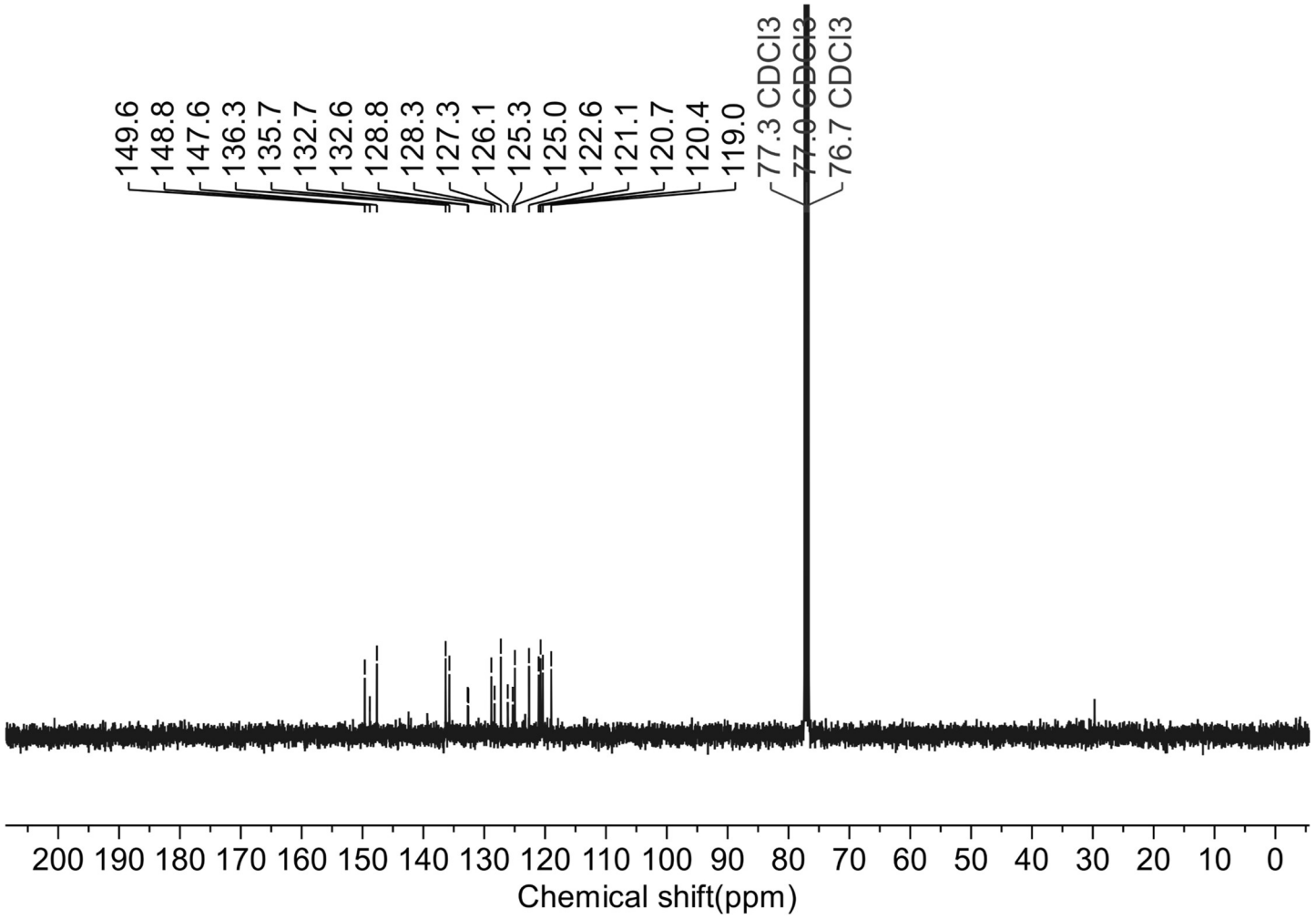

Benzo[4,5]imidazo[1,2-*a*]benzo[4,5]imidazo[2,1-*k*][1,10]phenanthroline (**4**): ^{1}H NMR (400 MHz, DMSO-d_6)

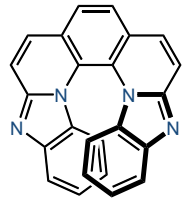

4

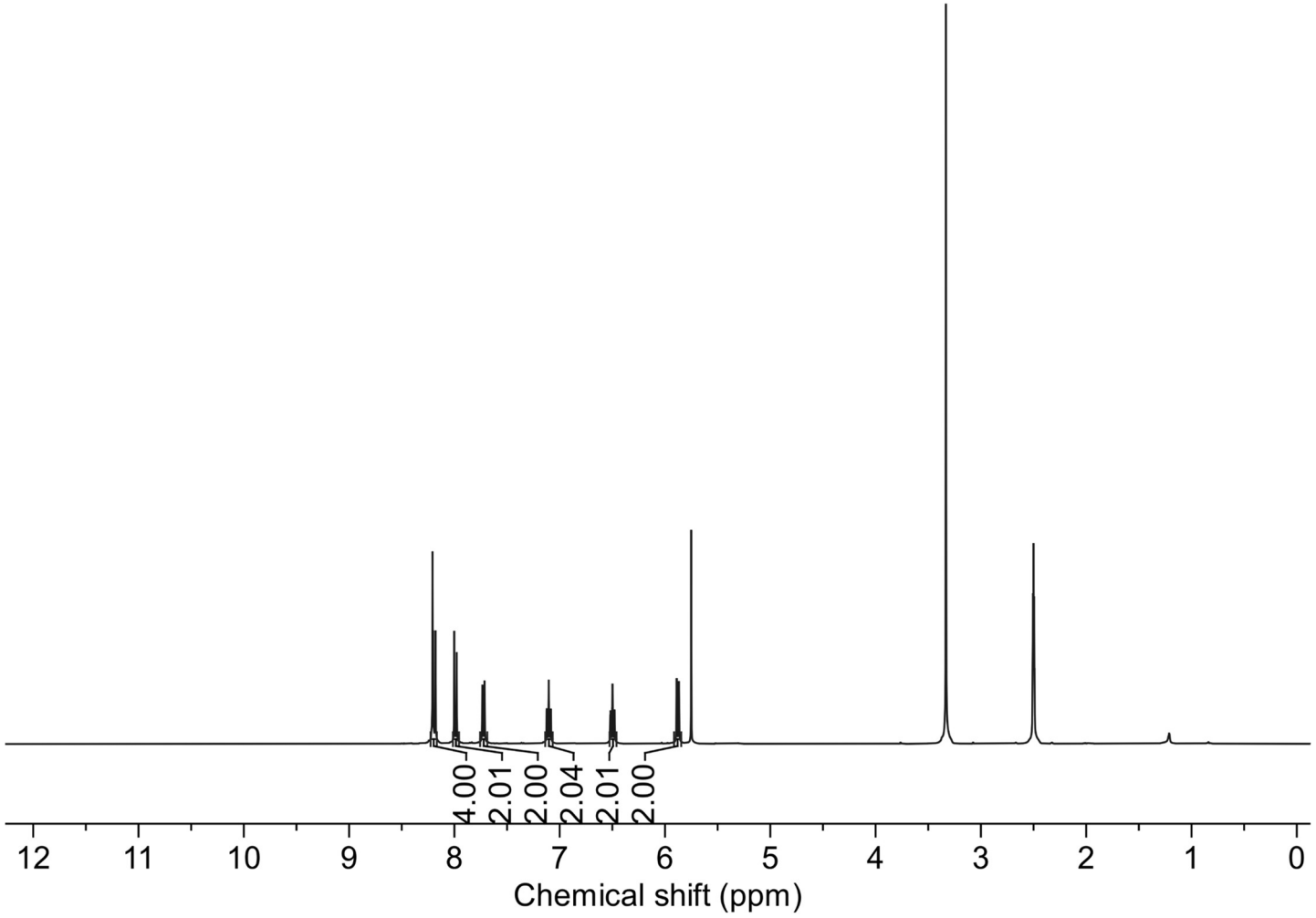

^{13}C NMR (100 MHz, DMSO-d_6)

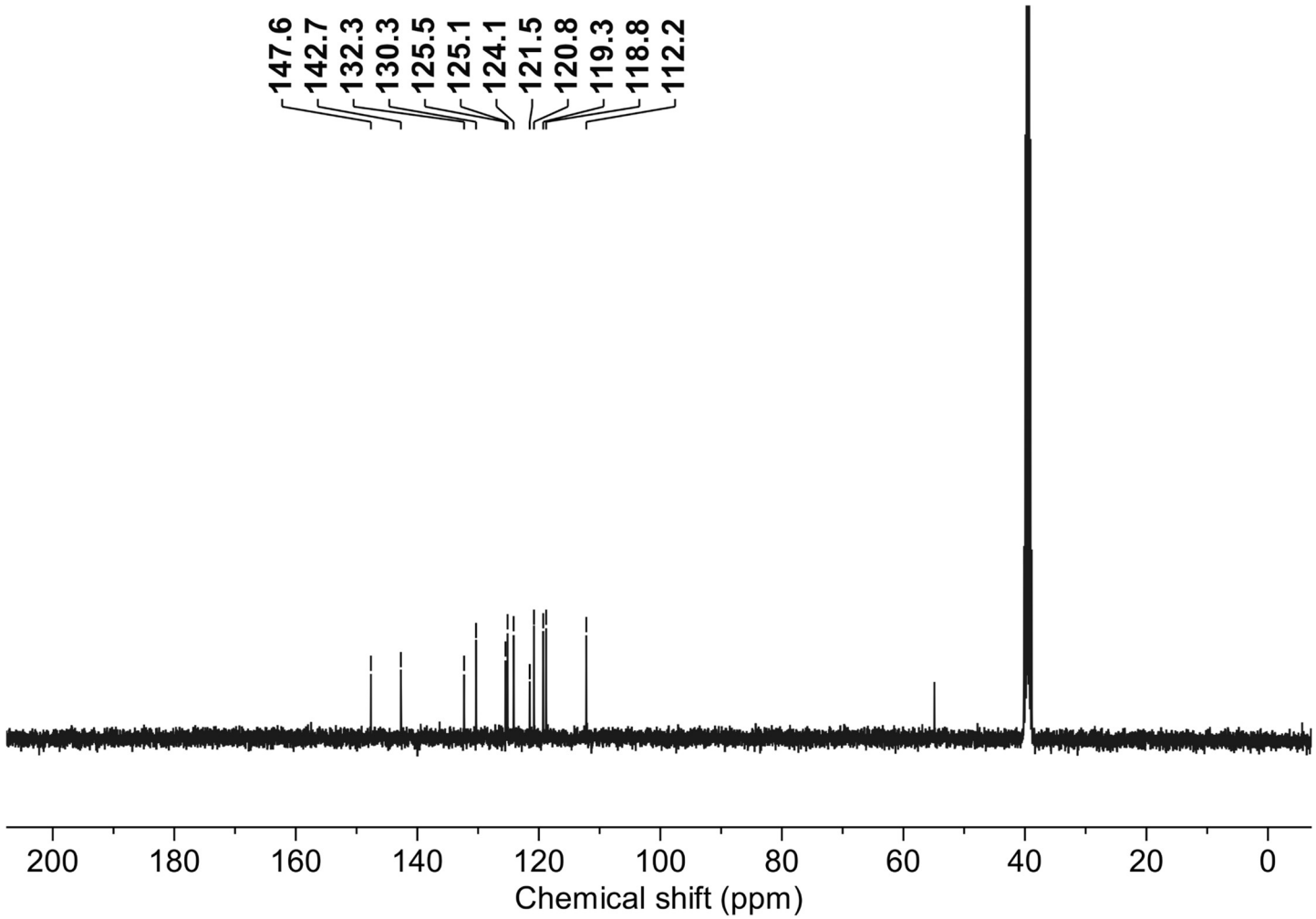

10,15-dimethoxybenzo[4,5]imidazo[1,2-*a*]benzo[4,5]imidazo[2,1-*k*][1,10]phenanthroline (**5**): ^{1}H NMR (400 MHz, DMSO-d_6)

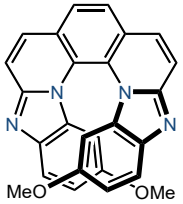

5

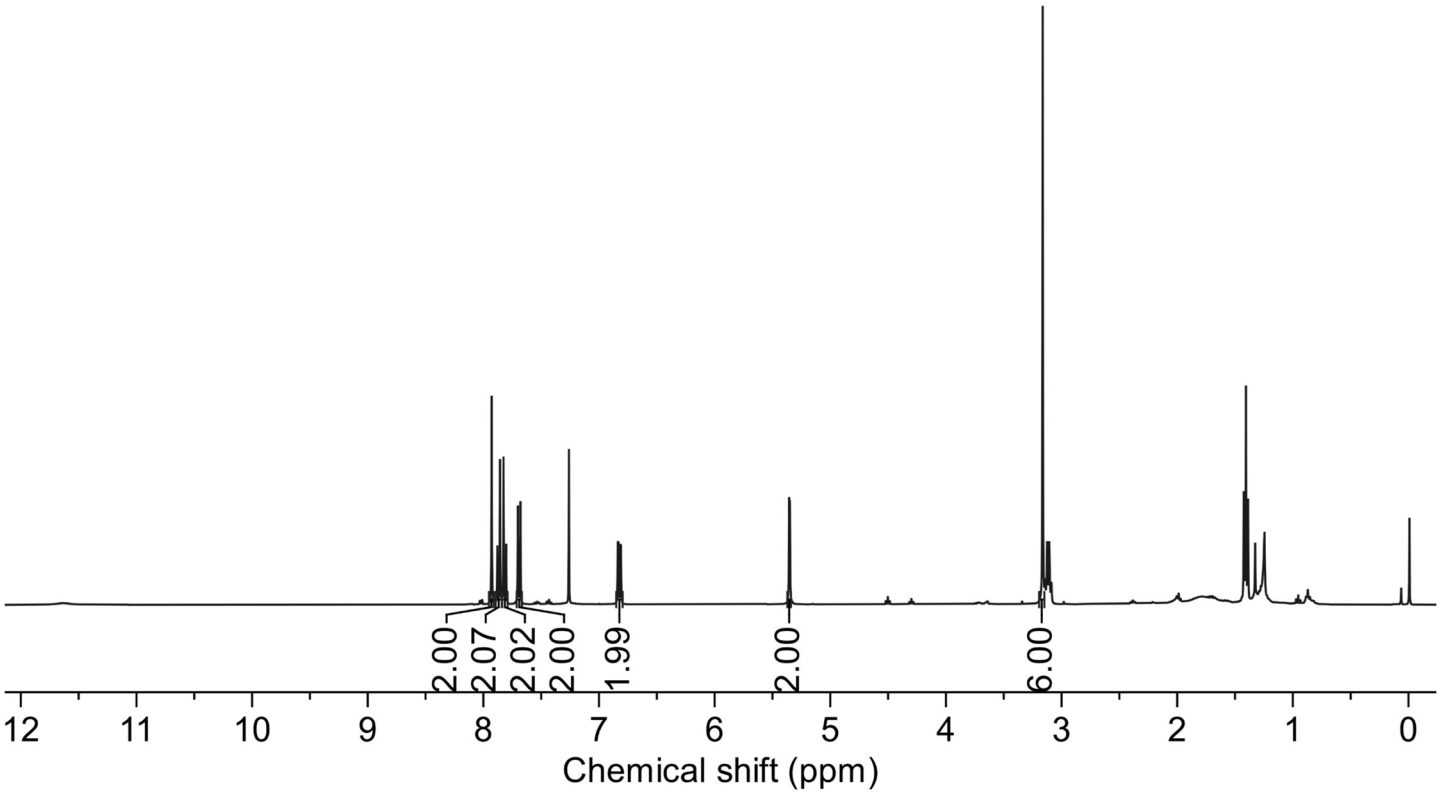

^{13}C NMR (100 MHz, DMSO-d_6)

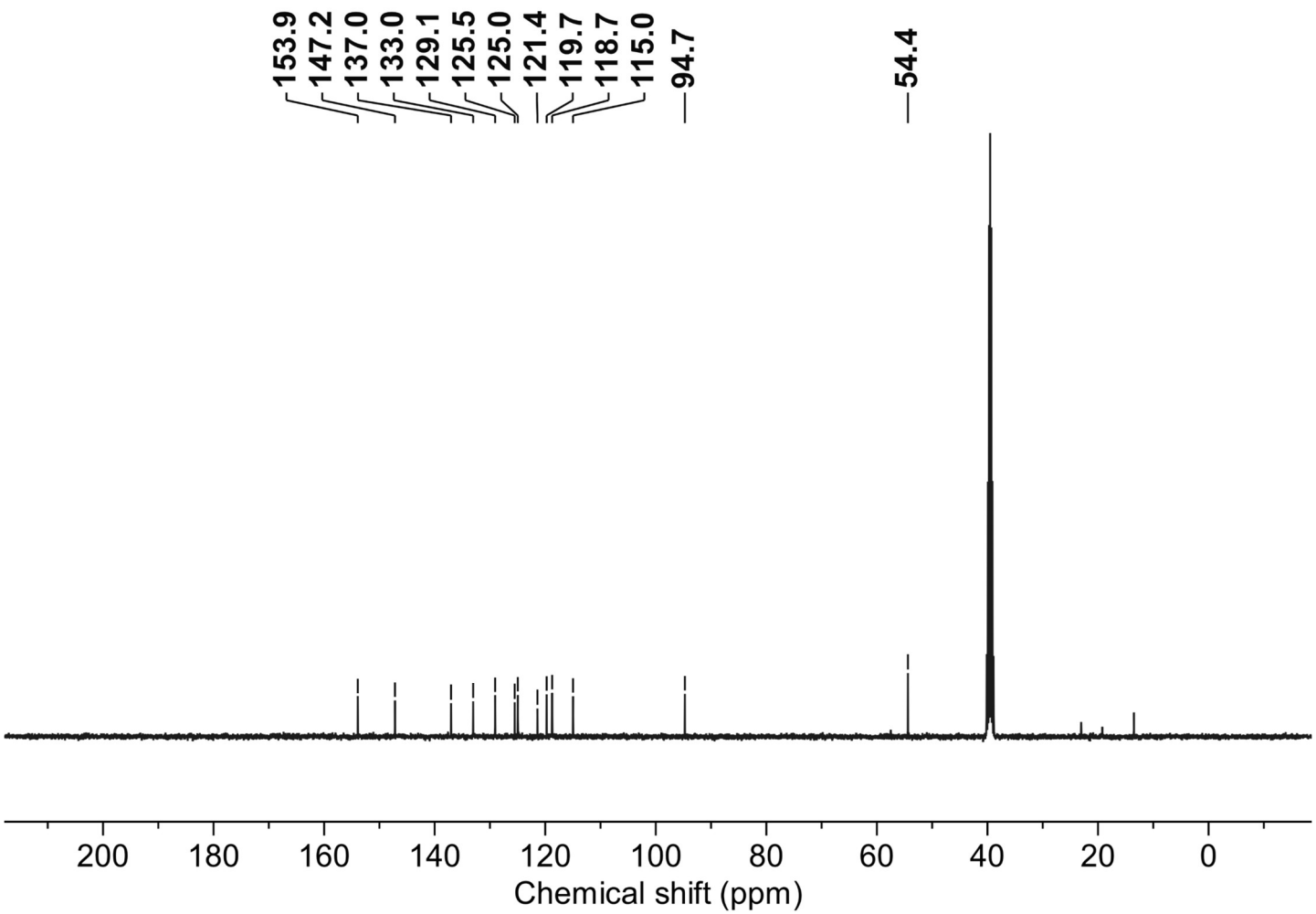

10,15-bis(cyclopentyloxy)benzo[4,5]imidazo[1,2-a]benzo[4,5]imidazo[2,1-k][1,10]phenanthroline (**6**): ^{1}H NMR (400 MHz, $CDCl_3$)

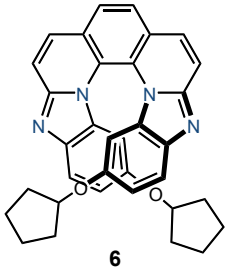

6

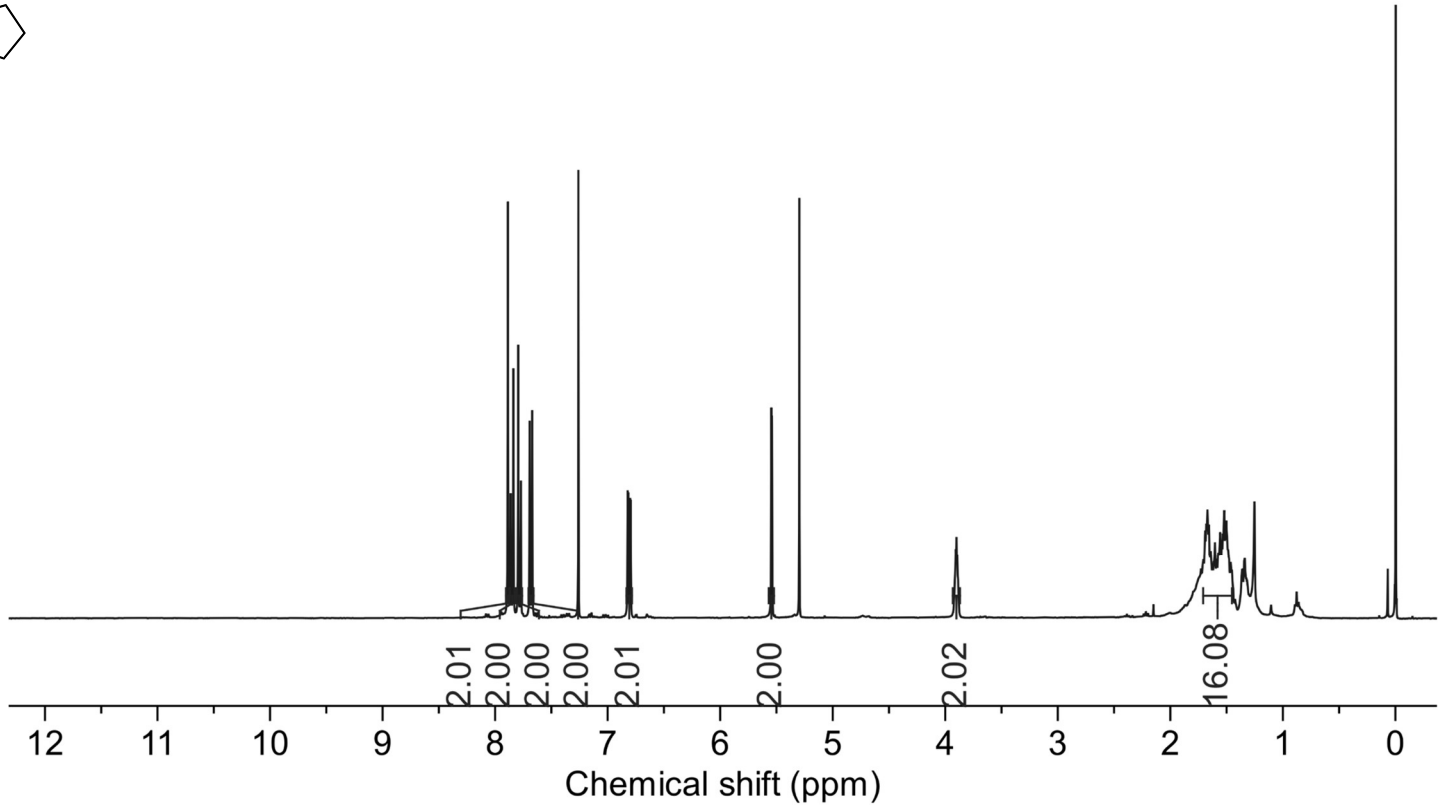

^{13}C NMR (100 MHz, $CDCl_3$)

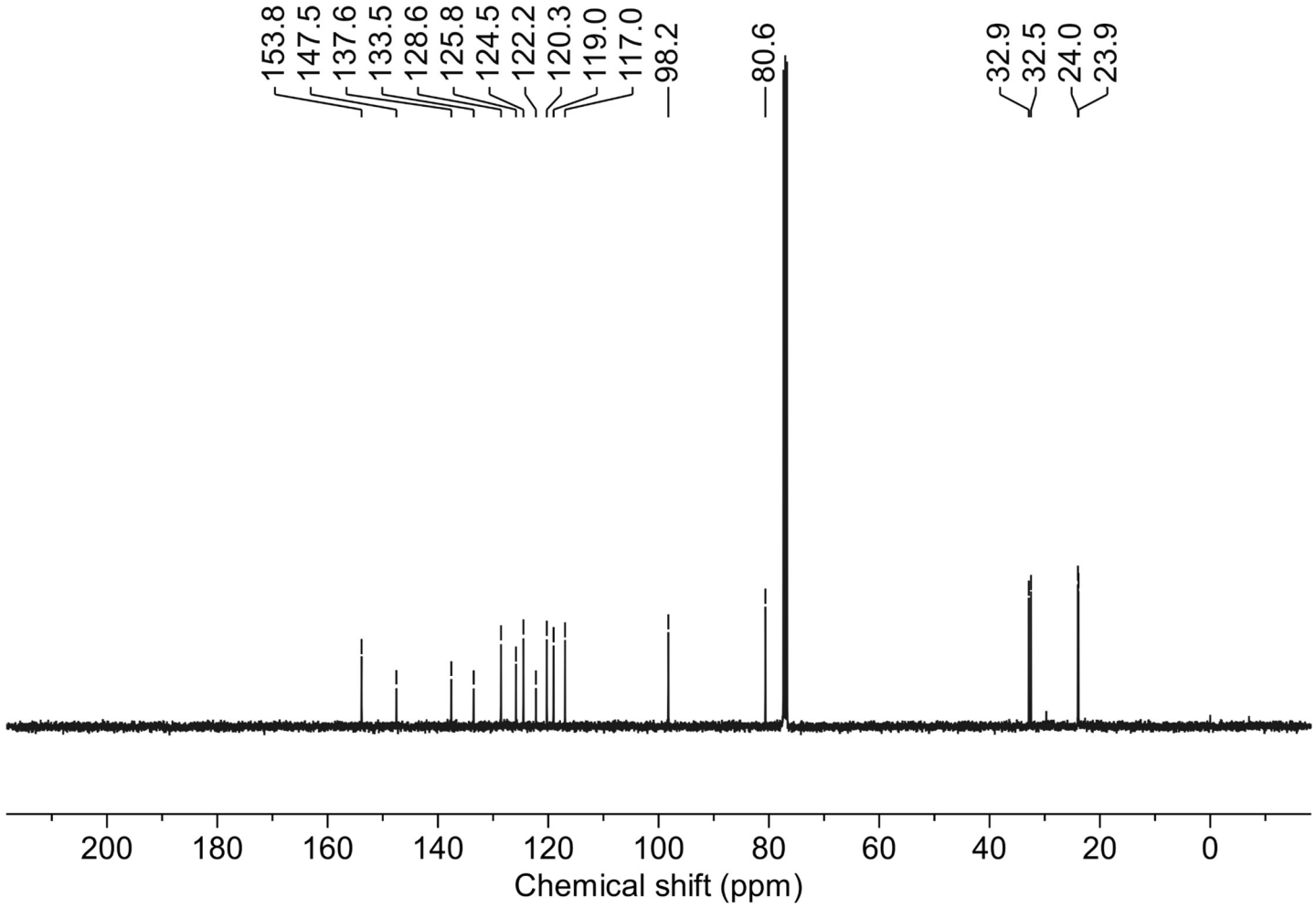

10,15-di-*tert*-butylbenzo[4,5]imidazo[1,2-*a*]benzo[4,5]imidazo[2,1-*k*][1,10]phenanthroline (7): ^{1}H NMR (400 MHz, $CDCl_3$)

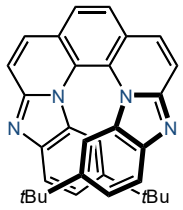

7

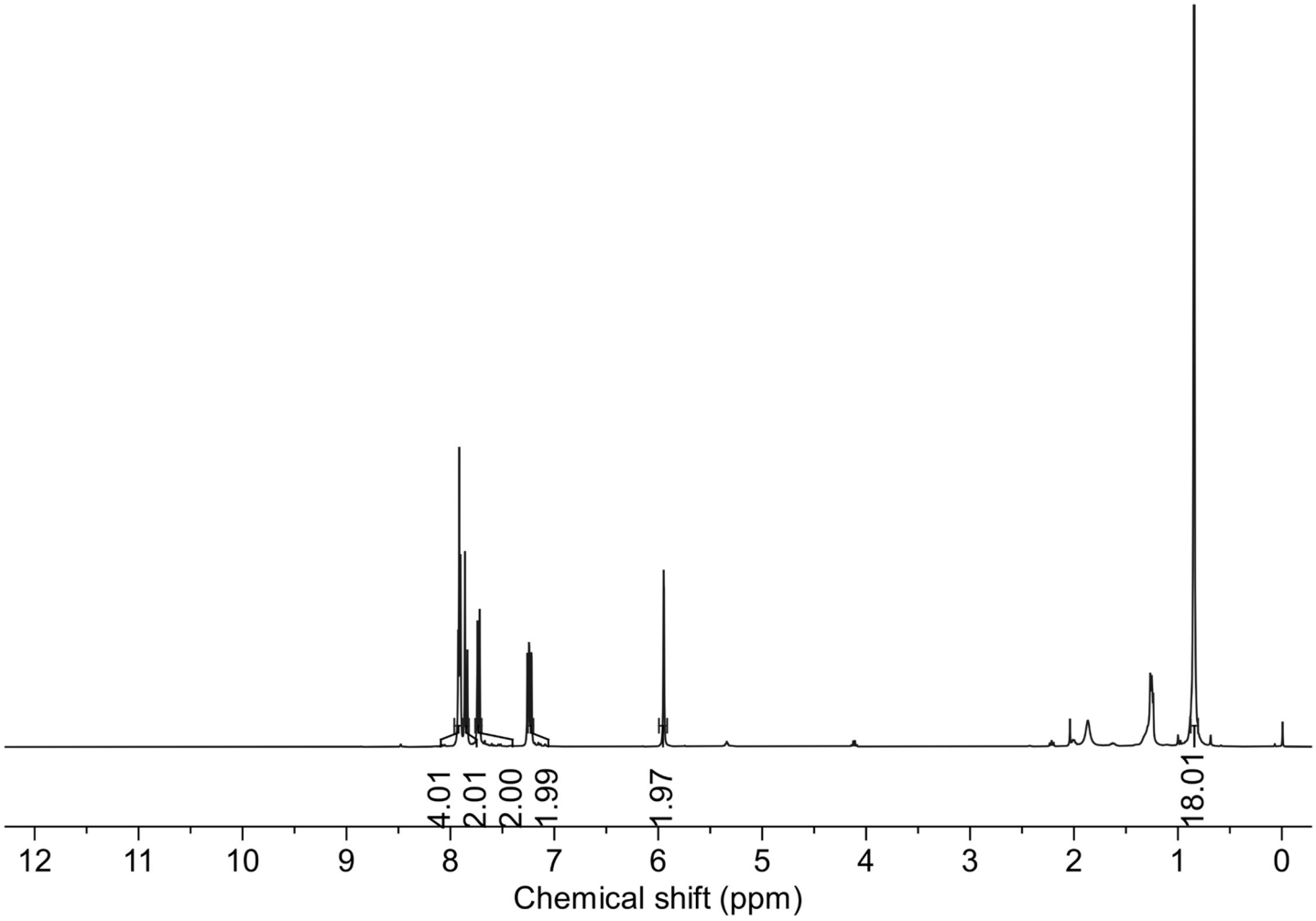

^{13}C NMR (100 MHz, $CDCl_3$)

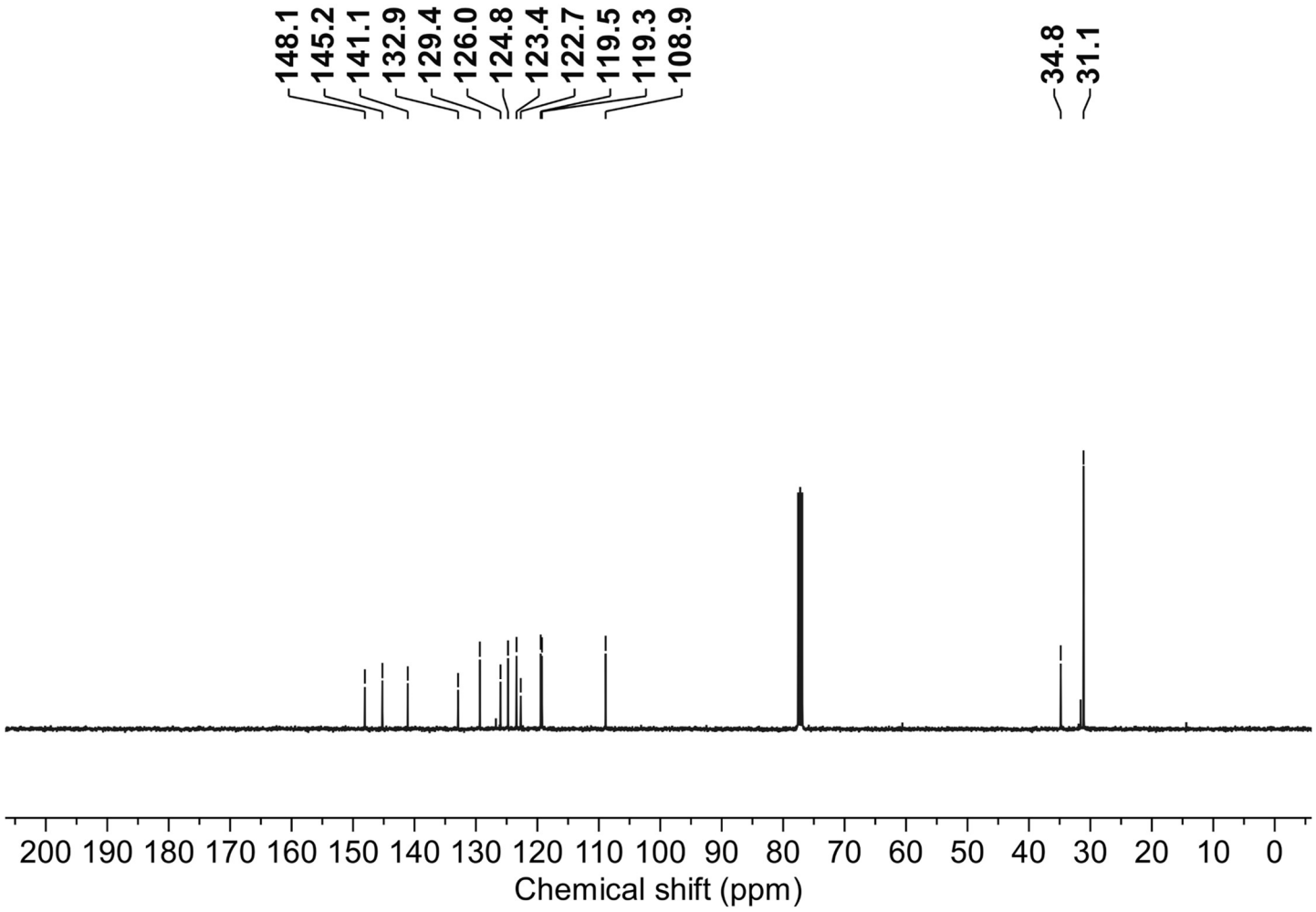

10,15-diphenylbenzo[4,5]imidazo[1,2-a]benzo[4,5]imidazo[2,1-k][1,10]phenanthroline (8): ^{1}H NMR (800 MHz, $CDCl_3$)

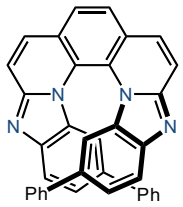

8

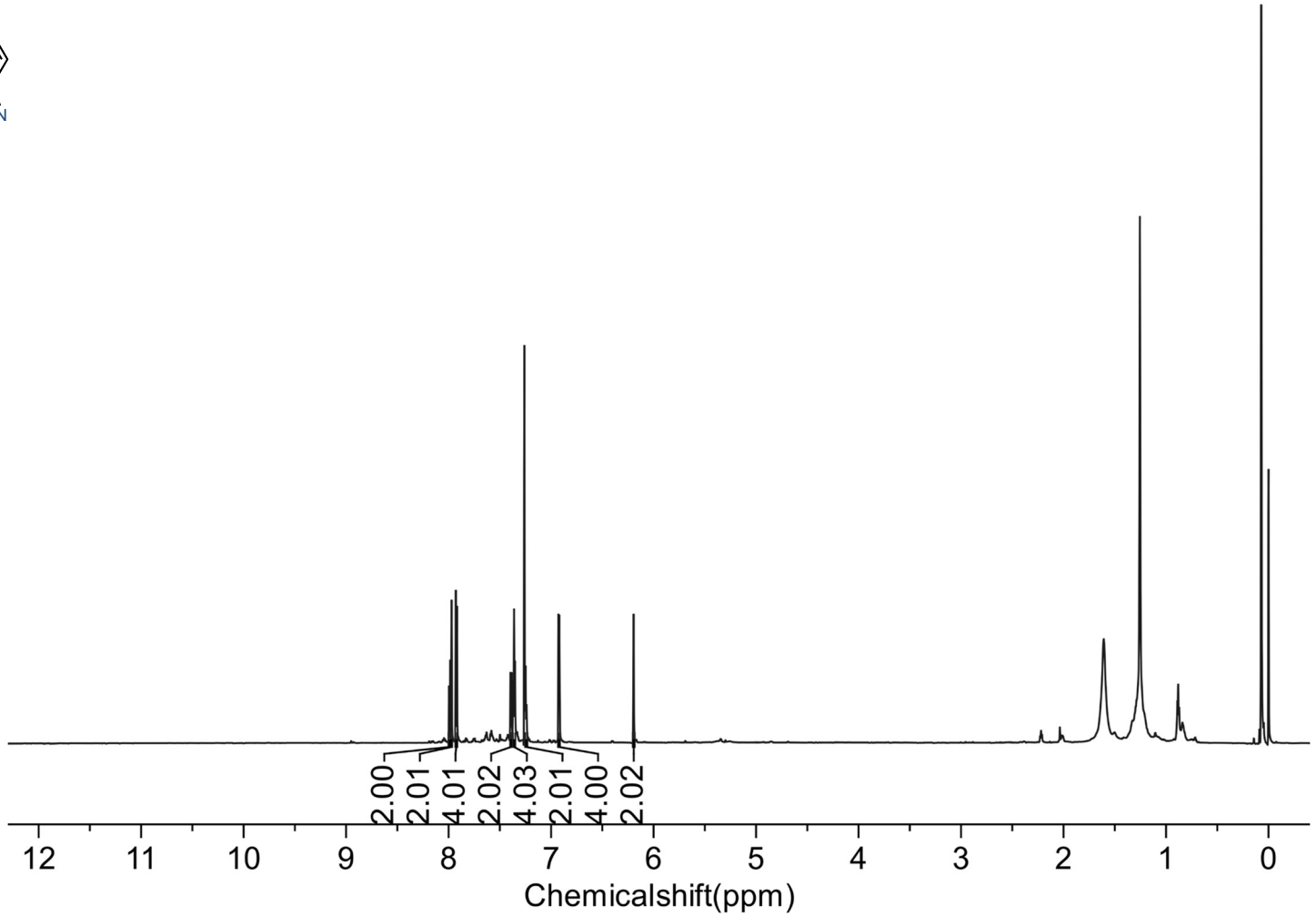

^{13}C NMR (200 MHz, $CDCl_3$)

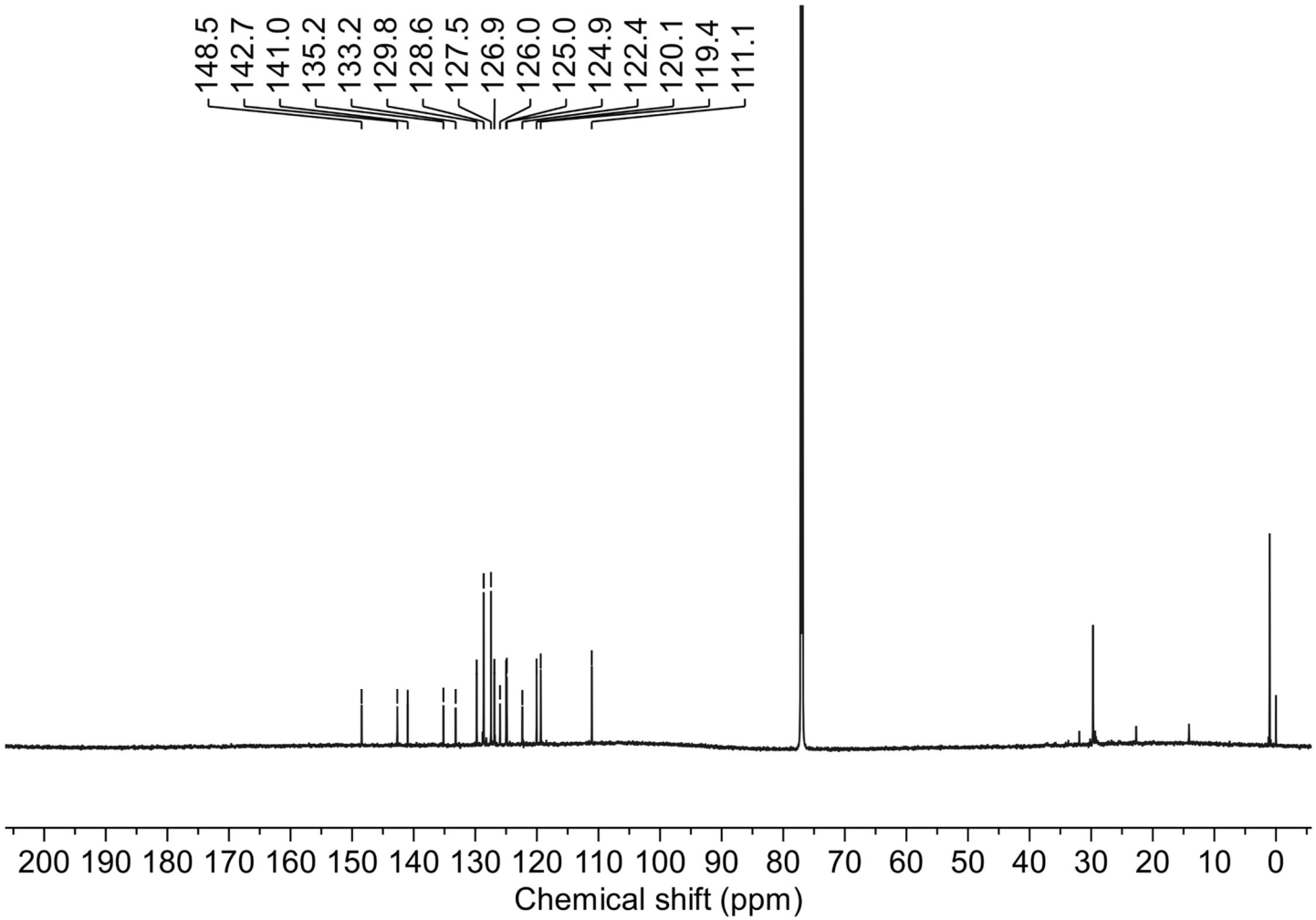

Dimethyl benzo[4,5]imidazo[1,2-*a*]benzo[4,5]imidazo[2,1-*k*][1,10]phenanthroline-10,15-dicarboxylate (**9**): ^{1}H NMR (400 MHz, $CDCl_3$)

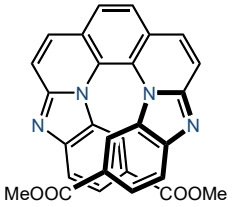

9

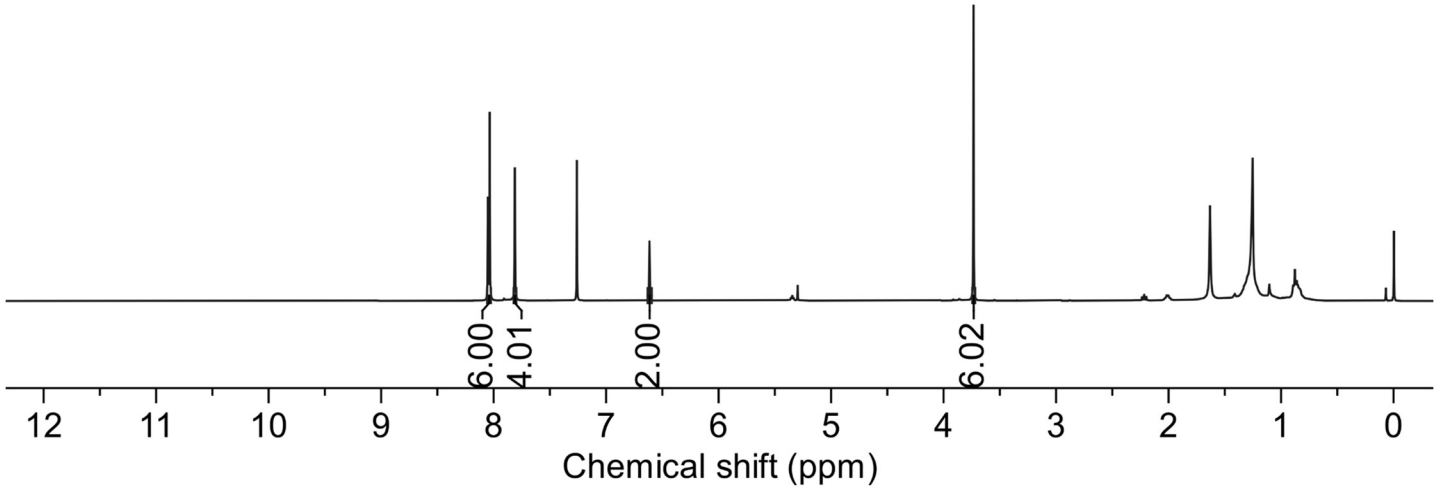

^{13}C NMR (200 MHz, $CDCl_3$)

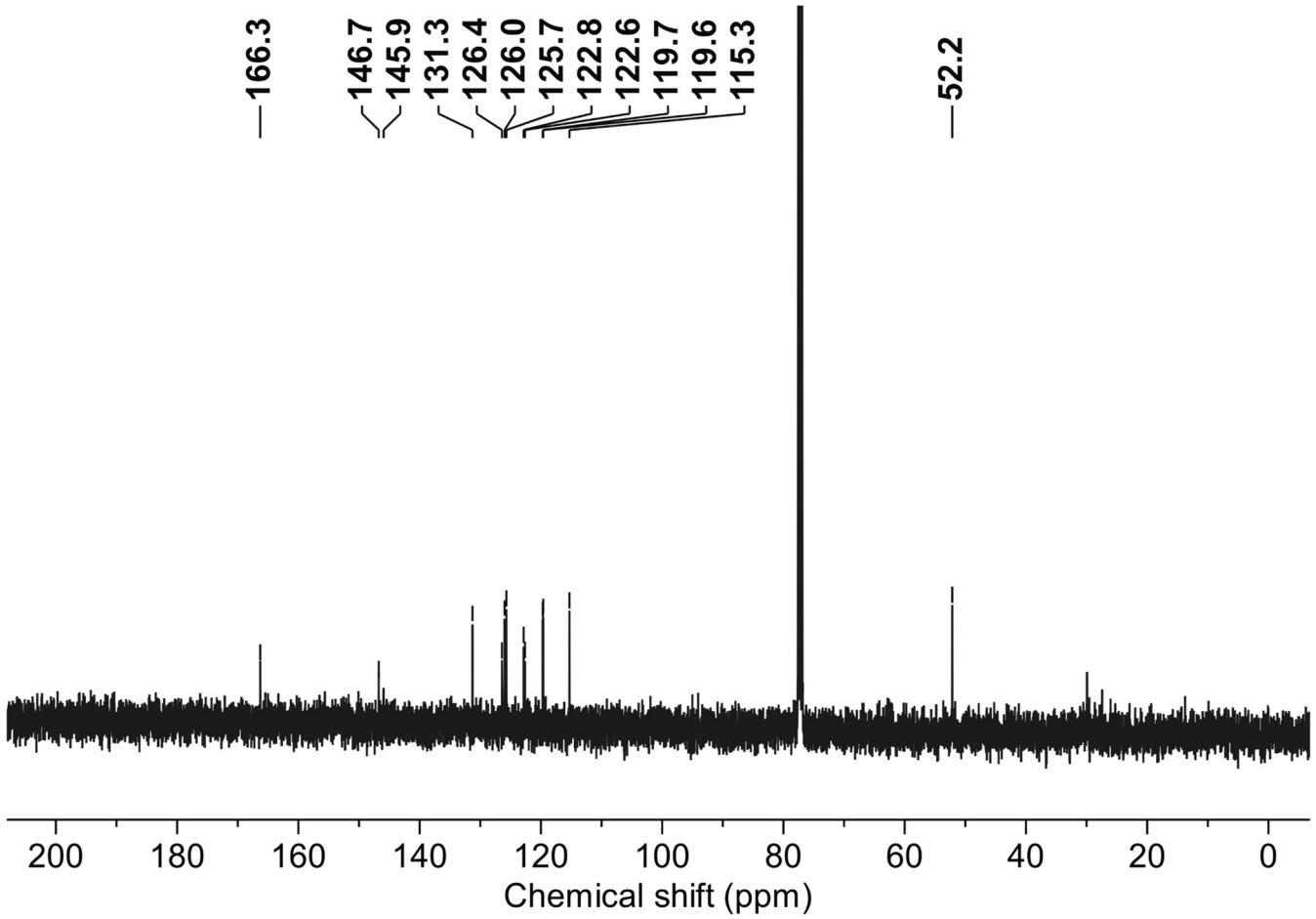

1,1'-(benzo[4,5]imidazo[1,2-a]benzo[4,5]imidazo[2,1-k][1,10]phenanthroline-10,15-diyl)bis(ethan-1-one) (**10**): ^{1}H NMR (400 MHz, $CDCl_3$)

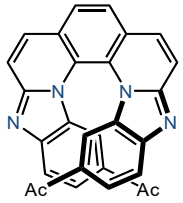

10

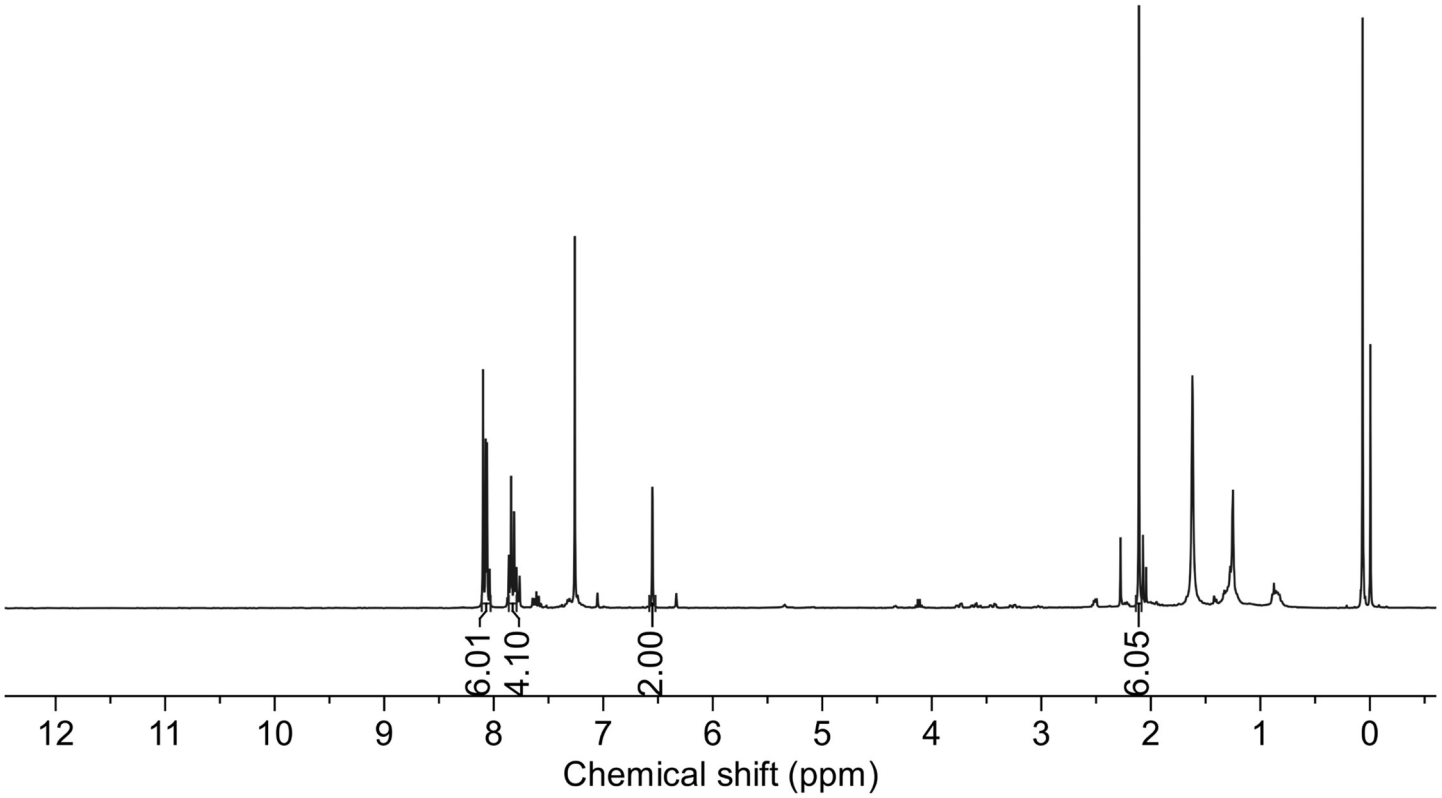

^{13}C NMR (100 MHz, $CDCl_3$)

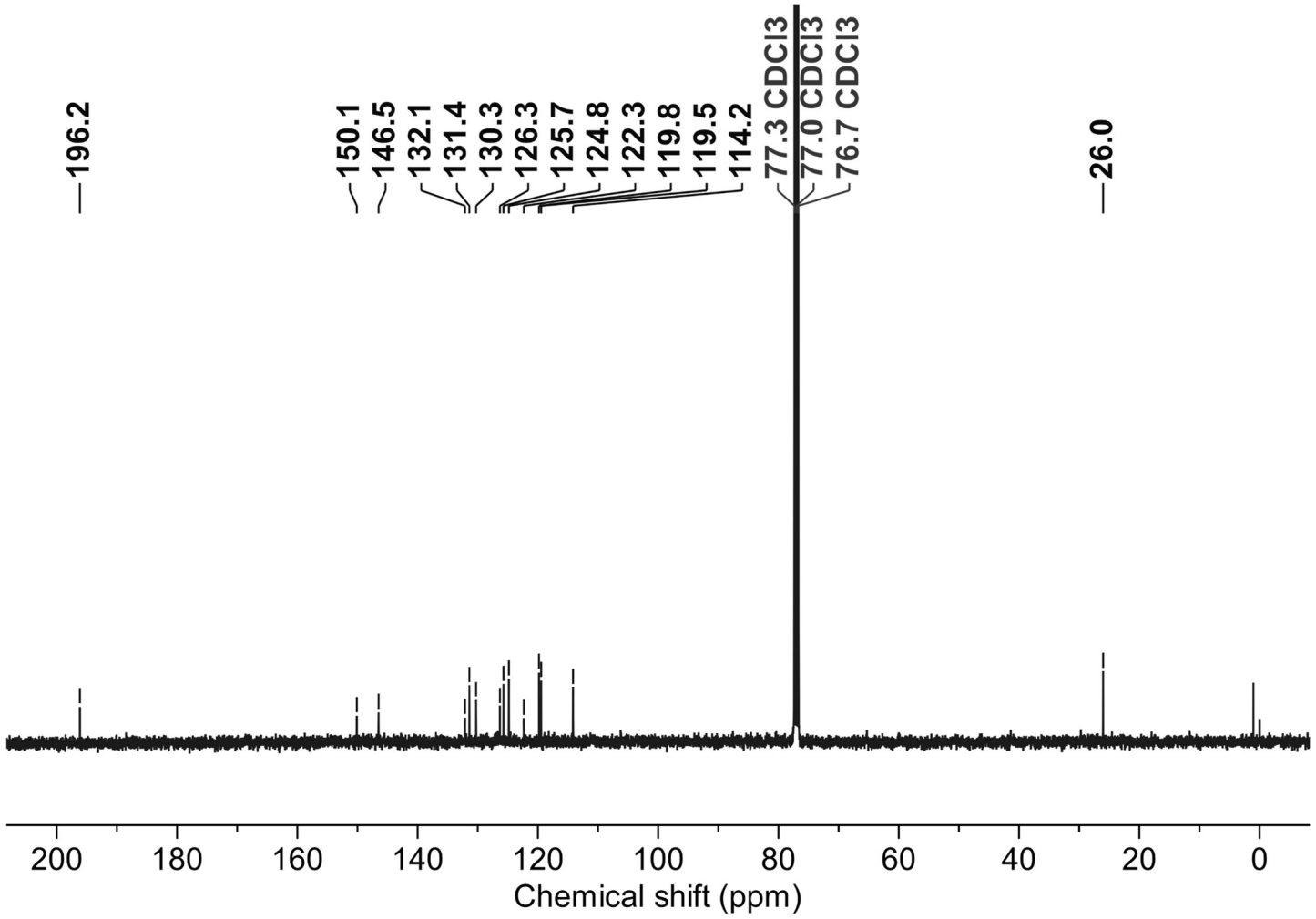

10,15-bis(trifluoromethyl)benzo[4,5]imidazo[1,2-*a*]benzo[4,5]imidazo[2,1-*k*][1,10]phenanthroline (11): ^{1}H NMR (400 MHz, DMSO-d_6)

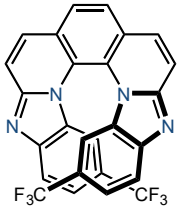

11

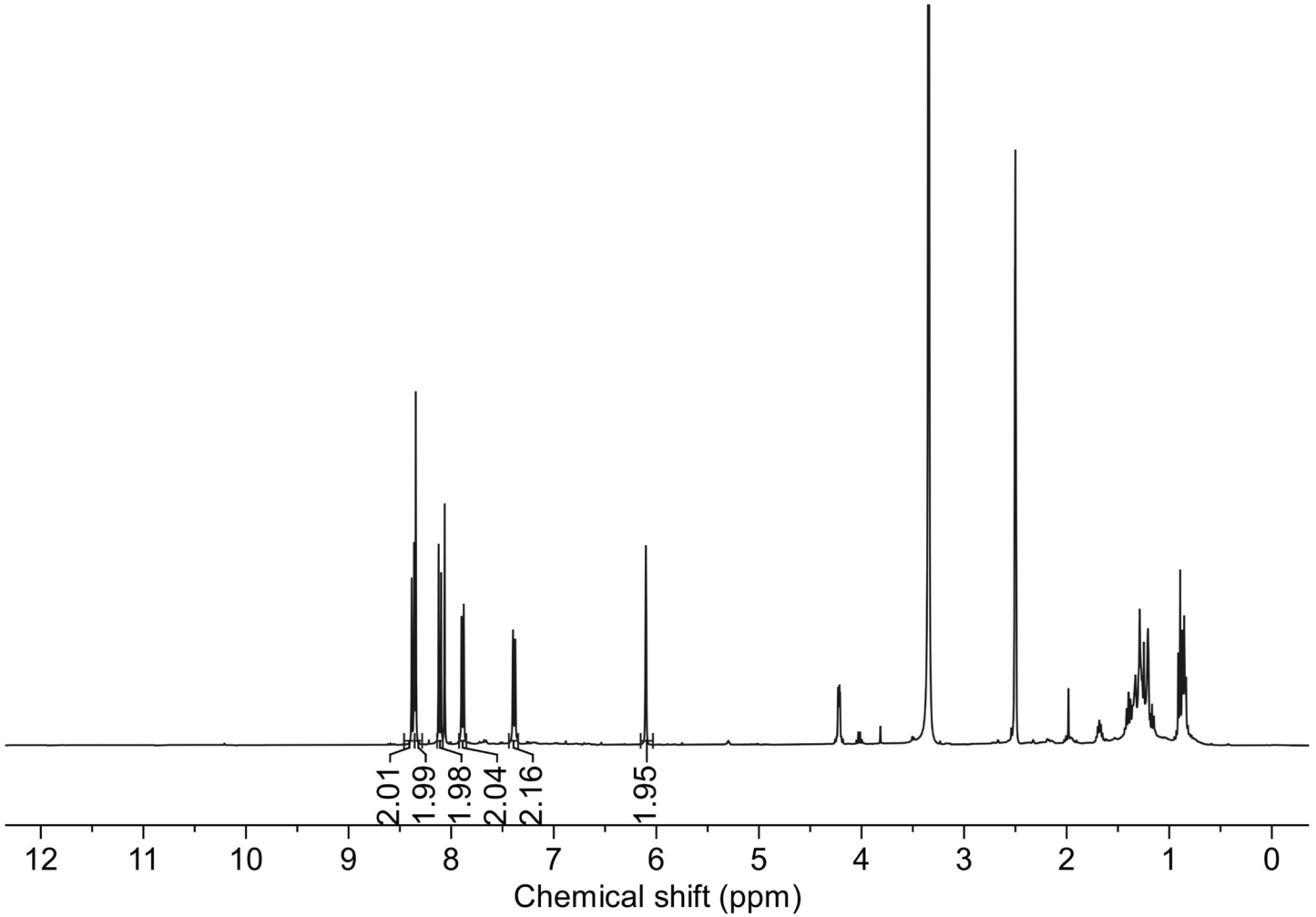

^{13}C NMR (100 MHz, $CDCl_3$)

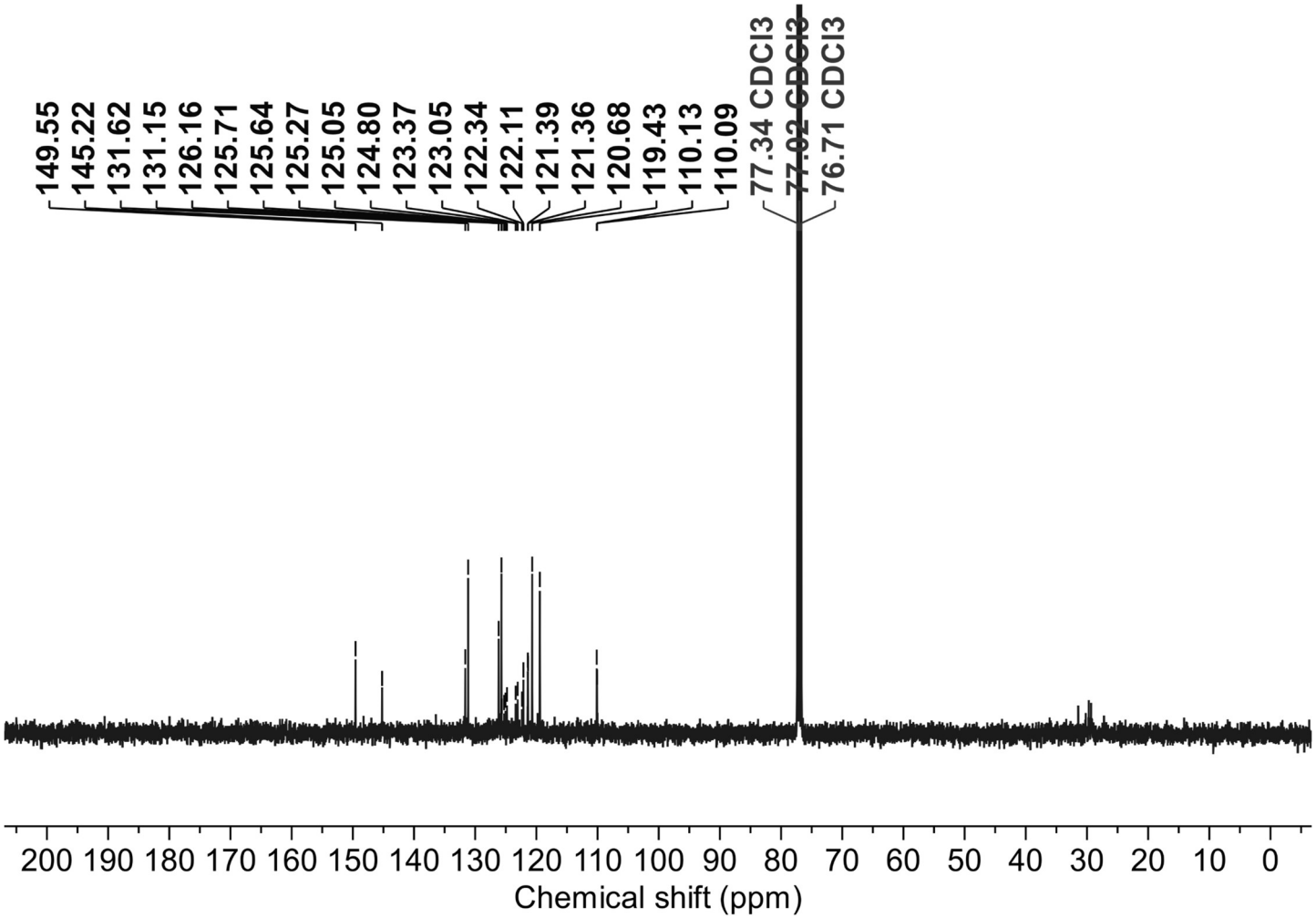

Pyrido[2',3':4,5]imidazo[1,2-a]pyrido[2',3':4,5]imidazo[2,1-k][1,10]phenanthroline (**12**): ^{1}H NMR (400 MHz, DMSO-d_6)

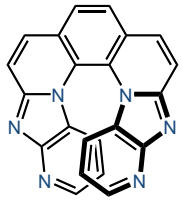

12

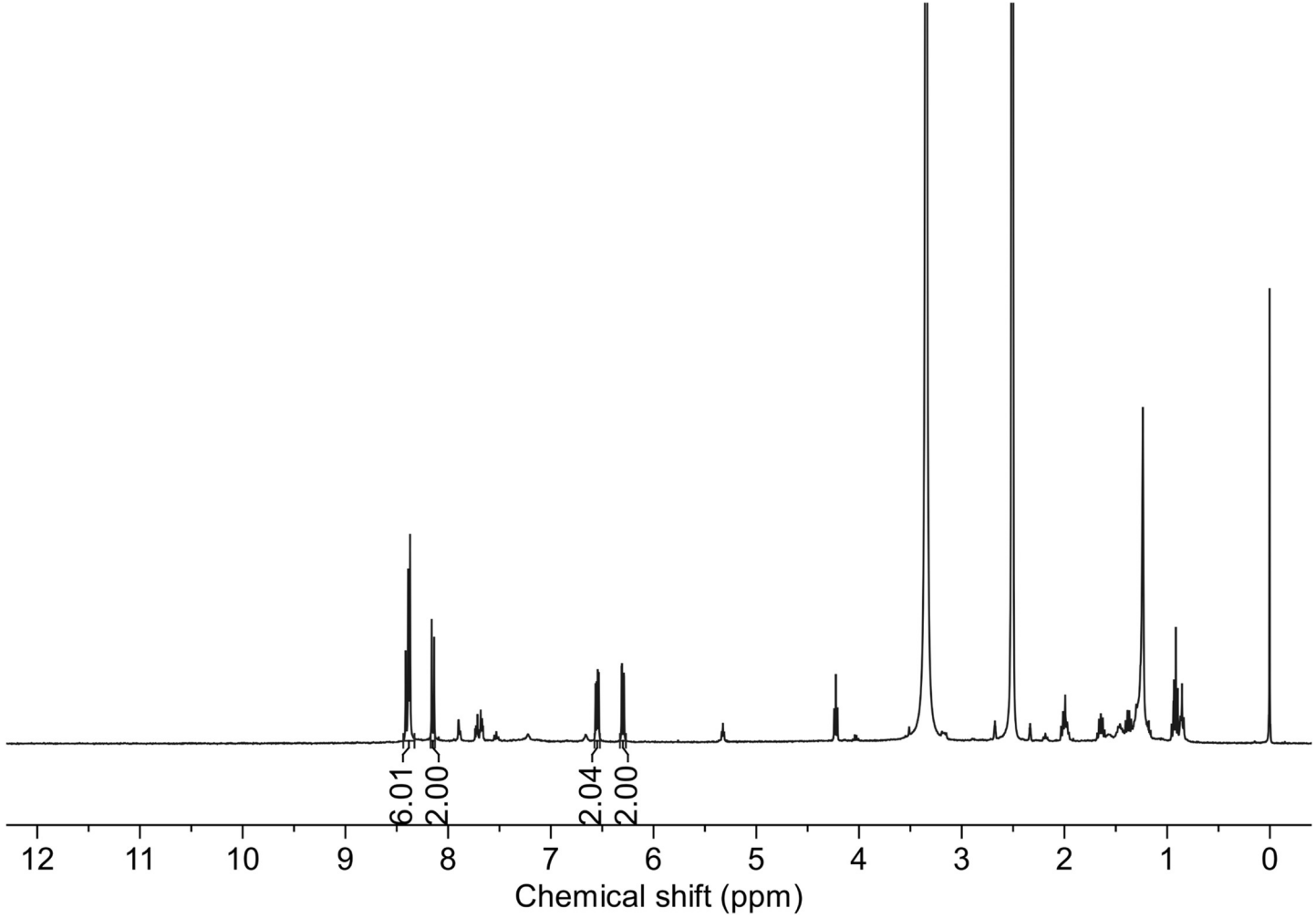

Quinolino[8',7':4,5]imidazo[1,2-*a*]quinolino[8',7':4,5]imidazo[2,1-*k*][1,10]phenanthroline (**13**): ^{1}H NMR (400 MHz, $CDCl_3$)

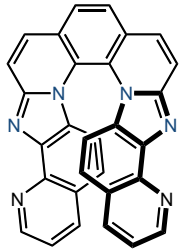

13

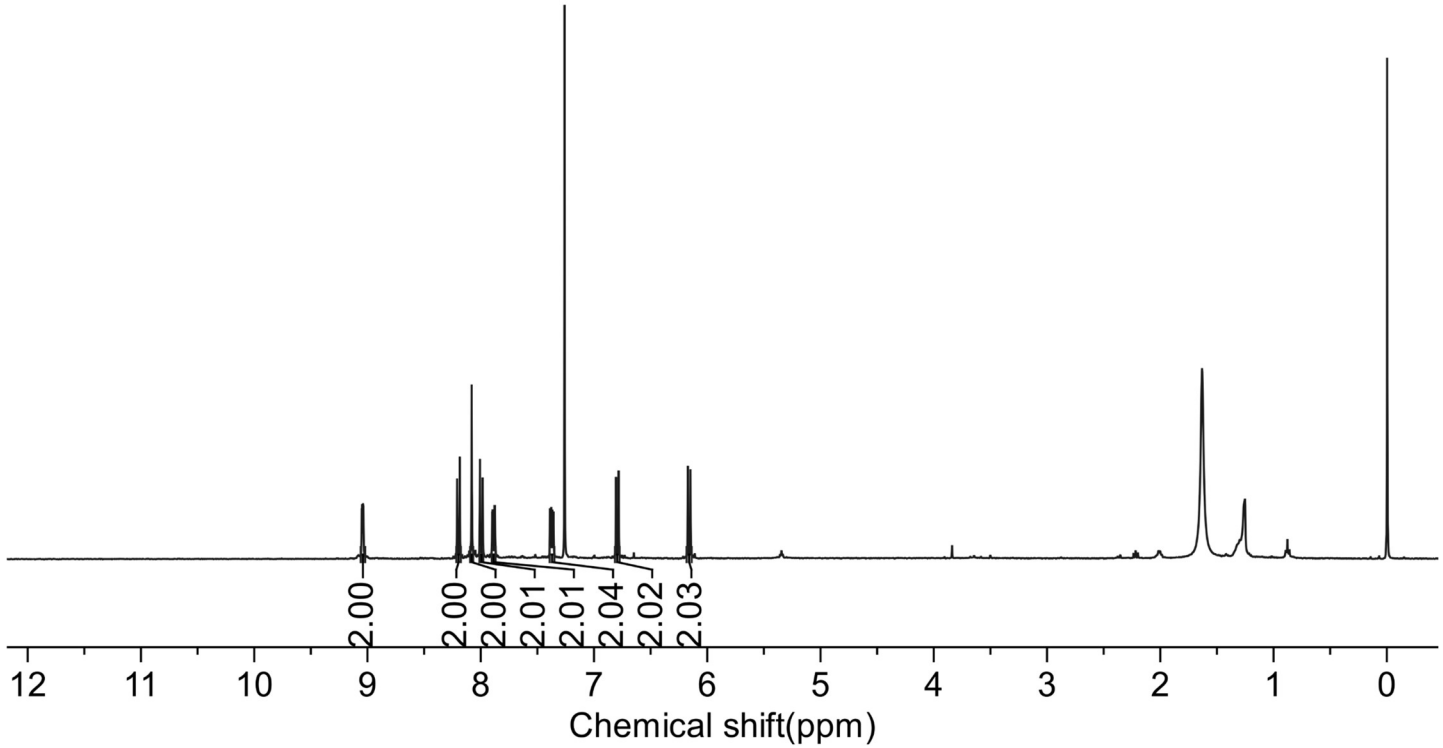

^{13}C NMR (100 MHz, $CDCl_3$)

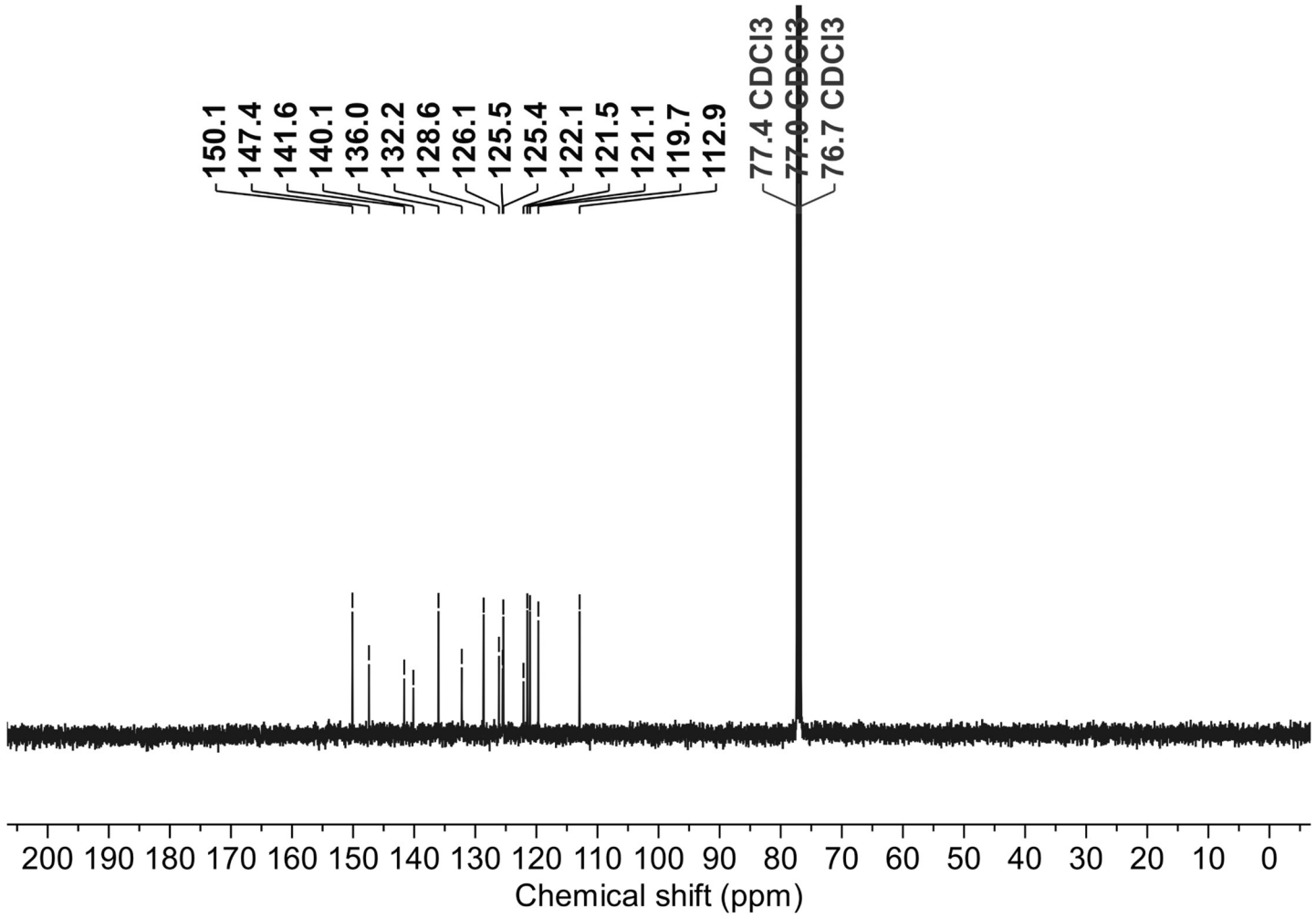

Naphtho[1',2':4,5]imidazo[1,2-*a*]naphtho[1',2':4,5]imidazo[2,1-*k*][1,10]phenanthroline (**14**): ^{1}H NMR (400 MHz, DMSO-d_6)

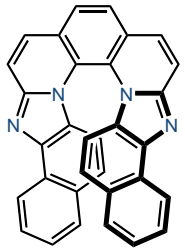

14

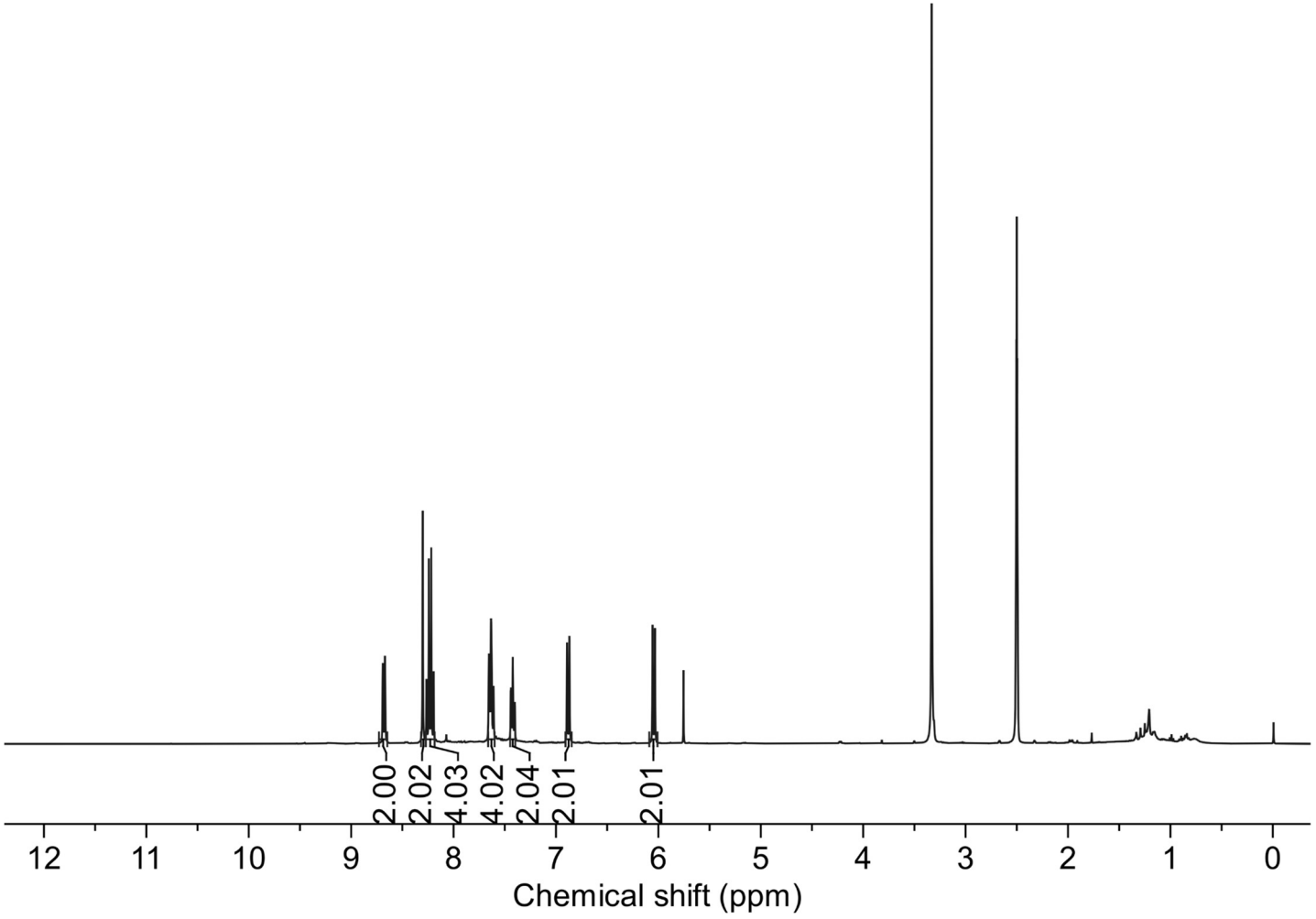

^{13}C NMR (100 MHz, DMSO-d_6)

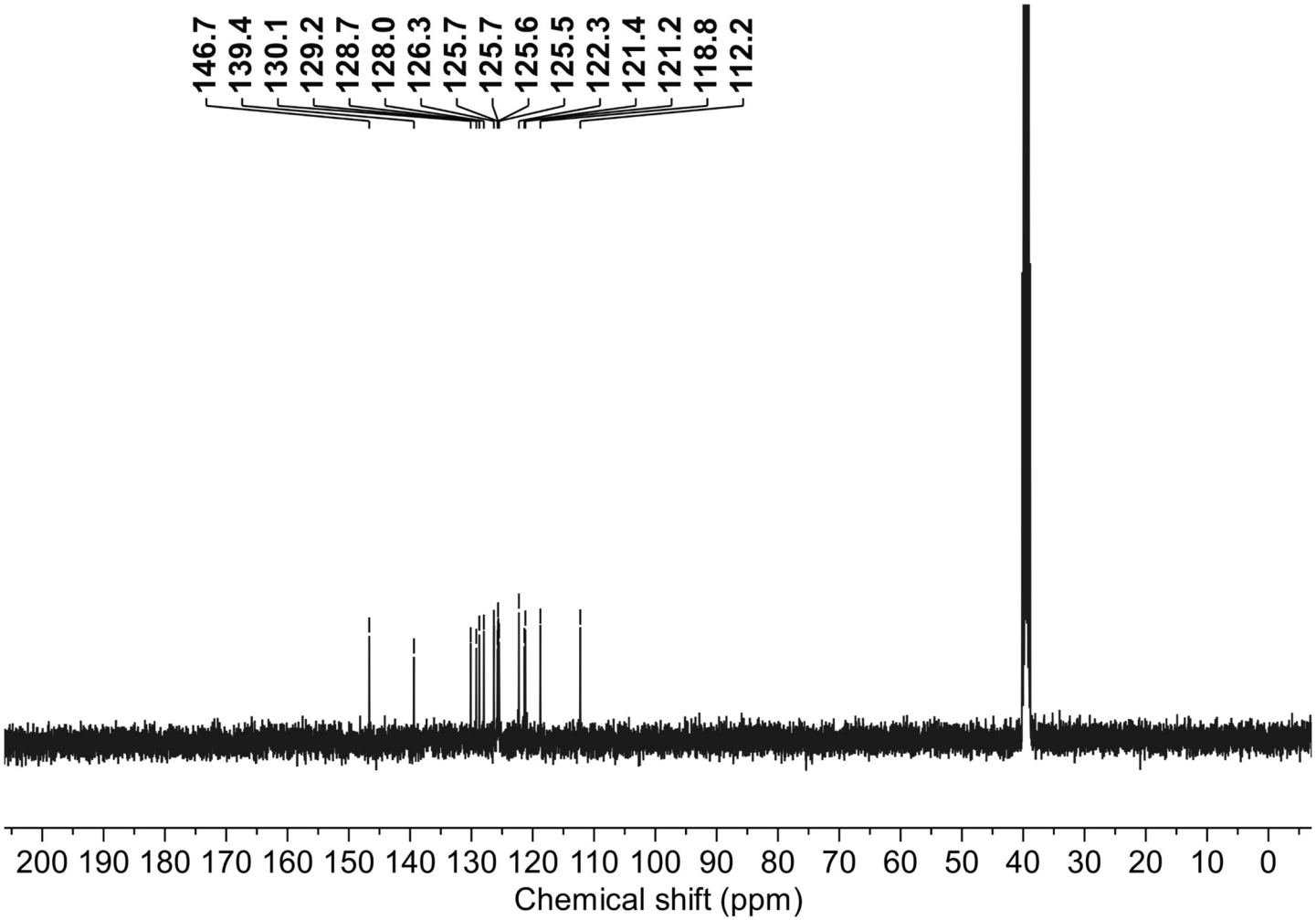

Naphtho[2',3':4,5]imidazo[1,2-*a*]naphtho[2',3':4,5]imidazo[2,1-*k*][1,10]phenanthroline (**15**): ^{1}H NMR (400 MHz,$CDCl_3$)

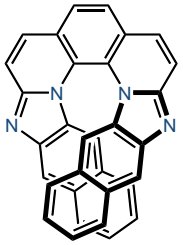

15

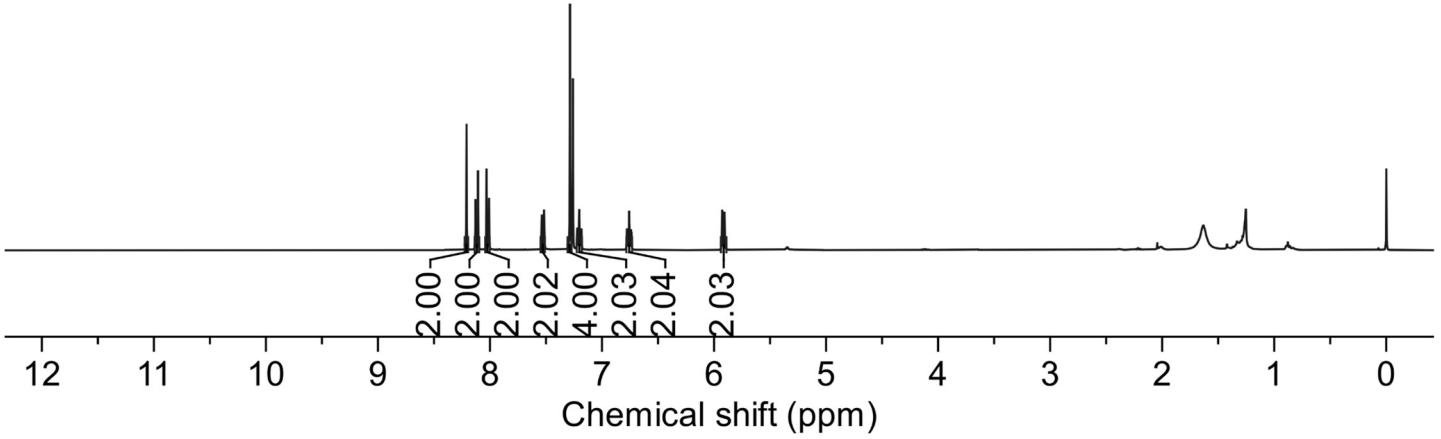

^{13}C NMR (100 MHz, $CDCl_3$)

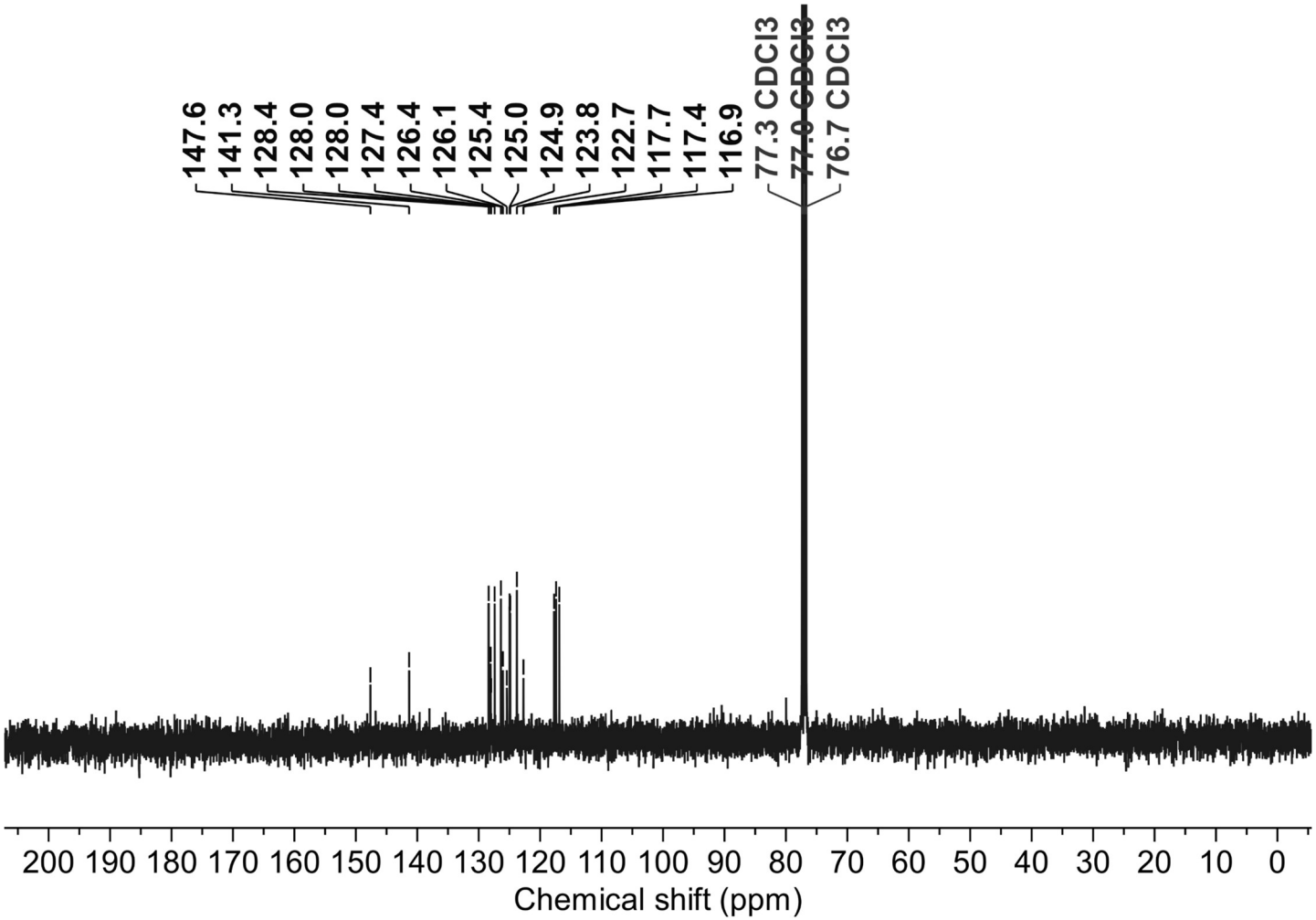

9,10,15,16-tetramethoxybenzo[4,5]imidazo[1,2-a]benzo[4,5]imidazo[2,1-k][1,10]phenanthroline (**16**): ^{1}H NMR (400 MHz, DMSO-d_6)

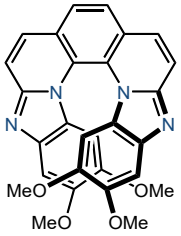

16

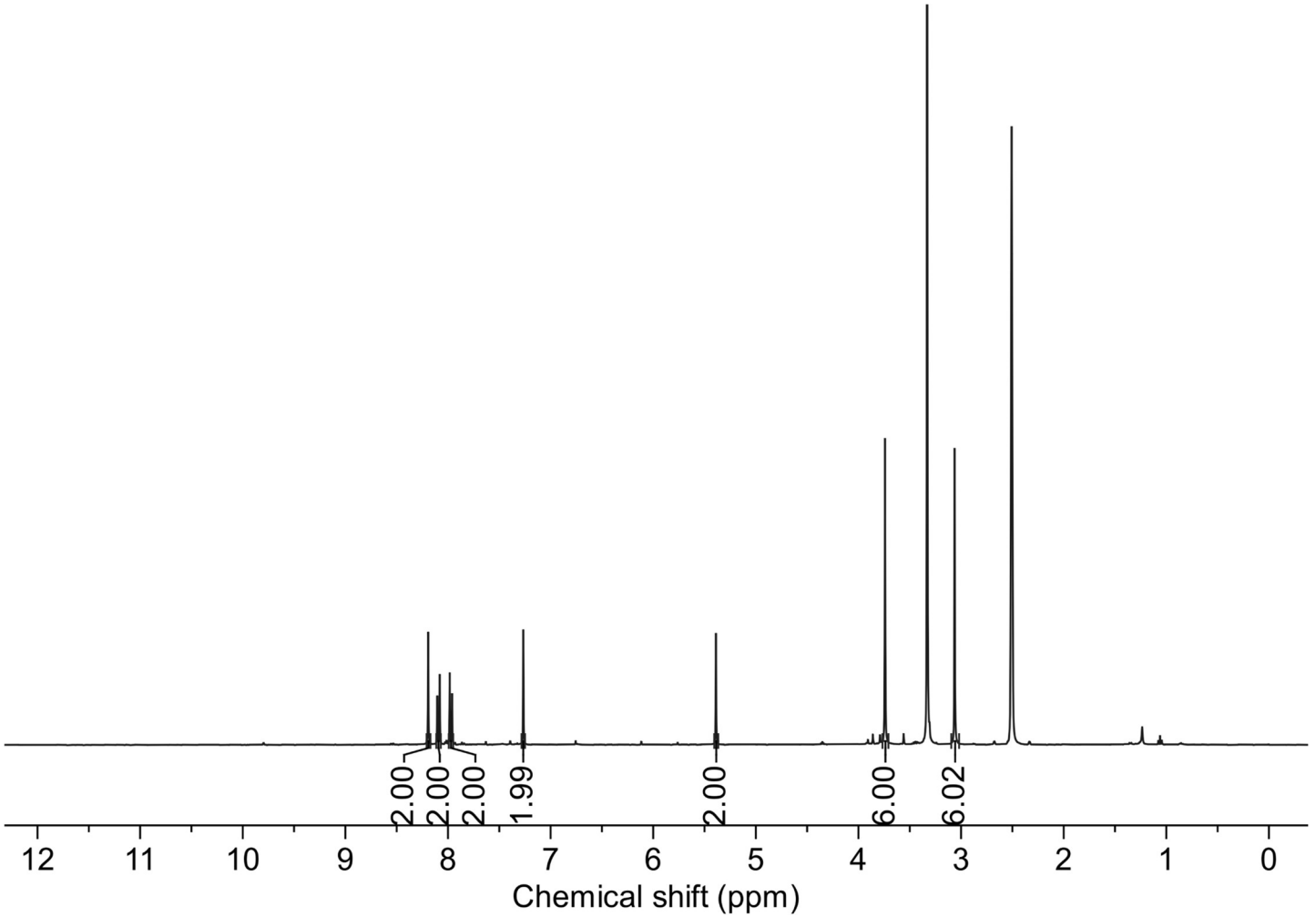

^{13}C NMR (100 MHz, $CDCl_3$)

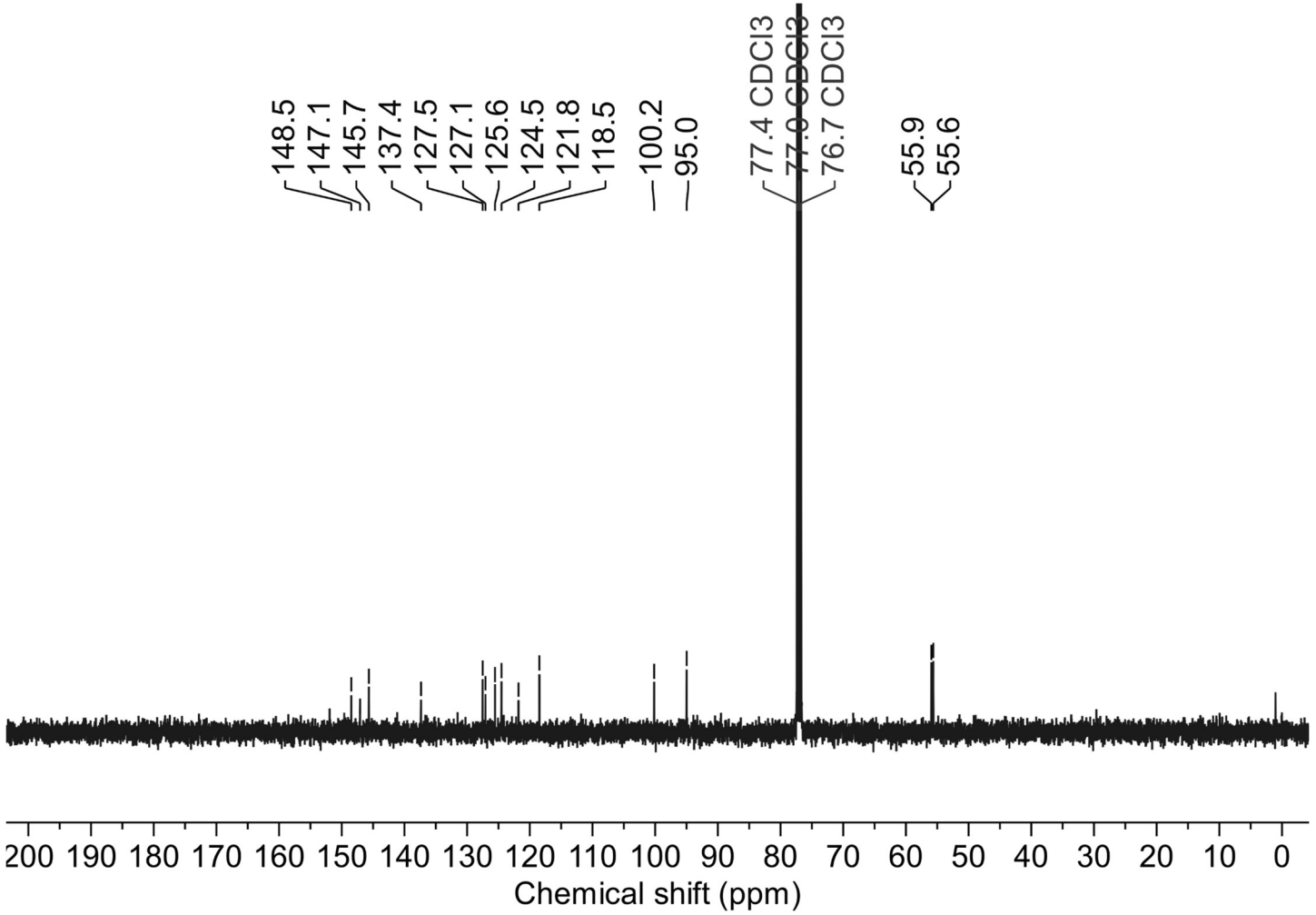

Pyrido[2''',1''':2'',3'']imidazo[4'',5'':3',4']benzo[1',2':4,5]imidazo[1,2-*a*]pyridine (**17**): ^{1}H NMR (400 MHz, $CDCl_3$)

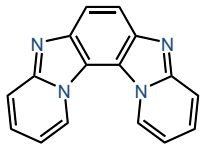

17

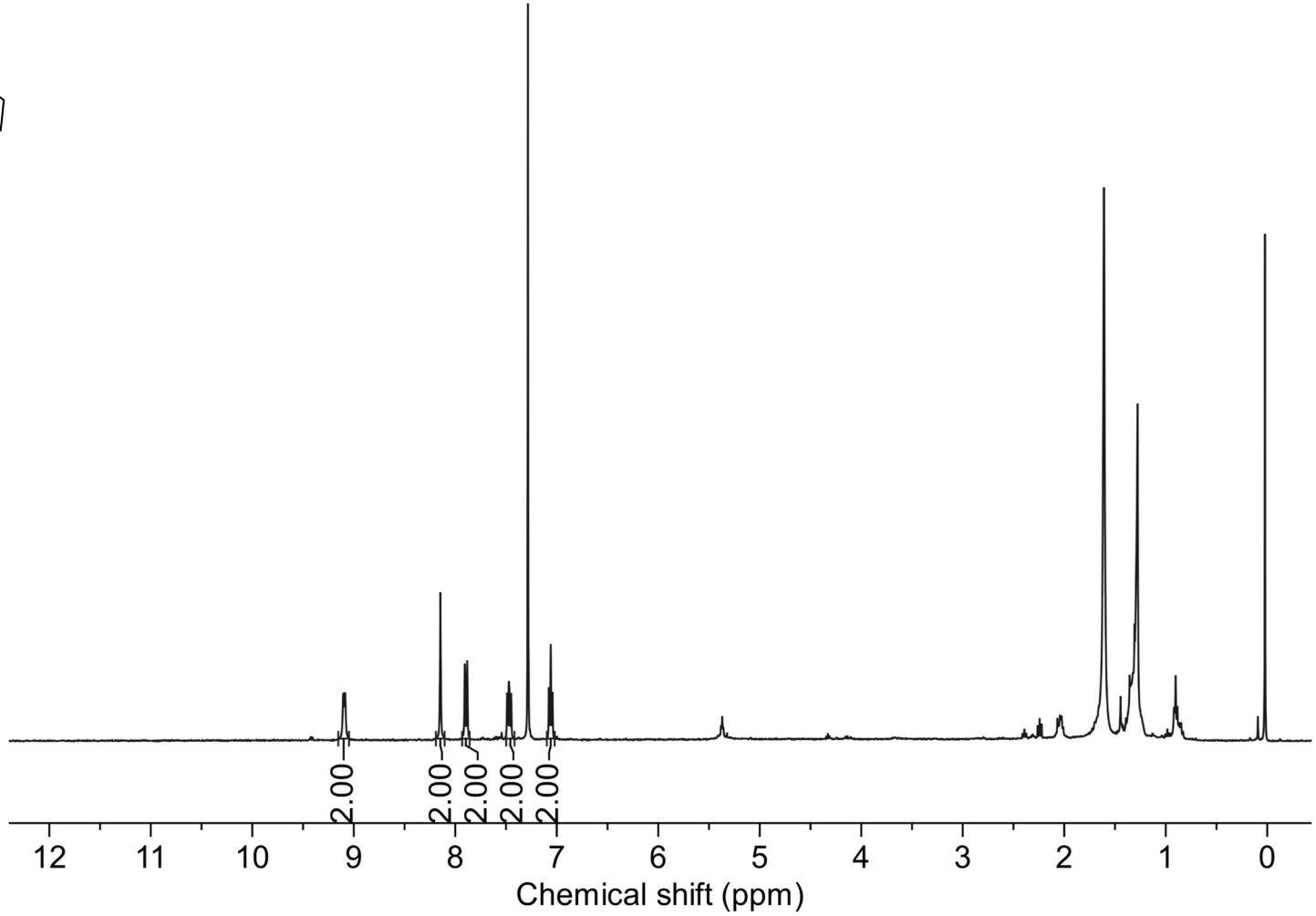

^{13}C NMR (100 MHz, $CDCl_3$)

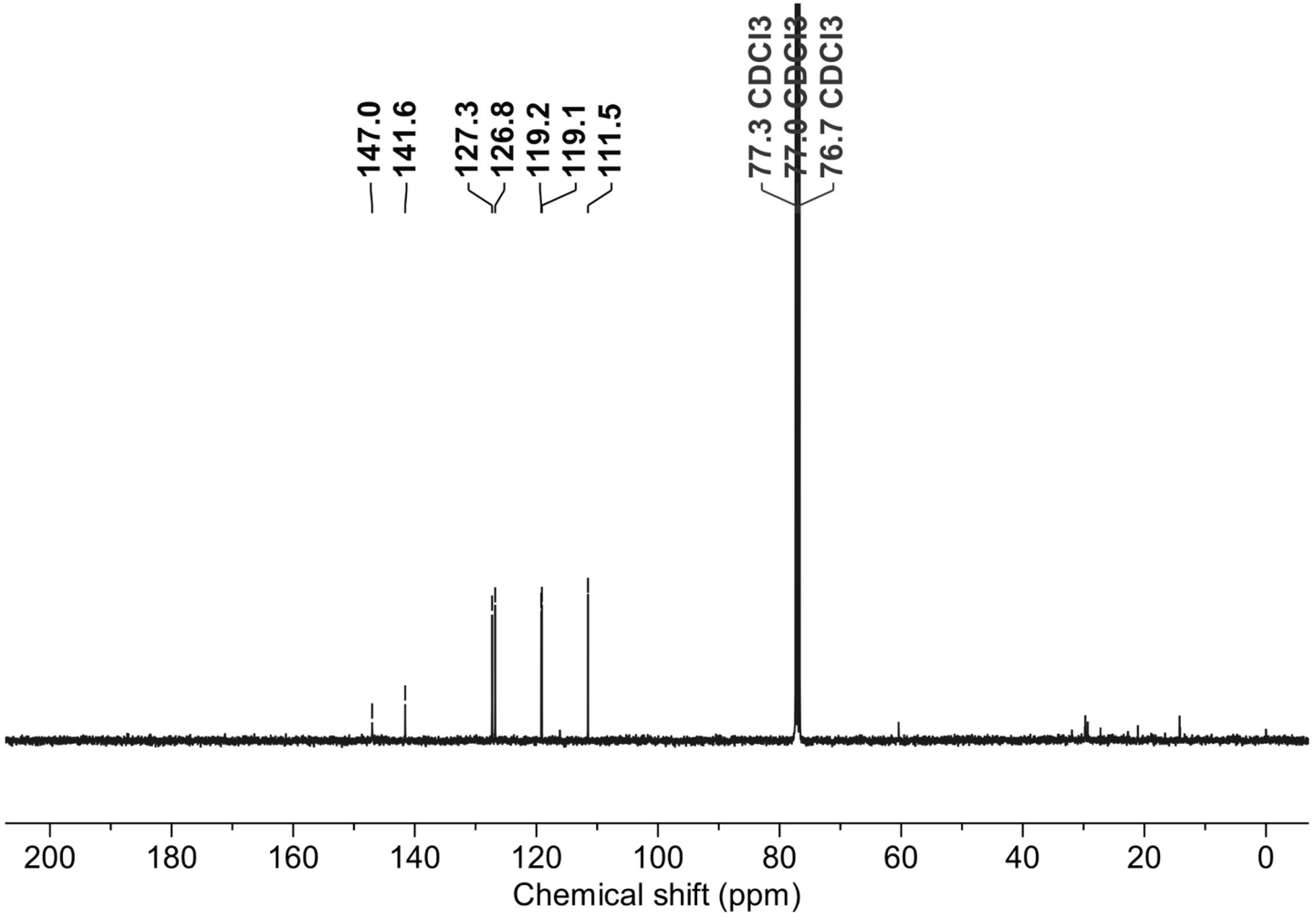

Pyrido[2''',1''':2'',3'']imidazo[4'',5'':3',4']benzo[1',2':4,5]imidazo[1,2-*a*]quinoline (**18**): ^{1}H NMR (400 MHz, $CDCl_3$)

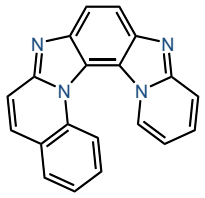

18

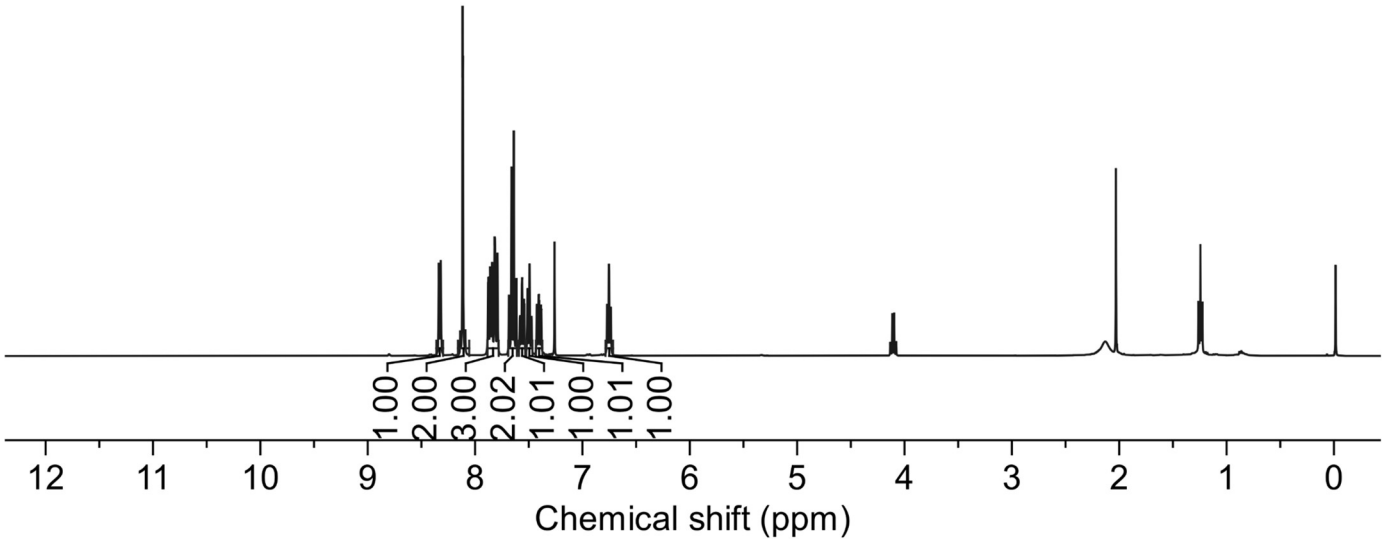

^{13}C NMR (400 MHz, $CDCl_3$)

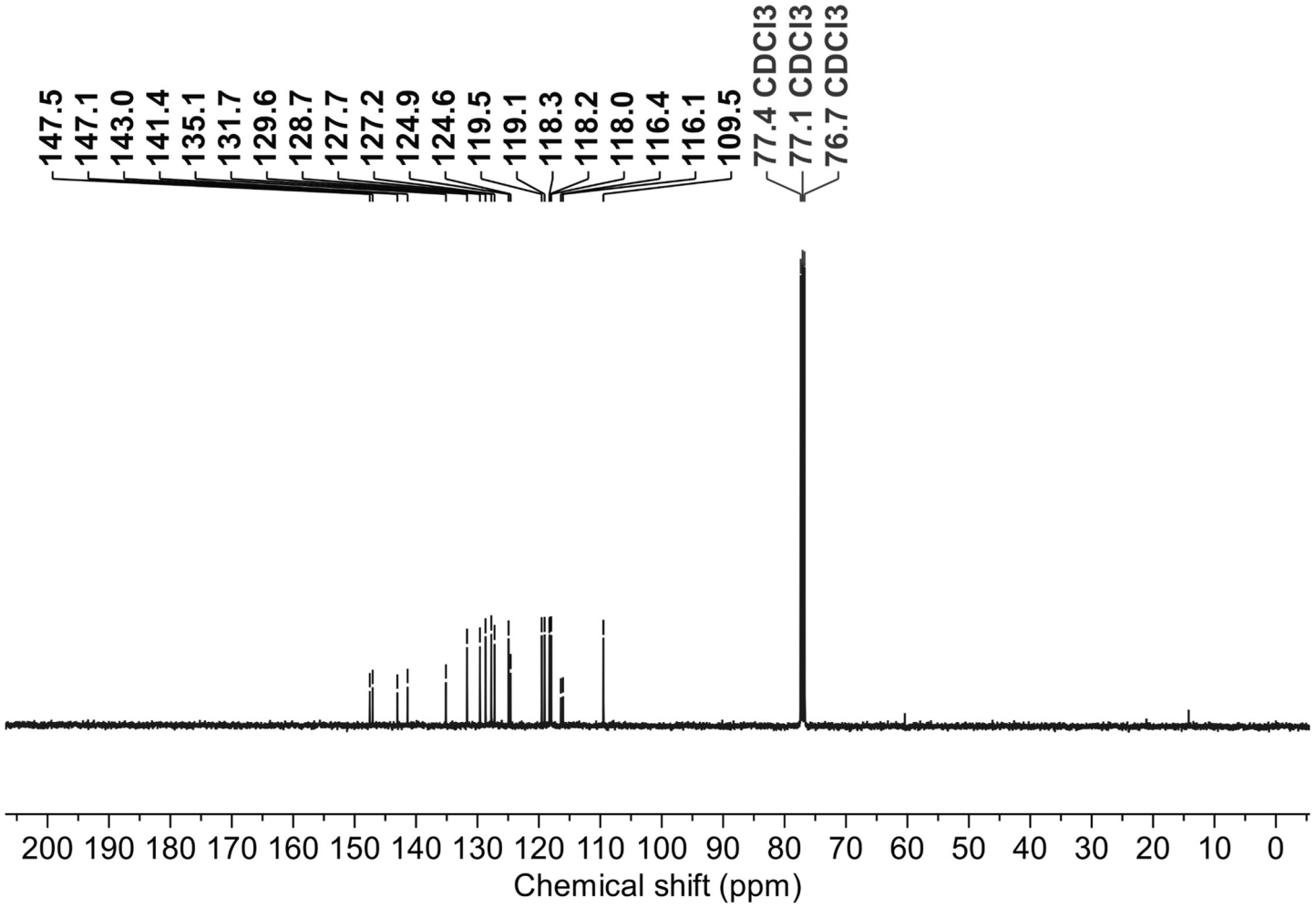

Quinolino[2''',1''':2'',3'']imidazo[4'',5'':3',4']benzo[1',2':4,5]imidazo[1,2-*a*]quinoline (**19**): ^{1}H NMR (400 MHz, $CDCl_3$)

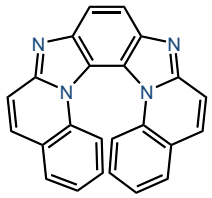

19

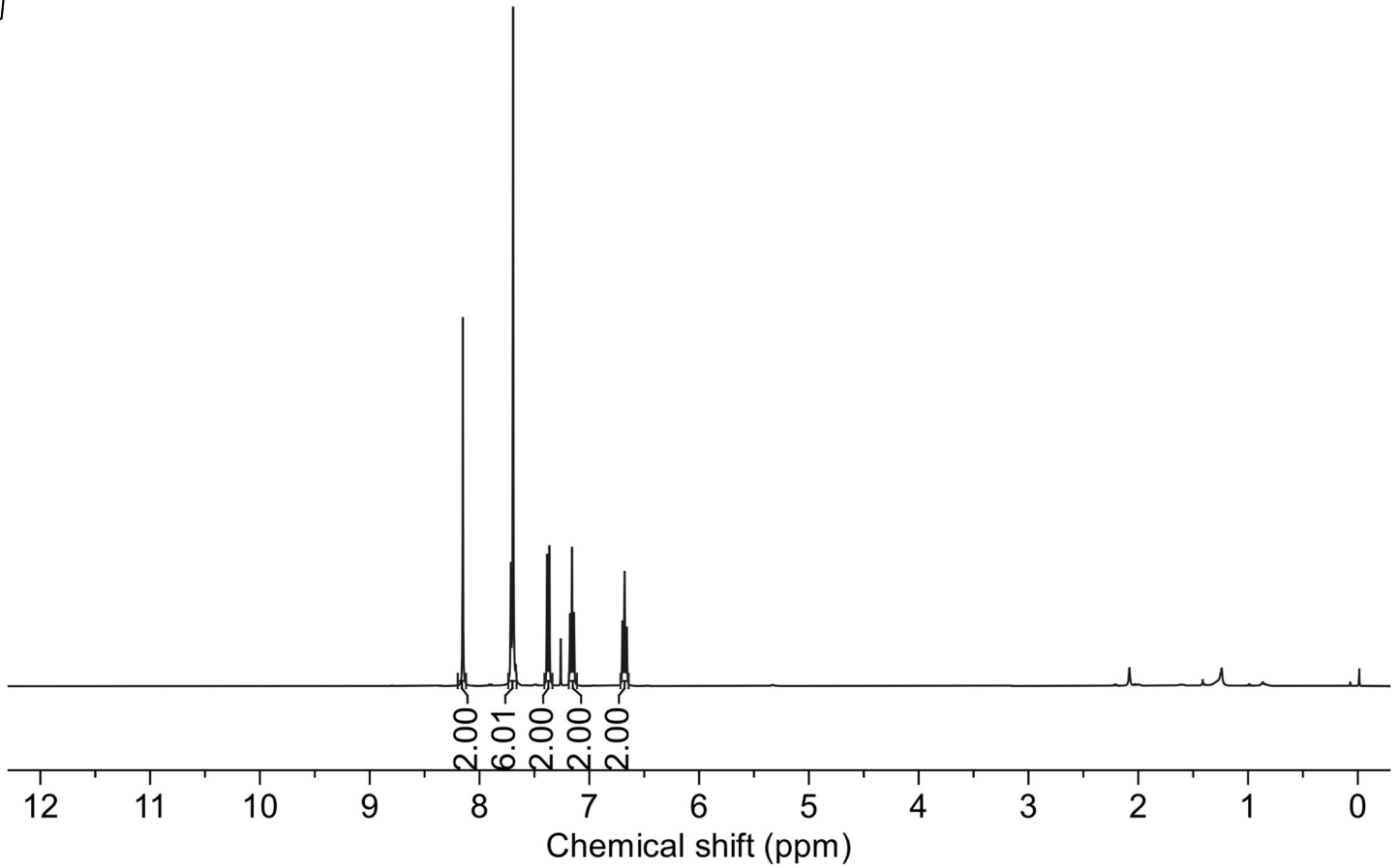

^{13}C NMR (100 MHz, $CDCl_3$)

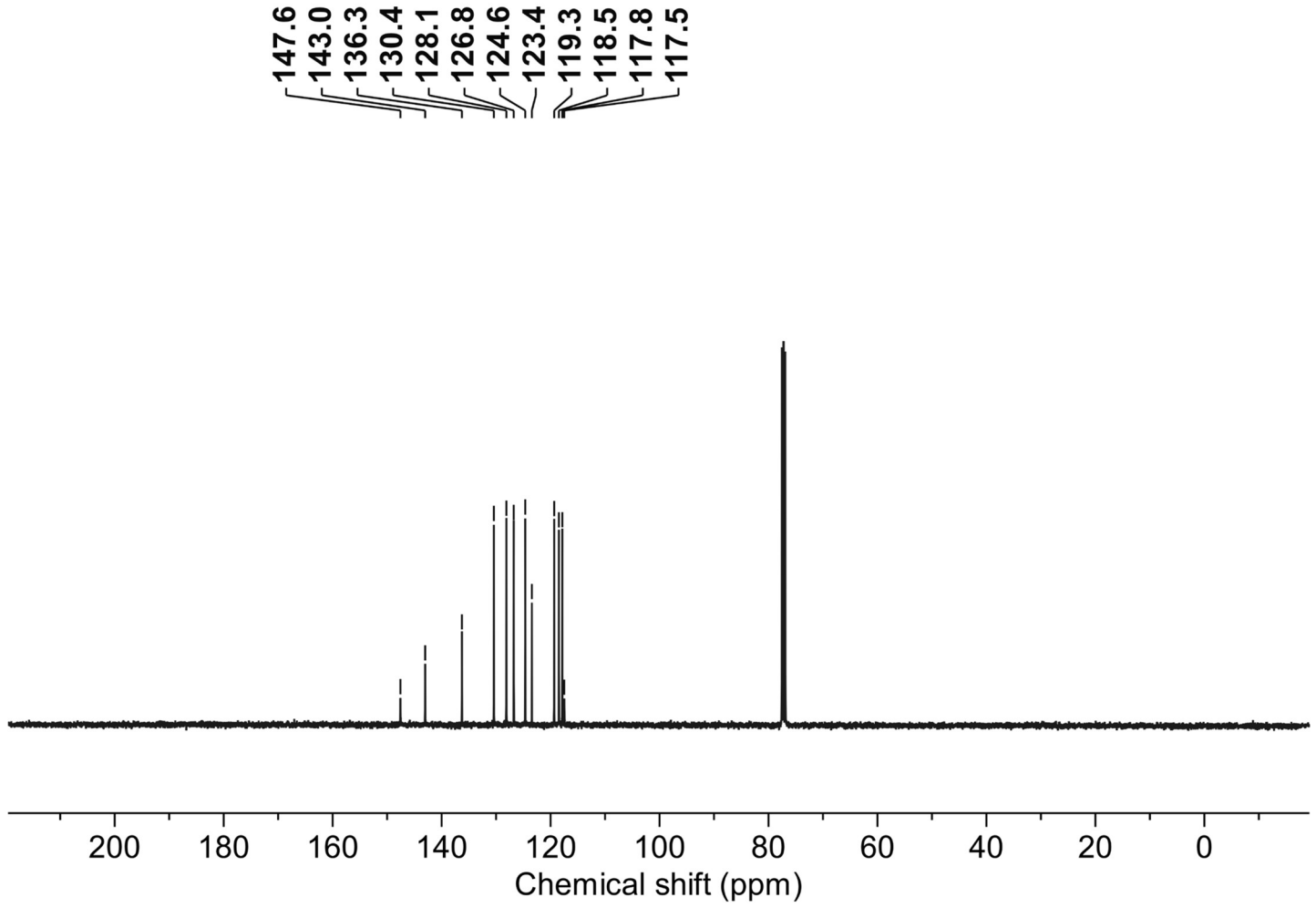

2,15-Dibromoquinolino[2”’,1”’:2”,3”]imidazo[4”,5”:3’,4’]benzo[1’,2’:4,5]imidazo[1,2-a]quinoline (**20**): ^{1}H NMR (400 MHz, DMSO-d_6)

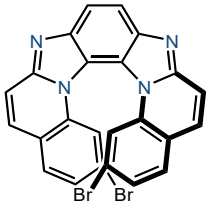

20

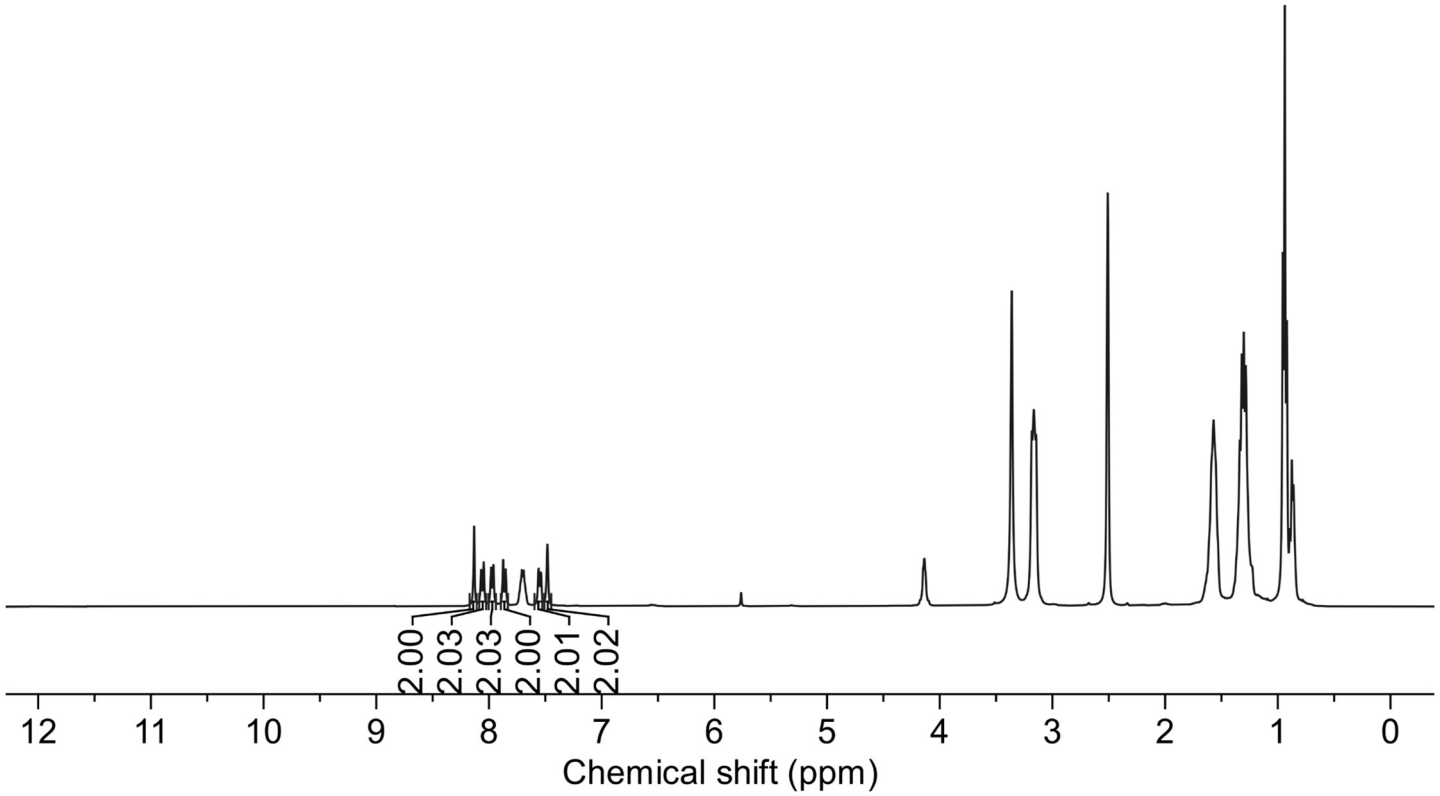

^{13}C NMR (100 MHz, $CDCl_3$)

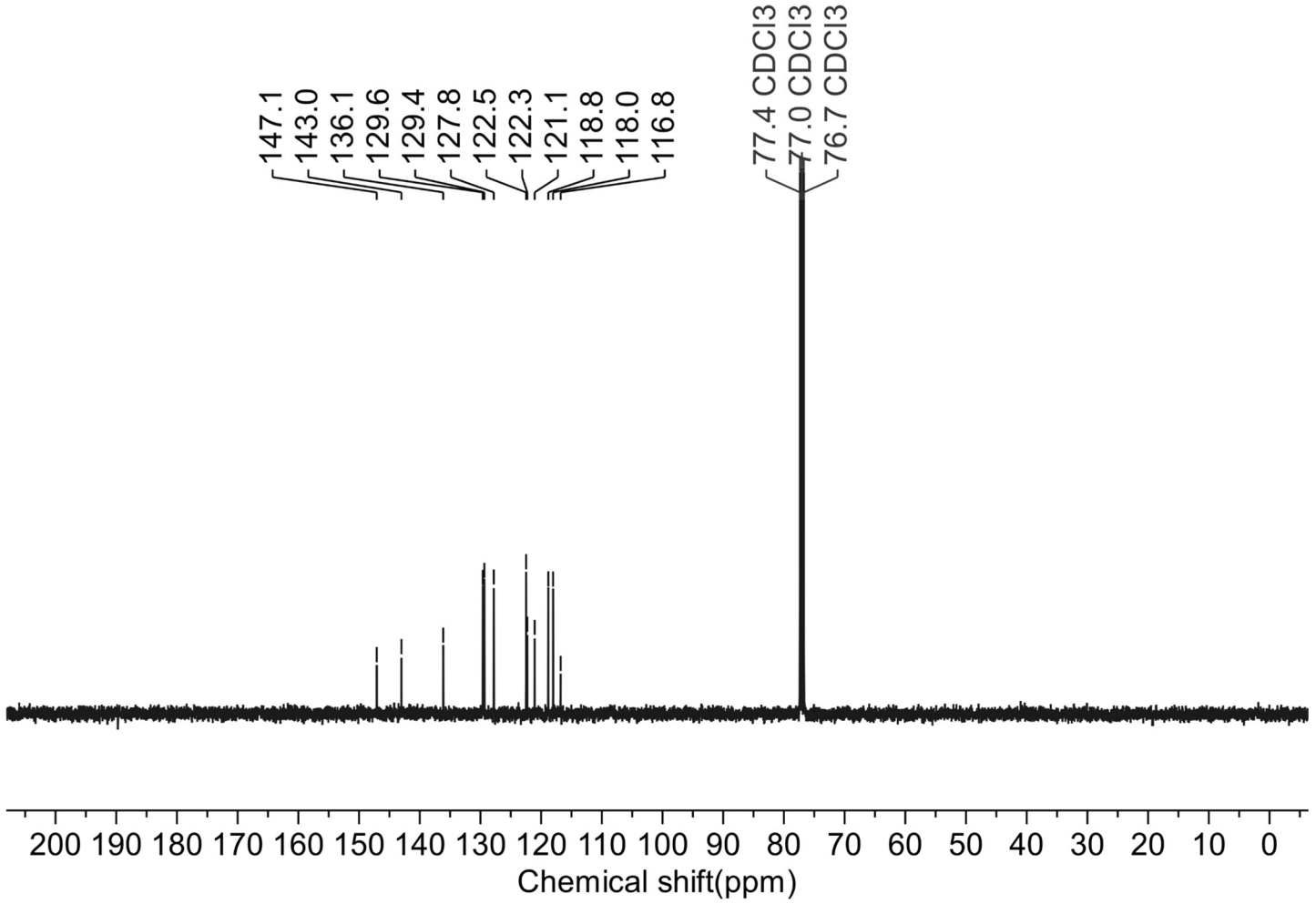

Quinolino[2''',1''':2'',3'']imidazo[4'',5'':3',4']benzo[1',2':4,5]imidazo[1,2-a][1,10]phenanthroline (**21**): ^{1}H NMR (400 MHz, $CDCl_3$)

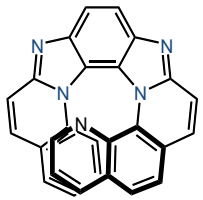

21

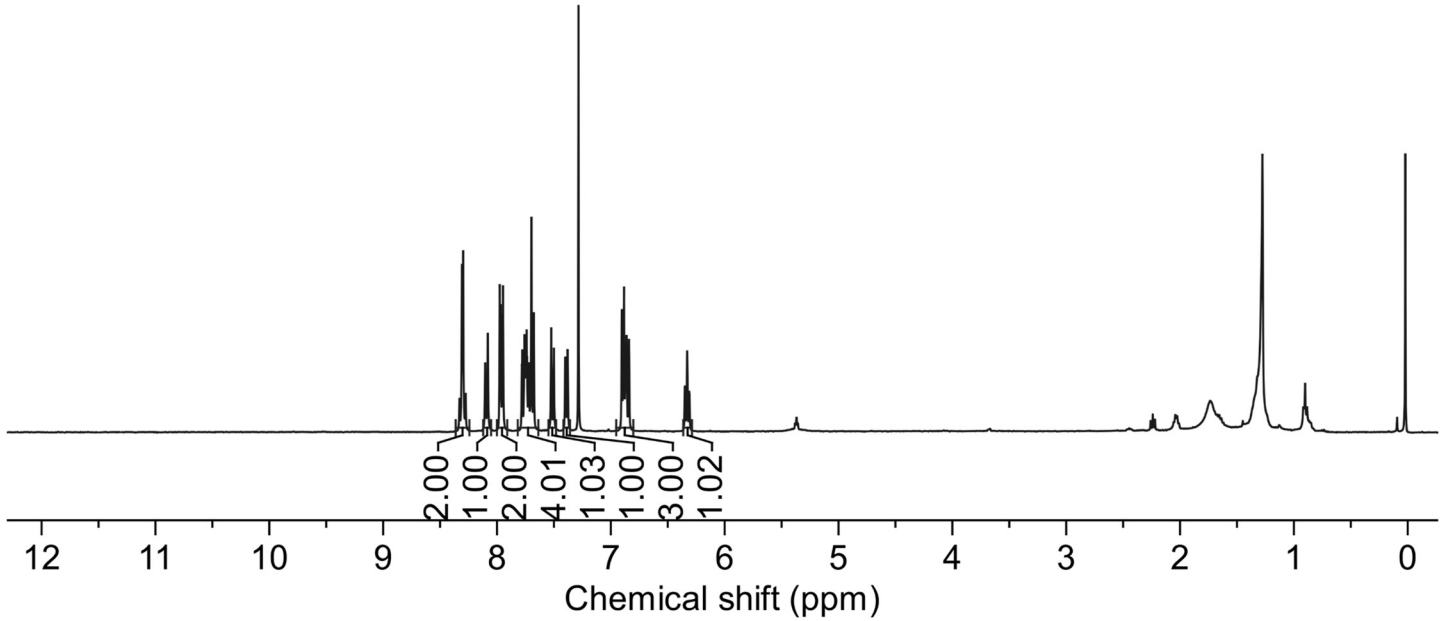

^{13}C NMR (100 MHz, $CDCl_3$)

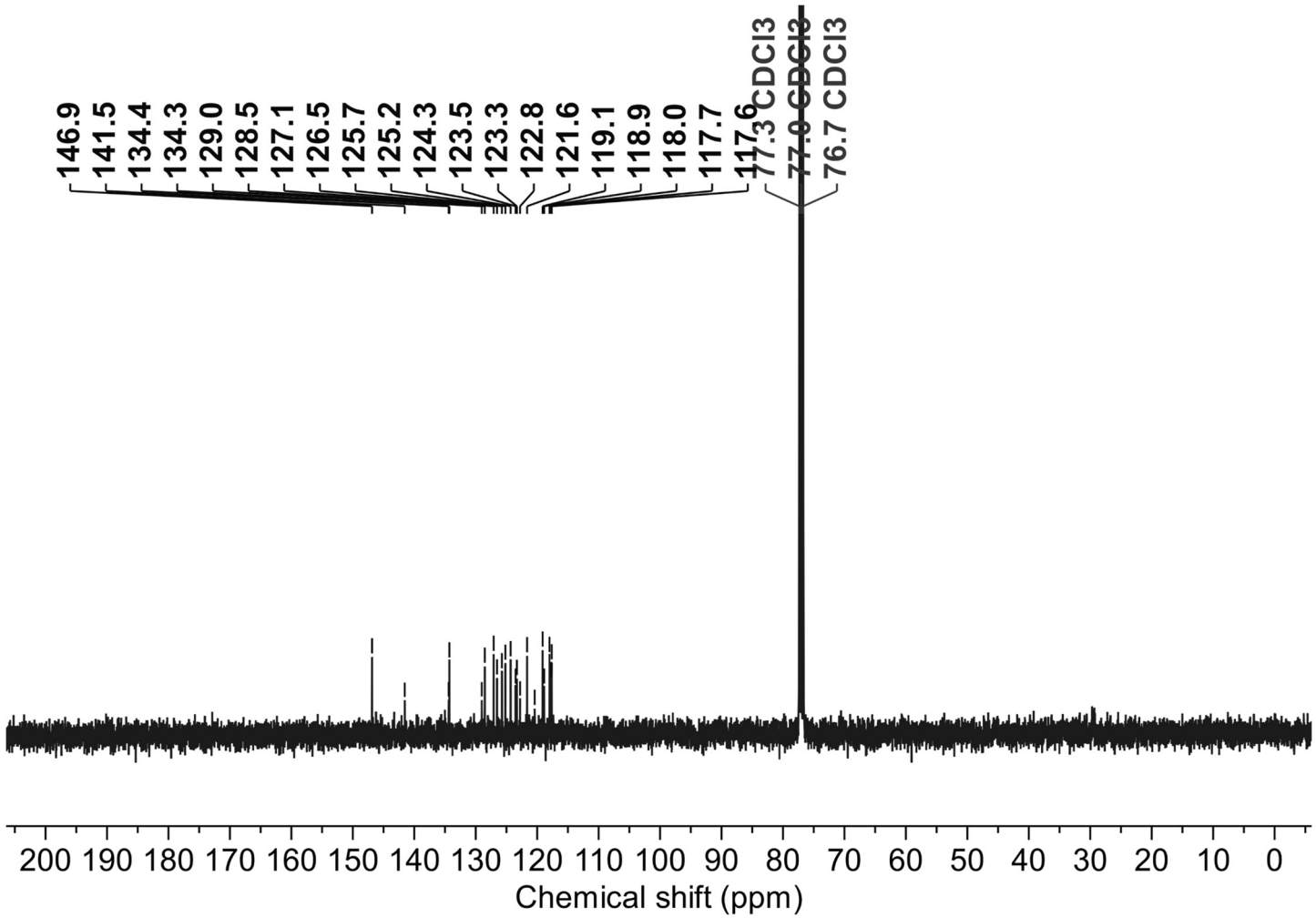

Phenanthoro[2''',1''':2'',3'']imidazo[4'',5'':3',4']benzo[1',2':4,5]imidazo[1,2-*a*]phenanthroline (**22**): ^{1}H NMR (400 MHz, $CDCl_3$)

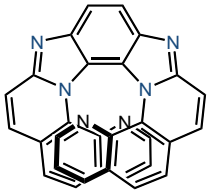

22

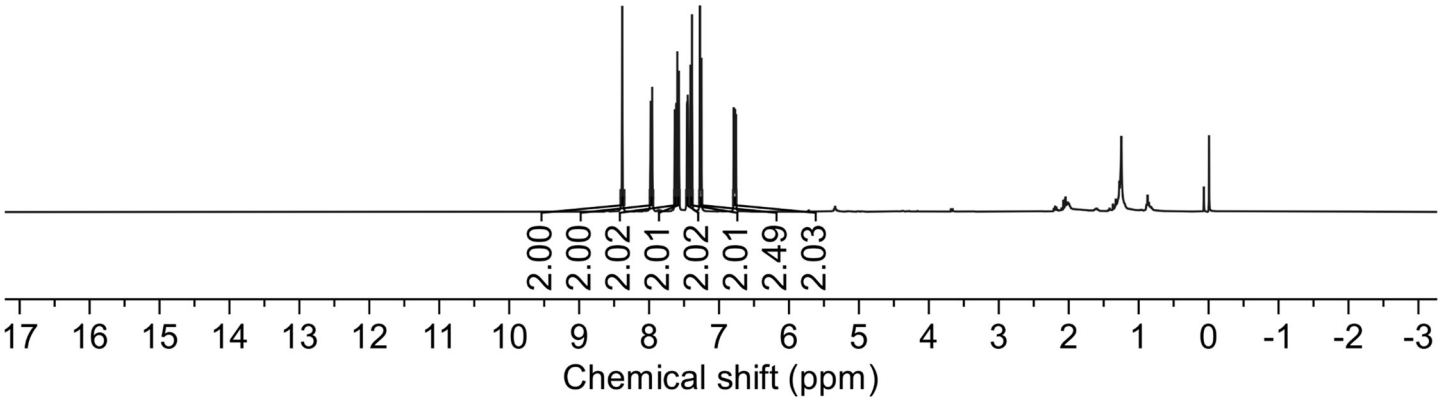

^{13}C NMR (100 MHz, $CDCl_3$)

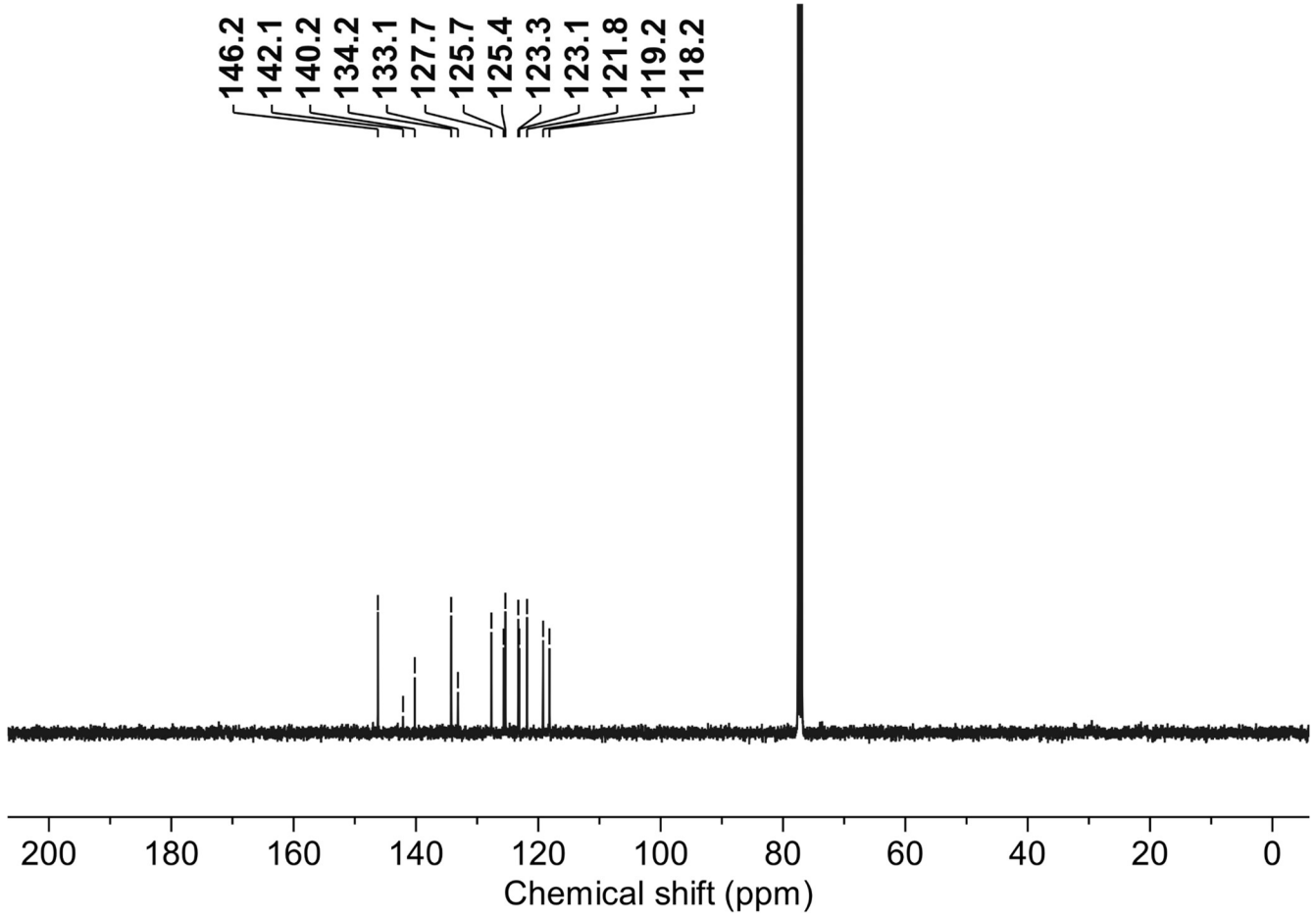

5,12-Di(N-((S)-1-phenylethyl)quinolino[2”’,1”’:2”,3”]imidazo[4”,5”:3’,4’]benzo[1’,2’:4,5]imidazo[1,2-a]quinoline (**23**): ^{1}H NMR (400 MHz, $CDCl_3$)

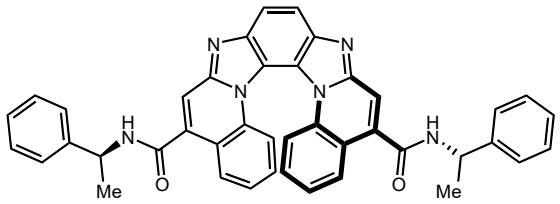

23

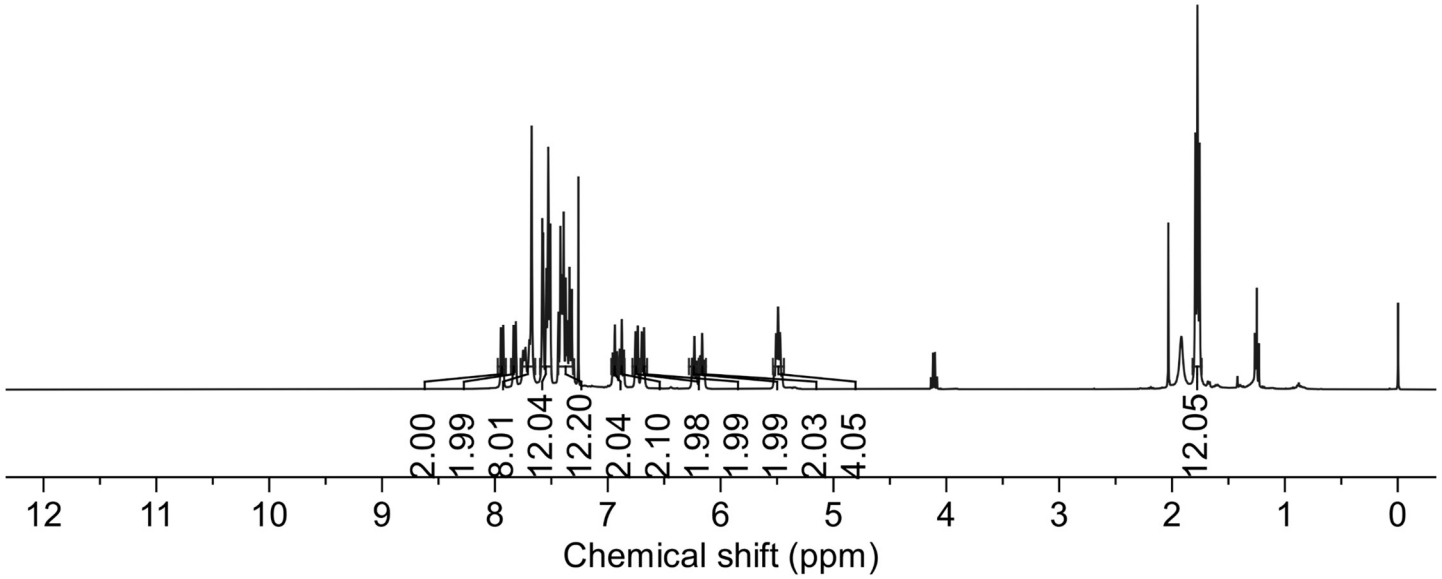

^{13}C NMR (100 MHz, $CDCl_3$)

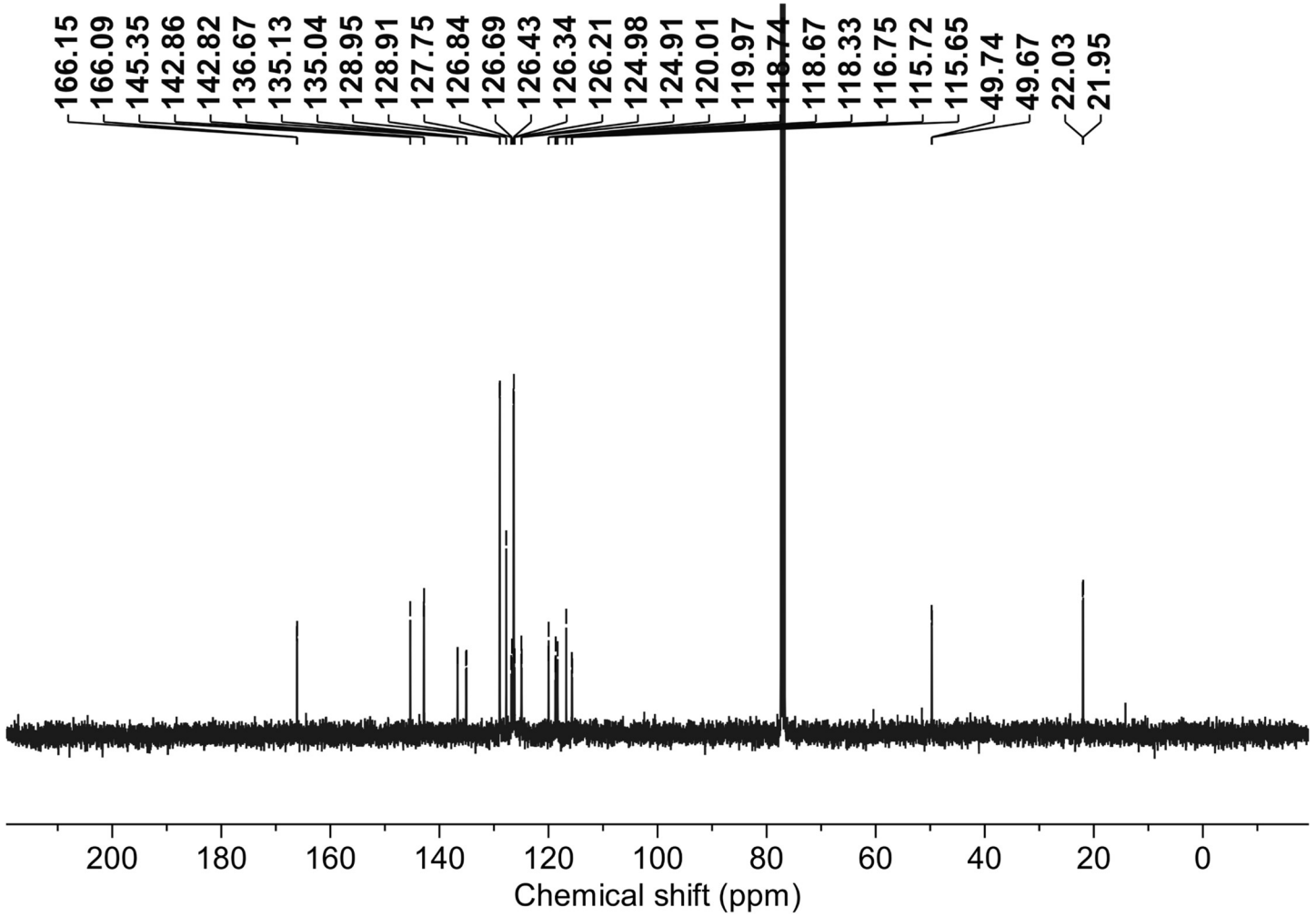

12 References

1. Otani, T. *et al.* Facile Two-Step Synthesis of 1,10-Phenanthroline-Derived Polyaza[7]helicenes with High Fluorescence and CPL Efficiency. *Angew. Chem. Int. Ed.* **56**, 3906–3910 (2017).
2. Otani, T. *et al.* Short-step synthesis and chiroptical properties of polyaza[5]–[9]helicenes with blue to green-colour emission. *Chem. Commun.* **56**, 4484–4487 (2020).
3. Rodríguez, R. *et al.* Mutual Monomer Orientation To Bias the Supramolecular Polymerization of [6]Helicenes and the Resulting Circularly Polarized Light and Spin Filtering Properties. *J. Am. Chem. Soc.* **144**, 7709–7719 (2022).
4. Zhang, D.-Y. *et al.* Highly Conductive Topologically Chiral Molecular Knots as Efficient Spin Filters. *J. Am. Chem. Soc.* **145**, 26791–26798 (2023).
5. Wang, Y., Zhang, Y., Wang, Y.-Y. & Yan, Q. Highly Conductive Chiral Organic Cages and Their Helical Assemblies Enable Efficient Spin Filtering. *J. Am. Chem. Soc.* **147**, 8751–8759 (2025).
6. Malatong, R. *et al.* Highly Durable Spin Filter Switching Based on Self-Assembled Chiral Molecular Motor. *Small* **19**, 2302714 (2023).
7. Suda, M. *et al.* Light-driven molecular switch for reconfigurable spin filters. *Nat. Commun.* **10**, 2455 (2019).
8. Zhu, Q. *et al.* Multistate Switching of Spin Selectivity in Electron Transport through Light-Driven Molecular Motors. *Adv. Sci.* **8**, 2101773 (2021).
9. Ko, C.-H. *et al.* Twisted molecular wires polarize spin currents at room temperature. *Proc. Natl. Acad. Sci.* **119**, e2116180119 (2022).
10. Bullard, G. *et al.* Low-Resistance Molecular Wires Propagate Spin-Polarized Currents. *J. Am. Chem. Soc.* **141**, 14707–14711 (2019).
11. Kettner, M. *et al.* Chirality-Dependent Electron Spin Filtering by Molecular Monolayers of Helicenes. *J. Phys. Chem. Lett.* **9**, 2025–2030 (2018).
12. Giaconi, N. *et al.* Efficient Spin-Selective Electron Transport at Low Voltages of Thia-Bridged Triarylamine Hetero[4]helicenes Chemisorbed Monolayer. *ACS Nano* **17**, 15189–15198 (2023).
13. Niu, W. *et al.* Lateral π-extended helical nanographenes with large spin polarization. *Chem. Sci.* **16**, 21446–21453 (2025).
14. Giaconi, N. *et al.* Spin polarized current in chiral organic radical monolayers. *J. Mater. Chem. C* **12**, 10029–10035 (2024).
15. Safari, M. R., Matthes, F., Schneider, C. M., Ernst, K. & Bürgler, D. E. Spin-Selective Electron Transport Through Single Chiral Molecules. *Small* **20**, 2308233 (2024).
16. Kiran, V. *et al.* Helicenes—A New Class of Organic Spin Filter. *Adv. Mater.* **28**, 1957–1962 (2016).
17. Rodríguez, R. *et al.* Weakly Self-Assembled [6]Helicenes: Circularly Polarized Light and Spin Filtering Properties. *Chem. – Eur. J.* **29**, e202302254 (2023).
18. Mishra, S. *et al.* Spin Filtering Along Chiral Polymers. *Angew. Chem. Int. Ed.* **59**, 14671–14676 (2020).
19. Bhowmick, D. K. *et al.* Spin-induced asymmetry reaction—The formation of asymmetric carbon by electropolymerization. *Sci. Adv.* **8**, eabq2727 (2022).
20. Wang, C. *et al.* Transverse Spin Selectivity in Helical Nanofibers Prepared without Any Chiral Molecule. *Phys. Rev. Lett.* **133**, 108001 (2024).
21. Mondal, A. K. *et al.* Spin Filtering in Supramolecular Polymers Assembled from Achiral Monomers Mediated by Chiral Solvents. *J. Am. Chem. Soc.* **143**, 7189–7195 (2021).

22. Sang, Y. *et al.* Ultrasound-Directed Symmetry Breaking and Spin Filtering of Supramolecular Assemblies from only Achiral Building Blocks. *Angew. Chem. Int. Ed.* **62**, e202215867 (2023).
23. Kulkarni, C. *et al.* Highly Efficient and Tunable Filtering of Electrons' Spin by Supramolecular Chirality of Nanofiber-Based Materials. *Adv Mater*. **32**, 1904965(2020).
24. Sun, S., Jiang, J., Jia, M., Tian, Y. & Xiao, Y. 1.5D Chiral Perovskites Mediated by Hydrogen-Bonding Network with Remarkable Spin-Polarized Property. *Angew. Chem. Int. Ed.* **64**, e202423314 (2025).
25. Kim, Y.-H. *et al.* Chiral-induced spin selectivity enables a room-temperature spin light-emitting diode. *Science* **371**, 1129–1133 (2021).
26. Park, Y. S. *et al.* Efficient solar-driven hydrogen peroxide production enabled by a perovskite electrochemical device integrated with a cobalt-based chiral catalyst. *Energy Environ. Sci.* **19**, 312–326 (2026).
27. Feng, S. *et al.* Chiral two-dimensional conjugated metal-organic frameworks with high spin polarization. *Nat. Commun.* **16**, 9473 (2025).
28. Chen, X. *et al.* Helical polymer metal–organic framework hybrids. *Nat. Synth.* **5**, 46–54 (2025).
29. Jiang, L. *et al.* Morphological chirality engineering in achiral CoNi-MOFs enables CISS-driven spin-selective oxygen evolution. *Nano Res.* **18**, 94907634 (2025).
30. Jiang, C. *et al.* Topology-Controlled Chirality and Spin Selectivity in Two-Dimensional Covalent Organic Frameworks. *J. Am. Chem. Soc*. **148**, 2551–2562 (2026).
31. Zhang, X. *et al.* Amplifying Chirality-Induced Spin Selectivity in Helical Covalent Organic Frameworks through Fullerene Encapsulation. *J. Am. Chem. Soc.* **147**, 26546–26556 (2025).
32. Liu, Z. *et al.* An Insight into the Relation of Spin-Polarization and Oxygen Evolution Enhancement with a Monolayer Chiral Covalent Organic Framework Model Catalyst. *J. Am. Chem. Soc.* **147**, 31975–31983 (2025).
33. Sun, X., Zhang, K.-Y., Zhou, S.-Z. & Fu, H.-H. Robust chirality-induced spin selectivity in topologically chiral molecular knots. *Nat. Commun.* https://doi.org/10.1038/s41467-025-67988-8 (2025)
34. Bloom, B. P., Kiran, V., Varade, V., Naaman, R. & Waldeck, David. H. Spin Selective Charge Transport through Cysteine Capped CdSe Quantum Dots. *Nano Lett.* **16**, 4583–4589 (2016).
35. Mishra, S. *et al.* Length-Dependent Electron Spin Polarization in Oligopeptides and DNA. *J. Phys. Chem. C* **124**, 10776–10782 (2020).
36. Labella, J., Bhowmick, D. K., Kumar, A., Naaman, R. & Torres, T. Easily processable spin filters: exploring the chiral induced spin selectivity of bowl-shaped chiral subphthalocyanines. *Chem. Sci.* **14**, 4273–4277 (2023).
37. Bian, Z. *et al.* Hybrid Chiral MoS_2 Layers for Spin-Polarized Charge Transport and Spin-Dependent Electrocatalytic Applications. *Adv. Sci.* **9**, 2201063 (2022).